REGULATION OF IMMUNE COMPLEX FORMATION AND CLEARANCE BY HISTIDINE-RICH GLYCOPROTEIN

by

Nick Naser Gorgani (B. Chem. Eng., M.B.B.S.)

This thesis submitted for the degree of Doctor of Philosophy at the Australian National Universioty

Division of Immunology and Cell Biology
The John Curtin School of Medical Research
The Australian National University

December 1998

STATEMENT

I certify that all experiments described in this thesis represent my own work, were done by me, and have not been previously submitted for a degree at this or any other university.

Nick Naser Gorgani,

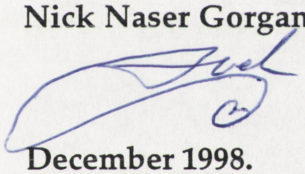

December 1998.

DEDICATION

To my parents

Ebrahim and Dursun Gorgani

who devoted their life for their children

ACKNOWLEDGEMENT

I wish to thank my supervisors Professor Chris Parish and Dr Joe Altin for their excellent supervision, advice and continuous support of my work. Especially, to Chris for his enthusiasm and encouragement in the scientific aspects of this thesis and my fellowship applications. I also wish to thank my advisor Dr Hilary Warren for her encouragement and in providing me with some materials necessary for my experiments. I wish to thank Damian Hall and Professor Don Winzor for their collaboration in the biosensor studies. Many thanks to Professor Paul Gatenby for his help in some aspects of this work, for supplying plasma of patients with SLE and RA and for encouraging me with my fellowship applications. Finally I wish to thank Dr. John Morrison for his assistance in interpreting the biosensor data.

I am indebted to many staff of the JCSMR for their support throughout my PhD studies. Especially, I would like to thank Karen Jakobsen, Ros Henderson and Pat Basnett. Many thanks to Mark, Stuart, Julie and Karen at the photography section of JCSMR and to Geoff Osborne and Sabine Gruninger at the FACS facilities for their continual help during my PhD.

I am grateful to many friends at the JCSMR who encouraged me in the continuation of my project, especially to Min Ru Qiu, Erin O'Neil, Tony Manderson, Allanna Hurne, Matthias Regner, Rolla Khoury and Mansoureh Eghbali. Also many thank to Robyn Watts for her proof reading of this thesis.

Special thanks to my parents Ebrahim and Dursun Gorgani who always encouraged me to keep up with their slogan "whatever you do try to create the best" and to my siblings Nader, Farhad, Matin, Nilay and Navid for their encouragement throughout my PhD studies.

Finally, the financial assistance of the Australian National University is gratefully acknowledged.

ABBREVIATIONS

A	absorbance
aAb	autoantibody
Ab	antibody
Abs	antibodies
ABTS	2,2'-azino-bis (3-ethylbenzthiazoline-6-sulfonic acid) diammonium
AEBSF	[4-(2-aminoethyl)-benzenesulfonyl fluoride hydrochloride]
Ag	antigen
Ags	antigens
AIDS	acquired immune deficiency syndrome
AMP	adenosine monophosphate
ANCA	anti-neutrophil cytoplasmic antigen
Arg	arginine
Asn	asparagine
ATIII	antithrombin III
Az	azide, NaN_3
BJ	bence jones
BJκ	bence jones kappa
BJλ	bence jones lambda
b-BSA	biotinylated BSA
b-HRG	biotinylated HRG
b-IgG	biotinylated IgG
b-IgM	biotinylated IgM
BSA	bovine serum albumin
BS3	*bis* (sulfosuccinimidyl) suberate
C	complement
CD	cluster designation
cDNA	complementary DNA
CICs	circulating immune complexes
Con A	concanavalin A
CR	complement receptor

DAF	decay accelerating factor
DEAE	diethyl amino ethyl
DMSO	dimethylsulphoxide
DNA	deoxyribonucleic acid
E	Maximum IAsys response at equilibrium
EDC	1-ethyl-3-(3-dimethylaminopropyl carbodiimide)
EDTA	ethylenediamine tetraacetic acid
ELISA	enzyme-linked immunosorbent assay
Ex	exon
FACS	fluorescence activated cell sorter
FBG	fibrinogen
FcR	Fc receptor
FcγRI	Fc gamma receptor I
FcγRII	Fc gamma receptor II
FcγRIII	Fc gamma receptor III
FcαRI	Fc alfa receptor I
FcεRI	Fc epsilon receptor I
FCS	fetal calf serum
FGF	fibroblast growth factor
FITC	fluorescine isothiocyanate
FITC-IgG	FITC-labeled IgG
FITC-STP	FITC-labeled streptavidin
FIU	fluorescence intensity unit
FPLC	fast performance liquid chromatography
GAG	glycosaminoglycans
Gly	glycine
Glu	glutamine
GN	glomerulonephritis
His	histidine

HMWK	higher molecular weight kininogen
HPR	histidine-proline-rich
HPRG	histidine-proline-rich glycoprotein
HRG	histidine-rich glycoprotein
HRG-1	form 1 HRG
HRG-2	form 2 HRG
HRP	horse radish peroxidase
HRP-STP	HRP conjugated streptavidin
HRR	histidine-rich region
I	intron
IC	immune complex
ICD	immune complex-associated/mediated diseases
ICF	immune complex formation
ICGN	IC-mediated glomerulonephritis
ICs	immune complexes
IFNγ	interferon gamma
Ig	immunoglobulin
IgG	immunoglobulin G
IgGκ	IgG with κ light chain
IgGλ	IgG with λ light chain
IgM	immunoglobulin M
IL	interleukin
K_d	dissociation constant
k_{obs}	observed rate constant
k_{off}	off rate
k_{on}	on rate
κ	kappa
LCDD	light chain deposition disease
Lys	lysine
λ	lambda
mAb	monoclonal antibody

MAC	membrane attack complex
MASP	MBP associated serine proteases
MBP	mannose binding protein
MCP	membrane cofactor protein
MHC	major histocompatibility complex
mRNA	messenger RNA
NHS	N-hydroxysuccinimide
NHS-LC- Biotin	sulfosuccinimidyl 6-(biotinamido) hexanoate
PBS	phosphate buffered saline
PBS-Az	PBS containing 3 mM NaN3
PBS-BSA	PBS containing 10 mg/ml BSA
PBS-BSA-Az	PBS-BSA containing 3 mM NaN3
PBS-BSA-Zn	PBS-BSA containing 20 μM Zn^{2+}
PBS-T	PBS containing 0.05 % Tween 20
PBS-BSA-T	PBS-BSA containing 0.05 % Tween 20
PBS-BSA-Zn-Az	PBS-BSA-Zn containing 3 mM NaN3
PLG	plasminogen
Pro	proline
PRR	proline-rich region
PVDF	polyvinyl difluoride
RA	rheumatoid arthritis
RES	reticuloendothelial system
RF	rheumatoid factor
RNA	ribonucleic acid
R_t	IAsys response at time t
R_o	IAsys response at time 0
SDS	sodium dodecyl sulfate
SDS-PAGE	SDS polyacrylamide gel electrophoresis
Ser	serine
SK	streptokinase
SLE	systemic lupus erythematosus

STP	streptavidin
t	time
T	polyoxyethylenesorbitan monolaurate (Tween-20)
Thr	threonine
TIN	tubulointerstitial nephritis
TSP	thrombospondin
TNFα	tumour necrosis factor alfa

PUBLICATIONS RESULTING FROM THIS THESIS

1 **Gorgani, N.N.**, Easterbrook Smith, S.B., Parish, C.R., Altin, J.G. (1997) Histidine-rich glycoprotein binds to human IgG and C1q and inhibits the formation of insoluble immune complexes. *Biochemistry* **36**, 6653-6662.

2. Hall, D.R., **Gorgani, N.N.**, Altin, J.G., Winzor, D.J. (1997) Theoretical and experimental considerations of the pseudo-first-order approximation in conventional kinetic analysis of the IAsys Biosensor Data. *Anal. Biochem.* **253**, 145-155.

3. **Gorgani, N.N.**, Parish, C.R. and Altin, J.G. (1998) A functional role for the kappa and lambda light chains of immunoglobulins. *Science* Submitted.

4. **Gorgani, N.N.**, Altin, J.G., Parish, C.R., (1998) Histidine-rich glycoprotein regulates the binding of monomeric IgG and immune complexes to monocytes *J. Immunol.* submitted.

5. **Gorgani, N.N.**, Altin, J.G., Parish, C.R., (1998) Histidine-rich glycoprotein blocks binbding of rheumatoid factor to immunoglobulin G. *Arthritis and Rheum.* submitted.

MEETINGS ABSTRACT

1. **Gorgani, N.N.**, Parish, C.R., Altin, J.G. (1997) Histidine-rich glycoprotein binds to human IgG and C1q and inhibits the formation of insoluble immune complexes. Australian society for immunology 1997 meeting Perth, 30 Nov-4 Dec.

2. Hall, D.R., **Gorgani, N.N.**, Altin, J.G., Winzor, D.J. (1997) A cautionary note on the analysis of IAsys biosensor data in terms of pseudo-first-order kinetic behavior. The 22 nd Annual Lorne Conference on Protein Structure and Fnction, 9-13 Feb.

ABSTRACT

Histidine-rich glycoprotein (HRG) is a relatively abundant plasma protein whose function is unclear, although it has been proposed that HRG may regulate processes as diverse as cell adhesion, coagulation and complement activation. This thesis will describe studies which indicate an important new functional role for HRG, namely the regulation of the size of immune complexes (ICs) and their subsequent uptake by monocytes. Preliminary studies prior to my PhD demonstrated that HRG co-purifies with C1q, based on enzyme linked immunosorbent assay (ELISA) results binds to purified C1q and immunoglobulin G (IgG) and can inhibit the formation of insoluble ICs. The aim of this thesis was to initially verify these preliminary findings and to further examine the functional significance of the interaction of HRG with ICs.

Studies outlined in Chapter 3 used the IAsys biosensor to verify that HRG interacts with C1q and IgG and established the kinetics of the interaction. Kinetic analyses of the HRG-C1q and HRG-IgG interactions revealed two distinct binding sites with dissociation constants (K_d) K_{d1} 7.8 nM and K_{d2} 37.3 nM for C1q, and one binding site with K_d 85 nM for IgG. The IgG and C1q binding regions on HRG were found to be located in the 30 kDa N-terminal region of the HRG molecule. The Fab region of IgG is likely to be involved in the HRG-IgG interaction since HRG also bound to F(ab')$_2$ fragments with an affinity similar to that seen with the complete IgG molecule. Interestingly, the binding between HRG and IgG was significantly potentiated (K_d reduced from 85.0 to 18.9 nM) by the presence of physiological concentrations of Zn^{2+} (20 μM). Conversely, the presence of Zn^{2+} weakened the binding of HRG to C1q (K_d increased from 7.80 to 29.3 nM). Modulation of these interactions by other divalent metal cations was less effective with relative potencies being $Zn^{2+}>Ni^{2+}>Cu^{2+}$. An examination of the effect of native and 30 kDa HRG on the formation of insoluble ICs between ovalbumin and polyclonal rabbit anti-ovalbumin IgG, revealed that physiological concentrations of HRG can markedly inhibit insoluble immune complex (IC) formation *in vitro*. The results show that human HRG binds to C1q and to IgG in a Zn^{2+}-modulated fashion, and that HRG can regulate the formation of insoluble ICs *in vitro*, thus indicating a new functional role for HRG *in vivo*.

Experiments described in Chapter 4 show that changing the heavy chain

isotype and the light chain type of IgG from κ to λ has a profound effect on the kinetics of the interaction of HRG with all IgG subclasses, the latter finding possibly providing a functional role for the κ and λ light chains of immunoglobulins (Igs). The binding of HRG to IgG subclasses was also modulated by the presence of Zn^{2+}. Interestingly, Zn^{2+} potentiated the binding of HRG to all IgG subclasses possessing κ light chain, whereas Zn^{2+} slightly inhibited the binding of HRG to IgG subclasses possessing the λ light chain. Thus, it was hypothesised that the ability of IgG molecules to interact with HRG and, consequently, form soluble versus insoluble ICs is dependent on the the IgG isotype and light chain type they express.

Since HRG has the ability to regulate the size of ICs and keeps ICs in a soluble form, this raised the intriguing question whether HRG, when incorporated in ICs, can regulate the binding of ICs to monocytes. Studies described in Chapter 5 of this thesis examined the ability of HRG to regulate the binding of monomeric IgG and ICs to monocytes. Initial studies demonstrated that HRG blocks the binding of monomeric IgG to the monocytic cell line THP1 but had no effect on the binding of ICs to these cells. Interestingly, under certain highly defined conditions, incorporation of HRG in IgG containing ICs potentiated the binding of ICs to THP1 cells in a Zn^{2+} dependent manner. Based on these observations it was hypothesised that the IgG binding domain of HRG can interact with Fc gamma receptor type I (FcγRI) on monocytes and block monomeric IgG binding. In contrast, if HRG interacts with monomeric IgG or IgG containing ICs the FcγRI binding site on HRG is masked and HRG enhances IC binding to monocytes, probably via its heparan sulfate binding domain.

Finally, the results described in Chapter 6 show that HRG, when incorporated in ICs, blocks the binding of rheumatoid factor (RF) to ICs and inhibits the subsequent insolubilisation of ICs by RF. These experiments provide the first report that a plasma protein, HRG, can block the binding of RF to ICs. Based on these data it is proposed that HRG may control the production of RF and the pathogenic effects arising from excessive production of RF *in vivo*. Chapter 6 also provides evidence that HRG can solubilise already formed insoluble ICs, a phenomenon which may be important in preventing the pathogenic effects of insoluble ICs deposited in tissues. In summary, these data imply that the presence of HRG in plasma is necessary for the effective clearance of ICs from the circulation *in vivo*.

TABLE OF CONTENTS

CHAPTER 1 Literature Review

CHAPTER 1

LITERATURE REVIEW

GENERAL INTRODUCTION

A key feature of the adaptive immune response to a pathogen is the secretion of pathogen-specific antibodies (Abs) by differentiated B lymphocytes. These secreted Abs then bind to their cognate antigens (Ags) to form soluble ICs which rapidly can become insolubilised. Under normal conditions, the ICs are cleared by the reticuloendothelial system (RES) with their clearance from the circulation being largely dependent on Fc receptors (FcR) and complement proteins/receptors. Prior to the commencement of my PhD studies, my preliminary research suggested that HRG may bind to human IgG and C1q, a result which allowed me to hypothesise that HRG may be another endogenous regulator of the formation and clearance of ICs. Thus, the aim of this thesis was to characterise the interaction of HRG with IgG subclasses and clarify the role of HRG in the formation and clearance of ICs, and the solubilisation of already formed insoluble ICs. Consequently, as background to the research work described in this thesis, Part I of this Chapter will describe general features and properties of HRG and Part II will address issues related to the insolubilisation and clearance of ICs and pathological conditions associated with the inappropriate deposition of ICs in tissues.

1.1 PART I HISTIDINE-RICH GLYCOPROTEIN

1.1.1 Introduction

HRG is a protein found in the plasma of many vertebrate species including human, cow, chicken, rabbit and mouse. HRG is synthesised by the liver at a relatively high rate, with the concentration of HRG in plasma being relatively high (~2 μM), suggesting that the protein could play important functional roles. Although a number of biological properties have been reported, namely binding to divalent metal ions (Morgan, 1978, 1981, 1985), heparin (Heimburger et al., 1972), heparan sulfate (Brown and Parish, 1994), thrombospondin (TSP) (Leung et al., 1984), fibrinogen (FBG) (Leung, 1986), and certain complement proteins (Chang et al., 1992a), hitherto the precise physiological function(s) of HRG remain to be determined. The aim of this review is to summarise recent findings on the structure, biological properties and clinical significance of HRG, and to highlight issues that appear crucial for a better understanding of the mechanisms by which HRG can regulate blood clotting and immune function.

1.1.2 Structure and biological properties of HRG

1.1.2.1 Structure of HRG

HRG, also known as histidine-proline-rich glycoprotein (HPRG), is a ~ 75 kDa plasma glycoprotein which was first discovered and isolated from human serum as a ~ 60 kDa α2-glycoprotein by Heimburger et al in 1972. Native human HRG has since been shown to be a glycoprotein which migrates at ~ 75-77 kDa on sodium dodecyl sulfate polyacrylamide gel electrophoresis (SDS-PAGE) gels (Rylatt et al., 1981). Evidence suggests that in humans the majority of HRG is synthesised by parenchymal cells of the liver for release into the blood stream (Koide et al., 1986; Corrigan et al., 1990; Hennis et al., 1991). This is also supported by the fact that patients with liver insufficiency show reduced levels of HRG (Saito et al., 1982). A small proportion of plasma HRG (0.14 %) has been shown to exist on the surface of platelets (Leung et al., 1983). It also has been suggested that HRG is present in the α-granules of platelets and is released following thrombin stimulation (Leung et al., 1983). However, both plasma and platelet HRG have been shown to react with Abs specific for human HRG indicating that the HRG from these two sources is immunochemically identical (Leung et al., 1983). Using anti-HRG Abs, HRG also was detected in human megakaryocytes isolated from normal marrow tissue (Leung et al., 1983). In mice, evidence also suggests that HRG may be produced by monocytes and macrophages (Sia et al., 1982). Blood clearance studies indicate that HRG in human plasma has a half life of approximately three days, thereby suggesting a rapid turn over of HRG *in vivo* (Lijnen et al., 1981a).

The primary structure of human HRG, as determined from the nucleotide sequence of its complementary DNA (cDNA), shows that HRG consists of 507 amino acids. Studies using circular dichroism, limited proteolysis, amino acid sequencing and cDNA sequencing have revealed that human HRG consists of a N-terminal region containing two cystatin-like domains (N1 and N2), a C-terminal domain and a histidine-proline-rich (HPR) domain (Figure 1.1A). The HPR domain contains a central histidine-rich region (HRR) which contains 12 tandem repeats of the 5 amino acid sequence Gly-His-His-Pro-His sandwiched between two proline-rich regions (PRR) (Koide et al., 1986). Histidines (His) are highly concentrated in the HRR (between residues 330 and 389), but proline (Pro) residues are more widely distributed with many being concentrated before and after the HRR. The high level of histidines in the HRR is most likely responsible for the highly hydrophilic nature of both the HRR, and native HRG

FIGURE 1.1 Gene and structure of HRG

The structure of native human HRG is depicted in (A). HRG is comprised of three domains namely the N1 and N2 amino-terminal domains, the HPR domain (binds heparin and heparan sulfates) which contains a central HRR and flanking PRR, and a C-terminal domain (binds plasminongen and plasmin). Residue 6 of the N1 domain is linked to residue 497 of the C-terminal domain by a disulfide bond. There are several disulfide bonds, as indicated, within domains N1 (60-71, 87-108) and N2 (199-222) and the PRR (264-294) which may render these domains resistant to cleavage by plasmin. The HRR is readily released into the surrounding medium upon cleavage by plasmin or kallikrein. As depicted, the N1, N2 and HRR domains contain three, one and two attached carbohydrates, respectively. In most humans, the six glycosylation sites are conserved (HRG-1) but a HRG polymorphism exists in which, due to Ser 186 being substituted with Pro 186, the glycosylation site in domain N2 is lost (HRG-2). Based on rabbit HRG structure, the two major plasmin cleavage sites flanking the HRR are indicated. As depicted in (B) the human HRG gene is composed of eight exon and seven intron. In terms of gene structure the first I occurs in the 5' untranslated region (B). The leader sequence of HRG (residues -18 to -1) is encoded by the second exon, Ex_2. The N1 amino-terminal domain of HRG (residues 1-112) is encoded by three exons namely Ex_2, Ex_3 and Ex_4, and the N2 amino-terminal domain (residues 113-229) is also encoded by three exons namely Ex_5, Ex_6 and Ex_7, whereas the PRR_1 (residues 255-314), HRR (residues 330-389), PRR_2 (residues 398-439) and C-terminal domains (residues 440-507) are all encoded by a single exon, Ex_8 (B).

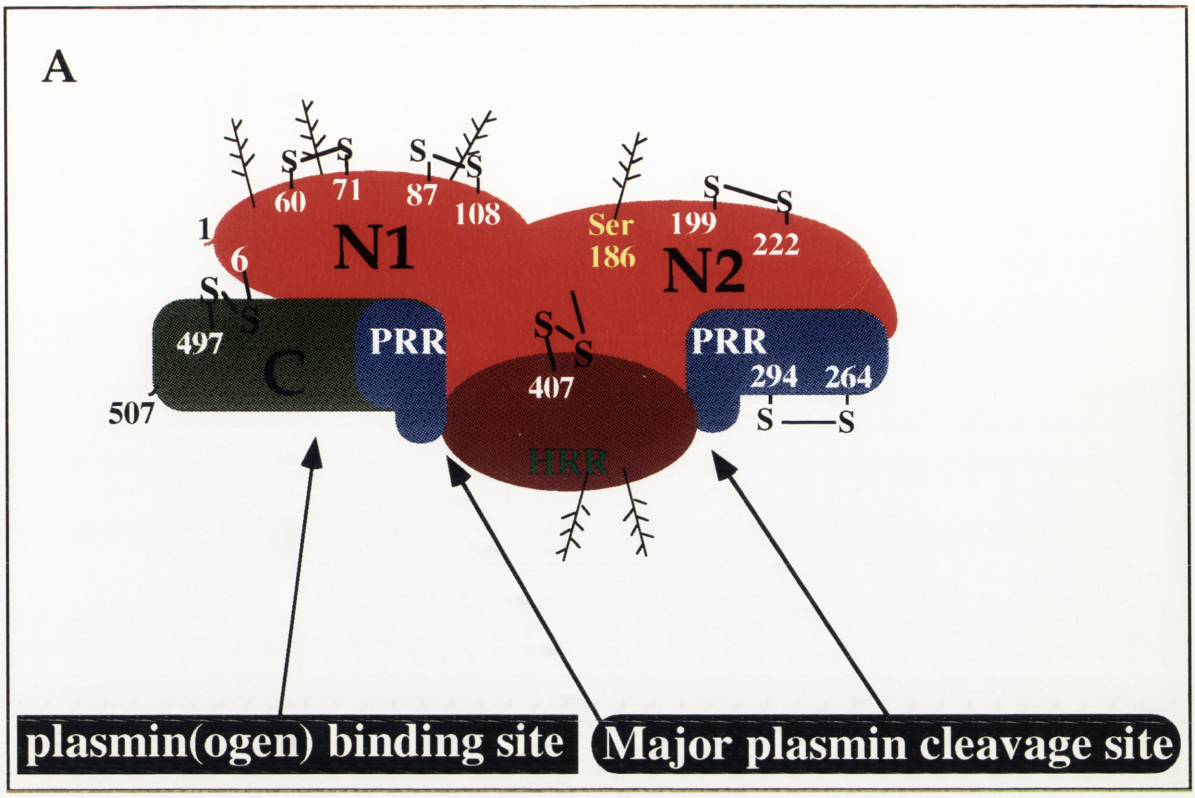

⟋⟋⟋	Attached Carbohydrate
S—S	Disulphide Bonds
PRR	Proline-Rich Region
HRR	Histidine-Rich Region
N1	N1 amino-terminal domain
N2	N2 amino-terminal domain
C	C-terminal domain

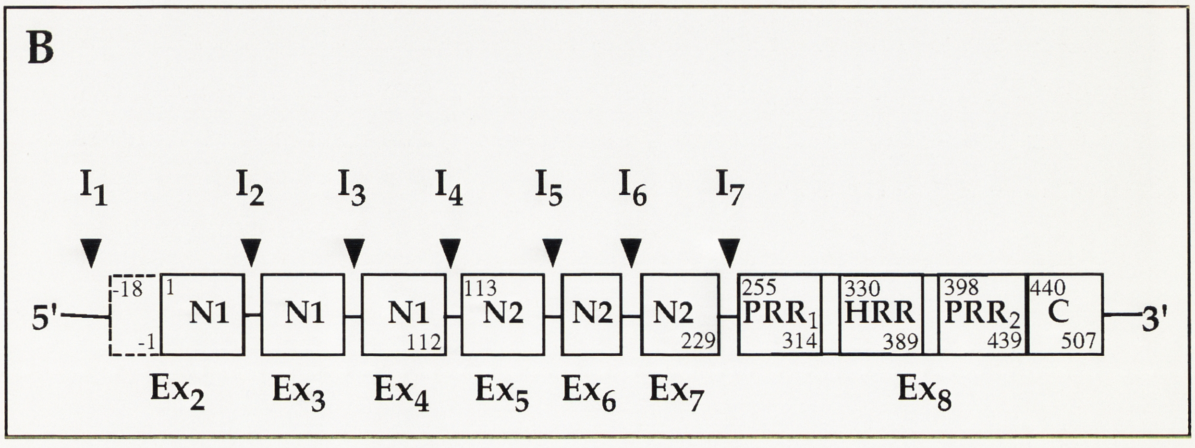

(Kyte and Doolittle, 1982). On the other hand, the presence of prolines may form bending and twisting conformations, providing a framework for the structure of the HRR of HRG (Figure 1.1A). The unusually high proportion of histidines and prolines, each of which exceeds 12% of the total amino acid content, is perhaps the most characteristic feature of the HRG sequence. The isoelectric point of HRG is approximately 6.45 suggesting that at physiological pH HRG is negatively charged.

The human HRG gene spans approximately 11 kb on chromosome 3q28-q29 and consists of eight exons (Ex) and seven introns (I) (Koide, 1988; Van Den Berg et al., 1990; Hennis et al., 1994) (Figure 1.1B). The HRG gene consists of 2067 nucleotides which includes 121 nucleotides of 5'-noncoding sequence, 54 nucleotides coding for a leader sequence of 18 amino acids, 1521 nucleotides coding for the mature protein of 507 amino acids, a stop codon of TTA , and 352 nucleotides of 3'-noncoding sequence followed by a polyA-tail of 16 nucleotides (Koide, 1988). The leader sequence of 18 amino acids in HRG contains a region rich in hydrophobic amino acids which is removed by the cleavage of an Ala-Val peptide bond by signal peptidase (Blobel et al., 1979) (Figure 1.1A and B). The I_1 occurs in the 5' untranslated region of the gene and the I_2 and I_3 are present within the N1 amino-terminal domain separating this domain into three exons (Ex_2, Ex_3, and Ex_4). I_4 occurs at the boundary between the N1 and N2 amino-terminal domains. The N2 amino-terminal domain is also encoded for by three exons (Ex_5, Ex_6, and Ex_7) separated by two I, I_5 and I_6. Intron 7 (I_7) separates the N2 amino-terminal domain from the HPR domain (Figure 1.1B). The HPR and C-terminal domains are encoded by exon 8 (Ex_8) which does not contain any I (Hennis et al., 1994) (Figure 1.1B).

Interestingly, the HRR of HRG has considerable homology (~50 %) with the HRR of higher molecular weight kininogen (HMWK), suggesting that the HRR of HRG and HMWK are evolutionally and functionally related (Koide et al., 1986; Koide, 1988). Furthermore, apart from the high level of homology in the HRR, the amino acid sequence of the N-terminal domain of HRG (between residues 30-75) is homologous (~ 43 %) to the amino acid sequence of the N-terminal domain of HMWK (between residues 54-98) (Koide et al., 1986; Koide, 1988). This homology is further strengthened by the demonstration that the disulfide bridge arrangement located at the N-terminal region of HRG is similar to that observed in cystatins, a family of cysteine proteinase inhibitors. This has led to the suggestion that HRG is a member of the cystatin superfamily which includes HMWK, α2-HS glycoprotein, and human cystatin C (Sorensen et al.,

1993). Hitherto, however, no proteinase inhibitory activity has been ascribed to HRG.

The secondary structure of HRG has not been completely solved, but predictions from the primary sequence show that human HRG may consist of 8% α-helices, 14% β-sheets, 46% β-turns and 32% random coils. The primary sequence of HRR suggests that this region only contains β-turn and random coil structures (Koide et al., 1986). Human HRG contains sixteen half-cystine residues, and twelve of these are involved in the formation of disulphide bridges (see Figure 1.1A) (Sorensen et al., 1993). As well as providing structural links for tertiary structure the six disulphide bridges can keep regions of the HRG molecule together after its cleavage by plasmin (see below). HRG has a number of potential N-linked glycosylation sites: namely asparagine-45 (Asn-45), Asn-69, Asn-107, Asn-326 and Asn-327; these account for some 14 % of the molecular mass of HRG being due to carbohydrate (Heimburger et al., 1972) (Figure 1.1A). These characteristics, coupled with its modular architecture, suggest that HRG possesses several independent binding sites, perhaps allowing it to bind several ligands simultaneously (Borza et al., 1996).

1.1.2.2 Proteolytic cleavage of HRG

Evidence suggesting that HRG can be cleaved by serum proteases like plasmin was first obtained by studies showing a lower recovery of native HRG from serum, than from plasma (Rylatt et al. 1981). More detailed studies using purified components *in vitro* indicate that native HRG (~ 75 kDa) is not cleaved by thrombin, but can be cleaved into polypeptides ranging from 9 to 67 kDa by treatment with serine (Ser) proteases like plasmin or kallikrein (Smith et al. 1985). Recent evidence suggests that arginine-295 (Arg-295) and lysine-413 (Lys-413) in the HPR region of HRG are the sites most susceptible to cleavage by plasmin, resulting in the release of the HPR region from the HRG molecule (Figure 1.1A) (Borza et al., 1996). The remaining fragment of HRG (termed the N/C fragment) comprises the 30 kDa N-terminal region connected to the C-terminal fragment by a buried disulphide bond with the separation of these two regions requiring further denaturation and reduction (Borza et al., 1996). While the C-terminal fragment of HRG can be readily cleaved into short peptides, the cystatin-like disulphide bonds within the 30 kDa N-terminal portion (see above) apparently stabilizes this portion making it resistant to further proteolysis by plasmin (Figure 1.1A) (Sorensen et al., 1993).

Cleavage of HRG by plasmin was demonstrated *in vivo* following streptokinase (SK) or urokinase therapy in patients with venous thrombosis (Smith et al., 1985). In these studies no intact HRG could be found 30 minutes after infusion of SK but the HRG fragments remained in the circulation (Smith et al., 1985). Interestingly, the cleavage of HRG by serum proteases also is reported to be inhibited by the pretreatment of the HRG with heparin, *in vitro* (Smith et al. 1985). Collectively, these findings suggest that in some patho(physio)logical conditions the regulated cleavage of HRG in the circulation may constitute a mechanism for regulating HRG's function *in vivo*.

1.1.2.3 Polymorphisms and levels of HRG in plasma

The existence of two molecular forms of HRG with a molecular weight difference of 2 kDa, namely 77 kDa HRG (form 1, HRG-1) and 75 kDa HRG (form 2, HRG-2), has been reported (Hennis et al., 1995). DNA sequencing of the HRG gene from homozygous HRG-1 and HRG-2 individuals showed five different polymorphisms in Ex 4, 5 and 7 with a Pro/Ser polymorphism at position 186 in Ex 5 being related to the two HRG isoforms: HRG-1 contains Ser, whereas HRG-2 contains Pro (see Figures 1.1A and B). The presence of Ser-186 in HRG-1 introduces an additional potential N-glycosylation site (Asn-184) with the consensus sequence Asn-X-Ser/Thr. Thus, the observed difference in the molecular size of HRG can be accounted for by differences in glycosylation, with HRG-1 (77 kDa) being more highly glycosylated than HRG-2 (75 kDa) (Hennis et al., 1995).

Evidence suggests that the level of HRG in human plasma can vary from 47 to 147 percent of the mean HRG level (Morgan et al., 1978; Saito et al., 1982). This variation can be accounted for by age (3%), environmental factors (27 %), and genetic influences (70%). The level of HRG in human plasma is age-dependent with HRG levels increasing by approximately 0.41 % per year (Drasin and Sahud, 1996). Approximately 85% of the genetic variability can be explained by the glycosylation differences observed in HRG-1 and HRG-2 (see above). Thus, HRG-1 homozygotes have HRG levels 50% higher, whereas HRG-2 homozygotes have HRG levels 50% lower, than the mean level of HRG. Heterozygotes have an intermediate level of the two forms of HRG, and are defined as the 100% level of HRG. It is presently unclear whether the differently glycosylated forms of HRG differ in their physiological function.

The remaining 15% of genetic variability has been attributed to other genetic differences (Hennis et al., 1995). It has been suggested that blood group-type may contribute to this previously unexplained genetic influence, as in healthy human subjects the level of HRG is significantly higher (125 %) in subjects possessing the AB blood group, than in subjects possessing either the A (103 %) or the O (105 %) blood-groups (Drasin and Sahud, 1996).

Furthermore, a family with congenital low levels of HRG (~20 % of normal) has been described, genetic analysis revealing that the low levels of HRG in these individuals is caused by a single nucleotide substitution (nucleotide guanine-429 (G429) to adenine (A) in Ex 3) of the HRG gene (see Figure 1.1B) which changes glycine 85 to glutamine in the first cystastin-like domain (termed Tokushima-HRG) of the HRG molecule. This substitution was reported to cause a change in the conformation of HRG leading to the degradation of the mutant HRG within the cell, and allowing only 20 % of the mutant HRG to be secreted into the surrounding medium (Shigekiyo et al., 1998).

1.1.2.4 Plasma levels of HRG in various disease states

Although, as outlined above, plasma HRG levels show considerable variation in healthy subjects (47 - 147 percent of the mean HRG level) (Morgan et al., 1978; Saito et al., 1982), significant differences in serum HRG levels have been observed in some conditions. For example, Morgan et al. (1978) first reported that serum HRG levels are decreased (~ 2-fold) in the second trimester of pregnancy, which is positively correlated with a known decrease in serum levels of the complement inhibitory protein C1-esterase inhibitor (Halbmayer et al., 1991, 1992). Moreover, the use of oestrogen, but not progestin, as an oral contraceptive results in a decrease in serum HRG levels (Haukkamaa et al., 1983). It has also been reported that the serum level of HRG is always low at birth (20-30 % of adult HRG) (Morgan et al., 1978), and increases steadily with age reaching the adult level at approximately 1 year of age (Corrigan et al., 1990). These findings suggest that plasma HRG levels are regulated by hormone- and age-dependent mechanisms in humans.

Interestingly, it has been reported that serum HRG levels are significantly decreased (~ 2-fold) in patients with sepsis and liver insufficiency (Lijnen et al., 1981a) and that the level of HRG in patients with advanced liver cirrhosis (7.0 ± 2.5 mg/dl) was decreased by 58% when compared to the HRG levels in healthy subjects (11.8 ± 2.7 mg/dl). The decreased serum level of HRG in these patients

was proportional to a previously described decrease in the level of albumin (~ 56%), antithrombin III (ATIII) (~ 66%) and α2-antiplasmin (~ 60%), but not to the change in levels of FBG and plasminogen (PLG), suggesting that the lower serum HRG level is due to a decreased synthesis of HRG by the liver (Saito et al., 1982) following liver damage. Moreover, studies on patients suffering from mild, moderate and severe liver cirrhosis showed no relationship between the level of plasma HRG and enhanced fibrinolysis in these patients. However, the level of HRG was found to decrease in both moderate and severe liver cirrhosis, but to increase in mild liver cirrhosis (Leebeek et al., 1989). These findings are consistent with the notion that the majority of HRG is synthesized by the liver (Koide et al., 1986).

Plasma levels of HRG are also lower in some immunological disorders and following administration of immunosuppressive steroids. For instance, it was reported that compared to healthy subjects (12.5 ± 3.0 mg/dl), the mean serum levels of HRG were significantly decreased (~ 40% decrease) in patients with asthma and chronic obstructive pulmonary disease receiving high-dose immunosuppressive steroid regimens (7.6 ± 2.9 mg/dl). The HRG level was found to decrease by ~ 55% (5.7 ± 1.8 mg/dl) in patients with acquired immune deficiency syndrome (AIDS) and even by ~65% (4.4 ± 1.1 mg/dl) in patients with end-stage renal disease after transplantation and steroid therapy. Collectively, these findings suggest that serum HRG levels are selectively decreased in patients with AIDS and those who are treated with immunosuppressive steroids (Morgan, 1986). A decrease in serum HRG levels in patients with acute inflammation and after surgical operations provides additional evidence that HRG plays some role in the immune system (Saigo et al., 1990a). In fact, these findings indicate that HRG is a negative acute phase reactant and may play an important role in acute inflammation (Saigo et al., 1990b). Other studies have shown that plasma HRG levels are dramatically decreased in patients with systemic lupus erythematosus (SLE) (Castel et al., 1983) suggesting an involvement of HRG in IC-associated/mediated diseases (ICD).

Interestingly, a family with a history of thrombosis possessed congenital high plasma levels of HRG (~ 2-3 fold higher than normal) suggesting that a high level of HRG may be a factor that leads to thrombotic disorders (Castaman et al., 1993). However, another family was identified with both congenital high levels of HRG and tissue PLG activator inhibitor-1 which did not suffer from

thrombotic disorders suggesting no correlation between venous thrombotic disease and high levels of HRG (Angles-Cano et al., 1993).

A family with congenital low levels of HRG (~20 % of normal) did not suffer from a higher incidence of thrombotic disorders, suggesting that HRG may not be a key regulator of fibrinolysis (Souto et al., 1996). Studies in healthy individuals with congenital low levels of HRG (20 - 30 % of normal range) also indicated that these levels were not associated with altered hemostatic function, immunologic function or levels of trace elements. These data suggest that HRG plasma levels are far in excess of those required to mediate HRG's normal physiological functions or other molecules exist which can substitute for HRG in its absence (Shigekiyo et al., 1995).

1.1.3 Ligands for HRG

A number of ligands have been described for HRG and Table 1.1 summarizes some of the physicochemical properties of the various HRG-ligand interactions. The sections below will discuss in more detail five important classes of ligands for HRG.

1.1.3.1 Heme and divalent metal cations

Early studies by Morgan (1978) revealed that HRG binds with moderate affinity to heme, divalent metal ions and organic ligands like bilirubin (Table 1.1). The binding of HRG to heme, although sensitive to inhibition by metal ions, was thought not to be of physiological relevance. The affinity of rabbit HRG (which is present at a plasma level of ~ 1 mg/ml) for divalent metal ions was found to follow the order Cu^{2+} ~ Hg^{2+} > Zn^{2+} ~ heme ~ Ni^{2+} > Cd^{2+} > Co^{2+} with no binding of Mg^{2+}, Mn^{2+} or Pb^{2+} being detected. Only the interaction of HRG with Zn^{2+} and Cd^{2+} was found to display cooperative binding. Since HRG competes with albumin and transferrin in binding divalent metal cations like Zn^{2+}, it was proposed that HRG can bind metal ions even in the presence of serum proteins, and therefore, that HRG plays an important role in metal ion transport and hemostasis (Morgan, 1981). Other studies, however, suggest that in normal human plasma, and in the plasma of patients with familial hyperzincemia, the majority of Zn^{2+} is bound to albumin, and not to other Zn^{2+}-binding proteins such as HRG and transferrin (Failla et al., 1982). Subsequent studies also revealed that albumin and α2-macroglobulin are the major transporters of Zn^{2+} in plasma and that HRG is not quantitatively

Table 1.1 Dissociation constants and stoichiometry of HRG with its ligands

Ligand	~ K_d (nM)	Stoichiometry HRG : Ligand	Binding domain
Heme	1,000-1,500	1 : 1	HRR
Zn^{2+}	1,000	1 : 10 - 20	HRR
Plasminogen/Plasmin	750-1,100 13.7 - 60.7*	1 : 2	C-Terminal
Fibrinogen/Fibrin	6.7	?	?
Heparin	7-10	1 : 1.5	HRR
Thrombospondin	7	3.5 : 1	?

* K_d when HRG immobilized.

important in the transport of Zn^{2+} (Cousins, 1989). These findings suggest that HRG is unlikely to play a major role in the transport of divalent metal ions *in vivo*.

Following digestion of native rabbit HRG (94 kDa) by plasmin, studies with the HRR (30 kDa fragment which is rich in His (29%), Pro (37%), Gly (16%) and carbohydrate (9%)) indicated that the HRR of HRG (see Figure 1.1A) retains much of the ability of intact HRG to bind metal ions and is the functional domain of HRG which binds Zn^{2+} and other metal ions in a pH-dependent manner (Morgan 1985). This also was consistent with studies showing that chemical modification of the His residues of HRG diminishes the binding of Zn^{2+} by HRG (Morgan, 1985). Interestingly, recent studies also have shown that protonation of the HPR region (below pH 6) can lead to conformational changes which can be transmitted via the disulphide bonds to other parts of the HRG molecule (see Figure 1.1A). This indicates that metal ion binding can change the conformation of HRG and, thereby, presumably regulate its function (Borza and Morgan, 1998).

The ability of HRG to interact with metal ions may be important in regulating HRG function (Guthans and Morgan, 1982). Despite some conflicting reports, substantial evidence suggests that metal ions are important modulators of HRG binding to other molecules, including heparin (see below). A number of *in vitro* studies have shown that this binding by human HRG is abolished in the presence of ethylenediamine tetra acetic acid (EDTA) (Lijnen et al., 1983b; Lane et al., 1986). On the other hand, it was reported that rabbit HRG can still bind heparin of different molecular weights in the presence of EDTA, suggesting that rabbit HRG can bind heparin in the absence of metal ions. This is consistent with the finding that the ability of HRG from different species to bind heparin is different (Burch et al., 1987). Other *in vitro* studies by Kazama and Koide (1992) reported that 20 μM Zn^{2+}, the amount that they suggested to be a physiological concentration, enhanced the ability of HRG to bind heparin and neutralize heparin's anticoagulant activity. Similarly, there is conflicting evidence as to whether metal ions affect the interaction of HRG with components of the immune system. For example, the binding of HRG to the complement component C9 was found to be enhanced in the presence of divalent cations such as Ca^{2+} and Mg^{2+} (Chang et al., 1992a), whereas the binding of [^{125}I]-labelled HRG to human peripheral blood T lymphocytes was unaffected by either 2 mM EDTA or 20 μM Zn^{2+} (Saigo et al., 1989). A possible explanation for these conflicting observations is the difference in the concentration of free Zn^{2+}

available to bind HRG in the assay systems used as in some studies 2% BSA (which binds Zn^{2+}) also was included in the reaction vessel (Saigo et al., 1989).

1.1.3.2 Heparan sulfates and heparin

Heparan sulfate is a sulfated glycosaminoglycan (GAG) which exists on the surface of cells as a constituent of proteoglycans or as a component of the extracellular matrix (reviewed by Jackson et al., 1991). Heparin, a highly sulfated form of heparan sulfate, is restricted to mast cell granules. GAGs include chondroitin sulfate, keratan sulfate, dermatan sulfate and hyaluronic acid. These GAGs consist of polymers of repeating disaccharide units, in which one of the sugars is either N-acetylgalactosamine or N-acetylglucosamine and the other a uronic acid. Different patterns of sulfation in the carbohydrate moieties gives further diversity to the structure of the GAGs. Heparan sulfate is one of the predominant GAGs covalently attached to cell surface proteoglycans. In patho(physio)logical conditions the release of heparan sulfate, by the action of heparanases that are produced by a number of cells such as leukocytes and platelets (Freeman and Parish, 1998), may play an important role in cell-cell and cell-matrix interactions and in cell migration (for review see Jackson et al., 1991).

The ability of HRG to bind heparin was first reported by Heimburger et al. in 1972. Subsequently, Koide et al. (1982, 1985) showed that HRG can be purified using a chromatographic procedure based on the ability of HRG to bind to heparin, and that the K_d of this interaction is ~ 7 nM, suggesting that HRG may interfere with the blood coagulation cascade during heparin administration *in vivo* (Lijnen et al., 1983b). As HRG is able to bind to many different cell types, and the binding is largely inhibitable by pretreatment of HRG with heparin, it would appear that heparan sulfates, and other GAGs present on the surface of cells may be natural receptors for HRG (Brown and Parish, 1994).

Despite extensive investigations, early studies (Lijnen et al., 1983b, 1984; Burch et al., 1987) failed to identify the region of HRG involved in heparin binding. Based on the observed similarities between the amino acid sequence of the N-terminal region of HRG and that of the N-terminal region of antithrombin III (ATIII) (~ 40 % homology), Koide et al. (1982) proposed that the N-terminal region of HRG is the domain involved in binding to heparin. This was in contrast to other studies showing that the pretreatment of HRG with deoxypyrocarboxylate, which modifies His residues, diminishes the heparin

binding ability of HRG, thereby suggesting an involvement of the His residues of HRG in heparin binding (Burch et al., 1987). Recent studies have, however, supported the view that the HRR of HRG is the domain involved in heparin binding (Figure 1.1A, Table 1.1) (Borza et al., 1996; Borza and Morgan 1998). Moreover, a study of the binding of HRG to immobilized GAGs revealed that HRG binds to GAGs only when the HRR of HRG is protonated and/or bound to metals ions like Zn^{2+} (Borza and Morgan, 1998). It was proposed that under conditions of local acidosis (eg. ischemia, hypoxia or inflammation), when the local pH is decreased by 1 to 1.5 unit below the physiological pH, or under conditions where the local metal ion concentration is increased (eg. upon the release of Zn^{2+} by activated platelets), HRG can bind to cell surface and extracellular matrix GAGs and co-immobilize other ligands such as PLG (Borza and Morgan, 1998).

1.1.3.3 Plasminogen/plasmin and fibrinogen/fibrin

Studies by Lijnen et al. (1980) revealed that HRG binds to both PLG and plasmin with moderate affinity having K_ds of 1.1 and 0.9 μM, respectively (Table 1.1). Subsequently it was proposed that HRG interacts with the high affinity Lys binding site of PLG (a triple loop structural (kringles) domain of plasmin(ogen) involved in Lys recognition which binds α_2-antiplasmin and fibrin) and can inhibit the interaction of plasmin(ogen) with α_2-antiplasmin and fibrin (Lijnen et al., 1980). Further studies of the interaction of HRG with PLG revealed that PLG interacts with the C- and N-terminal regions of HRG, and that both interactions are affected by ionic strength, but not by pH or Zn^{2+}. In particular, Lys residues in the C-terminal region of HRG were found to be essential for PLG binding (Figure 1.1A) (Sorensen et al., 1993; Borza and Morgan, 1997). However, PLG and heparin bound HRG independently, indicating that the PLG and heparin binding sites on HRG are distinct (Saez et al., 1995). Consistent with previous studies, HRG and PLG were found to interact with a K_d of ~ 0.75 μM and a stoichiometry of 1 : 1 (Table 1.1). Further studies revealed that immobilization of HRG onto a solid surface increases its affinity for native PLG and plasmin some 50-100 fold, giving K_ds of 60.7 nM and 13.7 nM, respectively (Table 1.1) (Silverstein et al., 1985b; Borza and Morgan, 1997). These findings suggest that HRG is likely to bind stronger to PLG when it is immobilized on cells through the interaction of its heparin binding (HRR) region with GAGs on cell surfaces.

In a related study Leung (1986) reported that HRG also binds strongly to FBG (K_d = 6.7 nM, Table 1.1), a finding which suggests that HRG can regulate the formation of fibrin clots (this point will be discussed later in section 1.1.5.1.1). However, the region(s) of HRG which interacts with FBG has not been defined.

1.1.3.4 Thrombospondin

Evidence indicates that a substantial amount of HRG (~ 0.14 % of the total HRG in plasma) exists on the surface of platelets (~ 370 ng/10^9 platelets) and can be released by stimulation of the platelets with thrombin (Leung et al., 1983). Moreover, HRG was found to bind with high affinity (K_d ~ 7 nM) to TSP (Table 1.1), a 450 kDa protein present in the α-granules of platelets, which is also released following stimulation of platelets with thrombin (Jaffe et al., 1982; Leung and Nachman, 1982). Interestingly, the binding of HRG to TSP did not interfere with the ability of TSP to bind FBG, and the HRG-TSP complex was still able to bind heparin and PLG (Leung et al., 1984). Each TSP molecule can form a complex with three molecules of HRG and three molecules of PLG, thereby creating a complex with the ability to bind cell surface heparan sulfates and to potentiate the generation of plasmin by tissue PLG activator. Furthermore, the binding to HRG of a first ligand (TSP or PLG) augments the binding of the second ligand (PLG or TSP), respectively (Silverstein et al., 1985a).

1.1.3.5 Complement components

Preliminary studies suggest that HRG immobilized on a nylon membrane, when incubated with normal human serum, interacts with factor D and components of the membrane attack complex (MAC) of complement, namely C8, C9 and S-protein (Chang et al., 1992a). The molecular basis of these interactions with HRG is unclear and the functional significance is unknown. Recently, it was also demonstrated that HRG interacts with the purified first component of complement, C1q, with high affinity (K_d ~ 10 nM) and that the 30 kDa N-terminal fragment of HRG was found to contain the C1q binding site (Gorgani et al., 1997; Chapter 3 of this thesis). However, the functional relevance of the interaction of HRG with C1q awaits further study.

1.1.4 Cell Surface Receptors for HRG

The ability of human HRG to interact with cell surface receptors was first demonstrated by Rylatt et al. (1981) who showed that HRG from the sera of many vertebrates can inhibit the autorosetting of murine lymphocytes and erythrocytes. Subsequent studies showed that HRG can bind to a number of different cell types including murine macrophages, erythrocytes, 3T3 fibroblasts, human peripheral blood T cells, the human monocytoid cell line U937, and Epstein Bar virus-transformed B cell lines. Despite the ability of HRG to bind to diverse cell types, the cell surface receptor(s) responsible for HRG binding have not been identified and it is unclear whether HRG interacts with these cells via similar receptors.

Interestingly, studies by Parish et al. (1984) demonstrated that native human HRG interacts with anionic carbohydrates, possibly sulfated polysaccharides, on murine erythrocytes. Furthermore, additional studies revealed that a 60 kDa fragment of HRG lacking the HRR is unable to bind to murine erythrocytes. These findings suggest that heparan sulfates on the erythrocyte surface are binding sites for HRG, although other anionic carbohydrates could be involved, and that the HRR of human HRG is the major functional domain which interacts with these sites on erythrocytes (Lijnen et al., 1983a) .

Following the initial observation that native human HRG binds to murine macrophages (Sia et al., 1982), studies by Chang et al. (1992b) demonstrated that HRG binds to inflammatory peritoneal macrophages, and that the 40 kDa N-terminal cystatin-like domain of HRG plays an important role in this binding (Chang et al., 1994). Moreover, since the pretreatment of HRG with heparin did not change the ability of HRG to bind to macrophages, the studies imply that HRG binds to a receptor on macrophages which is distinct from cell surface heparan sulfates. Additional studies using Abs provided evidence that HRG modulates Fc gamma receptor type 2 (FcγRII) expression on the surface of mouse inflammatory peritoneal macrophages (Chang et al., 1994), thus suggesting that HRG may interact with FcγRII on macrophages.

Studies on the interaction of HRG with human peripheral blood T lymphocytes indicated that HRG interacts with a 56 kDa cell surface protein which is immunochemically distinct from CD2 despite having a similar molecular weight (Saigo et al. 1989). Furthermore, kinetic analysis of the interaction of HRG with these cells indicated two distinct binding sites for HRG, namely a

high affinity binding site with a K_d of ~ 19 nM and a low affinity binding site with a K_d of ~ 500 nM (Saigo et al., 1989). Heparin at a 50-fold molar excess or bacterial heparinase pretreatment of the T cells did not inhibit HRG binding to the cells, suggesting that HRG does not interact with cell surface heparan sulfates. More recent studies employing flow cytometry, however, showed that the binding of human HRG to murine and human T cell lines is potentiated in the presence of physiological concentrations of Zn^{2+} and is largely inhibited by heparin (Olsen et al., 1996). The reason for this discrepancy is unclear although heparan sulfate may be a more important ligand on activated and/or transformed T cells than on resting, peripheral blood T cells. Similarly, it was reported that the binding of HRG to the monocytic cell line U937 and to Epstein Barr virus-transformed B cells is abolished by pretreatment with heparin (Saigo et al., 1989). HRG also was found to bind to heparan sulfate moieties on 3T3 fibroblasts and inhibit the binding of acidic fibroblast growth factor (FGF) and basic FGF to the heparan sulfates on these cells (Brown and Parish, 1994). The fact that HRG binding to these cell lines was inhibitable with heparin and other sulfated polysaccharides suggests that, similar to the erythrocyte cell surface, GAGs are a major receptor for HRG on many nucleated cells.

In summary, these findings suggest that HRG binds to at least three classes of cell surface receptors: GAGs, such as heparan sulfate, that exist on the surface of the majority of cells (eg. erythrocytes, T cells, monocytes, macrophages, fibroblasts), FcRs on macrophages, and a 56 kDa protein on the surface of human peripheral blood T lymphocytes.

1.1.5 Involvement of HRG in non-immune physiological processes

The ability of HRG to bind to several different plasma proteins and to interact with several different cell types (as outlined above) suggests it can potentially regulate a diverse range of physiological processes including blood clotting and aspects of immune function. The interaction of HRG with several physiological processes including the blood clotting system (fibrinolysis and coagulation) and regulation of apatite formation and muscle function are discussed in more detail below (section 1.1.5). The interaction of HRG with immune cells and other components of the immune system will be discussed in the next section (section 1.1.6).

1.1.5.1 Regulation of blood clotting by HRG

The plasma concentration of HRG deviates from the average normal level in various hematological disorders suggesting that HRG may play a role in the physiology of blood clotting. For example, individuals with genetically determined elevated levels of HRG have been shown to develop prothrombotic (increased clotting) abnormalities (Angles-Cano et al., 1993), whereas some patients with liver cirrhosis, who possess lower levels of plasma HRG, exhibit excessive bleeding and elevated fibrinolysis (Saito et al., 1982). The role of HRG in two aspects of the blood clotting system, namely fibrinolysis and coagulation, is discussed below.

1.1.5.1.1 Fibrinolysis

The notion that HRG can act as an antifibrinolytic agent followed from the observation that it can interact with moderate affinity with PLG (K_d = 1.1 μM) and plasmin (K_d = 0.9 μM). HRG is reported to be able to bind to the high affinity Lys binding site of plasmin(ogen) (similar to the interaction of 6-aminohexanoic acid with PLG) in normal human plasma and to inhibit the interaction of plasmin(ogen) with α_2-antiplasmin and fibrin. Thus it has been proposed that HRG, when bound to PLG, inhibits the interaction of PLG with fibrin clots and thus indirectly inhibits plasmin-mediated fibrinolysis (Lijnen et al., 1980). This antifibrinolytic effect of HRG would be expected to potentiate clotting in the microenvironment of fibrinogenesis. Consistent with this notion, the level of HRG and PLG is decreased in the plasma of patients with lymphocytic leukaemia undergoing L-asparaginase therapy, the side effects of which include thrombotic and haemorrhagic diathesis (Vellenga et al., 1984). However, the level of HRG is normal in patients with pulmonary thromboembolism, and this level does not change during SK therapy (despite the infused SK being biologically active). These findings fail to indicate a definitive role for HRG in fibrinolysis *in vivo* (Goodnough et al., 1985).

In contrast to the reported antifibrinolytic effect of HRG, other studies (Silverstein et al., 1985b; Borza and Morgan, 1997) showed that HRG, when immobilized on a surface (eg. on hydrazide or nickel chelate), can act as a profibrinolytic agent and enhance fibrinolysis. Although HRG in solution binds PLG with moderate affinity (~ 1 μM), immobilised HRG binds PLG with 50-100 higher affinity. The high affinity interaction of immobilised HRG with PLG has been shown to accelerate PLG activation by tissue PLG activator ~ 30 fold, thus

possibly leading to the generation of higher amounts of plasmin in the region of fibrin clots (Borza and Morgan, 1997). These findings suggest that HRG is likely to potentiate PLG activation when immobilized onto cells through the interaction of its heparin binding (HRR) region with GAGs on cell surfaces.

Evidence suggests that HRG binds strongly to FBG (K_d = 6.7 nM) (Leung, 1986). Although the presence of HRG does not affect the conversion of FBG to fibrin and the extent of fibrin polymerization, HRG is known to become incorporated into fibrin clots and to promote the formation of thinner and more distributed fibrils. These observations suggest that HRG can influence the stability and general structure of fibrin clots, especially in focal areas of active hemostasis and thrombosis (but not in plasma) where extensive release of platelet HRG may elevate the local HRG concentration (Leung, 1986). This interpretation also is consistent with the observation that bovine HRG is a substrate for bovine plasma factor XIIIa (fibrin stabilizing factor) (Halkier et al., 1994), and that activated factor XIIIa can catalyze the Ca^{2+}-dependent attachment of 1,4-[^{14}C]putrescine onto a glutamine residue on bovine HRG (Halkier et al., 1994). This suggests that in the presence of factor XIIIa HRG can become covalently linked to fibrin, thereby modifying the stability and structure of the fibrin clot formed (Halkier et al., 1994).

1.1.5.1.2 Coagulation

HRG is reported to bind heparin with high affinity (K_d = 7 nM) and to inhibit the neutralization of factor X and thrombin by the ATIII-heparin complex (Lijnen et al., 1983b). Evidence suggests that HRG interacts with heparin administered *in vivo*, and that it plays a role in regulating the anticoagulant effects of heparin administration in human by inhibiting the interaction of heparin with ATIII (Lijnen and Collen, 1983; Lijnen et al., 1984). Consistent with this view, the turn-over of HRG was found to be 2.9 ± 0.36 days in healthy individuals (Lijnen et al., 1981b), but this was lowered to 2.00 ± 0.14 days in patients with deep vein thrombosis during heparin administration (Lijnen and Collen, 1983). Furthermore, the effect of HRG on the anticoagulant activity of heparin was found to be due to a pH-dependent inhibition of the binding of heparin to thrombin and ATIII (Lane et al., 1986).

A study of the modulatory effects of HRG on the anticoagulant activity of heparin and dermatan sulfate in plasma and purified systems indicated that HRG binds to these sulfated polysaccharides and inhibits their ability to

prolong the thrombin time (Lijnen et al., 1984; Sakuragawa et al., 1985). HRG also inhibits the binding of heparin to monocytes, resulting in a failure of heparin to inhibit the procoagulant activity of monocytes at sites of inflammation and thrombosis (Leung et al., 1989). A number of studies report that HRG can play a procoagulant role by binding to heparin in fluid phase and blocking heparin's anticoagulant properties. It is also reported that HRG does not bind strongly to the heparin-like structures recognized by ATIII on vascular endothelial cells (even in the presence of divalent metal cations), suggesting that HRG is unlikely to play a major role in the endothelial cell-mediated inactivation of thrombin by ATIII (Shimada et al., 1989).

It has been shown that HRG forms a complex with purified TSP in fluid phase (Leung et al., 1984) and also interacts with TSP on the surface of activated platelets (Silverstein et al., 1985a), however, no functional relevance for the HRG-TSP interaction has been defined. It has been hypothesised that since one molecule of TSP can form a complex with three molecules of HRG and three molecules of PLG, with the binding of the first ligand augmenting the binding of the second ligand, the assembly of the trimolecular complex on the surface of various cells (eg. platelets) could regulate coagulation at sites of active fibrin deposition (Silverstein et al., 1985a). Consistent with this hypothesis, the incorporation of HRG in TSP-PLG complexes was found to augment both fibrin deposition and clot formation (Silverstein et al., 1985a). Other studies have demonstrated that HRG binds to human platelets in a Ca^{2+} and Mg^{2+} dependent manner, and remains bound to platelets once they have been activated by cross-linked IgG (Lerch et al., 1988). These latter findings also provide a mechanism by which HRG can be stored on the surface of platelets.

1.1.5.2 Regulation of apatite formation by HRG

Interestingly, recent studies indicate that HRG may be able to prevent metal salt-mediated kidney or blood vessel wall injury, by keeping metal salts in a soluble form (eg. inhibition of Ca^{2+} salt precipitation) in these organs. A baculovirus-derived recombinant form of human HRG produced by SF9 insect cells, was found to inhibit the precipitation of metal salts (apatite formation) in an *in vitro* system. This finding suggests that HRG could potentially play a role in the inhibition of phase separation and Ca^{2+} deposition at sites of tissue injury in blood vessels and kidneys (Schinke et al., 1997).

1.1.5.3 HRG and muscle function

Recently, a 75 kDa HRG-like protein from rabbit skeletal-muscle was found to be a component of adenosine monophosphate (AMP) deaminase, an enzyme that interacts with myosin and titin. This finding has raised the possibility that HRG also may be associated with muscle function. Rabbit AMP deaminase contains two subunits: one with deaminase catalytic activity, and the other possessing a high level of homology with rabbit HRG. This suggests the existence of a novel muscle-specific form of HRG (Ranieri-Raggi et al., 1997), a notion confirmed by the demonstration of the presence of a muscle-specific HRG in human skeletal muscle myofibrils by the use of rabbit anti-HRG Abs (Ranieri-Raggi et al., 1997). It has been suggested that the role of muscle-specific HRG may be to connect the catalytic site of AMP deaminase with myosin and titin, and that the HRR of the muscle form of HRG is responsible for the rapid clearance of AMP deaminase from the circulation (Ranieri-Raggi et al., 1997). Such clearance could occur in liver through an interaction of the muscle HRG with cell surface heparan sulfates and subsequent internalization of the enzyme by hepatocytes (Ranieri-Raggi et al., 1997).

In a related series of observations, HRG has been shown to inhibit the antiproliferative effects of heparin (or heparinoid GAGs) on cultured bovine arterial smooth muscle cells and to promote the proliferation of smooth muscle cells and atherogenesis (Hajjar et al., 1987). However, other heparin-binding proteins in plasma (such as FBG, fibronectin, ATIII and platelet factor 4) were found not to affect the action of heparin. It is possible, therefore, that HRG may play a role in cell growth and vessel repair of atheromatous vessel walls upon release of HRG from macrophages and platelets recruited in response to arterial injury (Hajjar et al., 1987).

1.1.6 Regulation of the immune system by HRG

Regulation of the immune system by HRG is indicated by studies which suggest that HRG inhibits autorosetting, binds to complement proteins, and binds to immune cells including macrophages, and T lymphocytes, altering their function. In addition, it has been reported that serum HRG levels are significantly decreased in patients with AIDS and in kidney transplant recipients on immunosuppressive steroid treatment (Morgan, 1986). These findings indicate an involvement of HRG in immune function which is discussed below.

1.1.6.1 Inhibition of rosette formation

Perhaps the first suggestion that HRG could play a role in regulating immune function followed from the observation that native human HRG is the major plasma protein in human serum which inhibits the formation of autorosettes between murine lymphocytes and autologous erythrocytes *in vitro* (Rylatt et al., 1981). HRG isolated from the sera of many vertebrates also was found to inhibit the autorosetting of murine lymphocytes and erythrocytes (Rylatt et al., 1981), suggesting that HRG from other species has similar activity. The physiological relevance of the *in vitro* phenomenon of autorosetting is not fully understood, but it is thought to provide insights into events associated with cell-cell interactions in the immune system.

Autorosetting has been studied most extensively in the human and murine systems. The T cell adhesion molecule CD2 has been shown to be involved in the human system (Kamoun et al., 1981; Kozarsky et al., 1993). Similarly it has been proposed that CD2 is also important in autorosetting in the murine system (Sem et al., 1991). However, an important difference between the two systems is that with murine cells, in contrast to human cells, products of the major histocompatibility complex are involved in the adhesion process (Sia et al., 1982).

The mechanism by which HRG inhibits autorosetting is unclear. Evidence suggests that in the murine system HRG may mask anionic carbohydrate structures on mouse erythrocytes recognised by lymphocytes (Lijnen et al., 1983a; Parish et al., 1984). In the human system, however, HRG inhibits rosetting between human peripheral blood T lymphocytes and sheep erythrocytes by masking erythrocyte binding receptors on the lymphocytes, suggesting that the molecular mechanism of rosette formation in the human and murine systems may be different. It should be noted, however, that the human system examined is not autorosetting but the binding of xenogeneic red cells to human lymphocytes. In the human system HRG was reported to bind to a CD2-unrelated 56 kDa protein on human peripheral blood T lymphocytes (Saigo et al., 1989) and partially inhibit rosette formation (Shatsky et al., 1989). Interestingly, the 60 kDa HRR of HRG (produced by plasmin cleavage of native 75 kDa HRG) retains its ability to bind PLG, but has no autorosette inhibitory activity, suggesting that the HRR is involved in blocking autorosette formation (Lijnen et al., 1983a). Through their ability to secrete HRG it has been suggested

that under certain conditions macrophages may locally regulate the binding of erythrocytes, and possibly other cell types, to lymphocytes in mice (Sia et al., 1982).

1.1.6.2 Inhibition of T cell proliferation

Studies on the effect of human HRG on the proliferation of resting peripheral blood T lymphocytes stimulated with immobilized CD3 monoclonal antibody (mAb) indicated that physiological concentrations of HRG inhibit proliferation by 80-90% when it is added to the cells at early stages (i.e. initial 2 hrs) of activation (Shatsky et al., 1989). The inhibition of proliferation was proposed to occur via inhibition of interleukin 2 receptor expression and of interferon gamma (IFNγ) release. However, HRG had no anti-proliferative activity when added to the T cells at later stages of activation, or when the T cells had been previously activated (Shatsky et al., 1989). The interaction of HRG with human peripheral blood T lymphocytes was not affected by the presence of either Zn^{2+} or EDTA, or by pre-incubating the HRG with heparin (Saigo et al., 1989). These observations are consistent with the binding of HRG to human peripheral blood T cells occurring predominantly through the binding of HRG to a binding site(s) distinct from heparan sulfates.

In contrast, studies with other cell types suggest that HRG can modulate cell proliferation by interacting with GAGs on the cell surface. Thus, HRG is reported to induce the proliferation of cultured arterial smooth muscle cells by inhibiting the anti-proliferative effects of heparin (Hajjar et al. 1987). Other studies indicate that human HRG can inhibit the proliferation of BALB/c 3T3 fibroblasts by interacting with heparan sulfate proteoglycans and inhibiting the binding of acidic and basic FGFs to these cells. These findings support a role for HRG in modulating the release of FGFs from the extracellular matrix/basement membrane, and also in inhibiting the interaction of FGFs with cell surface heparan sulfates, a key step in the triggering of cell division by FGFs (Brown and Parish, 1994).

1.1.6.3 Modulation of cell adhesion

Studies by Lamb-Wharton and Morgan (1993) demonstrated that HRG alters the morphology of human peripheral blood T cells and the human T cell line MOLT 3 and increases the concanavalin A (Con A) induced attachment of these

cells to the culture dish. Other studies, however, indicate that human HRG inhibits the adhesion of various human and murine T cell lines to culture dishes coated with components of the extracellular matrix, but at the same time promotes homotypic adhesion between the cells (Olsen et al., 1996). In these latter studies the effect was potentiated by the presence of physiological concentrations of Zn^{2+}, but was inhibited by the presence of heparin and certain other sulfated polysaccharides, suggesting that the binding of HRG to heparan sulfates on the surface of these T cell lines was important (Olsen et al., 1996). From these results it would appear that HRG could potentially modulate the adhesion of T cells to the surface of endothelial cells and platelets, and thus the migration of T cells to sites of inflammation (Lamb-Wharton and Morgan, 1993).

The ability of HRG to interact with TSP with high affinity (K_d = 7 nM) also is consistent with HRG playing a role in cell-cell interactions and cell migration. The involvement of TSP in cell-cell or cell-matrix interactions, and its presence on endothelial cells, fibroblasts and smooth muscle cells, raises the intriguing possibility that HRG, by binding to TSP, may interfere with the function of TSP (Leung et al., 1984; Jaffe et al., 1982). However, this suggestion has not been examined experimentally.

1.1.6.4 Modulation of the reticuloendothelial system

Following the initial observation that HRG interacts with murine macrophages (Sia et al. 1982), Chang et al. (1992b) demonstrated that murine HRG binds to immobilized oil-elicited inflammatory mouse peritoneal macrophages and regulates the binding and phagocytosis of opsonized sheep erythrocytes. The incubation of macrophages with native human HRG (125 ng/ml) for 1-2 hours at 37°C was found to potentiate, but incubation for more than 8 hrs was found to inhibit, their ability to bind and ingest opsonised erythrocytes. The effect of HRG was not dependent on the presence of either heparin (1-100 µg/ml) or IFNγ, but was dependent on the level of IgG on the erythrocyte surface. It remains to be established, however, whether HRG can inhibit the binding of antibody (Ab) coated erythrocytes to macrophages *in vivo*.

The N-terminal 40 kDa domain of HRG was found to bind to macrophages and to inhibit the binding and phagocytosis of IgG-opsonized sheep erythrocytes. The pretreatment of the human monocytic cell line THP1 with HRG (~ 0.04 - 4 µg/ml) for 18 hours resulted in increased cellular synthesis, but decreased cell surface expression of FcγRII, as assayed using a mAb to CD32 (Chang et al.,

1994). These studies suggested a role for HRG in regulating macrophage FcγR expression and FcγR-mediated phagocytosis, although the mechanisms underlying the time-dependent effect of HRG on macrophage endocytosis and expression of FcγRII is unclear. The experimental work described in Chapter 5 of this thesis provides some insight into this phenomenon.

1.1.6.5 Modulation of complement pathways

In humans the plasma levels of HRG are reported to decrease during inflammation and after surgery (Saigo et al. 1990a). Thus, unlike protein C or mannose binding protein (MBP), which are positive acute phase reactants in plasma, HRG was classified as a negative acute phase reactant and was suggested to play some role in inflammation (Saigo et al. 1990b). HRG also was found to interact with S-protein (vitronectin), factor D and components C8 and C9 of complement by *in vitro* ELISA assays (Chang et al., 1992a). However, the functional relevance of these interactions is unclear. On the other hand, evidence suggests that the addition of a mixture of HRG and normal human serum to a suspension of IgG-opsonized sheep erythrocytes potentiates lysis of the erythrocytes by the classical complement pathway in a HRG concentration-dependent manner (Chang et al., 1992a). Erythrocyte lysis is inhibited, however, when the HRG is preincubated with serum for 10 minutes before adding the mixture to the erythrocytes (Chang et al., 1992a). A similar effect is seen on the activation of the alternative complement pathway when HRG and serum are added to a suspension of rabbit erythrocytes (Chang et al., 1992a). These studies suggest that HRG can modulate complement function, although the molecular basis of this effect is unknown.

1.1.7 Concluding Remarks

Based on the information presented in the preceding sections it is clear that HRG is a multifunctional protein which deserves further detailed study. Overall the data suggest that HRG is a pre-existing plasma protein which modulates many biological processes, such as cell adhesion, coagulation, complement activation and immune responsiveness. The three domain structure of the molecule, with each domain being capable of binding unique families of ligands, is consistent with the multifunctional nature of HRG. In fact, HRG appears to be ideally placed to act as a linking molecule for disparate biological processes such as coagulation and complement activation.

1.2 PART II Formation and Clearance of Immune Complexes

Part II of this chapter will review two major features of ICs: the mechanism of formation of insoluble ICs and the clearance of ICs by the RES. Igs are a major component of ICs, and FcRs and complement components play major roles in the clearance of ICs. Therefore it is relevant, first of all, to very briefly review the general features, structure and functional properties of human Igs, FcRs and complement components.

1.2.1 Important molecules involved in IC formation and clearance

1.2.1.1 Immunoglobulins

The general properties of Igs are extensively reviewed elsewhere (Carayannopoulos and Capra, 1993; Max, 1993; Jefferis and Pound, 1992; Klein and Horejsi, 1997) and will be summarised below. Igs are composed of disulphide linked heavy and light chains, with each chain type consisting of a N-terminal segment of variable sequence, termed the variable region and a C-terminal region of constant sequence termed the constant region. The variable regions of individual heavy and light chains combine in three dimensional space to form a single antigen (Ag) binding site.

There are five classes of human Ig, namely IgM, IgD, IgG, IgA and IgE, which correspond to μ, δ, γ, α, and ε heavy chains (Table 1.2). Human IgG is divided into four subclasses namely, IgG1, IgG2, IgG3 and IgG4 and IgA is divided into two subclasses, IgA1 and IgA2. The heavy chains of all isotypes can be synthesised in two forms, either membrane-bound or secreted. The only difference between these two forms of Ig is the amino acid sequence of the C-terminal end of the heavy chains, with the membrane expressed Ig having an additional C-terminal membrane insertion sequence. The light chain of an Ig molecule can either be kappa (κ) or lambda (λ). Human Ig only has one type of κ light chain since the gene encoding the constant region of κ light chain only contains one segment, whereas there are four different functional human λ light chains, namely λ1, λ2, λ3 and λ6. The normal ratio of the different classes and subclasses of Ig in plasma may vary from species to species. For example, ~ 95 % of plasma Ig in mice contain the κ light chain but in humans the κ : λ ratio is ~ 6 : 4, whereas 95 % of horse light chains are the λ form and birds only express λ light chains. In humans the κ : λ light chain ratio has been shown to change

Table 1.2 Physicochemical Properties of Human Immunoglobulins

Properties	IgG1	IgG2	IgG3	IgG4	IgM	IgA1	IgA2	sIgA	IgD	IgE
Molecular weight (kDa)	146	146	170	146	970	160	160	385	184	188
Sedimentation coefficient	7S	7S	7S	7S	19S	7S	7S	11S	7S	8S
Heavy chain type	γ1	γ2	γ3	γ4	μ	α1	α2	α1 or α2	δ1	ε1
Number of heavy chain domains	4	4	4	4	5	4	4	4	4	5
Carbohydrate content (percent)	2-3	2-3	2-3	2-3	12	7-11	7-11	7-11	9-14	12
Number of oligosaccharides per chain	1	1	1	1	5	8	8	?	3	6
Serum levels (mg/ml) in adult	9	3	1	0.5	0.5-2	3	0.5	0.05	0.03	0.00005
Rate of synthesis (mg/kg/day)	33	33	33	33	3.3	24	24	-	0.4	0.002
Rate of catabolism (mg/kg/day)	7	7	17	7	8.8	25	25	-	37	71
Half-life (days)	23	23	8	21	5	6	6	-	3	2

Adapted from Klein and Horejsi, 1997; sIgA, secreted IgA.

during different pathological conditions. For example, in patients suffering from rheumatoid arthritis (RA) the production of Igs with the κ light chain has been shown to be significantly increased compared to healthy individuals (Riesen et al., 1976).

The Ig classes IgD, IgG, and IgE consist of two identical heavy chains and two identical light chains. However, IgM consists of a pentameric arrangement of this basic Ig structure, the five subunits being joined by disulphide bonds and a polypeptide termed the J-chain. IgA can exist in two forms, a monomer consisting of the basic four chain Ig structure and a dimer also linked by a polypeptide termed the J-chain (Table 1.2). Each Ig molecule consists of two Fab and one Fc region which are joined together by the hinge region of the heavy chains. Although there is ~ 95 % identity between the complete amino acid sequence of IgG subclasses, the hinge region shows great differences among the four IgG subclasses both in terms of amino acid sequence and number of residues. The hinge region determines the flexibility of an IgG molecule. It should be noted that in contrast to IgG, IgD and IgA molecules, the IgM and IgE have no defined hinge region. The flexibility of an Ig molecule also may be affected by the position of the disulphide bonds in its heavy and light chains. For example, the position of the cysteine residue in the heavy chain of IgG1 that links the heavy chain to the light chain may make the IgG1 molecule more flexible than other IgGs and hence influence different functions. In addition, the C-terminal cysteine residue of the κ light chain may form a more flexible Ig when compared to Ig molecules containing λ light chains in which the penultimate cysteine residue of the λ light chain forms a disulfide bond with the heavy chain. Each IgM molecule has 10 Ag binding sites, but presumably because of the lack of flexibility of the Fab arms, a single IgM molecule can only bind simultaneously a maximum of five antigenic determinants (Klein and Horejsi, 1997).

Igs are classified as glycoproteins since all of the Ig molecules contain some sort of carbohydrate. It has been shown that the type of oligosaccharide side chain is different and is characteristic for each class of Ig. The heavy chain of human IgG (regardless of subclass) contains only one N-linked oligosaccharide approximately at position 300, whereas other heavy chains contain either two or five oligosaccharides per molecule (Table 1.2). The N-linked oligosaccharides have a molecular weight of approximately 2500-3000 dalton and usually consist of ~ 15 monosaccharide units.

Human Igs are encoded for by genes located on three different chromosomes: the Ig heavy chain on chromosome 14q32, the κ light chain of Ig on chromosome 2p12-p11, and the λ light chain of Ig on chromosome 22q11. The heavy chain gene complex consists of 95 variable (V), 32 diversity (D), 9 joining (J) and 11 constant (C) segments, whereas, the κ light chain gene complex consists of 90 V, 5 J, and 1 C segments and the λ light chain gene complex consists of 60 V, 7 J, and 7 C segments (Klein and Horejsi, 1997). The two striking differences between κ and λ light chain gene are that the κ light chain gene contains only one C segment, whereas, the λ light chain gene contains seven segments only four of which are functional. The Ig genes rearrange before they are expressed as Ig on the cell surface of B lymphocytes, a process which has been extensively reviewed elsewhere (Lewis, 1994). Briefly, Ig diversity is generated by a rearrangement process where a single V, D and J or V and J segment is selected to produce the heavy chain or light chain variable region, respectively. Variation in the joining region between the segments, termed functional diversity, generates further sequence variation. Initially the rearranged VDJ segment is translocated adjacent to the μ chain locus, such that IgM is the first cell surface Ig expressed by B cells. However, by a process of class switching the rearranged VDJ segments can be subsequently translocated adjacent to other constant region loci, the nine different human heavy chain loci being arranged in the order μ, δ, γ3, γ1, α1, γ2, γ4, ε1, and α2 on chromosome 14. After the Ig heavy chain, either the κ light chain or λ light chain loci are rearranged. If the κ light chain is productively rearranged first then the cell expresses an Ig molecule that contains two identical heavy and two identical κ light chains. If the λ light chain locus rearrangement succeeds, the cell synthesises Igs with two identical heavy chains and two identical λ light chains (Max, 1993).

The functional properties of the different human Igs are summarised in Table 1.3. Igs protect the host against pathogens, either directly or indirectly. Among the five Igs, IgA and IgE may undertake functions against pathogens entering the host through mucosa or skin, respectively, whereas IgM and IgG mainly act against pathogens that have already entered the host and are present in the circulation. It has been shown that IgM Abs, after binding to their cognate Ag, are very effective at activating the classical complement pathway (see 1.2.1.3), whereas IgG Abs although activating the complement pathway in some cases, also coat cells or particles for uptake by phagocytic cells, such as macrophages and neutrophils, via FcR. Among the four IgG subclasses, IgG1 and IgG3 have the highest affinity for $Fc_{\gamma}R$ on phagocytic cells, whereas IgG4 has a lower

Table 1.3 Functional Properties of Human Immunoglobulins

Properties	IgG1	IgG2	IgG3	IgG4	IgM	IgA1	IgA2	IgD	IgE
Activate classical complement pathway	+	+/-	++	-	+++	-	-	-	-
Binds to macrophage Fc receptor	+	+/-	++	+	+	-	-	-	-
Presence in secretions	-	-	-	-	+	++	++	-	-
Cross placenta	+	+/-	+	+	-	-	-	-	-
React with protein A	+	+	-	+	-	-	-	-	-

Adapted from Klein and Horejsi, 1997.
Activity levels: +++ and ++, high; +, moderate; +/-, minimal; -, absent

affinity and IgG2 has the lowest affinity (Table 1.3). The binding affinity of IgG subclasses for the complement component C1q, the initiating component of the classical complement pathway, follows the hierarchy of IgG3 > IgG1 > IgG2 > IgG4. As a result of these differring affinities for C1q, human IgG3 and IgG1 can activate complement almost as efficiently as IgM, whereas IgG2 is a less efficient activator and IgG4 does not activate complement at all (Table 1.3).

IgA Abs function at body surfaces such as those associated with the digestive, respiratory and reproductive tracts (Table 1.3). IgA at the surface can prevent pathogens from entering the body by aggregating pathogens together. IgA also facilitates phagocytosis of pathogens via Fc alpha receptor ($Fc_{\alpha}R$) on phagocytes but this interaction is rather weak compared to the IgG $Fc\gamma R$ interactions. IgE Abs exist at lowest concentration in plasma and bind to Fc epsilon R ($Fc_{\varepsilon}R$) on mast cells and basophils. If an Ag can cross-link the IgE on mast cells, this clusters the $Fc_{\varepsilon}R$ and triggers the cells to release substances which are vasoactive and proinflammatory. IgE does not contain a hinge region and is therefore the most rigid Ig. IgD is usually co-expressed with IgM and appears on the cell surface of mature but immunologically naive B cells. However, the functional role of IgD is still unclear.

1.2.1.2 Fc receptors

FcR are members of the Ig-superfamily and are a set of heterogeneous cell surface molecules that bind to specific sites on Ig molecules (Reviewed by Hulett and Hogarth, 1994 and Unkeless et al., 1992). They are classified according to the Ig class that they recognise and the strength of the interaction (Table 1.4). FcR for IgG, IgA and IgE are well characterised, whereas FcR for IgM and IgD have been defined but have not been structurally characterised. Two high affinity FcR have been defined in humans, namely $Fc_{\gamma}RI$ and $Fc_{\varepsilon}RI$. Low affinity FcR are $Fc_{\gamma}RII$, $Fc_{\gamma}RIII$, $Fc_{\varepsilon}RII$ and $Fc_{\alpha}R$ (Table 1.4). Only the high affinity FcR can bind monomeric Ig molecules, whereas the low affinity FcR only can bind ICs or aggregated Igs (Unkeless et al., 1992; Hulett and Hogarth, 1994). Although three major classes of FcR for IgG have been described ($Fc_{\gamma}RI$, $Fc_{\gamma}RII$ and $Fc_{\gamma}RIII$), each class may be heterogenous and consist of different subclasses. This heterogeneity may arise from alternative messenger RNA (mRNA) splicing or may result from separate genes (Abrass, 1991; Sylvestre and Ravetch, 1994; Ravetch and Kinet, 1991).

Table 1.4 Properties of Human Fc Receptors

Receptors	Chromosome	Mw (kDa)	Affinity K_d (nM)	Specificity	Expression	Function
FcγRIA (CD64)	1q23	72	1-10	IgG3, IgG1	Macrophages Monocytes Neutrophils	Cell activation Endocytosis
FcγRIIA (CD32)	1q23	40	<200	IgG1, IgG3	Platelets, Monocytes Neutrophils Langerhan Cells	Cell activation Endocytosis Phagocytosis
FcγRIIB	1q23	40	<200	IgG1, IgG3	Macrophages Lymphocytes	? ?
FcγRIIC	1q23	40	<200		Myeloid Cells	Endocytosis
FcγRIIIA (CD16a)	1q23	50-70	<200	IgG1, IgG3	NK Cells Monocytes Macrophages	Cell activation Endocytosis
FcγRIIIB (CD16b)	1q23	50-70	<200	IgG1, IgG3	Neutrophils	
FcεRI	1q23	45-65	0.1	IgE	Mast Cells Basophils Langerhan Cells	Mast cell activation
FcεRIIa (CD23)	19p13.3	43	<200	IgE, CD21	B Cells	Endocytosis
FcαR	10q13.4	60	500	IgA, IgM	Epithelial Cells	Trancytosis

Adapted from Klein and Horejsi, 1997

Both high and low affinity FcR can only trigger a response in the cell's interior when clustered by ICs. Depending on the cell and Ab type the generated signal may lead to phagocytosis and/or killing of the Ab coated pathogen or pathogen infected cell and the release of inflammatory mediators (Unkeless et al., 1992). Although all FcR are membrane bound, the extracellular domain of $Fc_{\varepsilon}RII$ and $Fc_{\gamma}RIII$ may be cleaved enzymatically and may be released into the surrounding medium (Tosi and Berger, 1988; Fleit and Kuhnle, 1988). Additionally, in some instances, by splicing the mRNA $Fc_{\gamma}RII$ can be expressed without its transmembrane region ($Fc_{\gamma}RIIAa2$) and therefore can be released into the surrounding medium (Tartour et al., 1993).

The membrane-bound FcR consists of an extracellular region, a transmembrane region and a cytoplasmic tail. The extracellular region is comprised of one to three Ig-like domains which form the Fc binding region. Depending on the cell type they are expressed on, FcR may contain different intracellular domains. These differences in the cytoplasmic tail of FcR may lead to the generation of different signal transduction pathways and, therefore, may result in heterogeneous biological responses upon interaction of ICs with different cell types (Unkeless et al., 1992).

1.2.1.3 Complement components

The complement system is composed of approximately 30 proteins which, following activation by various stimuli, results in the assembly of a complex array of proteins which can lyse cell membranes/walls via the MAC and can facilitate uptake of foreign substances by phagocytes (Muller-Eberhard, 1992). Some complement components also have a proinflammatory role. The complement system can be activated by three different pathways, namely the classical, the alternative and the lectin pathways. Activation of any of these pathways ultimately leads to the assembly of the MAC (see below). Each pathway is comprised of a number of different components which, upon activation, results in the generation of complement 3 (C3) convertase and subsequent MAC assembly (see Figure 1.2).

The classical pathway can be activated by ICs containing certain IgG subclasses and/or IgM (see Table 1.3). Activation of the classical pathway leads to the production of a series of Ser proteases (C1s, C4b, C2b). In the presence of ICs, serum C1 binds to the Fc region of Ig molecules by the C1q globular head and releases associated C1 inhibitor (Golan et al., 1981). The C1 molecule changes

FIGURE 1.2 **Activation of complement**

The alternative, lectin, classical and lytic pathways of complement activation are depicted. The binding of activating surfaces to a C3b-like molecule ($C3(H_20)$) initiates the alternative pathway which leads to the formation of C3b. The lectin pathway of complement is initiated by the interaction of MBP with carbohydrates on the surface of bacteria which leads to the formation of C3b. The classical pathway is initiated when C1 recognizes IC and following a series of proteolytic reactions C3b is formed. The lytic pathway is initiated by the cleavage of C5 and the formation of MAC. Abbreviations are: C: complement, MBP: mannose binding protein, MASP: MBP-associated serine proteases, B: factor B, D: factor D, P: properdin, Adapted from Muller-Eberhard, 1992.

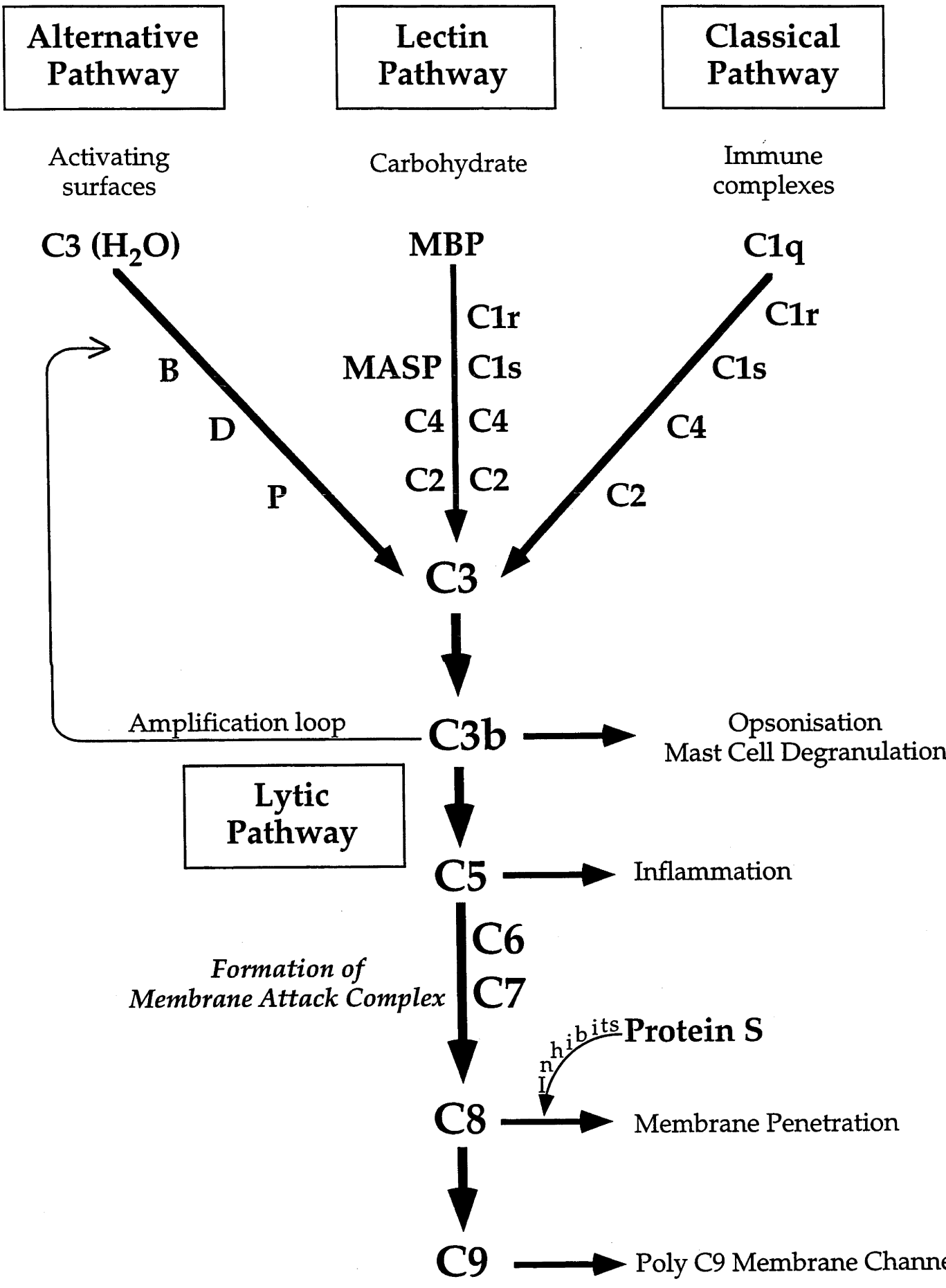
Alternative Pathway
Lectin Pathway
Classical Pathway
Activating surfaces
Carbohydrate
Immune complexes
C3 (H_2O)
MBP
C1q
B
D
P
MASP
C1r
C1s
C4
C2
C1r
C1s
C4
C2
C3
Amplification loop
C3b
Opsonisation
Mast Cell Degranulation
Lytic Pathway
C5
Inflammation
Formation of Membrane Attack Complex
C6
C7
Protein S
inhibits
C8
Membrane Penetration
C9
Poly C9 Membrane Channe

its conformation upon binding to ICs. One of the two C1r molecules becomes activated (perhaps by exposing the active site), cleaves the neighbouring C1r molecule and activates a proteolytic cascade which eventually results in the assembly of the C4bC2b complex, a potent C3 convertase which cleaves C3 to C3a and C3b (Porter and Reid, 1979; Nagasawa and Stroud, 1977; Golan et al., 1981; Isenman and Kells, 1982).

The alternative pathway of complement activates spontaneously at a very slow rate but, in the presence of activating surfaces such as bacteria, yeast, viruses, IgA containing ICs or insoluble ICs, the activation process is amplified leading to the deposition of C3b molecules on the surface of the pathogen or insoluble ICs. C3 spontaneously binds to one molecule of H_2O to form C3(H_2O) which changes the structure of C3 (Isenman et al., 1981; Pangburn et al., 1981) and allows it to bind factor B. The formation of the C3(H_2O)B complex exposes a site on factor B which is cleaved by plasma factor D (Muller-Eberhard and Gotze, 1972), leading to the production of Ba and Bb fragments and the subsequent release of the Ba fragment into the surrounding medium. The C3(H_2O)Bb complex acts as a mild C3 convertase and cleaves C3 to C3a and C3b (Lachmann and Hughes-Jones, 1984). At this stage if the C3b fragments generated encounter foreign particles or insoluble ICs, they bind to them by covalent ester or amide bonds and the bound C3bBb forms a potent C3 convertase which randomly deposits C3b on the parasite surface or insoluble IC (Figure 1.2). The C3(H_2O)Bb complex also is stabilized by properdin (factor P) (Fearon and Austen, 1975), a plasma protein with a structure similar to that of the cell adhesion molecule thrombospondin. Properdin also prevents the cleavage of C3 convertase by factor I, thereby further amplifying C3b deposition.

The third pathway of complement, the lectin pathway, is activated by bacterial surface carbohydrates (Kawakami et al., 1984). MBP, a protein analogous to C1q, is the first member of the lectin pathway which interacts with mannose and N-acetylglucosamine containing carbohydrates on the surface of bacteria (Weis et al., 1992; Holmskov et al., 1994). In plasma, MBP associates with a Ser protease called MBP-associated Ser protease (MASP) which is analogous to the $C1r_2C1s_2$ tetramer of the classical pathway (Matsushita et al., 1992). Upon recognition of mannose and/or N-acetylglucosamine on bacterial polysaccharides by the globular head of MBP, the MBP-bound MASP is activated (Ohta et al., 1990; Lu et al., 1990; Matsushita and Fujita, 1992). Activated MASP cleaves C4 and C2 and, therefore, triggers the assembly of C3

convertase by utilizing components of the classical complement pathway (Matsushita and Fujita, 1992) (see Figure 1.2).

Upon production of C3 convertase by any of the three complement pathways described above, the formed C3b can undertake two functions. Firstly, by binding to C3b receptors on phagocytic cells, it may potentiate the clearance of opsonised particles (or ICs), and secondly, by binding to the C3 convertase it forms the C5 convertase which initiates activation of the lytic MAC pathway of complement (Figure 1.2). Briefly, this complex cleaves C5 to C5a and C5b. C5a is an anaphylatoxin and C5b is involved in initiating the lytic pathway of complement. C5b gains a binding site for C6 and this complex binds C7 which produces a trimolecular complex with a hydrophobic domain (Davies et al., 1989). The trimolecular complex is released from C3b, inserts into the parasite membrane via its hydrophobic domain and gains a binding site for C8 and then C9 (Monahan and Sodetz, 1981). This multiprotein complex then binds more C9 to form C9 polymers and initiates a lytic lesion which forms a pore (Podack, 1984). As a defence mechanism the affected cell (eg. bacteria) may exocytose and release the attached MAC to the surrounding medium. Otherwise, in the absence of complement regulatory proteins (see below), the cell will be lysed.

As well as causing cytolysis of foreign organisms by the MAC and opsonisation of foreign organisms via complement receptors (CR1, CR2, CR3, and CR4) on phagocytes, the complement system also produces proteolytic fragments of complement components which induce inflammation. For example, C5a is chemotactic for neutrophils and activates the neutrophil oxidative burst. Similarly, C5a > C3a >> C4a stimulates mast cell degranulation which results in an increase in vascular permeability and smooth muscle contraction (anaphylaxis).

Another important feature of the complement system is that it represents a form of self non-self discrimination. A series of soluble and cell membrane proteins are expressed by vertebrates that inactivate complement and thereby prevent inadvertent destruction of self cells by the complement system. Among the soluble complement regulatory proteins is C1 inhibitor, a potent Ser protease that binds to activated form of C1 (C1q-2C1s-2C1r) and dissociates C1q from C1r and C1s (Ziccardi, 1981). Another soluble complement regulatory protein, factor I, is a Ser protease that degrades C3b and C4b in the presence of plasma cofactors C4 binding protein, factor H, membrane cofactor protein (MCP) or CR type 1 (CR1). Two other soluble proteins that regulate the lytic pathway of

complement are vitronectin (S Protein) and clusterin. It has been shown that vitronectin (Bariety et al., 1989) and clusterin (Tschopp et al., 1993) both bind to C5b-7 in fluid phase and inhibit its insertion into the lipid bilayer of the cell membrane. Recent findings also suggest that the plasma protein, HRG, can bind to C8, C9, S protein and factor D and may inhibit lysis of erythrocytes by the MAC (Chang et al., 1992b).

Rather than simply inactivating the complement cascade, some soluble complement regulatory proteins have additional functions. For example, factor I can cleave C3b to iC3b, C3c and C3dg and C4b to iC4b, C4c and C4d. This not only results in inhibition of further activation of C3 or C5 by either the classical or alternative complement pathways, but also generates biologically active components of C3b that bind to specific cell surface receptors. For example, iC3b and C3dg bind to CR3 and CR2, respectively, which in turn may mediate phagocytosis (Myones et al., 1988) or modify the immune response (Matsumoto et al., 1991).

Several cell surface molecules, such as decay accelerating factor (DAF) (Lublin and Atkinson, 1989), MCP (Cole et al., 1985; Liszewski et al., 1991) and CR1 (Holers et al., 1989; Fearon, 1983), have been shown to inhibit the activation of complement on self-tissues and prevent self tissue injury. These proteins inactivate C3 convertase and inhibit classical, lectin and alternative complement activation. It has also been shown that C8 binding protein and CD59 both bind to C8 and prevent the assembly of the MAC thus protecting self-cells from lysis (Hansch et al., 1981; Davies et al., 1989; Holguin et al., 1989; Yamashina et al., 1990).

It should be noted that tissues vary in their expression of these inhibitory proteins and, thus, the extent of protection against activation of complement is somewhat tissue-specific. For example, CR1 is detected on glomerular epithelial cells but not on renal endothelial or mesangial cells (Appay et al., 1990). It has also been demonstrated that nucleated cells are more resistant to complement activation compared to non-nucleated cells, such as erythrocytes and platelets, since nucleated cells can continually synthesise the inhibitory proteins (Ramm et al., 1984).

1.2.2 Immune complex formation

The binding of Abs to Ags leads to the formation of ICs. ICs can form following the interaction of Abs with intact microorganisms. However, in this section ICs that are formed by the interaction of Abs with soluble Ags such as proteins, carbohydrates or DNA will be considered. The term "immune complex formation" (ICF) refers to the interaction of Abs with their cognate Ags. This interaction was proposed to be similar to protein-ligand interactions since kinetic analyses of the interaction using immobilized Abs and soluble Ags revealed the reaction to be reversible. The reaction therefore could be written as:

$$xAb + yAg \rightleftharpoons Ab_xAg_y$$

This type of interaction may occur with mAb where the Ab recognises only one epitope on the Ag and the interaction is homogenous for the entire reaction. In this type of interaction the ligand can associate and dissociate. Therefore it is an Ag-dependent process. However, when polyclonal Abs are mixed with their cognate Ag, regardless of the ratio of Ag : Ab or reactant concentration, this reversible reaction follows a process of "insolubilisation" which leads to the formation of insoluble ICs (Gorgani et al., 1996). The insolubilisation process, which is an Ag-independent process, leads the entire process to become an "irreversible interaction" (see Scheme 1).

Insoluble ICs form when polyclonal Ab preparations are incubated with their cognate Ag, and this system has been widely used as a model to study ICF *in vitro*. Evidence suggests that two types of interactions may be important in ICF: the interaction between epitopes on the Ag and the Ag binding sites of the Ab molecules (Murphy et al., 1988), and the less well-defined interaction between the Fc region of Ab molecules (Møller, 1979; Møller and Steensgard, 1979; Rodwell et al., 1980; Møller and Bak, 1984; Cosio et al., 1987; Easterbrook-Smith et al., 1988; O'Brien et al., 1994). Moreover, it has been proposed that the formation of insoluble ICs occurs in three distinct steps, as shown in Scheme 1. These include the rapid formation of soluble Ag : Ab complexes within the first few seconds of the reaction (Step 1) (Ag-dependent), followed by the subsequent insolubilisation of these soluble complexes to form insoluble species in a process lasting several minutes (Step 2) (Ag-independent), and the coalescence of the larger species to form precipitates on a time scale of minutes to hours (Step 3) (Sittampalam and Wilson, 1984a, 1984b).

$$xAb + yAg \rightarrow Ab_xAg_y \quad \text{Step 1}$$
$$nAb_xAg_y \rightarrow (Ab_xAg_y)_n \quad \text{Step 2}$$
$$(Ab_xAg_y)_n \rightarrow \text{precipitate} \quad \text{Step 3}$$

Scheme 1: Formation of insoluble ICs

The experimental techniques that have been used to study ICF *in vitro* include sedimentation methods (Møller and Steensgard, 1979), electron microscopy (Murphy et al., 1988) and light scattering techniques (Murphy et al., 1988, Sittampalam and Wilson, 1984a, 1984b; Yarmush et al., 1988). Since the formation of insoluble ICs leads to the generation of a turbid suspension, and the turbidity or light scattering and absorbing properties of the suspension is related to the size of the particles in the suspension (Stacey, 1956), this method was widely used to study the mechanism of ICF and to elucidate effects of human plasma proteins, such as components of complement (eg. C1, C1q and C3b) which affect this process. Previously it was thought that the formation of insoluble ICs only leads to the formation of small size insoluble ICs (as shown in step 2) which then form precipitates (Easterbrook-Smith, 1993). However, recent studies (Gorgani et al., 1996) indicate that after insolubilisation of ICs they polymerise rapidly and this leads to the formation of very large insoluble ICs observable in a suspension by visual inspection (see below). The insolubilisation process, which presumably is vital for the effective functioning of humoral immunity, may increase the efficiency of Ab to tightly bind to Ag (see below).

As outlined in scheme 1, a major feature in the formation of precipitates (step 3) is the insolubilisation of soluble ICs (step 2) following the interaction of Ab with their cognate Ag (step 1). Since the size and resultant abnormal clearing of insoluble ICs has been proposed to be an important parameter in inducing some pathological conditions (Geronski et al., 1985), there have been many attempts to estimate the size of insoluble ICs. The use of electron microscopy or conventional light scattering (at a single wavelength) techniques only allowed the size of insoluble ICs to be estimated at the end of the reaction (Sittampalam and Wilson, 1984a, 1984b; Murphy et al., 1988; Yarmush et al., 1988) and no technique was available for the continuous accurate measurement of the size of complexes during the insolubilisation of ICs. However, in 1993 a technique was developed which allowed one to continuously measure the increase in the size of insoluble ICs by measuring the light scattering properties of the suspension

at different wavelengths (Easterbrook-Smith, 1993), although the problem of sedimentation of large insoluble ICs led to inaccuracies.

In order to overcome this problem a continuous mechanical stirring of the reaction solution has been employed to accurately determine the rate of increase in the size of ICs formed between ovalbumin and anti-ovalbumin IgG (Gorgani et al., 1996). The results suggest that the formation of insoluble ICs in a continuously stirred solution occurs in at least two phases by a mechanism dependent on the concentration of the Ab, the Ag : Ab ratio and the ionic strength of the reaction medium. In this system, initiation of ICF by mixing the Ab and Ag led to the generation of insoluble ICs of radii up to approximately 100 nm (scheme 1, step 2), and was followed by a rapid increase in the size of ICs (Figure 1.3A, B and C) (scheme 1, step 3). By employing continuous mechanical stirring of the solution, the rapid polymerisation and formation of very large insoluble ICs in the second phase of the reaction could readily be quantified (Figure 1.4) (Gorgani et al., 1996).

Similar patterns of ICF were obtained when $F(ab')_2$ fragments of IgG were used instead of whole IgG (compare Figure 1.3A and B) but the formation of insoluble ICs with a 100 nm radius (scheme 1, step 2) was ~ 70 fold slower. These observations suggest that Fc-Fc interactions lead to a 70-fold faster insolubilisation of ICs when compared to IgG molecules that lack this region. The similarity between the polymerisation phase (scheme 1, step 3) of ICs containing whole IgG and those containing $F(ab')_2$ fragments of IgG suggests that the rapid polymerization occurs even with IgG molecules that lack the Fc region and hence the Fc-Fc interaction. The results suggest that the polymerization phase is not dependent on the Fc-Fc interaction but presumably involves a Fab-Fab interaction (Figure 1.3A and B). Interestingly, insoluble ICs in Ag excess and Ab excess also underwent rapid polymerization after reaching the critical size of 100 nm suggesting that the Ag : Ab ratio has its major effect on the rate of phase 1 insolubilisation (scheme 1, step 2) with rapid phase 2 polymerization (scheme 1, step 3) occuring at all Ag : Ab ratios (Figure 3.1C). This study also presented evidence that ionic interactions play a role in step 2 insolubilisation of ICs since there was a sodium halide concentration-dependent inhibition of the insolubilisation of ICs containing both whole IgG or $F(ab')_2$ when the average radius of ICs was <100 nm (Gorgani et al., 1996).

Since the insolubilisation process results in an increase in turbidity and absorbance, the kinetic parameters (eg. on-, off-rates) for the insolubilisation of

FIGURE 1.3 **The effect of Ab concentration on the size of ICs formed from ovalbumin and IgG or F(ab')$_2$.**

The formation of insoluble ICs was initiated by adding ovalbumin to give an Ag : Ab ratio of 0.03 : 1 (w/w) to solutions of anti-ovalbumin IgG at 1.0 (▲), 0.75 (○), 0.5 (●), 0.375 (□) and 0.25 (■) mg/ml in PBS. The radii of the ICs that formed as a function of time at different wavelengths was determined as described (Gorgani et al., 1996) and shown in (A). (B). The formation of insoluble ICs using F(ab')$_2$ fragment of IgG instead of IgG. The formation of insoluble ICs was initiated by adding ovalbumin to give an Ag : Ab ratio of 0.03 : 1 (w/w) to a solution of F(ab')$_2$ (made from of anti-ovalbumin IgG) at 0.56 (■), 1.15 (□), 1.71 (●), 2.25 (○) mg/ml in PBS. (C). The effect of Ag : Ab ratio on the size of insoluble ICs that formed. The formation of insoluble ICs was initiated by adding ovalbumin to give Ag : Ab ratios (w/w) of 0.015 : 1 (■), 0.03 : 1 (□), 0.045 : 1 (●), and 0.06 : 1 (○), to solutions of anti-ovalbumin IgG (0.5 mg/ml) in PBS. In each instance the absorbances associated with light scattering by the ICs at different wavelengths were measured, and the size of the ICs were calculated as described (Gorgani et al., 1996).

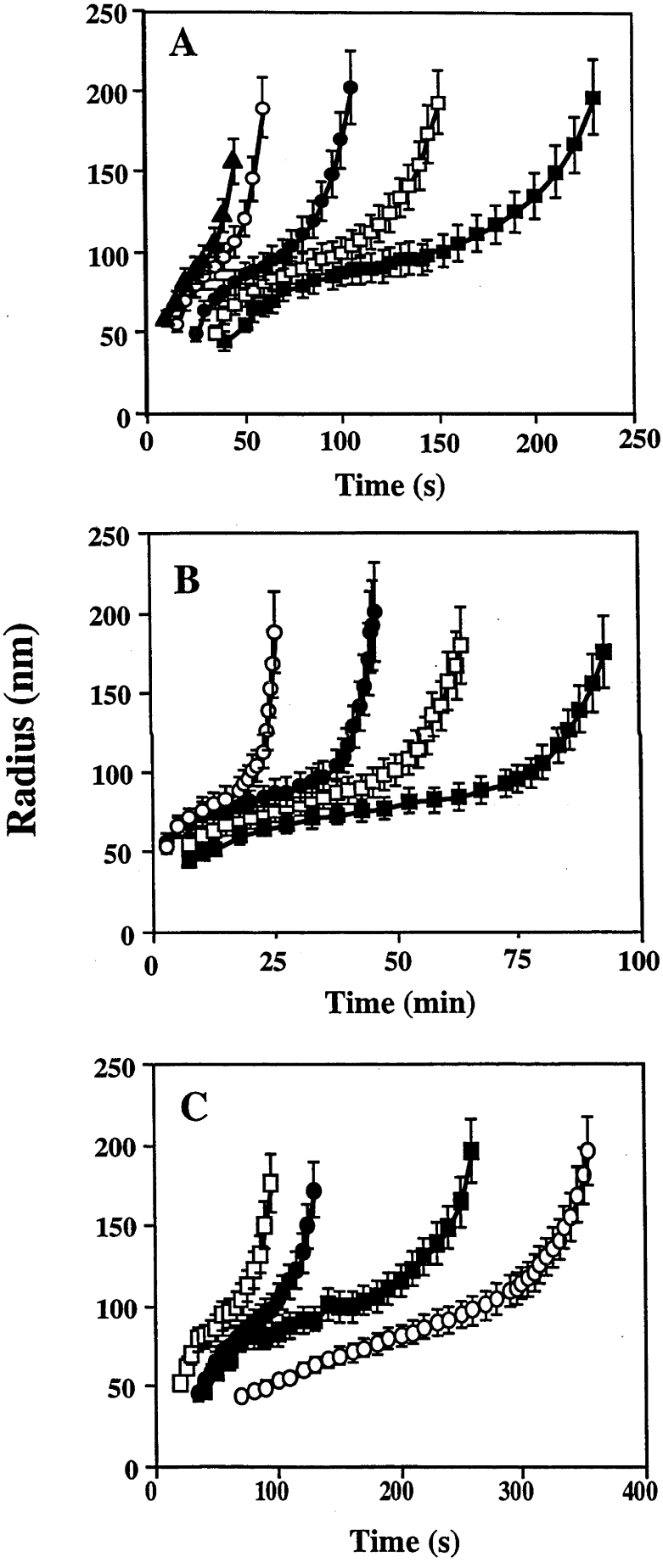
A
B
C
Radius (nm)
Time (s)
Time (min)
Time (s)
0
50
100
150
200
250
0
25
50
75
100
0
100
200
300
400

FIGURE 1.4 **Rapid polymerisation of insoluble ICs.**

Photographs show insoluble ICs that were formed at 0 (A), 5 (B), 10 (C), 15 (D), 30 (E), 60 (F), 120 (G), 300 (H) and 600 (I) seconds after the initiation of the reaction by mixing 1 mg/ml of anti-ovalbumin IgG with ovalbumin at an equivalence Ag : Ab ratio in a stirred reaction vessel.

A

B

C

D

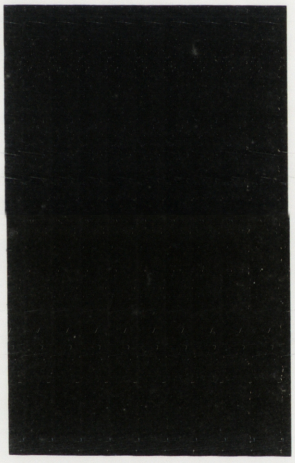

E

F

G

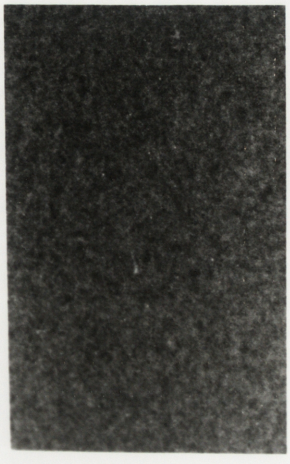

H

I

ICs can be determined using absorbance measurements obtained at 350 nm. For each concentration of IgG and ovalbumin at an equivalence Ag : Ab ratio, the initial absorbance values of the insolubilisation phase (scheme 1, step 2) (as depicted in Figure 1.3A) could be fitted to the equation:

$$A = A_o \times e^{k_{obs}\, t} + c$$

Where t is time, A is the absorbance due to light scattering by the insoluble ICs at time t, A_o is the absorbance due to light scattering by the insoluble ICs at time 0, k_{obs} is the observed rate constant for insolubilisation of ICs and c represents a net displacement (constant). For each concentration of ICs, k_{obs} was calculated by fitting the absorbance data to the exponential curve and then the k_{obs} was plotted versus concentrations of IgG assuming that the initial concentration of ICs is correlated with the initial concentration of IgG (Ag : Ab ratio is constant). This plot revealed that the off-rate of this process is zero and the on-rate is 42075 $M^{-1}s^{-1}$. These results therefore indicate that the insolubilisation process is an irreversible process with a pseudo-on rate of 42,075 $M^{-1}s^{-1}$ (Gorgani et al., unpublished observations).

1.2.3 Mechanisms of IC clearance

In primates ICs are cleared in different ways depending on the site at which they are formed. For example, in the case of formation in the circulation, ICs bind to erythrocytes and are transferred to the liver or spleen to be cleared by resident macrophages in these organs, whereas in the case of formation in lymph nodes, ICs may be cleared by macrophages and dendritic cells, and if ICs are formed in other tissue they may be cleared by tissue macrophages.

1.2.3.1 Erythrocyte-IC clearance mechanism

ICs formed in the circulation activate complement and are rapidly opsonized following fixation of C3b and C4b. Both C3b and C4b bind erythrocyte CR1, thus C3b or C4b opsonised ICs can bind erythrocyte CR1. CR1 only exists on the surface of erythrocytes in humans and other primates (Nickells et al., 1995). In contrast to leukocytes, the erythrocyte CR1 is clustered and allows C3b and/or C4b opsonised-ICs to bind multivalently. Although circulating leukocytes such as neutrophils and monocytes possess CR1 on their surface, it has been calculated that 85% of CR1 in the circulation is associated with erythrocytes. It is likely, therefore, that most circulating ICs (CICs) which are

not bound to FcR on leukocytes may bind erythrocyte CR1 (Hebert, 1987; Hebert, 1991; Hebert et al., 1991a, 1991b). ICs that are bound to erythrocytes are prevented from being deposited in tissues and remain bound until the erythrocytes traverse the liver or spleen, at which point the ICs are released from the erythrocyte surface and taken up by macrophages. The transfer of ICs from erythrocytes to macrophages occurs quickly and involves the binding of the Fc region of ICs to FcR on macrophages. The erythrocytes then re-enter the circulation and may be able to undertake the same function again. Studies in nonhuman primates have shown that decreased binding of ICs to erythrocyte CR1 results in a decreased uptake of ICs by the liver or spleen but increased deposition of ICs in the kidney (Waxman et al., 1984; Waxman et al., 1986), indicating the importance of the erythrocytes CR1 in the clearance of CICs.

1.2.3.2 Clearance of ICs by reticuloendothelial system

The clearance of ICs may occur via the ingestion of ICs by phagocytic cells of the RES. Phagocytic cells are divided into two classes: those whose function relates to the body's defence such as neutrophils, eosinophils, monocytes and macrophages, and those that are non-professional phagocytes such as epithelial cells, platelets, fibroblasts, lymphocytes, mast cells and various mucous membranes. The ingestion occurs predominantly via IgG-FcR interactions and also through CRs if the complement component C3b is attached to the ICs. ICs are one of the most potent activators of macrophages, the binding of ICs to FcR converting a macrophage from a resting state into a primed (activated) state which then leads to the ingestion and digestion of ICs. Hitherto, IgG, IgA and the C3b fragment of C3 are the opsonins that facilitate phagocytosis. As described earlier in section 1.2.1.2, receptors for the Fc region of Igs are heterogenous and present on many cells of the immune system. Several types of FcR are expressed by phagocytes: $Fc_{\gamma}RI$ (CD64) which is expressed on monocytes; $Fc_{\gamma}RIIa$ (CD32a) which is expressed on all major types of phagocytes; $Fc_{\gamma}RIIIb$ (CD16b) which is expressed on neutrophils; and $Fc_{\alpha}RI$ (CD89) which is expressed on monocytes, macrophages and neutrophils (Table 1.4). Upon binding of ICs containing the appropriate IgG isotype to these receptors they induce phagocytosis. At least three CRs are expressed on the phagocyte surface: CR1 (CD35), CR3 (CD11b/CD18) and CR4 (CD11c/CD18). These receptors can promote phagocytosis only if the particles are also attached to the phagocytic cells via FcR or fibronectin.

The binding of ICs or opsonised particles to FcR leads to receptor clustering which brings together protein kinases bound to the cytoplasmic regions of the FcR. Subsequently, the protein kinases are phosphorylated and signal transduction pathways initiated that lead to the formation of actin filaments and pseudopodia and eventual phagocytosis. Complement receptors collaborate with FcR to enhance the intensity of phagocytosis. Upon attachment of ICs to FcR and CRs on the cell surface, they are engulfed and retained in vesicles which fuse together to form large vesicles called phagosomes. Phagosomes containing ICs then move towards the cell centre and fuse with lysosomes. The ingested ICs then are digested by a wide variety of enzymes (hydrolases) present in the lysosomes and specific granules in the cytoplasm of the phagocytic cell. The ICs in the phagosomes may be digested to amino acids, sugars, lipids and nucleotides which can then cross the phagosome membrane to be re-used by the ingesting cell. The killing of a phagocytosed microorganism also can be achieved by mechanisms such as the respiratory burst which involves the formation of oxygen derivatives such as the superoxide anion (O_2^-), hydrogen peroxide (H_2O_2), hydroxyl radicals ($^{\cdot}OH$) and singlet oxygen ($^1O_2$). Upon release of these substances into the phagosome they act as oxidants causing lethal changes in the ingested microorganisms.

1.2.3.3 Tissue injury caused by phagocytes

In some instances where ICs are too large (eg. Ab-coated multicellular parasites or very large hydrophobic insoluble ICs) or strongly adhere to self tissues, the phagocytic cells may bind but may not be able to ingest the ICs. In such circumstances they may release their lysosomal contents to the cell exterior in an attempt to destroy the particle. The release of such enzymes and other soluble substances to the cell exterior may cause local tissue damage. This process may happen in the synovium of patients with RA where the phagocytic cells fail to ingest the high concentrations of ICs (presumably adhering to the tissues) and may release hydrolases into the extracellular space which leads to tissue injury (Robinson et al., 1994; Mannik and Person, 1994; Edwards and Cambridge, 1998).

1.2.4 Factors which regulate IC formation and clearance

1.2.4.1 The nature of the Ag and the Ab response it induces

The physical nature of an Ag can have a profound affect on the class, subclass, charge, and affinity of Ab that are produced against it and, in turn, the class and

subclass of the Ab determines complement fixing ability, rate of clearance and ability of ICs to initiate inflammatory reactions (Gauthier and Abrass, 1992, Milstein, 1986). For example, it has been shown that polysaccharide Ags with repeating antigenic determinants are most likely to induce IgM production, IgG1 is mostly produced against soluble protein Ag, whereas IgG2 is mostly produced in response to carbohydrate Ag. In contrast, IgA is produced against Ag entering through mucosal surfaces such as the respiratory or gastrointestinal tracts (Gauthier and Abrass, 1992; Milstein, 1986; Purkerson and Isakson, 1992).

Another important factor is whether the Ag source is chronic or transient in nature. For example, exogenous Ag such as drugs may only cause transient IC-mediated tissue damage, with eventual clearance of the drug resulting in recovery of the affected tissue, whereas an Ab response to an endogenous Ag, which always exists at low concentrations, may lead to the gradual formation of ICs and chronic progression of ICD. Similarly, in the case of exposure to a replicating virus such as hepatitis C virus, if the virus is not efficiently eliminated the infection may cause chronic ICD.

1.2.4.2 Rheumatoid factors

RFs are Abs that can recognize other Abs (Panush et al., 1971). They are usually of low affinity and, therefore, only bind to Ig in ICs rather than monomeric Ig (Johnson and Page Faulk, 1976; Normansell, 1971; Carson et al., 1981). It is believed that persistant ICs can activate RF producing B cells, with the resultant RF either binding to the persistant ICs and aiding their clearance or enhancing their pathological effects (Pisko et al., 1982; Coulie and Van Snick, 1983; Nemazee and Sato, 1983). Three types of RFs have been identified, namely Ab against the constant domains of the Fc or Fab regions of IgG or against the Ag combining site of Ab (anti-idiotypic) (Zanetti and Wilson, 1986). A characteristic feature of RA is the production of RFs against the Fc region of IgG molecules (Stewart et al., 1997). Ab against the constant domains of the Fab regions of IgGs were detected in the plasma of SLE and RA patients (Nasu et al., 1980). Anti-idiotype Abs have been detected in several models of IC formation in the glomerulus. These Abs may add to glomerular immune deposits and potentially could contribute to the chronicity of some forms of immunologic nephritis (Zanetti and Wilson, 1986). The precise role of anti-idiotype Abs in glomerular injury associated with tissue-bound primary ICs is not clear. However, it would be expected that the binding of these anti-idiotype Abs to

primary ICs may change the size, complement fixing ability and other biological properties of ICs trapped in tissues (Abrass, 1997).

1.2.4.3 Regulation of IC formation by complement

It has been known for many years that following activation of the classical pathway, complement inhibits formation of insoluble ICs (Heidelberger, 1941) and activation of the alternative pathway causes solubilisation of already formed insoluble ICs (Miller and Nussenzweig, 1975). Moreover, inhibition of formation of insoluble ICs has been shown to occur via interaction of C1 with soluble ICs (Schifferli et al, 1985) and this action is potentiated by C4b and C3b (Schifferli et al, 1982). In addition, a recombinant soluble form of FcγRII has been shown to inhibit IC precipitation (Gavin et al., 1995). An additional important consequence of the interaction of complement with ICs is to promote the clearance of ICs from the circulation by promoting the binding of ICs to erythrocyte CR1 and mononuclear phagocytic cells (see section 1.2.3). These findings suggest that complement deficiency, either environmentally induced or genetically based, may induce ICDs (Lachmann and Walport, 1987).

1.2.4.3.1 Environmentally induced depletion of complement

In some infectious diseases the presence of a high load of foreign Ag or the persistance of Ag (eg. chronic viral hepatitis) may lead to a profound depletion of complement since under these conditions the activation and catabolic rate of complement would be much higher than its synthesis. In such circumstances, the absence of complement or other regulatory plasma proteins may compromise the normal pathway of IC clearance.

The plasma level of complement components has been used as a tool for the diagnosis of ICD that are associated with hypocomplementaemia. These studies indicated that some ICD can cause hypocomplementaemia, whereas others do not (Table 1.5). It has been shown that the level of complement components C3 and C4 was usually decreased in the plasma of patients suffering from hypocomplementaemia-associated ICD (Table 1.6). In cases where ICs induced activation of the classical complement pathway the levels of both C3 and C4 were similarly decreased. However, in cases where activation of the alternative pathway predominated, the C3 component was reduced more than C4 (Hebert et al., 1991c). Despite the fact that the majority of ICD are associated with hypocomplementaemia, in some ICD plasma complement

Table 1.5 Immune Complex-Mediated Diseases with or without Complement Depletion

Conditions coincident with low plasma levels of complement
SLE
Membranoproliferative glomerulonephritis
Cryoglobulinemia
Glomerulonephritis of chronic infection
Postinfectious glomerulonephritis
Rheumatoid vasculitis
Idiopathic vasculitis
Drug-induced SLE
Repeated injection of foreign protein
Hypersensitivity to drugs
Chemotherapy for malignancy with immune complex formation
Thyroid diseases and glomerulonephritis
Jejunoileal bypass with vasculitis
B-cell lymphoproliferative disorder with immune complex formation
Conditions coincident with high plasma levels of complement
Systemic infections
Chronic inflammatory diseases (eg. RA)
Conditions with normal plasma levels of complement
IgA nephropathy
Idiopathic membranous nephropathy
Henoch-Schonlein purpura
Goodpasture's syndrome
Immunotactoid and fibrillary glomerulonephritis
C1q glomerulopathy

Adapted from Hebert et al., 1991c and 1997

Table 1.6 Complement Deficiency and Immune Complex Diseases

Complement Deficiency	Percent of Deficient Individuals	
	with ICD	with SLE
C1q, C1r or C1s	~ 50-90 %	Yes severe (94 %)
C1 inhibitor	Less than 25 %	?
C2	~ 50-90	Yes (33 %)
C3	More than 90 %	No (17 %)
C4	More than 90 %	Yes severe (75 %)
Factor H or I	Less than 25 %	?
C5, 6, 7, 8, 9	Less than 10 %	?

Adapted from Walport and Davies, 1996 and Hebert et al., 1997

levels do not change or are rarely associated with hypocomplementaemia (Hebert et al., 1991c) (Table 1.5). In addition, it has been shown that some conditions may actually raise serum complement levels (Table 1.5).

There is substantial evidence that the processing of ICs is abnormal in diseases such as SLE, which are associated with hypocomplementemia. In fact, two abnormalities have been detected in IC transport in patients with SLE and hypocomplementemia. Firstly, low plasma levels of complement result in the formation of larger ICs, which fix less complement and may not bind efficiently to erythrocyte CR1. Secondly, erythrocytes of patients with SLE carry reduced numbers of CR1 (Miyakawa et al., 1981; Iida et al., 1982). Although there is a genetic polymorphism in CR1 expression (Klopstock et al., 1965; Wilson et al., 1982) the bulk of evidence indicates that the reduction in CR1 is an acquired process (Walport and Lachman, 1988). There is evidence showing that CR1 is enzymatically cleaved from erythrocytes during the interaction of erythrocytes containing ICs with mononuclear phagocytic cells in the liver or spleen (Walport et al., 1987; Cosio et al., 1990; Birmingham et al., 1990; Davies et al., 1990a, 1990b). These abnormalities may result in a reduction in the binding of ICs to erythrocytes and may increase IC deposition in blood vessel walls. *In vitro* studies have indicated that the binding of ICs to erythrocyte CR1 prevents injury to endothelial cells by reducing the pro-inflammatory reaction of ICs with neutrophils (Beynon et al., 1994). These observations provide evidence that erythrocyte CR1 may act as a buffer for toxic ICs in the circulation and prevent their interaction with other cell types while delivering ICs to the fixed mononuclear phagocytic cells in the liver or spleen (Davies et al., 1995).

Major abnormalities in IC processing by the mononuclear phagocytic system were observed in humans with acquired complement deficiency (Davies et al., 1992). The uptake of ICs by spleen showed complete complement dependence (Davies et al., 1993), a correlation being observed between defective uptake by spleen and the degree of hypocomplementaemia (Davies et al., 1992). In contrast, the uptake of ICs by the liver was increased in patients with hypocomplementaemia compared to normal subjects but the ICs were rapidly released from the liver back into the circulation. It was proposed that in normal subjects the complex of C3b-IC may engage both FcR and C3b receptors on liver phagocytes (Kupffer cells) and may result in efficient uptake and internalization of ICs, whereas in SLE patients the absence of C3b may result in a less efficient interaction of ICs with FcR and consequently impaired uptake. Based on this

model, uptake of ICs by splenic phagocytes appears to be totally C3b receptor dependent.

1.2.4.3.2 Effect of genetic deficiencies in complement and complement regulatory proteins on IC clearance

Although most complement deficiencies are known to be environmentally induced, a number of genetic deficiencies in complement have been shown to be associated with a high incidence of ICDs (Table 1.6). For example, 30 of 32 patients with hereditary C1q deficiency (or C1 deficiency) have a dramatically high prevalence of ICDs (Bowness et al., 1994) indicating that the presence of C1q (or whole C1) may be necessary to prevent the development of ICDs (Schifferli, 1987; Schifferli et al., 1982, 1985, 1987). It should be noted, however, that although C1q deficient patients are shown to develop SLE, the presence of whole C1 rather than just C1q may be necessary for the prevention of ICDs.

The most striking feature of these genetic deficiencies is that deficiencies in complement components involved in the classical or lectin pathways (eg. C1, C2, C4) are associated with a very high incidence of ICDs, particularly SLE (Table 1.6). In contrast, deficiencies in components associated with the alternative pathway or the MAC result in a much lower incidence of ICDs (Table 1.6). Interestingly, C3 deficiency is associated with a high incidence of other ICDs but not SLE.

1.2.5 IC-mediated diseases

Under normal conditions the interaction of Abs with their cognate Ags should result in the clearance of ICs by the RES. However, due to a range of genetic defects (eg. see Table 1.6) (Leber and McCluskey, 1974; Theofilopoulos and Dixon, 1980; Schifferli, 1996) or to the excessive formation of ICs which may saturate FcR and deplete complement components (eg. C1, C3, see Table 1.5), ICs may escape RES clearance (Walport and Davies, 1996; Hebert et al., 1997). The escaped-ICs are pathogenic macromolecules with properties that are entirely different from Ags or Igs themselves. Escaped-ICs may bind to tissues by nonspecific mechanical means, eg. in renal glomeruli, in joints or in blood vessels. Persistance of these trapped ICs in tissues can lead to localized accumulation of activated complement components and the attraction of phagocytic cells (see below) (Theofilopoulos, 1980; Theofilopoulos and Dixon,

1980). The escaped-ICs also may interact with phagocytic cells in tissues leading to activation of the local phagocytic cells and a resultant release of cytokines, vasoactive substances, and activators of the coagulation cascade (Wener and Mannik, 1986; Haakenstad et al., 1976). Collectively these effects are proinflammatory and may cause localized tissue damage and, ultimately, pathological effects.

Kidneys, joints and blood vessel walls are the most common sites susceptible to deposition of plasma CICs since the capillaries in renal glomeruli (to form urine) and synovia (to form synovial fluid) are the vessels in which plasma is ultrafiltered at high hydrostatic pressure (Abbas et al., 1991). Since the kidney receives 25% of cardiac output, the Ags, Abs and ICs are delivered to the kidney at a high rate. The glomerular capillary wall provides a surface upon which circulating proteins may be trapped non-specifically or may directly interact with constituents of the capillary wall. Almost all glomerular diseases are mediated by abnormal regulation of the immune system and most of them are mediated by ICs (Abrass, 1997).

Necrosis and cellular infiltrates (predominantly composed of neutrophils) are the two morphological hallmarks of ICDs. Sites of necrosis often contain fibrin because of leakage of plasma proteins and is termed "fibrinoid necrosis". In this section ICDs are discussed where organ dysfuction results primarily from tissue damage caused by the deposition of ICs, presumably resulting from abnormal regulation of IC processing and clearance.

1.2.5.1 Glomerulonephritis

Glomerulonephritis (GN) is one of the most characteristic pathological conditions, caused by the deposition of blood borne ICs in the glomerulus. Diseases that are associated with GN are listed in Table 1.7. ICs can accumulate in the glomerulus in three ways, namely (a) ICs may initially form in the circulation and as a consequence of impaired clearance they may be deposited in the glomerulus, (b) ICs may be formed *in situ* by Ab reacting with Ag, such as DNA, trapped in the glomerulus and (c) ICs may result from Ab reacting directly against intrinsic glomerular Ag.

The size of ICs is shown to be an important factor in their localization in the glomerulus (Wener and Mannik, 1986). In IC-mediated GN (ICGN) latticed insoluble ICs accumulate in the mesangium and subendothelial space, whereas

Table 1.7 Pathological Conditions Caused by CICs

Glomerulonephritis (GN) (Kidney)	**Tubulointerstitial Nephritis (TIN)** (Kidney)	**Vasculitis** (Blood vessel wall)	**Arthritis** (Joint)
SLE	SLE	SLE	SLE
IgA Vasculitis	IgA Nephropathy	RA	RA
Cryoglobulinemia	Cryoglobulinemia	Cryoglobulinemia	Polyarthritis Nodosa
Goodpasture's Syndrome	Serum Sickness	IgA Vasculitis	Acute Rheumatic fever
Membranous Nephropathy	Sjorgen Nephropathy	Polyarthritis Nodosa	
Hypocomplementemia		Hypocomplementemia	
		Giant-Cell Arteritidis	
		Henoch-Schonlein Purpura	
		Lymphomatoid granulomatosis	
		Churg-Strauss Syndrome	
		Wegener's Granulomatosus	
		Hypersensitivity Vasculitis Syndrome	

Adapted from Haynes, 1992 and Abrass, 1997

small soluble ICs penetrate the glomerular basement membrane and deposit in the subepithelial space (Mannik et al., 1983; Agodoa et al., 1983). These features of ICs indicate that ICs containing the same Ag can cause various type of ICGN. It also has been demonstrated that the affinity of Ab for Ag may affect the IC deposition sites. For example, in animals the formation of membranous nephropathy (Table 1.7) was induced by the injection of low affinity Ab which deposited ICs in the subepithelial space rather than in the mesangium or subendothelial space (Iskandar and Jennette, 1983; Steward, 1979). On the other hand, injection of high affinity Ab resulted in the formation of large insoluble ICs which were either cleared by phagocytosis or were deposited in the mesangium and subendothelial space (Steward, 1979). In non-inflammatory glomerular disease it has been shown that CICs can also indirectly initiate glomerulosclerosis when the Ig deposits are not detected but the immune system is still activated in the glomerulus (Savin, 1993).

Deficiencies in FcR function have also been shown to be related to diseases such as ICGN. A number of studies have clearly indicated that the saturation or impairment of FcR-mediated phagocytosis leads to IC deposition in various organs (Kijlstra et al., 1978; Mauer et al., 1972). Futher studies have demonstrated that the enhancement of FcR-mediated phagocytosis minimizes the accumulation of immune deposits in the kidneys (Abrass, 1984). In addition to facilitating the clearance of ICs, FcR are crucial for the initiation of inflammatory responses which are amplified by cytokines and complement (Sylvestre and Ravetch, 1994). FcR ligation also has been shown to increase expression of IL-10 (Tripp et al., 1995) which in turn increases the expression of FcR. Thus by a positive feedback, FcR ligation enhances phagocytosis. Glomerular epithelial and mesangial cells of the kidney have been shown to express FcR and ingest ICs. However, they may not be able to digest large and insoluble ICs (Mancilla-Jimenez et al., 1984; Neuwirth et al., 1988). These features of epithelial and mesangial cells may contribute to the accumulation of ICs in the glomerulus (Furness, 1993).

1.2.5.2 Tubulointerstitial nephritis

Tubulointerstitial nephritis (TIN) is an example of a pathological condition caused by IC deposition and cell-mediated destruction. Although the abnormality occurs in the interstitial tubules of the kidney, the mechanisms causing TIN are similar to the ones which affect the glomerulus of the kidney. Diseases that are associated with TIN are listed in Table 1.7. The disease is

classified according to the site that Abs bind to Ags and cause inflammation. The consumption of drugs such as penicillins, cephalosporins, and phenytoin have been implicated in TIN. It has been proposed that the CICs containing Ab and drugs may passively deposit in the interstitium and cause the disease or they may cause TIN by cell-mediated mechanisms.

A number of bacterial (eg. streptococcal) and viral infections have been implicated in TIN since Ab against streptococci have been shown to cross-react with the non-collagen-like domain of collagen IV which exists in the tubular basal membrane (Lehman et al., 1975). Tubular cells may be infected with cytomegalovirus and express new Ag which in turn become a target for Ab or cell-mediated immunity. CICs can also deposit in the renal interstitium of patients suffering from systemic disease such as serum sickness, IgA nephropathy, cryoglobulins, SLE and Sjorgen nephropathy (Table 1.6). When accompanied by GN they may lead to renal malfunction.

1.2.5.3 Vasculitis

Vasculitis is a pathological condition characterized by inflammation and necrosis of blood vessels, resulting in vessel occlusion and ischemia of tissues presumably due to lack of nutrient transport by involved vessels (Fauci et al., 1978; Cupps and Fauci, 1981, 1982; Fauci, 1983; Andrassy et al., 1983; McCluskey and Bhan, 1983; Haynes et al., 1986; Smoller et al., 1990; Smiley and Moore, 1989). The deposition of ICs in and around blood vessel walls is responsible for the initiation of vasculitis lesions in many of the syndromes listed in Table 1.7. Also there is evidence for pathogenic ICF in specific vasculitis syndromes. For example, in polyarthritis nodosa (hepatitis B associated vasculitis) ICs containing hepatitis B surface Ag are present in the circulation and tissues (Gocke et al., 1970) and can induce vasculitis ranging from urticarial vasculitis to systemic necrotizing vasculitis (Dienstag, 1981).

Several investigators have outlined mechanisms for the pathogenesis of vascular damage when ICs are not cleared by normal mechanisms. For example, pathogenic ICs can activate complement components that participate in the amplification phase of the inflammatory response via generation of chemotactic factors for neutrophils and monocytes such as C5a. Further activation of complement can lead to the assembly of the MAC, thereby causing cellular damage. Further phagocytic activation causes release of proteolytic enzymes (eg. elastase, cathepsin, proteinase 3), reactive oxygen metabolites and

proinflammatory substances such as leukotrienes, and prostaglandins. As a consequence of the resultant vessel damage, platelets may adhere to locally damaged endothelium, aggregate and obstruct blood vessels, and induce vessel necrosis and clot formation (Fauci et al., 1978; Van Es et al., 1984; Tosca and Stratigos, 1988). It is noteworthy that local characteristics of the blood vessels themselves may influence IC deposition. For example, structural and hemodynamic differences among various blood vessels may result in ICs being deposited at the branch point of vessels (Giacomelli and Weiner, 1974; Huttner et al., 1970).

Although the deposition of pathogenic ICs is responsible for the initiation of the vasculitis syndromes, other mechanisms may perpetuate the disease and cause further vessel damage. These include the production of Ab of the IgG4 subclass against lysosomal enzymes in neutrophils (anti-neutrophil cytoplasmic Ag, ANCAs) and monocytes (Van Der Woude et al., 1985; Kallenberg et al., 1991), anti-endothelial cell Ab-mediated vessel damage (Cines et al., 1984; Brasile et al., 1989), vessel damage due to pathogenic cellular immune responses and granuloma formation (Cupps and Fauci, 1981; Fauci, 1983; Fauci et al., 1978), and vessel damage or altered vessel function mediated directly by infectious agents (Dorff and Lind, 1976; Fernald, 1982; Liu et al., 1989).

1.2.5.4 Arthritis

Arthritis is a pathological condition characterized by inflammation of the joints. Many types of arthritis progress from a stage dominated by an inflammatory infiltrate in the joint to a later stage in which a neovascular pannus invades the joint and begins to destroy the cartilage (eg. in RA). Diseases that are associated with arthritis are listed in Table 1.7. In chronic joint inflammation the disease manifestation involves largely the activation of cellular immunity. However, it also has been suggested that the deposition of pathogenic ICs in both soluble and insoluble forms may, at least in part, cause joint inflammation (Edwards and Cambridge, 1998). The finding that cell-free synovial fluid of patients with RA contains soluble and insoluble ICs that can activate reactive oxidant production by macrophages supports this view (Robinson et al., 1994). Recent plasmapheresis studies (Balint, 1996) on the removal of CICs from different patients with ICDs (including RA), using a protein A/silica column, indicate that the removal or clearance of CICs may be of clinical benefit in these autoimmune disorders. Moreover, the majority of ICs in the synovium of inflammed joints in RA were found to contain IgG but not IgM and the majority of the IgG in the soluble and insoluble ICs was of the IgG4 subclass, indicating

that increased deposition of IgG4 in the joint may contribute to the pathogenesis of the disease (Zach et al., 1995).

1.2.6 Treatment of IC-mediated diseases

It has been proposed that IC deposits in tissues are in equilibrium with CICs (Abrass, 1997). Therefore reduction of ICs in the circulation may be a viable therapeutic approach for ICDs (Balint, 1996). For example, stimulating phagocyte function was shown to enhance plasma clearance of CICs and reduce glomerular deposits, whereas a reduction in the mononuclear phagocytic system (eg. after splenectomy) results in increased amounts of ICs in the circulation and their subsequent deposition in glomeruli (Abrass, 1984). Similarly, removal of ICs by plasmapheresis through a protein A column has been of some clinical benefit (Balint, 1996).

As described above, the majority of self tissue destruction caused by the deposition of ICs in tissues is mediated by the activation of complement pathways. Under such circumstances, one beneficial way of treating patients would be to temporarily attenuate the activation of complement. Four basic approaches could be used to diminish the biological activity of complement: (1) administration of agents like cobra venom factor that can deplete key components of complement such as C3 (Savige et al., 1989). (2) Administering agents that inhibit complement activation. Heparin is the only clinically available inhibitor of complement activation, but for efficient inhibition heparin has to be administered at a dose much greater than that needed to achieve anti-coagulation (Waxman et al., 1984). Soluble recombinant forms of CR1, MCP and DAF are candidates which can reduce complement-induced injury in experimental models of a number of diseases (Causer et al., 1995). However, because these recombinant proteins are immunogenic they only can be used for acute, not chronic treatment. It has been proposed that the release of CR1 might be a natural mechanism for the control of complement activation since CR1 on activated neutrophils has been shown to be cleaved and released into the surrounding medium (Danielsson et al., 1994). (3) Intravenous injection of high doses of Igs has been used to absorb activated complement components before they can bind to tissues and initiate further complement activation. Following such treatment the Fc portion of the injected IgG absorbs C3b and C4b (Ruiz de Souza et al., 1993) and aggregated IgG (~10 % of total injected Ig) binds C1 (Qi and Schifferli, 1995). (4) Complement components were removed from the circulation by plasmapheresis which was successful in controlling disease

progression in some cases (Shumak and Rock, 1984). However, other plasma components including Ab and coagulation factors are removed following plasmapheresis.

Vasculitis is the most common pathological condition associated with ICs and is caused by the deposition of ICs in blood vessels. Although some vasculitis syndromes can be controlled with a combination of cytotoxic drugs and glucocorticosteroids, therapy for vasculitis is usually not optimal and many vasculitis syndromes are refractory to therapy. A novel approach has been used to inhibit the proinflammatory effects of ICs trapped in the vasculature by administering mAbs that deplete leukocyte subsets, block the action of key leukocyte adhesion molecules or interfere with proinflammatory cytokine action. For example, administration of a combination of anti-CD4 and anti-CD52 Abs, which deplete CD4+ T cells and neutrophils respectively, in patients with positive ANCAs resulted in resolution of vessel inflammation (Mathieson et al., 1990). Similarly, use of CD11b mAbs which block Mac-1-mediated adhesion by myeloid cells inhibited inflammation and immune mediated vessel injury in many cases (Rosen and Gorden, 1989). It has also been found that interleukin 1 receptor antagonists are potent inhibitors of a wide variety of IL1-mediated proinflammatory functions and have been in human trials for the treatment of RA (Eisenberg et al., 1990, 1991). Other novel biological agents, which target tumour necrosis factor alpha (TNFα), including TNFα-blocking mAbs (Kavanaugh, 1998), and recombinant soluble TNF alpha receptors (Lorenz and Kalden, 1998; Moreland, 1998) are currently being used in clinical trials for the treatment of RA.

1.3 PART III Aims of this study

As outlined above (Part II), the clearance of ICs from the circulation is largely shown to occur via FcR and complement proteins. However, during my PhD studies I examined the ability of an additional plasma protein, HRG, to regulate the formation and clearance of ICs. As reviewed in Part I of this Chapter, HRG has been shown to bind to many ligands associated with the immune and blood clotting systems. Furthermore, preliminary studies suggested that HRG binds to human IgG and C1q, a result which allowed me to hypothesise that HRG may be another endogenous regulator of the formation and clearance of ICs. The aim of this thesis was to characterise the interaction of HRG with IgG subclasses and clarify the role of HRG in the formation and clearance of ICs, the interaction of RF with ICs and the solubilisation of already formed insoluble IC.

CHAPTER 2

MATERIALS AND METHODS

2.1 Reagents

Human myeloma IgG1κ, IgG1λ, IgG2κ, IgG2λ, IgG3κ, IgG3λ, IgG4κ, IgG4λ and IgMκ were purchased from Sigma, Calbiochem-Novabiochem and Accurate Chemicals. Bence Jones (BJ) proteins were a generous gift from Dr Bob Raison, University of Technology, Sydney. Human IgG (isolated from pooled human serum), human C1q, human IgM, bovine serum albumin (BSA, fraction V), ovalbumin (grade V), heparin (bovine lung) polyoxyethylenesorbitan monolaurate (Tween-20), dimethylsulphoxide (DMSO), phosphate-citrate buffer with sodium perborate capsules and 2,2'-azino-bis (3-ethylbenzthiazoline-6-sulfonic acid) diammonium (ABTS) were purchased from Sigma Chemical Co., St. Louis, MO. Biotinylated mAb specific for κ or λ light chains of rat IgG were purchased from Pharmingen, San Diego, CA. Carboxymethyl dextran cuvettes for the IAsys biosensor, 1-ethyl-3-(3-dimethylaminopropyl carbodiimide) (EDC), N-hydroxysuccinimide (NHS) and ethanolamine were purchased from Fisons Affinity Sensors, Cambridge, UK. Streptavidin (STP) was purchased from Progen Industries, Australia. The homobifunctional reagent *bis* (sulfosuccinimidyl) suberate (BS3), sulfosuccinimidyl 6-(biotinamido) hexanoate (NHS-LC- Biotin), gentle Ag/Ab elution buffer (a cuvette regeneration buffer gentle to the dextran matrix) and horseradish peroxidase (HRP)-conjugated STP (HRP-STP), were purchased from Pierce, Rockford, IL. Avid Al beads were purchased from BioProbe, Tustin, CA. Fluorescine isothiocyanate (FITC) conjugated STP (FITC-STP) was purchased from Amersham Life Science Limited, Buckinghamshire, UK. mAb MRII against FcγRI was kindly provided by Dr Hilary Warren (Canberra Hospital, ACT).

2.2 Purification of proteins

2.2.1 Purification of human C1q and 30 kDa fragment of HRG

Human C1q was purified from human serum using Biorex-70 ion-exchange chromatography followed by Sephacryl S-300 gel filtration as previously described (Tenner et al., 1981). Slight modifications of this procedure (namely omitting the $(NH4)_2SO4$ precipitation step) resulted in the co-purification of two other proteins. Reduced SDS-PAGE analysis demonstrated that purification of C1q by this procedure resulted in the co-purification of two proteins of 32 and 34 kDa. The proteins were electrophoretically transferred onto a Problott polyvinyle difluoride (PVDF) membrane, and after staining with Coomassie

Brilliant Blue, the 32 and 34 kDa bands were excised and subjected to N-terminal sequencing using an Applied Biosystems Inc 473A model sequencer.

2.2.2 Purification of native human HRG

Native human HRG of 75 kDa molecular weight was purified from fresh human plasma as previously described (Rylatt et al., 1981) by equilibrating a phosphocellulose column with loading buffer comprising 10 mM sodium phosphate (pH 6.8) containing 1 mM EDTA and 0.5 M NaCl. The plasma was mixed with EDTA and NaCl to final concentrations similar to the loading buffer and with [4-(2-aminoethyl)-benzenesulfonyl fluoride hydrochloride] (AEBSF) (ICN Pharmaceutical Inc., Costa Mesa, CA) at 100 μg/ml and aprotinin (a trypsin inhibitor) at 2 μg/ml. The plasma was passed through the equilibrated column and unbound protein was removed by extensive washing of the column with the loading buffer. Bound HRG was then eluted from the column using the same buffer containing 2M NaCl. Since the 30 kDa HRG co-purified with C1q, the C1q purification procedure also was used to purify the N-terminal 30 kDa fragment of HRG.

2.2.3 Purification of rabbit anti-ovalbumin IgG

Rabbit anti-ovalbumin IgG was purified from immunized rabbit serum by Na_2SO_4 precipitation and ion-exchange chromatography using a diethyleaminoethyl (DEAE)-Sephacel column. The IgG was collected from the break through peak as described (Easterbrook-Smith et al., 1988).

2.2.4 Purification of rat anti-ovalbumin IgG

Rat anti-ovalbumin IgG was purified using commercially available Avid-Al beads which contain a ligand with high affinity for IgG. The rat serum was passed through the column and then the column was washed extensively with 10 mM sodium phosphate (pH 7.2) plus 150 mM NaCl (phsophate buffered saline, PBS) containing 3mM NaN_3 (PBS-Az). The bound IgG was eluted using 0.1 M sodium acetate buffer, pH 3.0, and dialysed against PBS before storing the IgG in small aliquots at -20°C until use. The purity of IgG was always > 95%.

2.3 Conjugation of proteins

2.3.1 FITC conjugation of proteins

The protein (2 mg/ml) to be conjugated was extensively dialysed against 0.05 M boric acid, 0.2 M NaCl (pH 9.2). 50 µl of FITC (5 mg/ml) (Molecular Probes Inc, Eugene, OR) dissolved in DMSO was added to 1 ml of protein and the mixture incubated for 2 hours at room temperature in the dark. Unreacted FITC was removed by subjecting the sample to five cycles of concentration and dilution in an Amicon ultrafiltration apparatus (Amicon Inc, Beverly, MA). FITC-proteins were sterile filtered using a DynaGard 0.2 µm filter (Microgon Inc, Laguna Hills, CA), before storing at 4°C until use.

2.3.2 Biotinylation of proteins

The proteins to be biotinylated (eg. IgG, HRG, IgM, BJ proteins, BSA) were dissolved in PBS at a concentration of 1 mg/ml and then reacted with NHS-LC-biotin (1 mg/ml) (Pierce, Rockford, IL) for 30 min at room temperature. The reaction was stopped by the addition of Tris-HCl buffer (pH 8.0) to a final concentration of 100 mM. Unreacted biotin was removed by washing the sample extensively (five cycles of concentration and dilution) in a Centricon 10 microconcentrator (Amicon Inc), before storing the biotinylated proteins at -20°C in small aliquots until use.

2.4 Preparation of heat aggregated IgG

Human IgG (2 mg/ml) in PBS was heat aggregated by incubation at 63°C for 40 min and then chilling on ice for 2 h. The aggregated IgG was separated from non-aggregated IgG by fast performance liquid chromatography (FPLC) gel filtration using a Superose 12 column (Pharmacia, Uppsala, Sweden). The aggregated IgG was collected in the exclusion volume peak.

2.5 Preparation of Bence Jones proteins

The κ and λ BJ proteins (BJκ and BJλ) were a generous gift from Dr Bob Raisen, University of Technology, Sydney. The lyophilised proteins were dissolved in PBS. SDS-PAGE analysis showed that BJκ consisted of two bands of mol. wt. ~ 22 kDa and ~ 44 kDa, whereas the BJλ consisted of only a single band of mol. wt. ~ 44 kDa. These proteins were subjected to gel filtration using a Superose 12

FPLC column with the monomeric form of BJκ being separated from the dimeric form, whereas BJλ showed only a single peak as the dimer form. The dimeric form of both proteins was biotinylated (as in section 2.3.2) and was used in all biosensor studies.

2.6 SDS-PAGE

The purity of protein preparations was checked by SDS-PAGE analysis which was carried out as described (Laemmli, 1970). Aliquots of proteins were boiled in either reducing or non-reducing sample buffer and electrophoresed on a 12.5% or 10% acrylamide gel. After electrophoresis protein bands were identified by Coomassie Brilliant Blue staining of the gel. The purity of the HRG and IgG preparations as judged by the intensity of the contaminating bands was always > 95%.

2.7 Precipitin curve analysis of ICs containing rabbit IgG and ovalbumin

Anti-ovalbumin IgG (1 mg/ml) was mixed with different concentrations of ovalbumin at Ag : Ab ratios in the range of 0.005-0.06 (w/w) in PBS containing 10 mg/ml BSA (PBS-BSA) and 3 mM NaN_3 (azide) (PBS-BSA-Az) to a final volume of 1 ml and incubated overnight at 37°C. The insoluble ICs in each suspension were collected by centrifugation (104 x g, 1 min), washed three times in PBS, and then dissolved in 0.2 M NaOH. The extent of IC formation was then calculated by measuring the absorbance of each solution at 280 nm, assuming E 0.1% (w/v) = 1.4 for IgG.

2.8 Formation of insoluble ICs

2.8.1 Formation of insoluble ICs containing ovalbumin and rabbit anti-ovalbumin IgG

The formation of insoluble ovalbumin : anti-ovalbumin IgG ICs was carried out by incubating rabbit polyclonal anti-ovalbumin IgG (or rat polyclonal anti-ovalbumin IgG) in PBS-Az and different amounts of HRG and/or C1q for 5 min in a quartz reaction vessel (final volume 1 ml) maintained at 37°C. The formation of insoluble ICs was initiated by the addition of ovalbumin at an equivalence Ag : Ab ratio. Since the absorbance due to light scattering of a suspension of particles is related to the average size of the particles, the

formation of insoluble ICs was monitored by measuring the absorbance of samples at 350 nm, using a Varian Cary-1 spectrophotometer as described (Gorgani et al., 1997).

2.8.2 Formation of insoluble ICs containing RF and human IgG.

The formation of insoluble ICs was initiated by the addition of human IgG (from pooled human serum) to solutions of anti-human IgG Abs. Insoluble IC formation was studied in three different systems namely: (1) rabbit anti-human IgG (Fc) Ab (69 μg/ml) were incubated without or with different concentrations of HRG in PBS-Az in a quartz reaction vessel (final volume 1 ml) maintained at 37°C. Insoluble IC formation was initiated by the addition of human IgG which was either treated or untreated with HRG at different Ag : Ab ratios. (2) RF (8 IU/ml) was incubated in PBS-Az without or with different concentrations of HRG and insoluble IC formation was initiated by addition of heat-aggregated human IgG which was either treated or untreated with HRG at different Ag : Ab ratios. (3) biotinylated human IgG (b-IgG, from pooled human serum) (30 μg/ml) was incubated without or with different concentrations of HRG for 20 minutes and then STP was added to form ICs in a quartz reaction cuvette. After 20 minutes incubation, RF (8 IU/ml) which was treated or untreated with HRG, was added to the mixture of STP and b-IgG to initiate the formation of insoluble ICs. In all instances the formation of insoluble IC was monitored by measuring the absorbance of samples at 350 nm using a Varian Cary-1 spectrophotometer as described (Gorgani et al., 1997).

2.9 Solubilization of preformed insoluble ICs by HRG.

Ovalbumin at Ag : Ab ratios between 0.005 and 0.05 was added to a solution of rabbit anti-ovalbumin IgG (900 μg/ml) in PBS-BSA-Az containing 20 μM Zn^{2+} (PBS-BSA-Zn-Az) in an Eppendorf tube. Tubes were rotated for 1 hr at 37°C, and then the mixtures were further rotated for 12 hours at 37°C without or with addition of 150 μg/ml of HRG. In some experiments different concentrations of HRG were incubated with preformed insoluble ICs containing anti-ovalbumin IgG (900 μg/ml) and ovalbumin at equivalence Ag : Ab ratio to assess the effect of different concentrations of HRG on the solubilisation of preformed insoluble ICs. In all instances, after 12 hours rotation of insoluble ICs with or without HRG, the samples were centrifuged at 104 x g for 1 minute to collect insoluble ICs. The pellets were washed three times in PBS and then dissolved in 0.2 M NaOH. The absorbance of each solution was measured at 280 nm assuming

that the E 0.1% (w/v) = 1.4 for IgG. The percent precipitation was calculated for each sample and was plotted against the ovalbumin/IgG ratio (w/w) or plotted against the concentration of HRG.

2.10 Cell culture

The human THP1 and U937 monocyte cell lines, and human Jurkat ($CD4^+$) leukaemic T-cell line and human MT4 ($CD4^+$) T-cell line were all cultured in RPMI-1640 (Gibco, Gaithersburg, MD) supplemented with 10% heat-inactivated fetal calf serum (FCS) (Commonwealth Serum Laboratories, Melbourne, Australia) and antibiotics (penicillin 120 mg/l, streptomycin 200 mg/l, neomycin 200 mg/l) at 37°C in a 5% CO_2 atmosphere. The cell lines were routinely subcultured at ~ 0.25 x 10^6 cells/ml and allowed to grow to the maximum concentration of ~ 1 x 10^6 cells/ml.

2.11 Immunofluorescent flow cytometry

The cultured cells were transfered to plastic 50 ml Falcon tubes (Becton Dickinson, Lincoln Park, NJ) and centrifuged at 1500 rpm (450 x g) for 5 minutes. Supernatants were discarded and the cells were washed three times in PBS. The concentration of cells was determined using a haemocytometer and the cell suspensions pelleted and resuspended in PBS-BSA or PBS-BSA containing 20 μM Zn^{2+} (PBS-BSA-Zn) buffer to a final concentration of 1 x 10^7 cells/ml. The cell suspensions were then pipetted (25 μl/well) into each well of a 96-well V-bottomed plastic plate (Nunc, Roskilde, Denmark), human HRG was added at different concentrations (25 μl/well), and the mixture incubated for 1 hr on ice. The cells were washed three times by centrifugation (800 x g, 1 min) with the appropriate buffer to remove the unbound HRG, and b-IgG or FITC-IgG conjugate was added in the appropriate buffer and incubated with the cells for 1 hour on ice. The cells were washed three times by centrifugation and bound biotinylated IgG (b-IgG) was detected by incubating the cells with FITC-STP (~ 50 μg/ml). After removing unbound FITC-STP by centrifugation, the cells were resuspended in PBS-BSA or PBS-BSA-Zn buffer (50 μl/well), and fixed by the addition of 4% paraformaldehyde in PBS (50 μl/well).

The fluorescence intensity unit (FIU) of the cells was measured by flow cytometry using a FACScan (Becton Dickinson, Mountain View, CA). In some experiments cell populations were gated, according to the forward and side scatter, to eliminate the fluorescence deriving from dead cells, aggregated cells

or large insoluble ICs. The results obtained for each sample were analysed by the program "Cell Quest". Using this program, the Median FIU value of each fluorescence intensity histogram was determined and plotted against the concentration of ligand or inhibitor used.

2.12 Ovalbumin immunization of rats

Ovalbumin was dissolved in PBS at 10 mg/ml and mixed with complete Freund's adjuvant at a 1 : 1 ratio (v/v). Then 200 µl of this mixture was injected subcutaneously at four sites into DA rats. After 28 days the injection was repeated except that incomplete Freund's adjuvant was used. Twenty one days later the rats were injected intraperitoneally with 1 mg of ovalbumin in normal saline and 7 days later rats were bled, and their serum were collected.

2.13 ELISA assays

2.13.1 Binding of C1q to immobilized HRG

HRG (125 nM) was coupled for 1 hr to Maxi-sorb ELISA trays in 0.1 M $NaHCO_3$ buffer (pH 9.0). The trays were blocked with PBS-BSA and then incubated with C1q in PBS-BSA for 1 hr. Bound C1q was detected using a monoclonal mouse anti-C1q Ab (BUS-1) followed by incubation with a HRP-conjugated sheep anti-mouse Ab and colour development using o-phenylenediamine dihydrochloride (2.5 mg/ml) in a 0.05 M sodium citrate, 0.1 M sodium phosphate buffer (pH 5.0) containing 0.03% (v/v) hydrogen peroxide as substrate. The binding of C1q was dose-dependent in the concentration range tested (15-125 nM). Under these conditions non-specific binding was assessed using the mouse mAb anti-DNP-9 (a mAb to 2,4 dinitrophenyl) as a control. No significant level of non-specific binding could be detected using the control mAb, indicating that the signal observed using the BUS-1 mAb reflects C1q specific binding.

2.13.2 Binding of rabbit IgG to immobilized HRG

An ELISA assay was also used to study the binding of rabbit anti-ovalbumin IgG to immobilized HRG. HRG coupled Maxi-sorb ELISA trays were incubated with rabbit IgG (0.03-2 µM) in PBS-BSA overnight at room temperature. Bound IgG was detected using a HRP-conjugated polyclonal goat anti-rabbit Ab followed by colour development. Parallel experiments in which a HRP-conjugated polyclonal goat anti-sheep Ab was used instead of HRP-conjugated

goat anti-rabbit Ab, or in which BSA was coated onto the wells instead of HRG, indicated that the binding was specific for HRG.

2.13.3 Binding of human IgG , IgG subclasses, IgM and Bence Jones proteins to immobilized HRG

The binding of biotinylated forms of human IgG (from pooled human serum), IgG subclasses (myeloma derived), IgM and BJ proteins to immobilized human HRG was examined by ELISA. HRG (20 µg/ml) was immobilized on Maxi-Sorb ELISA trays by incubating in 0.1 M $NaHCO_3$ buffer (pH 9.6) for 1 hr at 37°C. The trays were blocked with PBS-BSA-Az for 1 hr at 37°C and then incubated with biotinylated proteins in the concentration range between 1.6 - 100 µg/ml in PBS-BSA-Az for 3 hours at 37°C. Unbound proteins were washed away three times with PBS-BSA containing 0.05 % Tween-20 (PBS-BSA-T). Bound biotinylated proteins were detected by incubating the trays with HRP-STP (in 1/500 dilutions) in PBS-BSA for 1 hr at 37°C. This was followed by incubating the trays with the colourimetric HRP substrate ABTS (0.2 mg/ml) for 30 minutes at 37 °C in a 0.05 M sodium citrate, 0.1 M sodium phosphate buffer (pH 5.0) containing 0.03% (v/v) sodium perborate (a substitute for hydrogen peroxide). The absorbance of the solution of each well was measured at 405 and 490 nm using an ELISA plate reader (dual end measurement). The results showed that the binding of these proteins to immobilized HRG was dependent on the concentration of added protein. There was no colour development in control experiments when either the trays were coated with BSA instead of HRG or when, instead of incubating the tray with biotinylated proteins they were incubated with biotinylated BSA (b-BSA). These control experiments, therefore, indicated that the binding of these proteins was specific for HRG.

2.14 Determination of binding constants using the biosensor

An IAsys resonant mirror biosensor (Affinity Sensors, Cambridge, UK) (Cush et al., 1993; Buckle et el., 1993) with a carboxymethyl dextran sensing cuvette was used to determine the kinetic constants and affinities of the binding of HRG to immobilized ligands (eg, IgG, C1q, IgM, BJ proteins). Except where indicated, all experiments were performed in PBS-BSA-T and at a temperature of 25°C. The BSA (1%, w/v) was included in the buffer to reduce non-specific binding. The reaction vessel was stirred continuously by the aid of a propeller. Binding was measured at 2 sec intervals, and the readout from the biosensor was in units of

arc-sec. Each binding reaction was routinely followed for 5 min. All binding experiments were performed at least in duplicate. The "Fast Fit" program supplied by Fisons was used to evaluate the kinetic constants (George et al., 1995).

2.14.1 Coupling of STP or C1q to the dextran matrix

STP or C1q was coupled via ε-amino groups to the carboxymethyl dextran sensing surface of the IAsys biosensor cuvette using EDC and NHS (Cush et al., 1993; Buckle et el.,1993). This was done by equilibrating the cuvette in PBS buffer containing 0.05 % Tween-20 (PBS-T) and then reacting the cuvette with a mixture of EDC/NHS for 7 min. Unreacted EDC/NHS was washed away with PBS-T followed by three washes with 0.01 M sodium acetate buffer (for immobilization of STP the pH was adjusted to 4.5 and for C1q immobilization the pH was adjusted to 5.0 using 2 M acetic acid). STP (50 μg/ml) or C1q (10 μg/ml) in indicated acetate buffer was added to the cuvette and allowed to react with the activated carboxyl groups for 5 min. Uncoupled STP or C1q was removed by washing with the appropriate acetate buffer, and unreacted succinimidyl groups were blocked by incubating with ethanolamine (1 M, pH 8.5) for 2 min. The cuvette was washed three times with the appropriate acetate buffer, and then washed with PBS-T followed by a wash with 10 mM HCl to remove any non-covalently bound protein. Consistent with studies using other proteins (eg. George et al., 1995), under these conditions there was no evidence that the 10 mM HCl wash affected the ability of the immobilised C1q to interact with soluble HRG since binding constants did not change significantly after repeated washing of the cuvette with 10 mM HCl, even when the first HCl wash of the cuvette was omitted to avoid possible denaturation of the immobilised C1q. A biosensor response of ~ 500 arc sec for the immobilized STP and 1800 arc sec for immobilized C1q were observed. According to the data provided by the manufacturer this response represents the coupling of 3 ng of STP and 11 ng of C1q per mm^2 of sensing surface.

2.14.2 Binding of biotinylated proteins to the biosensor surface

Biotinylated proteins (eg. b-IgG or biotinylated IgM (b-IgM)) were coupled to the immobilised STP as follows. Biotinylated protein (50 μg/ml) in PBS-T (eg. IgG or HRG) was added to the STP coupled dextran cuvette equilibrated in PBS-T, and allowed to bind to the immobilized STP for 5 min. Nonspecifically bound

biotinylated protein was removed by washing three times with PBS-T, followed by three washes with 10 mM HCl for 2 min (for three cycles).

2.14.3 Binding of protein ligands to proteins on the biosensor surface

Before immobilization of the biotinylated proteins on the STP-dextran, non-specific binding between the protein ligands and the STP-dextran was assessed by the addition of different amounts of the non-biotinylated protein ligands in PBS-BSA-T to the cuvette. Under these conditions no significant level of nonspecific binding of any of the protein ligands used in these study could be detected.

Preliminary experiments were performed to establish the concentration range of protein-ligand suitable for kinetic analysis. PBS-T was added to the protein coupled cuvette to establish a baseline (5 min) and protein-ligand was then added in PBS-T at different concentrations. Binding of the protein-ligand was studied by monitoring the association phase for 5 minutes. Subsequently, the cuvette was washed with PBS-T and the dissociation phase was monitored for 5 min. Bound protein-ligand was removed (cuvette regeneration) by washing with either 10 mM HCl or the gentle Ag/Ab elution buffer (Pierce). The baseline was then re-established after washing the cuvette with PBS-T. In the HRG inhibition experiments, HRG (15 μg/ml) was added to the cuvette, allowed to reach equilibrium for 5 minutes and then unbound HRG washed away before addition of protein-ligand. As previously (George et al., 1995), we found no evidence that the 10 mM HCl cuvette regeneration wash significantly affected the ability of the proteins to subsequently interact with immobilized proteins on the cuvette surface.

2.14.4 Evaluation of the kinetic constants

2.14.4.1 Conventional method of analysis of the biosensor data

The IAsys biosensor was provided with a digital DECpc 450D2LP computer. Data obtained with the biosensor were transferred directly to the "Fast Fit" program (Fison Applied Sensor Technology). This program uses an iterative curve fitting to derive the observed rate constant and the maximum response at equilibrium due to ligand binding at the particular ligand concentration. The association of a soluble ligand with an immobilized macromolecule can be described by the pseudo first order equation $R_t=R_0+E(1-e^{-k_{obs}t})$, when only one

binding site is available for the ligand (Cush et al., 1993). In this equation: R_t is the IAsys response at time t in units of arc secs (this is proportional to the concentration of ligand-protein complex at time t, $R_t \alpha$ [Ligand-Protein]$_t$), R_0 is the IAsys response at time t=0 in units of arc secs induced by the addition of the ligand solution to the buffer in the cuvette (this represents a net displacement of the biosensor signal and its value is determined by the Fast Fit program for each binding curve analysed, $R_0 \alpha$ [Ligand-Protein]$_0$), E is the maximum IAsys response in units of arc secs due to bound ligand at equilibrium (E α [Ligand-Protein]$_\infty$), and K_{obs} is the observed rate constant (termed k_{on} in Fast Fit) given by $K_{obs} = k_{on}[Ligand] + k_{off}$ (George et al., 1995). For two binding sites the "Fast Fit" program uses the equation $R_t=R_0+E_1(1-e^{-k_{obs1}t})+E_2(1-e^{-k_{obs2}t})$ to derive the kinetic constants (Cush et al., 1993). In this equation E1 and E2 are the maximum response at equilibrium due to binding of the ligand to the high and low affinity binding site, respectively; and k_{obs1} and k_{obs2} represent the observed rate constants for the high and low affinity binding site, respectively. This equation assumes that, at equilibrium, the ligand-protein complex is stable; thus, the equilibrium line must be parallel to the starting baseline ([Ligand-Protein]$_\infty$) and at least 80-90% of the data must be taken into account when fitting data to a curve for either single or double exponential binding.

2.14.4.2 Kinetic constants for HRG-C1q, HRG-IgM and HRG-IgG interactions

A linear relationship between k_{obs} and ligand concentration was obtained when the binding data for the interaction of HRG with immobilized C1q was fitted to a double exponential curve, whereas the binding data for the HRG-IgM interaction was fitted only to a single exponential. Using this method the k_{on} (on-rate) and k_{off} (off-rate) values for the interaction are given by the slope and y-intercept of the plot, respectively.

The binding of HRG to λ containing IgG subclasses (IgGλ) could only be fitted to a single exponential and not to a double exponential. A linear relationship was obtained by plotting k_{obs} versus ligand concentration for the interaction of HRG with these IgG subclasses (IgGλ). In contrast, no linear relationship was obtained by plotting k_{obs} versus ligand concentration for the interaction of HRG with immobilized human IgG (from pooled human serum) or human IgG subclasses containing κ light chain (IgGκ), indicating that the data does not fit an exponential curve. Therefore, in these instances, similar to other kinetic analyses (George et al., 1995), the first region of the progress curve that best fits the single

exponential term (assuming that thermodynamic equilibrium is reached) was used to evaluate the parameters for the highest affinity interaction. This was done by plotting $Ln((E-(R_t-R_0))/E)$ versus time and selecting the linear region of this plot.

In some instances the Fast Fit program was used to extrapolate the dissociation data to the baseline for determination of the k_{off}. Values of K_ds obtained by using the relationship $K_d=k_{off}/k_{on}$ were in good approximation with those obtained by Scatchard analysis of the extent of association (not shown).

CHAPTER 3

HISTIDINE-RICH GLYCOPROTEIN BINDS TO HUMAN IgG AND C1q AND INHIBITS THE FORMATION OF INSOLUBLE IMMUNE COMPLEXES

Abstract

Purification of the complement component C1q from human serum using an established method resulted in the co-purification of two 30 kDa proteins with a N-terminal sequence identical to human HRG. Therefore, to explore the possibility that HRG can interact with C1q, the ability of 75 kDa (native) and the 30 kDa proteins (presumably proteolytic N-terminal fragments of HRG) to bind to C1q was examined, using both ELISA and optical biosensor techniques. Both forms of HRG were found to bind to the human complement component C1q and also to purified human and rabbit IgG by ELISA. Kinetic analyses of the HRG-C1q and HRG-IgG interactions using the IAsys biosensor indicate two distinct binding sites with affinities K_{d1} 0.78×10^{-8} M and K_{d2} 3.73×10^{-8} M for C1q, and one binding site with affinity K_d 8.5×10^{-8} M for IgG. Moreover, the fact that both native and 30 kDa HRG bind to C1q and to IgG, suggests that the IgG and C1q binding regions on HRG are located in the 30 kDa N-terminal region of the HRG molecule. The Fab region of IgG is likely to be involved in the HRG-IgG interaction since HRG also bound to $F(ab')_2$ fragments with an affinity similar to that seen with the complete IgG molecule. Interestingly, the binding between HRG and IgG was significantly potentiated (K_d reduced from 85.0 to 18.9 nM) by the presence of physiological concentrations of Zn^{2+} (20 μM). Conversely, the presence of Zn^{2+} weakened the binding of HRG to C1q (K_d increased from 7.80 to 29.3 nM). Modulation of these interactions by other divalent metal cations was less effective with relative potencies being $Zn^{2+}>Ni^{2+}>Cu^{2+}$. An examination of the effect of native and 30 kDa HRG on the formation of insoluble ICs between ovalbumin and polyclonal rabbit anti-ovalbumin IgG, revealed that physiological concentrations of HRG can markedly inhibit insoluble IC formation *in vitro*. The results show that human HRG binds to C1q and to IgG in a Zn^{2+}-modulated fashion, and that HRG can regulate the formation of insoluble IC *in vitro*, thus indicating a new functional role for HRG *in vivo*.

3.1 Introduction

It is well established that certain autoimmune diseases, such as SLE and RA, are associated with the production of auto antibody (aAb) (Mountz et al., 1994). Moreover, *in vitro* studies have shown that aAb can be cross-linked with their cognate Ag to form insoluble ICs (Sittampalam & Wilson, 1984a), which can precipitate in target tissues (e.g. joint synovial membrane) and lead to a lack of nutrient transport and consequent tissue injury. Evidence suggests that the effective clearance of CICs is necessary to limit IC-mediated tissue injury (Charlesworth et al., 1982). Protective measures may include mechanisms which inhibit insoluble IC formation, as well as those which promote solubilisation of formed insoluble ICs.

Evidence suggests that the complement components C3b and C1q, can modulate the formation of insoluble IC, *in vitro*. Upon activation of the complement cascade the generation of complement C3b and its covalent binding to the Fc (Cγ2 or hinge domains) and/or Fab portion of IgG molecule, may both inhibit the formation of insoluble IC and promote their solubilisation (Anton et al., 1994; Schifferli, 1987; Takata et al., 1984). In contrast, C1q (a constituent of the C1 component of complement) is reported to enhance the formation of insoluble IC by binding to IgG molecules via the Cγ2 domain (Burton et al.,1980) and may lead to the cross-linking of IgG molecules (Geronski et al., 1985; Easterbrook-Smith et al., 1988). The interaction of C1q with the Fc region of IgG molecules in ICs may also activate the complement cascade by the classical pathway (Schifferli, 1987). In addition, C1q is reported to bind to specific receptors on normal endothelial cells through its collagen-like fragment and to act as an FcR for circulating IgG ICs (Zhang et al., 1986). In contrast, studies on the anti-opsonic effect of serum suggest that C1q inhibits the interaction between IgG and the FcR on neutrophils (Hakansson et al., 1982). Recently, it has been shown that a recombinant form of FcγRII also inhibits the formation of insoluble ICs (Gavin et al., 1995).

In order to compare the effects of rabbit and human C1q on the formation of insoluble IC between ovalbumin and rabbit anti-ovalbumin IgG *in vitro*, rabbit and human C1q was purified using an established method. During these studies two proteins with a N-terminal sequence identical to HRG co-purified with C1q (Gorgani et al., unpublished observation), suggesting that C1q may form a complex with this protein. Preliminary data also suggested that HRG may associate with IgG molecules. HRG is a 75 kDa protein present in human

plasma at a concentration of 150 μg/ml, and was first described by Heimburger et al. (1972). The protein has since been isolated from the plasma of other species such as mouse, rabbit, cattle and chicken. *In vitro* studies have implicated HRG in divalent metal ion binding component of serum (Guthans and Morgan, 1982), regulation of the coagulation cascade (Leung et al., 1984; Leung, 1986), regulation of growth factor action (Brown and Parish, 1994) and regulation of immune function (Rylatt et al., 1981; Saigo et al., 1990a, 1990b; Chang et al., 1992a, 1992b; Olsen et al., 1996). Its precise physiological role, however, remains to be determined.

In this study an ELISA and the IAsys resonant mirror biosensor were used to study the binding of human HRG to human C1q and IgG, and to determine the kinetic constants for these interactions. In addition, light scattering techniques (Easterbrook-Smith et al., 1988) were used to examine the effects of human HRG and C1q on the formation of insoluble IC between ovalbumin and polyclonal rabbit anti-ovalbumin IgG. The results show that physiological concentrations of HRG bind strongly to C1q and to IgG, and inhibit the formation of insoluble IC *in vitro*, suggesting a previously undescribed functional role for HRG.

3.2 Results

3.2.1 Human C1q co-purifies with and binds to HRG

My preliminary studies showed that purification of the complement component C1q from human serum using an established procedure (Tenner et al., 1981) employing Biorex-70 ion exchange chromatography followed by Sephacryl S-300 gel filtration resulted in the co-purification of a contaminating protein of 30-35 kDa molecular weight which migrated as a 32-34 kDa doublet under reducing conditions (see Figure 3.1). N-terminal amino acid sequencing of the two protein bands seen under reducing conditions, after their electrophoretic transfer to PVDF membranes, indicated that the residues identified in the N-terminal sequence of both bands (VSPTDXSAV) were identical to that reported for the N-terminal sequence of HRG (VSPTDCSAV) (Koide et al., 1986). Since the purification of forms of HRG in this molecular weight range (Heimburger et al., 1972), presumably derived from the cleavage of native 75 kDa HRG by plasmin and kallikrein in serum, has been reported (Smith et el., 1985; Lijnen and Collen, 1983) these findings suggested that the 30-35 kDa protein co-purified with C1q may be derived from the cleavage of native HRG (75 kDa) (see Figure 3.1) and that HRG may interact with C1q.

The possibility that C1q can interact with HRG was initially explored using an ELISA assay. Significant binding of soluble human C1q to 30-35 kDa and to 75 kDa (native) HRG, each immobilized onto the wells of a 96-well plate, was detected by the ELISA assay (data not shown). In order to validate these preliminary experiments the strength of the interaction between HRG and C1q was studied using the IAsys biosensor. C1q was immobilized onto the biosensor cuvette using the EDC/NHS procedure and the binding of soluble HRG to the immobilized C1q was studied by adding different concentrations of HRG in PBS-BSA-T. The biosensor traces in Figure 3.2A show that the binding of soluble HRG to immobilized C1q over a 5 min period exhibits saturation kinetics with near-maximal binding occuring with 320 nM HRG (see Figure 3.2A). Under these conditions no non-specific binding of HRG to the dextran matrix could be detected (not shown). Analysis of the data obtained from these studies using the Fast Fit program indicated that the data did not fit to a single exponential function but that it could be fitted to a double expontential function, indicating that HRG reacts at two different sites on immobilised C1q with about five-fold difference in affinity. The k_{off} and k_{on} for the higher affinity binding site was found to be $1.04 \pm 0.57 \times 10^{-3}$ s^{-1} and $1.39 \pm 0.095 \times 10^{5}$ M^{-1} s^{-1}, respectively. The

FIGURE 3.1 **SDS-PAGE analysis of native HRG and 30 kDa proteins co-purified with C1q.**

Native HRG and the 30 kDa proteins co-purified with C1q were analysed by SDS-PAGE (12.5 % gel) under reduced and non-reduced conditions, and then stained with Coomassie Brilliant Blue. Lane M, reduced molecular weight marker proteins; lane A, non-reduced 30 kDa HRG ; lane B, reduced 30 kDa HRG; lane C, non-reduced native HRG; lane D, reduced native HRG.

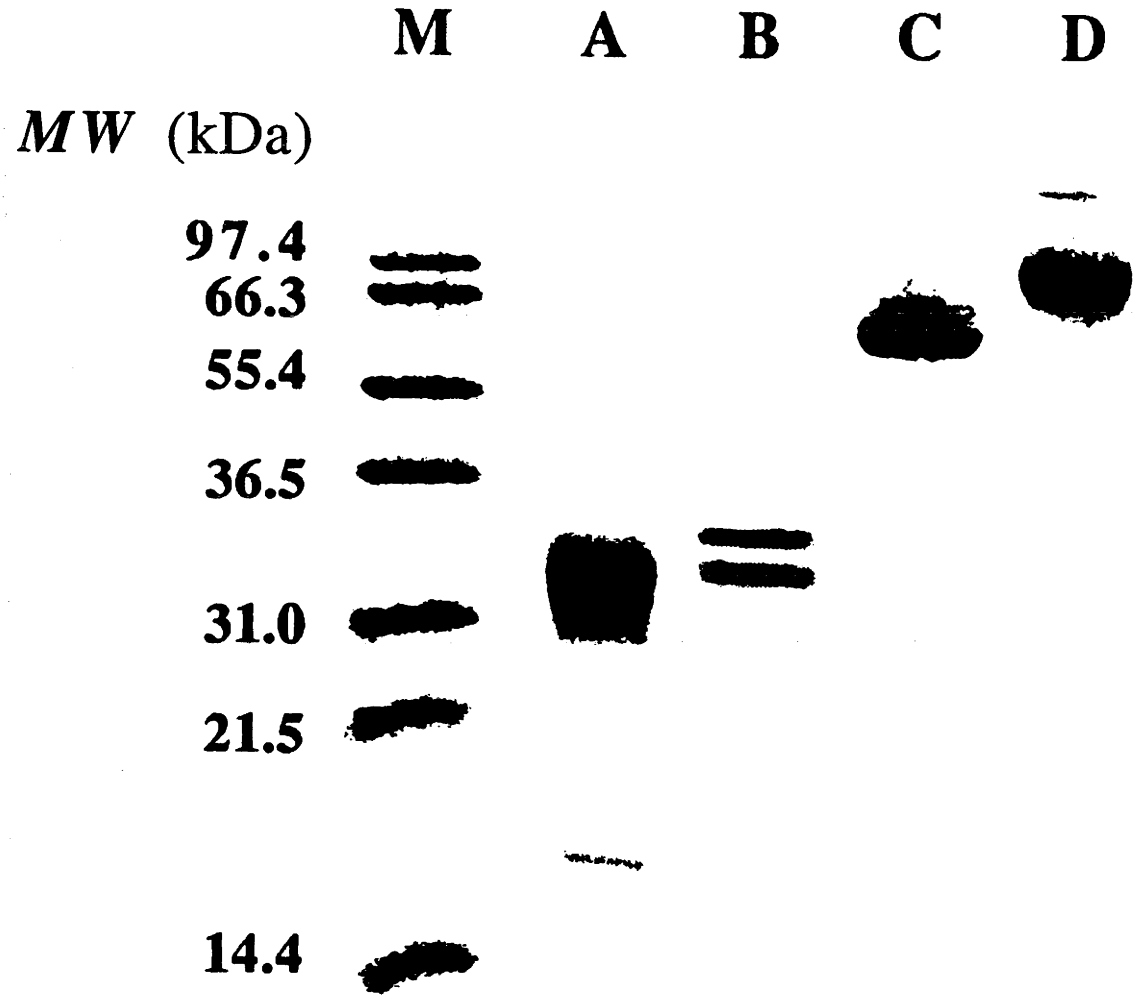
M
A
B
C
D
MW (kDa)
97.4
66.3
55.4
36.5
31.0
21.5
14.4

FIGURE 3.2 **Determination of the binding constants for the binding of soluble HRG to immobilized C1q.**

The IAsys resonant mirror biosensor was used to study the binding of HRG to C1q immobilized onto the biosensor surface. After establishing a baseline in PBS-BSA-T the indicated concentration of HRG was added to the cuvette and the association phase was monitored for 5 min. Overlay plots of the responses observed following the addition of different concentrations of HRG in the range of 20 to 320 nM are shown in (A). The cuvette was then washed with PBS-BSA-T and the dissociation phase was monitored for 5 min (not shown). For each concentration of HRG the values of $k_{obs(1)}$ and $k_{obs(2)}$ (rate constants) were determined by the linearization procedure using the Fast Fit program. As shown in (B), the plot of k_{obs} values related to high (●) and low (■) affinity binding sites against HRG concentration gives two straight lines with slopes of k_{on} and intercepts with the y-axis of k_{off}. Error bars show the ±SEM of triplicate experiments performed for each concentration of HRG; the absence of error bars indicates an error $< \pm 0.001$.

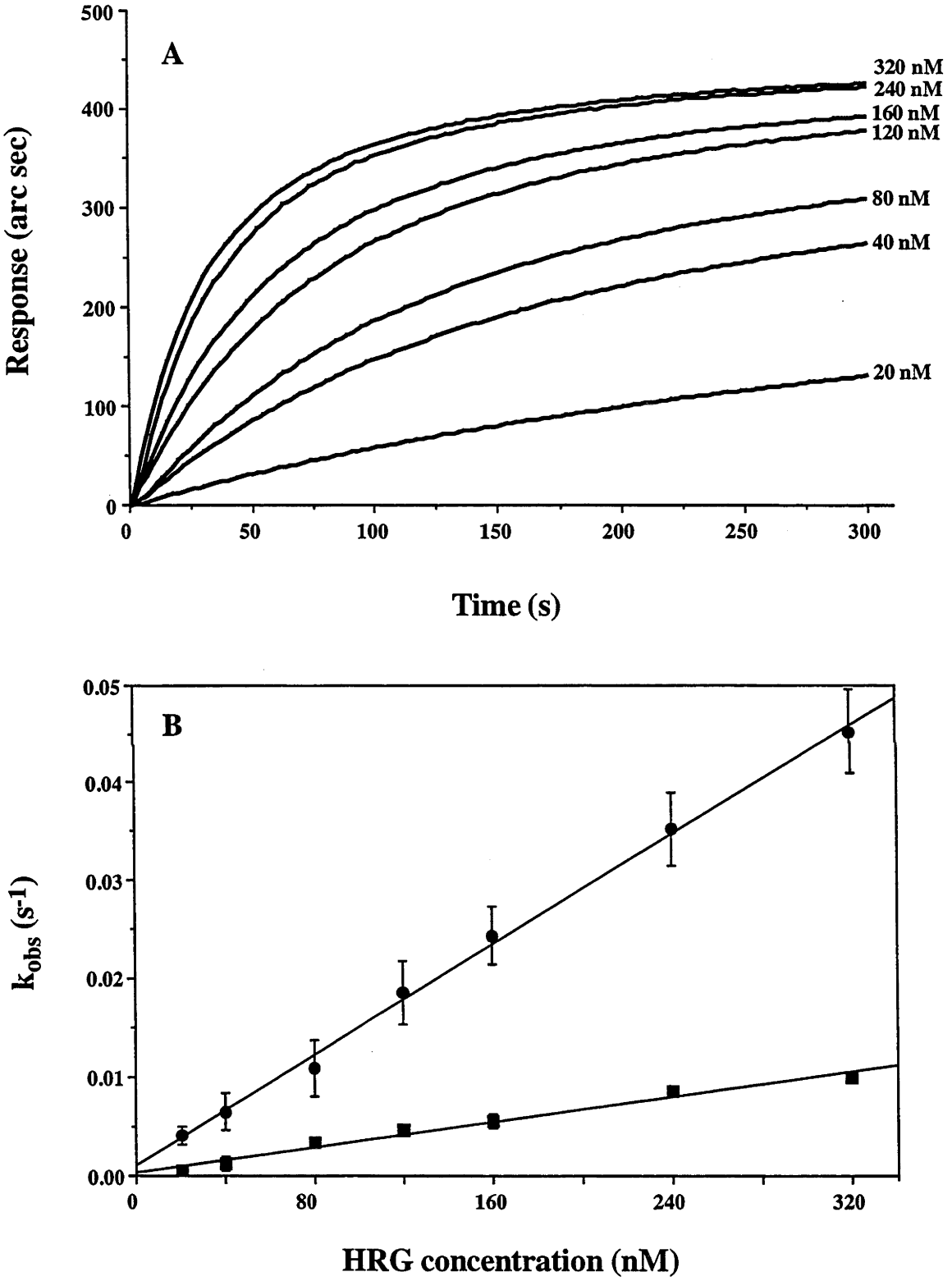
A
Response (arc sec)
500
400
300
200
100
0
0
50
100
150
200
250
300
Time (s)
320 nM
240 nM
160 nM
120 nM
80 nM
40 nM
20 nM
B
k_{obs} (s^{-1})
0.05
0.04
0.03
0.02
0.01
0.00
0
80
160
240
320
HRG concentration (nM)

Kd for this interaction (as shown in Figure 3.2B and Table 3.1) as determined either by Scatchard analysis of equilibrium binding data (not shown), or by using the relationship $K_d=k_{off}/k_{on}$, was found to be $0.78 \pm 0.46 \times 10^{-8}$ M. The k_{on} for the lower affinity binding site was determined from the slope of the plot shown in Figure 3.2B and found to be $0.32 \pm 0.027 \times 10^5$ M^{-1} s^{-1}. The k_{off} value was obtained from the intercept of the plot shown in Figure 3.2B ($k_{off}=3.60 \pm 2.30 \times 10^{-4}$ s^{-1}). According to the manufacturer k_{off} values in the range ($10^{-3} > k_{off} > 10^{-5}$ s^{-1}) need to be determined from the dissociation phase. Therefore, for the low affinity binding site the k_{off} value was determined by extrapolating the dissociation data to the baseline and then fitting to a curve using the Fast Fit program (not shown). The k_{off} was similar for all concentrations of HRG tested; the average $k_{off} = 1.17 \pm 0.16 \times 10^{-3}$ s^{-1}. The dissociation constant as determined using $K_d=k_{off}/k_{on}$ was $3.73 \pm 0.81 \times 10^{-8}$ M.

The binding of soluble C1q to immobilized HRG was studied also by immobilizing biotinylated HRG (b-HRG) via STP coupled to the dextran surface of the biosensor cuvette and adding C1q in solution at different concentrations in the range of 2.5-250 nM. The binding of soluble C1q to immobilized HRG over a 5 min period was dependent on the C1q concentration. There was no detectable non-specific binding of C1q to the immobilized STP (not shown). The binding was saturable at the higher C1q concentrations with near-maximal binding occurring with about 250 nM C1q. The k_{on} and k_{off} for the reaction as determined using the Fast Fit program were found to be $7.08 \pm 0.19 \times 10^5$ M^{-1} s^{-1} and $6.4 \pm 2.0 \times 10^{-3}$ s^{-1}, respectively, and the dissociation constant was $0.92 \pm 0.30 \times 10^{-8}$ M (see Table 3.1).

3.2.2 Human HRG binds to IgG

The ability of HRG to bind to C1q with high affinity, and the reported ability of C1q to enhance the formation of insoluble IC *in vitro*, prompted me to explore the possibility that HRG also binds to IgG. Preliminary experiments in which the binding of polyclonal rabbit anti-ovalbumin IgG to immobilized human HRG was examined using an ELISA assay indicated that HRG also interacts with rabbit IgG and that the binding is concentration dependent. A similar dose dependent increase in the binding was observed when the $F(ab')_2$ fragment of rabbit IgG was used instead of IgG, and when 30 kDa human HRG was used instead of native HRG (data not shown).

TABLE 3.1 **Rate and dissociation constants for the interaction of HRG with C1q and IgG/(Fab')$_2$.**

Kinetic constants were calculated by applying the "Fast Fit" program to the binding data obtained using the IAsys biosensor for the conditions indicated. In each instance the constants represent the mean ± SEMs of three independent experiments. The set of data in control represent constants related to the interaction in PBS-BSA-T.
* Off-rate (k_{off}) for these interactions were determined by using the dissociation phase.

Interaction	k_{on} ($M^{-1}s^{-1}$) x 10^{-5}	k_{off} (s^{-1}) x 10^{3}	K_d (M)x10^{8}
HRG to immob. C1q (high affinity)			
Control	1.39 ± 0.095	1.04 ± 0.57	0.78 ± 0.46
+ 20 mM Zn^{2+}	1.25 ± 0.043	3.63 ± 0.88	2.93 ± 0.80
+ 20 mM Zn^{2+} and 1 mM EDTA	1.48 ± 0.078	0.68 ± 0.33	0.47 ± 0.25
HRG to immob. C1q (low affinity)			
Control	0.32 ± 0.027	1.17 ± 0.16*	3.73 ± 0.81
+ 20 mM Zn^{2+}	0.22 ± 0.014	0.79 ± 0.23*	3.67 ± 1.28
+ 20 mM Zn^{2+} and 1 mM EDTA	0.34 ± 0.020	1.35 ± 0.36*	4.05 ± 1.29
C1q to immob. HRG	7.08 ± 0.19	6.4 ± 2.0	0.92 ± 0.30
HRG to immob. IgG			
Control	1.0 ± 0.054	8.60 ± 1.0	8.50 ± 1.50
+ 20 mM Zn^{2+}	1.40 ± 0.031	2.70 ± 0.67	1.89 ± 0.46
+ 20 mM Zn^{2+} and 1 mM EDTA	0.70 ± 0.033	13.0 ± 0.69	18.0 ± 1.83
HRG to immob. $F(ab')_2$	0.55 ± 0.029	4.70 ± 0.87	8.30 ± 1.7

The HRG-IgG interaction was further studied with the biosensor using immobilized IgG. For these experiments biotinylated human IgG was immobilized by binding to STP coupled to the dextran surface, and the binding of different concentrations of HRG to the immobilized b-IgG was monitored over a 5 min period. The data in Figure 3.3A indicates that native human HRG binds to human IgG, and that the binding is concentration dependent in the range of 10-400 nM HRG. The binding was saturable with near-maximal binding occurring with 400 nM HRG. The k_{obs} value for the binding of each concentration of HRG was calculated using the linearization procedure and the Fast Fit program. The plot of k_{obs} against the corresponding HRG concentration is shown in Figure 3.3B and gives a straight line with a slope of k_{on} ($1.0 \pm 0.054 \times 10^5$ M^{-1} s^{-1}) and an intercept with the y-axis of k_{off} ($8.6 \pm 1.0 \times 10^{-3}$ s^{-1}). The dissociation constant was $8.5 \pm 1.5 \times 10^{-8}$ M (see Table 3.1).

Experiments also were carried out to study the binding of human IgG to immobilized human HRG. For these studies the HRG was coupled to the dextran surface using EDC/NHS procedure or via the biotin-STP linkage (as above) or was chemically linked to a cuvette with an amino-silane surface using the amino reactive homobifunctional cross-linker BS3. Although the binding of C1q to HRG immobilized via the biotin-STP linkage was fast, strong and concentration dependent, under these conditions no significant binding of soluble human or rabbit IgG to the immobilized HRG could be detected. Thus, it appears that the direct covalent cross-linking of the HRG to the biosensor cuvette, as well as linking the HRG via biotin-STP, each can destroy the IgG binding site on the HRG.

The biosensor also was used to investigate the binding of human HRG to immobilized F(ab')2 fragments of rabbit IgG. For these experiments biotinylated F(ab')2 fragments were immobilized by binding to STP coupled to the dextran cuvette, and HRG was added at a concentration range of 10-625 nM in PBS-BSA-T. As previously, the binding and dissociation of HRG was carried out for 5 min. A dose-dependent increase in the binding of HRG to F(ab')2 fragments was observed. After calculating the k_{obs} for each concentration of HRG using the linearization and Fast Fit program the k_{on} and k_{off} of the reaction were found to be $0.55 \pm 0.029 \times 10^5$ M^{-1} s^{-1} and $4.70 \pm 0.87 \times 10^{-3}$ s^{-1}, respectively, and the dissociation constant was $8.30 \pm 1.70 \times 10^{-8}$ M (see Table 3.1). This dissociation constant is similar to that observed with the whole IgG molecule.

FIGURE 3.3 **Determination of binding constants for the interaction of soluble HRG with immobilized IgG.**

The IAsys resonant mirror biosensor was used to study the binding of HRG to biotinylated human IgG immobilized onto the biosensor surface by coupling to immobilized STP. The biosensor cuvette was equilibrated in PBS-BSA-T and HRG was added at the indicated concentrations and the association phase was monitored for 5 min. The cuvette was then washed with PBS-BSA-T and the dissociation phase was monitored for 5 min. The overlay plots for the different concentrations of HRG are shown in (A). The value of k_{obs} (rate constant) related to each concentration of HRG was determined by linearisation using the Fast Fit program and the results are shown in (B). The plot of k_{obs} against HRG concentration gives a straight line with a slope of k_{on} and an intercept with the y-axis of k_{off}. Error bars show the ±SEM of triplicate experiments performed for each concentration of HRG.

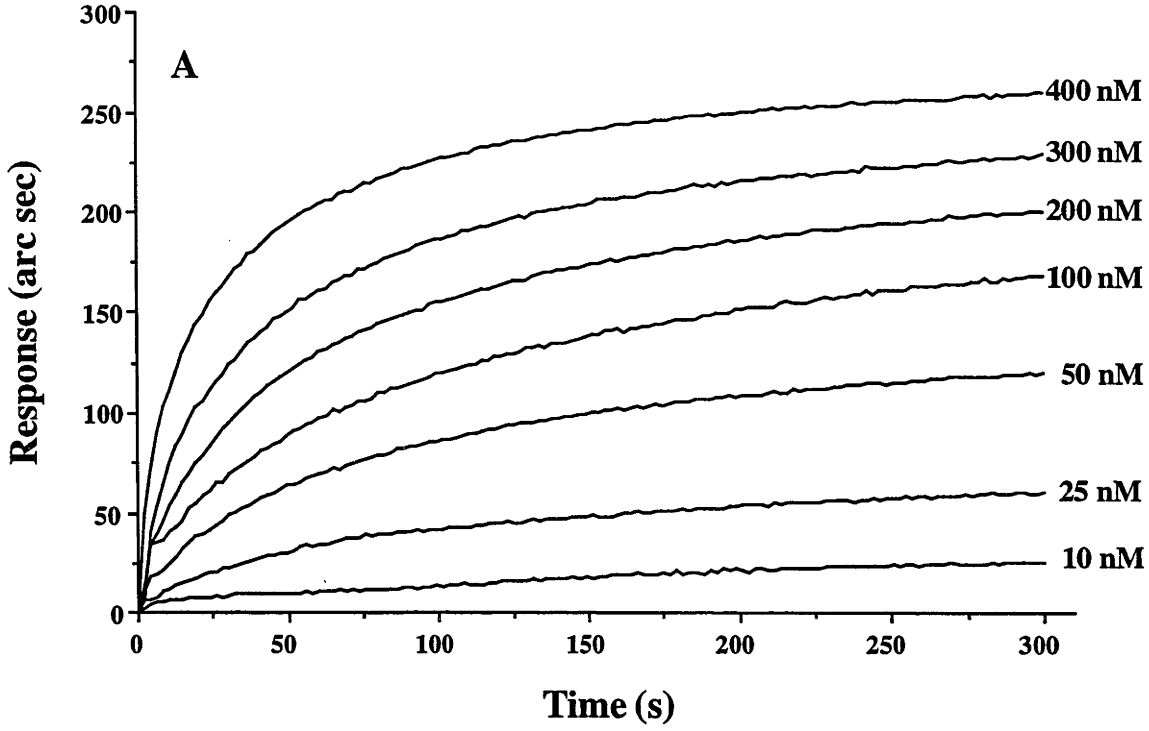
A
Response (arc sec)
Time (s)
400 nM
300 nM
200 nM
100 nM
50 nM
25 nM
10 nM
0
50
100
150
200
250
300

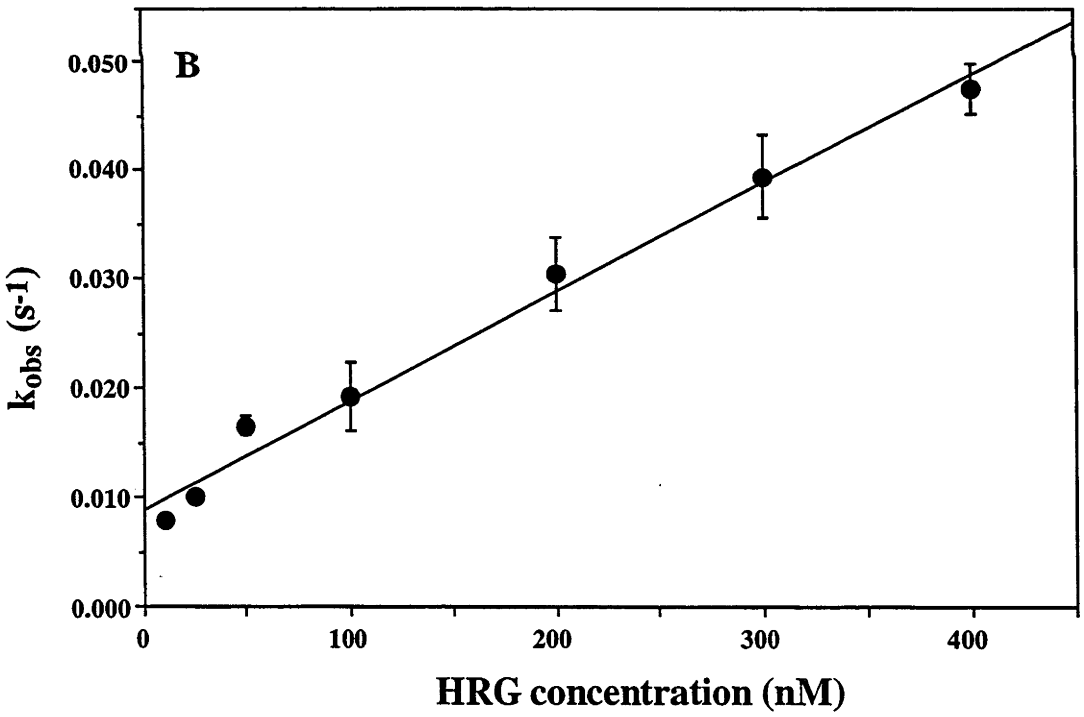
B
k_{obs} (s^{-1})
HRG concentration (nM)
0.000
0.010
0.020
0.030
0.040
0.050
0
100
200
300
400

3.2.3 Effect of Zn^{2+} on the binding of HRG to human IgG and to C1q

HRG is reported to bind divalent metal cations like Zn^{2+}, which can alter the ability of HRG to interact with heparin and to bind to T cells and elicit T cell responses (Kazama and Koide, 1992; Olsen et al., 1996). To determine whether Zn^{2+} also can affect the ability of HRG to interact with IgG or with C1q, binding studies using the biosensor also were carried out in the presence of 20 μM added Zn^{2+}, with and without 1 mM EDTA. These studies showed that mixing the HRG (100 nM) with different concentrations of Zn^{2+} (2.5-20 μM) increases the binding of HRG to the immobilized human IgG. The increase was positively correlated with the amount of added Zn^{2+} and the potentiation was $Zn^{2+}>Ni^{2+}>Cu^{2+}$ (not shown). As shown in Figure 3.4A the presence of Zn^{2+} potentiated the binding of HRG to immobilized IgG by 2-3 fold. In contrast, the presence of 1 mM EDTA markedly reduced the binding (probably by binding to trace metal ions in the PBS buffer) compared to that seen in the absence of added Zn^{2+} (see Figure 3.4A, and compare Figure 3.3B and 3.4B). The on-rate of the interaction between HRG and immobilized IgG increased from $1.0 \pm 0.054 \times 10^5$ M^{-1} s^{-1} in the absence of added Zn^{2+} (control) to $1.40 \pm 0.031 \times 10^5$ M^{-1} s^{-1} in the presence of added Zn^{2+}. Similarly, the presence of Zn^{2+} decreased the off-rate from $8.60 \pm 1.0 \times 10^{-3}$ to $2.7 \pm 0.67 \times 10^{-3}$ s^{-1}. Collectively, these changes in the on- and off-rates produced by Zn^{2+} resulted in approximately a five-fold increase in the affinity of HRG for IgG. Moreover, experiments carried out in the presence of Zn^{2+} and EDTA indicated that the on-rate of the interaction was decreased from $1.4 \pm 0.031 \times 10^5$ M^{-1} s^{-1} to $0.70 \pm 0.033 \times 10^5$ M^{-1} s^{-1} by the addition of 1 mM EDTA. These experiments also showed that in the presence of EDTA the off-rate of the reaction was increased from $2.70 \pm 0.67 \times 10^{-3}$ to $13.0 \pm 0.69 \times 10^{-3}$ s^{-1}, and the dissociation constant was increased from $1.89 \pm 0.46 \times 10^{-8}$ M to $18.0 \pm 1.83 \times 10^{-8}$ M following the addition of the EDTA. The two-fold reduction in the affinity of HRG for IgG produced by EDTA suggests that some metal ions may already be bound to the HRG, perhaps as a result of trace amounts of metal ions being present in the PBS used in these experiments.

Similar experiments carried out using immobilized C1q instead of IgG showed that, in contrast to the results observed with IgG, the affinity of HRG for immobilized C1q was decreased in the presence of 20 μM Zn^{2+}. At the two different HRG concentrations tested (50 and 600 nM) the inhibition of binding was dependent on the Zn^{2+} concentration (2.5-50 μM). Similar to the IgG-HRG interaction, the potencies of inhibition was $Zn^{2+}>Ni^{2+}>Cu^{2+}$. As shown in

FIGURE 3.4 **The effect of Zn^{2+} on the binding of native HRG to immobilized IgG.**

Pooled IgG (from human serum) was immobilized onto the biosensor surface and the binding of HRG to the immobilized IgG was measured in the absence and presence of 20 μM Zn^{2+}. For each experiment a baseline was established in PBS-BSA-T-Zn for 5 min before adding HRG at the indicated concentration (in the same buffer). HRG binding was followed for 5 min and the cuvette was washed with the same buffer before monitoring the dissociation phase (data not shown). For some experiments a baseline in buffer also containing 1 mM EDTA (PBS-BSA-T-Zn-EDTA) was obtained for 5 min before adding HRG in the same buffer. The interaction also was followed for 5 min before washing the cuvette with PBS-BSA-T-Zn-EDTA and monitoring the dissociation phase (data not shown). The maximum binding (in units of arc sec) versus ligand concentration is shown in (A). For each concentration of HRG the rate constant (k_{obs}) was determined by linearisation using the Fast Fit program. The measured k_{obs} values obtained from experiments carried out in PBS-BSA-T-Zn (●) and in the presence of 20 μM Zn^{2+} and 1 mM EDTA in the reaction buffer (■), were plotted against HRG concentration and are shown in (B). Error bars show the ±SEM of triplicate experiments performed for each concentration of HRG.

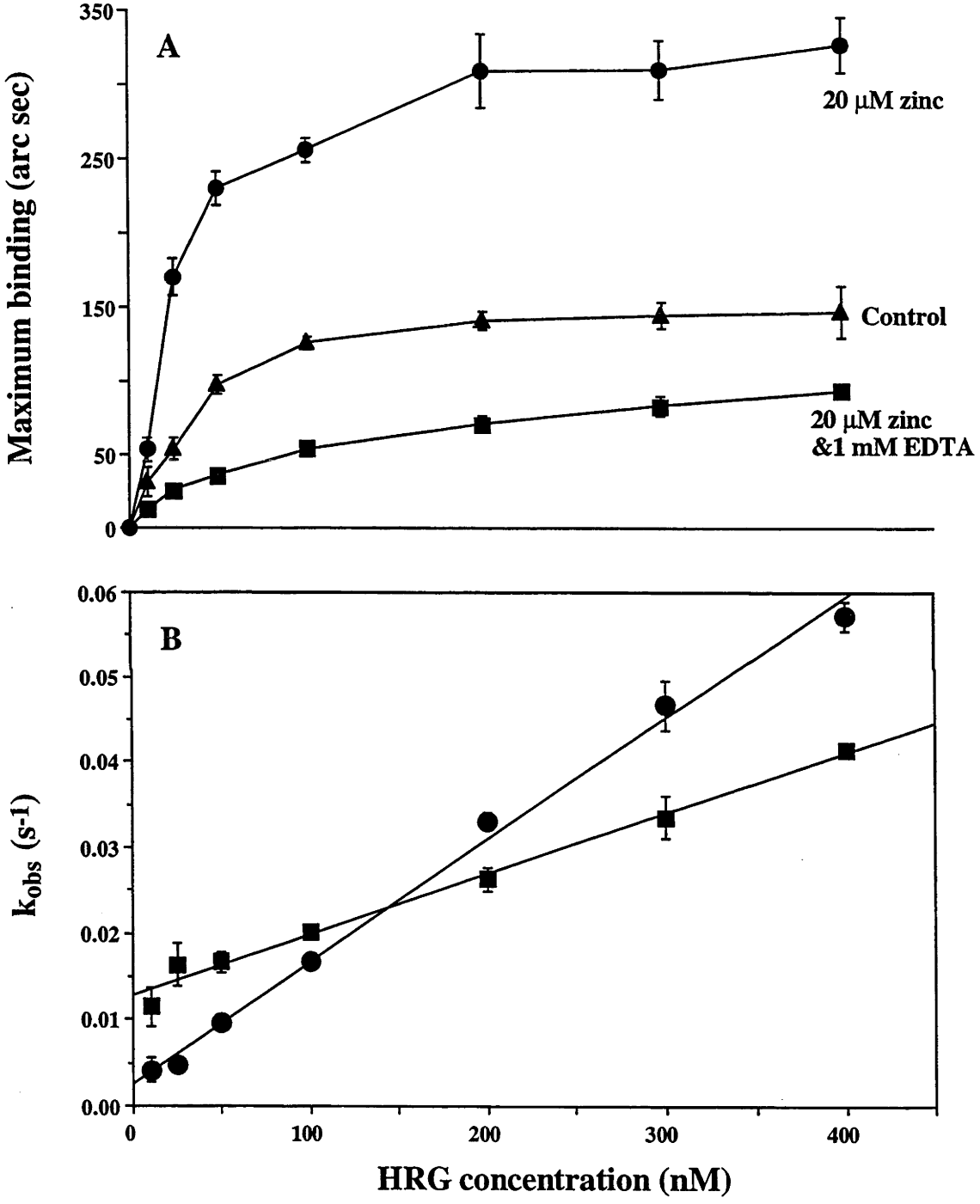
A
Maximum binding (arc sec)
350
250
150
50
0
20 μM zinc
Control
20 μM zinc
&1 mM EDTA
B
k_{obs} (s^{-1})
0.06
0.05
0.04
0.03
0.02
0.01
0.00
0
100
200
300
400
HRG concentration (nM)

FIGURE 3.5 **The effect of Zn^{2+} on the binding of native HRG to immobilized C1q.**

C1q was immobilized onto the biosensor surface and the binding of HRG to the immobilized C1q was measured in the absence and presence of 20 μM Zn^{2+} as described in the legend of Figure 3.4. The association phase of the interaction (in units of arc sec) versus time (for 600 nM HRG) is shown in (A). For each concentration of HRG the rate constants related to high ($k_{obs(1)}$) and low ($k_{obs(2)}$) affinity binding sites were determined by linearisation using the Fast Fit program. The measured $k_{obs(1)}$ and $k_{obs(2)}$ values obtained from experiments carried out in PBS-BSA-T-Zn (●) and in the presence of 20 μM Zn^{2+} and 1 mM EDTA in the reaction buffer (■), were plotted against HRG concentration and are shown for the high affinity site in (B) and for low affinity site in (C). Error bars show the ±SEM of triplicate experiments performed for each concentration of HRG.

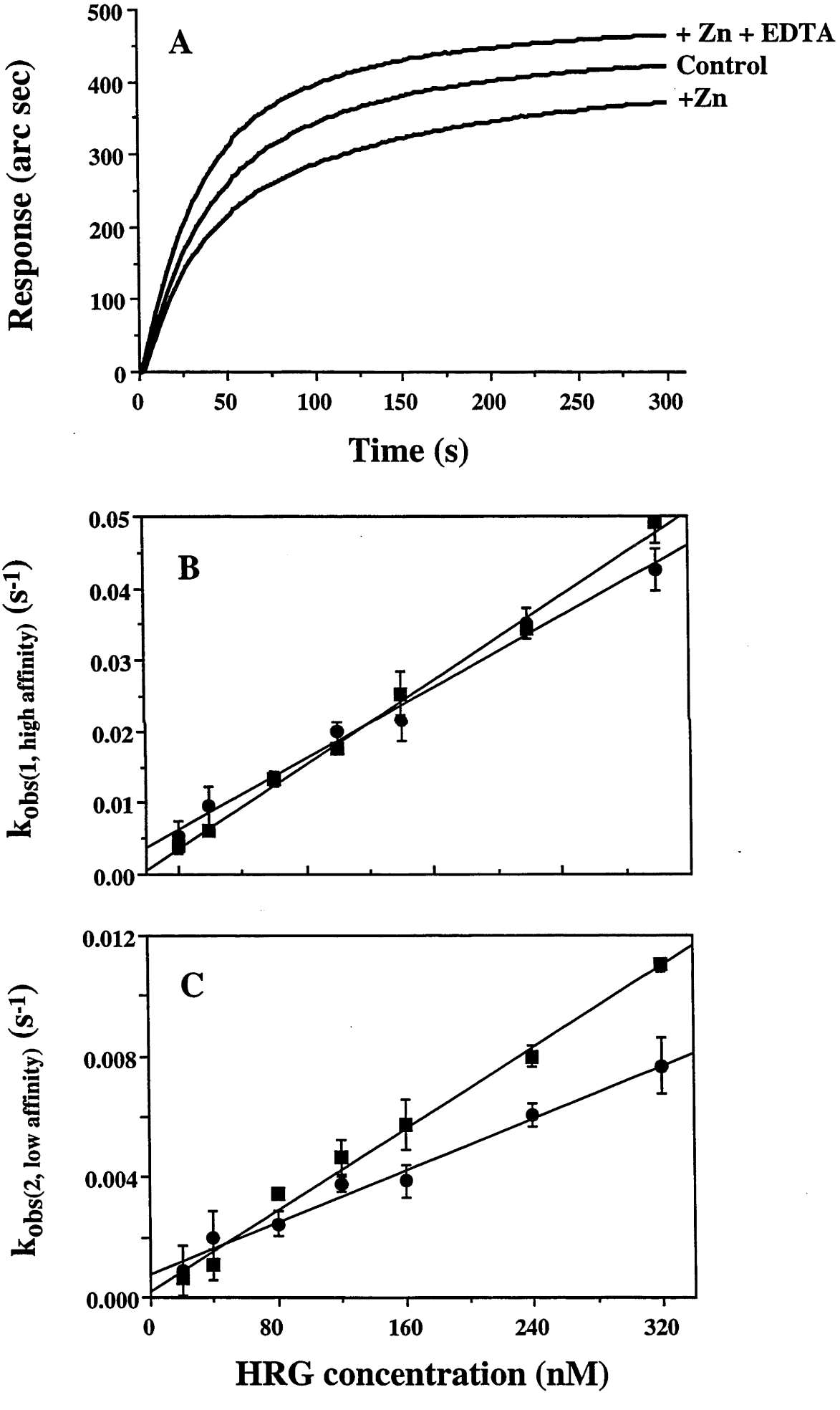
A
+ Zn + EDTA
Control
+Zn
Response (arc sec)
Time (s)
B
$k_{obs(1, high affinity)}$ (s^{-1})
C
$k_{obs(2, low affinity)}$ (s^{-1})
HRG concentration (nM)

FIGURE 3.6 **Effect of 30 kDa and native HRG and C1q on the formation of insoluble ICs.**

The formation of insoluble ICs was initiated by the addition of ovalbumin at an equivalence Ag : Ab ratio to a solution of IgG (175 μg/ml) pre-incubated with native HRG or C1q. To evaluate the inhibitory effect of 30 kDa HRG, the 30 kDa HRG was pre-incubated with a solution of IgG (200 μg/ml) and then ovalbumin was added at an equivalence Ag : Ab ratio. ICF was monitored as a function of time by measuring the absorbance at 350 nm associated with light scattering produced by the insoluble ICs that formed in the mixtures. The results in (A) show the increase in absorbance as a function of time due to formation of insoluble ICs for a control experiment (Δ, no additions), and for experiments carried out in the presence of 25 μg/ml C1q (□), and 150 μg/ml native HRG (o). The results in (B) show the time to reach 50% maximum absorbance as a function of the concentration of native HRG (●), 30 kDa HRG (o) or C1q (■). Each set of results is representative of 5 experiments performed in triplicate.

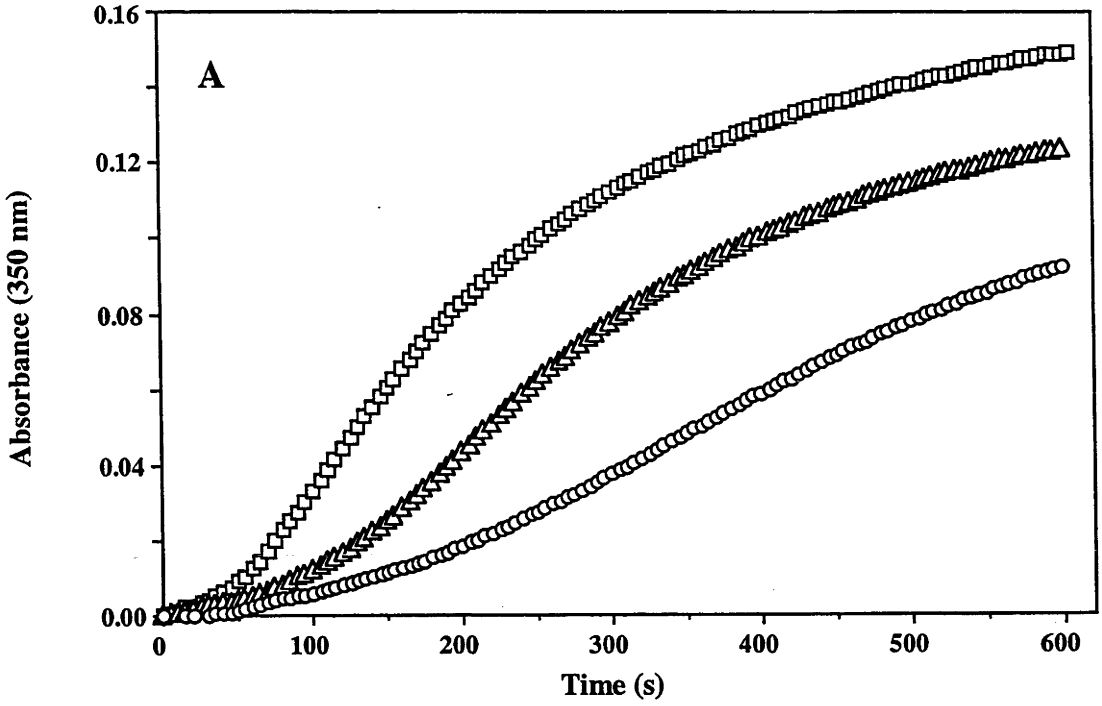
A
Absorbance (350 nm)
0.16
0.12
0.08
0.04
0.00
0
100
200
300
400
500
600
Time (s)

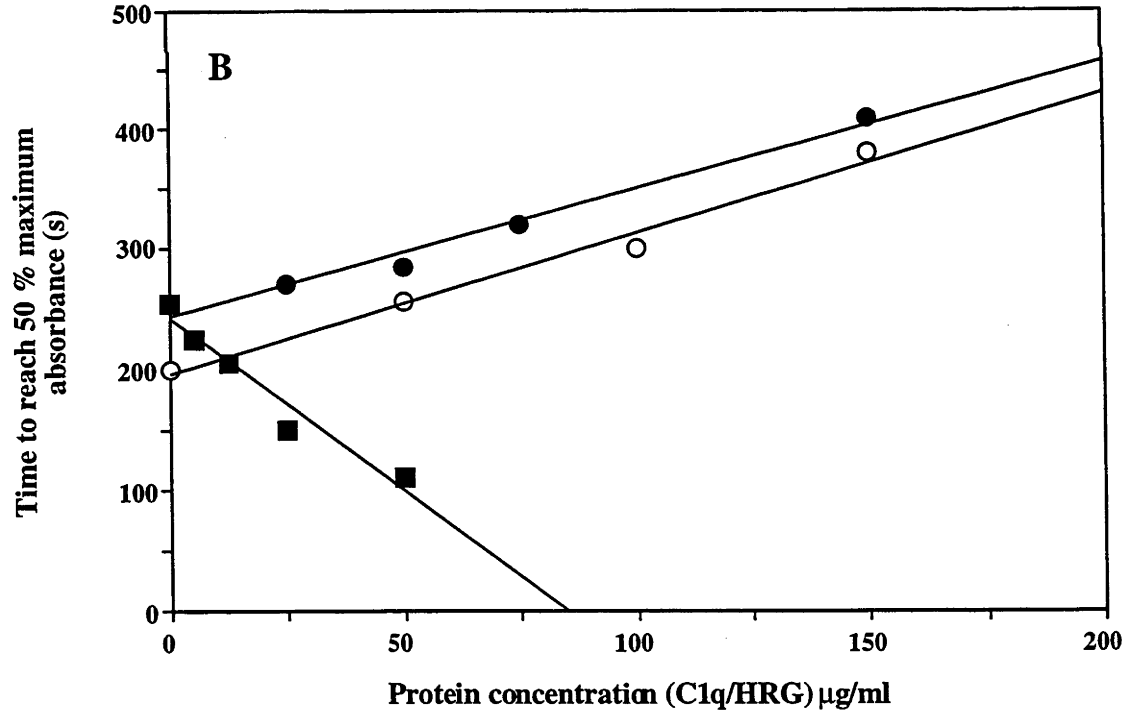
B
Time to reach 50 % maximum absorbance (s)
500
400
300
200
100
0
0
50
100
150
200
Protein concentration (C1q/HRG) µg/ml

FIGURE 3.7 **Effect of native human HRG on the formation of insoluble ICs in the presence of human plasma.**

The results in (A) show the absorbance change due to the formation of insoluble ICs which was initiated by the addition of ovalbumin to a solution of IgG (175 μg/ml, at equivalence Ag : Ab ratio) pre-incubated in PBS (Δ), PBS containing a 1 in 10 dilution of whole human plasma (O), or containing a 1 in 10 dilution of human plasma in which the levels of HRG were reduced to <10% of normal levels by phosphocellulose chromatgraphy (□). ICF was monitored as described in the legend to Figure 3.6. In addition, similar experiments were carried out in which the IgG was pre-incubated with plasma containing the reduced levels of HRG (at 1 in 10 dilution in PBS) and also containing the indicated concentration of added purified native HRG. Each point in (B) shows the time to reach 50% maximum absorbance, and is a representative result of three separate measurements performed at the indicated concentration of HRG.

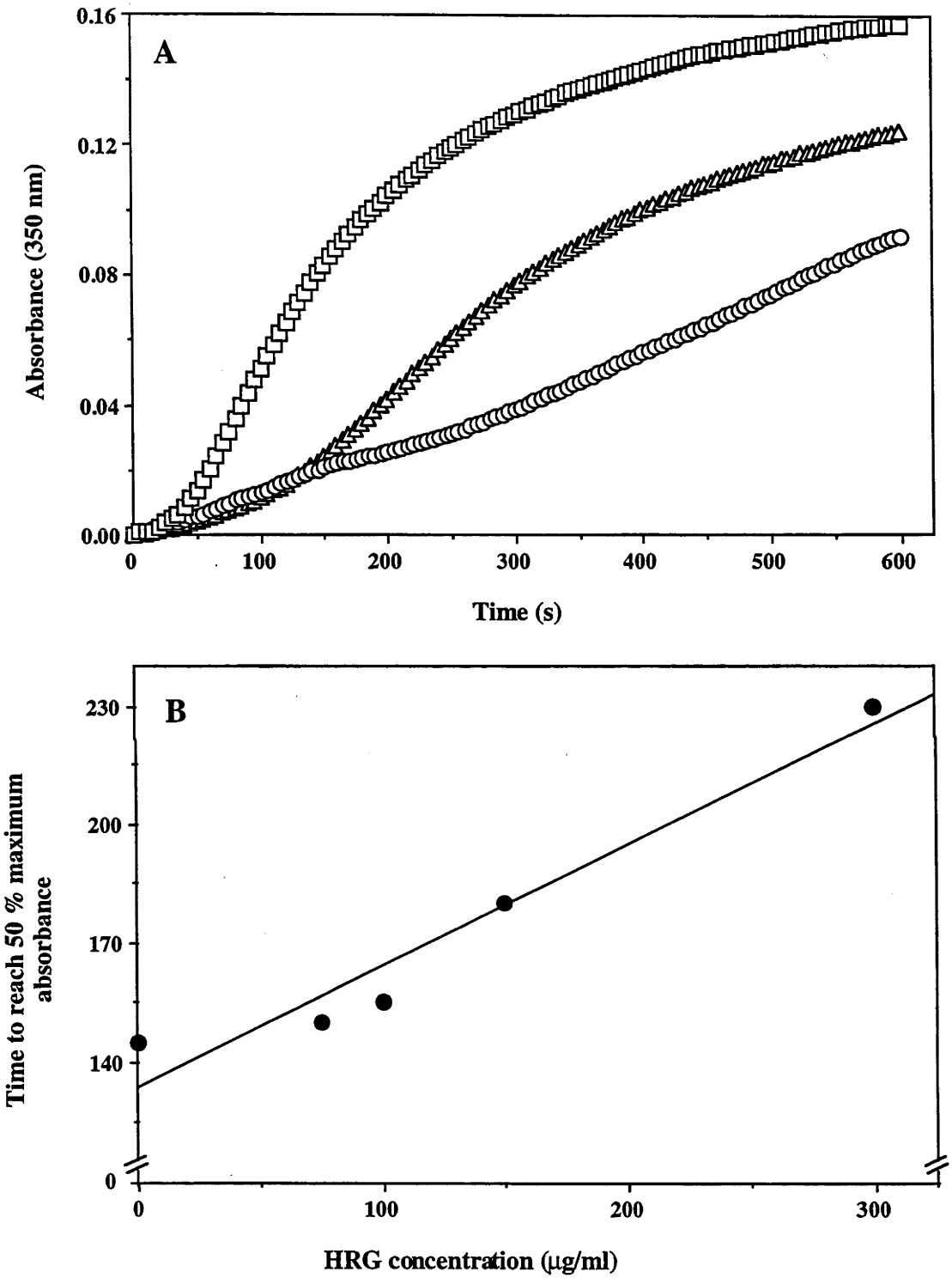
A
Absorbance (350 nm)
0.16
0.12
0.08
0.04
0.00
0
100
200
300
400
500
600
Time (s)
B
Time to reach 50 % maximum absorbance
230
200
170
140
0
0
100
200
300
HRG concentration (μg/ml)

incubated with whole human plasma, and potentiated when pre-incubated with plasma in which the level of HRG was reduced to <10% of that in normal human plasma by passing through a phosphocellulose column as described (Rylatt et al., 1981). Furthermore, the potentiating effect of pre-incubating with the plasma containing reduced levels of HRG on insoluble IC formation was abrogated when exogenous human HRG was included in the pre-incubations of this plasma with IgG (see Figure 3.7B). These findings are consistent with previous studies showing that C1q enhances the formation of insoluble IC (Easterbrook-Smith et al., 1988), and suggest that the presence of HRG can inhibit the formation of insoluble IC under physiological conditions.

3.3 Discussion

The present study shows that HRG binds C1q and IgG with relatively high affinity compared to other HRG ligands (eg. PLG and heparin) and, as a consequence, effectively inhibits the formation of insoluble IC between ovalbumin and anti-ovalbumin IgG *in vitro*. The co-purification of HRG with C1q was first reported by Haupt and Heimburger (1972), but they provided no evidence that the two proteins can interact. Furthermore, previous studies have shown that HRG purified from human serum consists of two identical 30 kDa subunits, held together by ionic interactions (Heimburger et al., 1972). In the present study two bands of similar molecular mass (~ 30 kDa) were observed to co-purify with C1q and N-terminal sequencing indicated that the two molecules have a N-terminal sequence identical to HRG. The possibility that C1q could bind to HRG was first suggested by our observation that the two 32-34 kDa contaminating proteins were not separated from C1q (400 kDa) by gel filtration on a Sephacryl S-300 column. These findings, therefore, provided evidence that C1q can interact with HRG.

The binding of HRG to immobilized human C1q was detected by optical biosensor techniques. The fact that biosensor data for the binding of HRG to immobilized C1q could be fitted to the double exponential relationship suggests that the binding of HRG to C1q occurs with two dissociation constants namely $0.78 \pm 0.46 \times 10^{-8}$ M and $3.73 \pm 0.81 \times 10^{-8}$ M. It would appear, therefore, that at least two distinct binding sites are involved in the HRG-C1q interaction. This notion is supported also by the dissociation phase in which, after the dissociation of the protein ligand from immobilized C1q (presumably from a lower affinity binding site), re-association also could be detected (probably due to the re-binding of HRG to the higher affinity binding site) (not shown). The binding of human C1q to immobilized human HRG could be detected by ELISA and optical biosensor techniques. Kinetic studies of the binding of C1q to immobilized HRG using the biosensor showed the binding to have a dissociation constant of $0.92 \pm 0.30 \times 10^{-8}$ M (see Table 3.1). The fact that the results indicate a single homogeneous response (ie. no heterogeneous interactions) provides evidence that either hexameric C1q (Reid, 1974) is required to form the HRG binding site, and/or that the tail region of the hexameric structure (as opposed to the head region) is involved in the interaction with HRG. While a precise determination of the stoichiometry of the binding between HRG and C1q awaits the use of other techniques such as

ultracentrifugation, the present results show that HRG and C1q interact with high affinity.

The present studies using ELISA and optical biosensor techniques also show that HRG binds to immobilized IgG, and the results are consistent with the previous observation that a trace amount of IgG is present in HRG preparations when the HRG is purified using carboxymethyl cellulose (Haupt and Heimburger, 1972). Biosensor analyses indicate that binding of soluble HRG to immobilized IgG is dependent on the concentration of soluble HRG and that the complex has a dissociation constant of $8.50 \pm 1.50 \times 10^{-8}$ M (Figures 3.3A and B). Interestingly, a similar dissociation constant was observed when the $F(ab')_2$ fragment of rabbit IgG was used instead of whole IgG. Thus, the binding of HRG to immobilized $F(ab')_2$ was concentration dependent, and the dissociation constant was $8.30 \pm 1.70 \times 10^{-8}$ M (see Table 3.1). These findings suggest that HRG binds to IgG with a modest affinity resembling that of low affinity FcR (Van de Winkel and Anderson, 1991), and that the HRG-IgG interaction occurs predominantly via the Fab region of IgG. The IgG and C1q binding sites of HRG are likely to be located on the 30 kDa N-terminal domain of the HRG molecule since this domain interacted with both C1q and IgG in ELISA assays.

Although HRG interacts with immobilized IgG, no binding of human or rabbit IgG to immobilized HRG could be detected when the HRG was immobilised directly onto the biosensor surface using the homobifunctional cross-linking reagent BS3. Similarly, despite the fact that both native and b-HRG bound to immobilised IgG with the same affinity, no binding of IgG to HRG could be detected when the HRG was immobilised by the biotin-STP linkage, even if the first 10 mM HCl wash of the cuvette was omitted to avoid the possibility of denaturation of the HRG (data not shown). Additional studies showed that soluble HRG which had been exposed to 10 mM HCl for 5 min (before being neutralised with PBS) still retained its ability to bind to immobilised IgG in biosensor studies, and that IgG still bound to HRG when immobilised in an ELISA assay (not shown). The most likely explanation consistent with these observations is that the free ε-amino groups on the HRG involved in the biotinylation and cross-linking reaction are located close to the IgG binding region(s), and that this region(s) is stearically hindered upon the immobilisation of the HRG.

Consistent with our recent finding that physiological concentrations of Zn^{2+} potentiate the binding of HRG to T cells (Olsen et al., 1996), the present study

shows that Zn^{2+} also potentiates the binding of HRG to IgG. The affinity of the binding of HRG to immobilized IgG was increased about 5-fold in the presence of a physiological concentration of Zn^{2+} (20 μM). Interestingly, the presence of added Zn^{2+} induced a two-fold increase in the on-rate of HRG binding, but reduced the off-rate of the reaction to ~ 20% of that observed in the absence of added Zn^{2+}. These results suggest that the presence of Zn^{2+} leads to a faster and stronger interaction between HRG and human IgG. In contrast, the high affinity binding of HRG to immobilized C1q was markedly inhibited by Zn^{2+} with the dissociation constant increasing from $0.78 \pm 0.46 \times 10^{-8}$ M in the absence of added Zn^{2+}, to $2.93 \pm 0.80 \times 10^{-8}$ M in the presence of 20 μM added Zn^{2+}. The results suggest that Zn^{2+} can potentiate the ability of HRG to interact with some ligands (eg. IgG) while at the same time inhibit the ability of HRG to interact with other ligands (eg. C1q).

The mechanism by which Zn^{2+} potentiates the interaction between HRG and IgG is unclear. It has been shown that divalent metal cations like Zn^{2+} interact with the HPR domain of HRG (Morgan, 1985). Further studies have shown that protonation of the HPR domain of HRG transmits a conformational change to the rest of the molecule and may regulate its physiological function (Borza et al., 1996). In this study the potencies of enhancement by other divalent metal ions such as Ni^{2+}, Cu^{2+} or Zn^{2+} did not follow the lyotropic series but was more specific for Zn^{2+} and Ni^{2+} than for Cu^{2+}, suggesting that the binding of divalent cations to the HRG molecule does not depend only on charge-charge interactions. It is conceivable that a conformational change induced by the binding of Zn^{2+} may also explain the potentiation of the interaction between HRG and immobilized IgG.

Similarly, the inhibitory effect of Zn^{2+} on the binding of HRG to C1q may be due to a Zn^{2+}-induced conformational change in the HRG molecule which results in a reduced affinity for C1q. These features of the HRG molecule may also reflect its ability to regulate diverse physiological functions. Thus, the potentiation of the HRG-IgG interaction by Zn^{2+} may result in more effective inhibition of insoluble IC formation, whereas the ability of Zn^{2+} to inhibit the HRG-C1q interaction may indicate an ability of HRG to regulate the classical complement pathway (see below).

A major finding from the present work is that physiological concentrations of either 30 kDa or native HRG can inhibit the formation of insoluble IC between ovalbumin and polyclonal rabbit anti-ovalbumin IgG *in vitro*. This finding

suggests that HRG may also play a role in regulating insoluble IC formation *in vivo*, and is consistent with the observation that HRG is an acute phase reactant (Saigo et al., 1990b). Our results indicate that 30 kDa HRG is as effective as native HRG in inhibiting insoluble IC formation (Figure 3.6B), suggesting that the N-terminal region of HRG is involved in the interaction of HRG with IgG. Despite the fact that HRG binds to C1q with high affinity, in preliminary studies I was unable to detect any effect of HRG on insoluble IC formation in the presence of C1q. A possible explanation for this latter observation is that other plasma proteins also are involved in regulating insoluble IC formation. Alternatively, it is possible that the failure to detect any effect is due to the fact that a stirred reaction vessel was not employed in the present studies and C1q enhances insoluble IC formation in the second phase of the progress curve when the insoluble ICs are larger than 100 nm in radii (Gorgani et al., 1996).

Interestingly, C3b is the only plasma protein previously reported to modulate the formation of insoluble IC by covalently binding to the Fc and/or Fab region of IgG (Anton et al., 1994), and evidence suggests that this interaction may be an important factor in both inhibiting insoluble IC formation, and promoting solubilisation of already formed insoluble IC (Schifferli, 1987; Takata et al., 1984). C3b is produced, however, only after activation of the complement pathway which may result in the concommitant release of other complement proteins not involved in regulating insoluble IC formation. Interestingly, it is also reported that HRG-depleted serum has less complement functional activity than whole serum (Chang et al., 1992a). This is consistent with the present studies suggesting that, whereas whole human plasma inhibits the formation of insoluble ICs in a dose-dependent manner, human plasma containing reduced levels of HRG (<10% of that in normal plasma) enhanced the formation of insoluble ICs (see Figure 3.7A). Moreover, the enhancement of insoluble IC formation by plasma containing these reduced levels of HRG was inhibited by the addition of physiological concentrations of purified native HRG (Figure 3.7B). These observations suggest that HRG is a key plasma inhibitor of insoluble IC formation and is able to inhibit this process in the presence of plasma proteins, thereby supporting the notion that this function of HRG is physiologically relevant.

Recently I have shown that the process of formation of insoluble IC can be divided into two phases (Gorgani et al., 1996). Initially the radii of the complexes increase slowly with time (during the process of insolubilisation) until the average radius reaches a critical size (approximately 100 nm for

ovalbumin and rabbit anti-ovalbumin IgG-containing ICs). This is followed by a phase of rapid increase in the radii (polymerization phase), leading to the formation of very large complexes. Interestingly, the enhancement of insoluble IC formation by C1q occurs in the second phase of the progression curve when IgG containing ICs are insoluble (Gorgani et al., 1996). The present study shows that HRG inhibits only the first phase of the progression curve when the mean radius of ICs is less than critical size and soluble IgG-containing ICs are present (not shown). The enhancing effect of C1q on insoluble IC formation may not be physiologically relevent, therefore, if ICs are kept under critical size in radius by the non-covalent interaction of HRG with soluble IgG ICs in early stages of disease or by the covalent binding of C3b to IgG ICs in chronic disease states.

It has been proposed that the production of aAb may be responsible for the induction of ICD, eg. RF, against the IgG molecule in patients suffering from RA. It has also been shown that goat anti-human IgG and human IgG molecules can aggregate and insolubilise *in vitro* (Sittampalam and Wilson, 1984a). In addition, Charlesworth et al., (1982) have shown that the effective clearance of CICs is necessary to limit IC-mediated tissue injury in a mouse model of infectious mononucleosis. These observations may imply that the clearance of circulating insoluble IC (in early stages) is also necessary to limit insoluble IC mediated tissue injury in patients suffering from other ICD, such as RA or SLE. At the molecular level an inhibition of the insolubilisation of soluble ICs (which can lead to the formation of very large hydrophobic particles [Gorgani et al., 1996]), may play an important role in the initiation and pathogenesis of the ICD. The mechanism by which insoluble IC precipitate in target tissues (eg. kidney or synovium of patients suffering from SLE or RA, respectivly) is still unclear, although, inhibition of the insolubilisation process may be a factor which can limit this process and thus the pathogenesis of ICD.

CHAPTER 4

DIFFERENTIAL BINDING OF HISTIDINE-RICH GLYCOPROTEIN TO HUMAN IgG SUBCLASSES

Abstract

In Chapter 3 it was shown that human HRG interacts with high affinity with pooled human IgG. In this Chapter myeloma proteins consisting of the different human IgG subclasses were examined for their ability to interact with human HRG. Using the optical biosensor it was found initially that IgG subclasses differed substantially in their affinity of interaction with HRG. However, the most striking finding was the observation that whether the IgG subclasses contained κ or λ light chains had a dramatic effect on the kinetics of the HRG interaction. Thus, it was found that the on-rate for the binding of HRG to κ light chain containing IgG1 and IgG2 (IgG1κ and IgG2κ) was ~ 4- and ~ 10- fold faster than the on-rate for the binding of HRG to λ light chain containing IgG1 and IgG2 (IgG1λ and IgG2λ), respectively. In contrast, the on-rate for the binding of HRG to IgG3λ and IgG4λ was found to be 9- and 20-fold faster than the on-rate for the binding of HRG to IgG3κ and IgG4κ, respectively. Furthermore, the binding of HRG to IgGs containing κ light chains was generally enhanced in the presence of Zn^{2+}, an effect particularly apparent with IgG1κ, but Zn^{2+} had no effect or slightly inhibited the binding of HRG to immobilized IgG subclasses expressing λ light chains. Interestingly, HRG also bound to BJ proteins. The binding of HRG to κ light chain BJ (BJκ) was two fold faster than the binding of HRG to λ light chain BJ (BJλ) and the presence of physiological concentrations of Zn^{2+} enhanced the binding of HRG to BJκ but inhibited the binding of HRG to BJλ, giving rise to a 14-fold higher affinity of HRG for BJκ than BJλ in the presence of Zn^{2+}. HRG also bound to IgM with a low affinity and the presence of Zn^{2+} actually decreased the affinity of HRG for IgM by 4-fold. Collectively, these data suggest that the ability of HRG to bind to IgG subclasses is influenced by both the heavy chain and light chain isotypes and the presence of Zn^{2+}.

4.1 Introduction

Autoimmune diseases such as RA and SLE are often associated with an excessive production of aAb and the formation of insoluble ICs in the blood circulation. The failure of insoluble ICs to be cleared from the circulation may result in their deposition in specific target tissues, and this may be an important factor in the pathogenesis of ICD (reviewed by Walport and Davies, 1996). The pathology associated with ICD may be caused, at least in part, by the ability of the deposited insoluble ICs to activate the complement pathway and to induce inflammation in the target tissue. In addition, the deposition of insoluble ICs can limit nutrient transport, and consequently, cause tissue injury. For example, patients with RA or SLE have been shown to have high levels of the aAb RF in their sera and affected tissues (Heimer et al., 1982; Nasu et al., 1980). Evidence suggests that RF may form complexes with IgG containing insoluble ICs (self-association) and precipitate in the tissue causing tissue injury and disease (Winchester, 1975).

Interestingly, evidence suggests that aAb of several different isotypes can be found in the sera of patients with RA, and that the form of aAb most frequently found in the affected synovia of these patients is the IgG form of RF (Brown et al., 1982). For example, B cell hybridomas generated from mononuclear cells isolated from the synovial tissue of RA patients are reported to secrete Igs which are predominantly IgG1 containing κ light chains, and IgG2 containing λ light chains (Randen et al., 1993). Moreover, compared to patients that lack aAbs, the overall ratio of κ : λ is often increased in the sera of patients with aAb (Riesen et al., 1976). This raises the possibility that specific IgG subclasses may play a role in the pathogenesis of RA or SLE. However, the functional role of the different Ig classes/subclasses and more particularly, that of the constituent light chains (κ and λ) in the development of ICD is not well understood.

Although the formation of insoluble ICs can occur as a result of the interaction of an Ab with its cognate Ag, the molecular mechanism(s) which regulates the formation, polymerization and precipitation of ICs in the blood circulation and in tissues, is not well understood. Evidence indicates that the formation of insoluble ICs may be regulated by the activation of the classical complement pathway. Thus, the complement component C3b is known to inhibit the formation of insoluble ICs and to promote the solubilisation of already formed insoluble ICs (reviewed by Schifferli, 1987). I have shown that the formation of insoluble ICs occurs in at least two distinct phases: an initial phase of insoluble

IC formation followed by a second phase of rapid polymerization (Gorgani et al., 1996). In addition, the results in Chapter 3 demonstrate that physiological concentrations of HRG bind strongly to IgG, and can inhibit the formation of insoluble ICs between ovalbumin and polyclonal rabbit anti-ovalbumin IgG *in vitro* (Gorgani et al., 1997). These findings raise the question of whether HRG can interact with the different IgG subclasses (which can possess either κ or λ light chains) with the same affinity.

The work in this chapter employs the IAsys biosensor to determine the affinities of the interaction between HRG and different IgG subclasses, and hence establish whether different IgG subclasses differ in their ability to interact with HRG. The effect of the light chain type (κ or λ) on the binding of HRG to IgG was also examined. It was found that different IgG subclasses varied in the ability to interact with HRG. However, the most striking finding was that the on-rate for the binding of HRG to IgG1κ and IgG2κ was found to be ~ 4- and 10-fold higher than the on-rate for the binding of HRG to IgG1λ and IgG2λ, respectively. In contrast, the on-rate for the binding of HRG to IgG3λ and IgG4λ was found to be 9- and 20-fold higher than the on-rate for the binding of HRG to IgG3κ and IgG4κ, respectively. Furthermore, the binding of HRG to IgGs with the κ light chains was enhanced in the presence of Zn^{2+}, but Zn^{2+} slightly inhibited the binding of HRG to immobilized IgG with the λ light chain. These findings provide, for the first time, convincing evidence that the light chain type of IgG has a profound effect on the binding of HRG to IgG subclasses and hence indicates functional differences between the κ and λ light chains of Igs.

4.2 Results

4.2.1 Binding of HRG to IgG subclasses possessing κ light chains

The studies in Chapter 3 showed that HRG binds to immobilized human IgG (from pooled human serum) with high affinity (K_d = 85 ± 15 nM) (see Chapter 3). To determine whether HRG binds with a similar affinity to each different IgG subclass, preliminary experiments were carried out to examine the binding of biotinylated IgG1κ, IgG2κ, IgG3κ and IgG4κ to immobilized HRG in an ELISA assay. In these studies the binding of each IgG subclass to the immobilized HRG could be detected by incubation with HRP-STP conjugate followed by color development as described in Materials and Methods (Chapter 2). The experiments indicated that each of the four different subclasses of IgG binds to immobilized HRG in a concentration-dependent manner. Moreover, the dissociation constants (K_d) for the binding of IgG(κ) to immobilized HRG, as determined by Scatchard analysis after plotting (1/maximum bound) versus (1/IgG concentration), was found to follow the relationship IgG2κ > IgG1κ >>> IgG3κ > IgG4κ (data not shown).

To further characterise the interaction of HRG with IgG subclasses, the binding of native human HRG to each of the four IgG subclasses possessing the κ light chain also was examined using the IAsys biosensor. For these studies 20-60 ng of biotinylated human IgG (of the indicated subclass possessing κ light chain) was immobilized via STP coupling onto the surface of a dextran cuvette, and the binding of soluble HRG to the immobilized IgG subclass was carried out following equilibration of the cuvette in PBS-BSA-T. Thus, HRG was added in PBS-BSA-T and the association phase for the binding of native human HRG to the immobilized IgG1κ was monitored for 5 minutes. Subsequently, the cuvette was washed three times with PBS-BSA-T buffer (to bring the liquid phase HRG concentration to zero) and the dissociation phase was monitored for 5 minutes. The biosensor profiles for the binding of different concentrations of HRG to immobilized human IgG1κ are shown in Figure 4.1A. The data show that the binding of HRG to IgG1κ is dependent on the HRG concentration in the range of 10-400 nM, and that within this concentration range the binding of HRG is saturable with near-maximal binding (~500 arc sec) occurring at a HRG concentration of 400 nM. The binding of HRG was significantly inhibited (> 80%) when the HRG was pre-incubated, before addition to the cuvette, with soluble IgG1κ (IgG1κ/HRG molar ratio > 4, data not shown) suggesting that the HRG interacted specifically with IgG1κ. The observed rate constant for each

FIGURE 4.1 **Determination of the binding constant for the interaction of HRG with immobilized IgG1κ.**

The binding of human HRG to IgG1κ was examined using the IAsys biosensor. Human IgG1κ was biotinylated and then immobilized onto the carboxymethyl dextran sensing surface of the biosensor cuvette by coupling to immobilized STP. The cuvette was equilibrated in PBS-BSA-T for 5 minutes to obtain a base line and then (at time zero) HRG at the indicated concentration was added to the cuvette in the same buffer. For each concentration of HRG the association or binding of HRG to the immobilized IgG1κ was monitored for 5 minutes. The overlay plots representing the binding of HRG to the immobilized IgG1κ are shown in (A). Subsequently, the contents of the cuvette were removed, and the cuvette was washed three times with PBS-BSA-T before monitoring the dissociation phase for 5 min (not shown). The value of k_{obs} for the binding curve for each HRG concentration was determined using the linearization method (FAST FIT program) and each value plotted against the concentration of HRG (B). The plot of k_{obs} against HRG concentration gives a straight line (●); the slope represents k_{on} and the y-intercept represents k_{off} for this interaction. Error bars represent the ± SEM obtained from three separate experiments for each concentration of HRG.

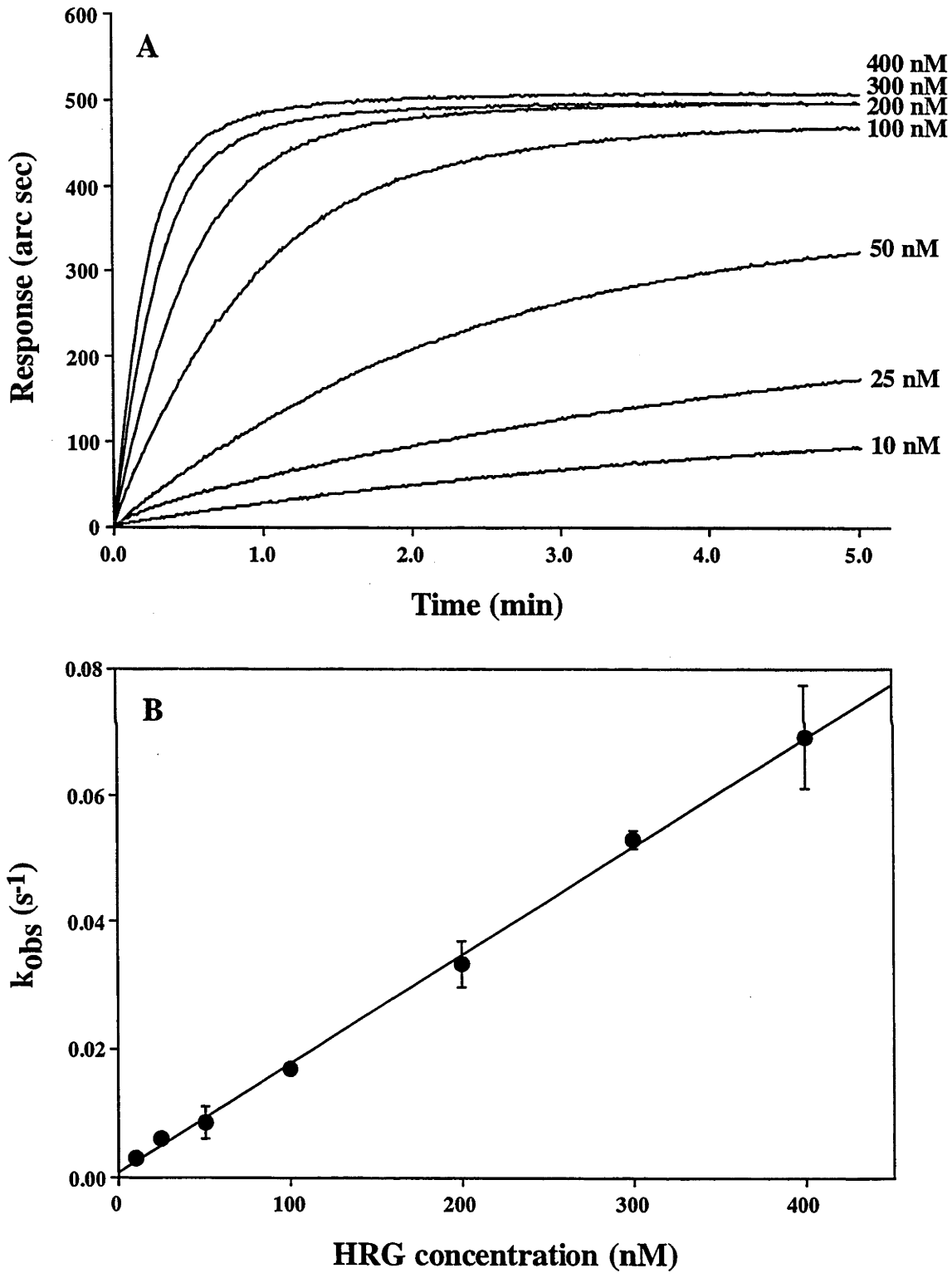
A
600
500
400
300
200
100
0
Response (arc sec)
400 nM
300 nM
200 nM
100 nM
50 nM
25 nM
10 nM
0.0
1.0
2.0
3.0
4.0
5.0
Time (min)
B
0.08
0.06
0.04
0.02
0.00
k_{obs} (s^{-1})
0
100
200
300
400
HRG concentration (nM)

binding curve, at the indicated concentrations of HRG, was obtained by fitting the curve to the single exponential expression using the "FAST FIT" program as previously described (Gorgani et al., 1997, see Chapter 3). A plot of the observed rate constant (k_{obs}, s^{-1}) against the concentration of HRG (nM) approximated a straight line (see Figure 4.1B), with the line of best fit revealing that HRG binds to immobilized IgG1κ with an on-rate of $1.73 \pm 0.04 \times 10^5$ $M^{-1}s^{-1}$ (slope of the plot) and an off-rate of $0.53 \pm 0.02 \times 10^{-3}$ s^{-1} (intercept with the y-axis) (see Table 4.1). The dissociation constant for this interaction was determined either using the relationship $K_d=k_{off}/k_{on}$, or by Scatchard analysis of the maximum amount of bound HRG at equilibrium; both methods gave a K_d of 3.04 ± 0.13 nM (see Table 4.1).

Similar biosensor experiments carried out to study the interaction of soluble HRG with immobilized IgG2κ, IgG3κ and IgG4κ, (each immobilized on to separate biosensor cuvettes) also indicated that the binding of HRG to each of these subclasses was saturable and dependent on the HRG concentration. As previously, the biosensor profiles for the binding of HRG (at each concentration) to each IgG subclass was fitted to a single exponential to derive the k_{obs}. As shown in Figure 4.2B and Table 4.1 the on-rate, off-rate and K_d for the interaction of HRG with IgG2κ were found to be $2.76 \pm 0.27 \times 10^5$ $M^{-1}s^{-1}$, $1.36 \pm 0.22 \times 10^{-3}$ s^{-1} and 5.04 ± 1.29 nM, respectively. Interestingly, the on-rate for the interaction of HRG with IgG3κ was $0.13 \pm 0.004 \times 10^5$ $M^{-1}s^{-1}$ (see Figure 4.2C) and that for HRG with IgG4κ was $0.11 \pm 0.005 \times 10^5$ $M^{-1}s^{-1}$ (see Figure 4.2D); these values are ~ 15-30 fold slower than those observed for IgG1κ or IgG2κ. Further analysis showed that the off-rate and K_d for the interaction of HRG with immobilized IgG3κ were $1.92 \pm 0.11 \times 10^{-3}$ s^{-1} and 147.57 ± 13.01 nM, respectively. The corresponding values for IgG4κ were different, being off-rate $= 2.86 \pm 0.16 \times 10^{-3}$ s^{-1} and $K_d = 268.01 \pm 26.98$ nM. The on-rates for the binding of HRG to the four different IgG subclasses therefore follows the series IgG2κ > IgG1κ >>> IgG3κ > IgG4κ (see Figure 4.2 and Table 4.1). These studies show that the kinetics of the binding of HRG to IgG depends on the IgG subclass, with HRG having a faster binding rate and higher affinity for IgG1κ and IgG2κ, than for IgG3κ and IgG4κ.

4.2.2 Binding of HRG to IgG subclasses possessing λ light chains

The finding that HRG differs in its ability to interact with different subclasses of IgG containing the κ light chain, suggested that differences also may exist in the ability of HRG to interact with subclasses of IgG containing the λ light chain.

TABLE 4.1 **Rate and dissociation constants for the interaction of HRG with different IgG subclasses and Bence Jones proteins.**

Kinetic constants for the conditions indicated were determined by applying the "Fast Fit" program to the binding data obtained using the IAsys biosensor. All experiments were performed by the addition of HRG to a dextran cuvette containing the immobilized protein in PBS-T-BSA buffer (pH 7.4). Each constant represents the mean ± SEMs of three independent experiments. Asterisks indicate that changing the light chain type from κ to λ for a particular IgG subclass significantly affected the HRG-ligand binding constant.

* $p < 0.05 > 0.01$; ** $p < 0.01 > 0.001$; *** $p < 0.001$

Interactions	k_{on} ($M^{-1}s^{-1}$) x 10^{-5}	k_{off} (s^{-1}) x 10^{3}	K_d (nM)
IgG with κ light chains			
HRG to immob. IgG1κ	1.73 ± 0.04	0.53 ± 0.02	3.04 ± 0.13
HRG to immob. IgG2κ	2.76 ± 0.27	1.36 ± 0.22	5.04 ± 1.29
HRG to immob. IgG3κ	0.13 ± 0.004	1.92 ± 0.11	147.57 ± 13.01
HRG to immob. IgG4κ	0.11 ± 0.005	2.86 ± 0.16	268.01 ± 26.98
HRG to immob. BJκ	0.77 ± 0.04	2.56 ± 0.29	35.21 ± 4.89
HRG to immob. IgMκ	0.036 ± 0.005	7.11 ± 0.10	1989.50 ± 50.50
IgG with λ light chains			
HRG to immob. IgG1λ	0.44 ± 0.02***	8.07 ± 1.36*	188.73± 43.26*
HRG to immob. IgG2λ	0.27 ± 0.01*	3.07 ± 0.20*	111.93±2.68***
HRG to immob. IgG3λ	1.16 ± 0.09***	12.20 ± 2.10**	109.31 ± 28.95
HRG to immob. IgG4λ	2.16 ± 0.03***	20.8 ± 0.77**	96.10 ± 4.78*
HRG to immob. BJλ	0.38 ± 0.02**	2.87 ± 0.042	76.35 ± 5.60*

FIGURE 4.2 **Determination of the binding constants for the interaction of HRG with immobilized IgG1, IgG2, IgG3 and IgG4.**

The binding of human HRG to each of 8 different IgG subclasses (IgG1κ, IgG1λ, IgG2κ, IgG2λ, IgG3κ, IgG3λ, IgG4κ and IgG4λ) was examined using the IAsys biosensor. Each human IgG subclass was biotinylated and then immobilized onto a carboxymethyl dextran biosensor cuvette by coupling to immobilized STP. Subsequently, different concentrations of HRG was added to the cuvette and the association and dissociation of HRG was monitored exactly as described in the legend for Figure 4.1. The k_{obs} values for the binding of HRG to each IgG subclass was determined by fitting the biosensor data to a single exponential. The results in (A) shows plots of the k_{obs} against HRG concentration for the binding of HRG to IgG1κ (●) and to IgG1λ (■). Similarly, the results in (B) show plots of k_{obs} against HRG concentration for the binding of HRG to IgG2 subclasses (IgG2κ ●, IgG2λ ■). Also the results in (C) shows plots of the k_{obs} against HRG concentration for the interaction of HRG with IgG3κ (●) and with IgG3λ (■), whereas, the plots of k_{obs} against HRG concentration for the interaction of HRG with IgG4 subclasses are shown in (D) (IgG4κ ●, IgG4λ ■). Error bars represent ± SEM obtained from three separate experiments for each concentration of HRG.

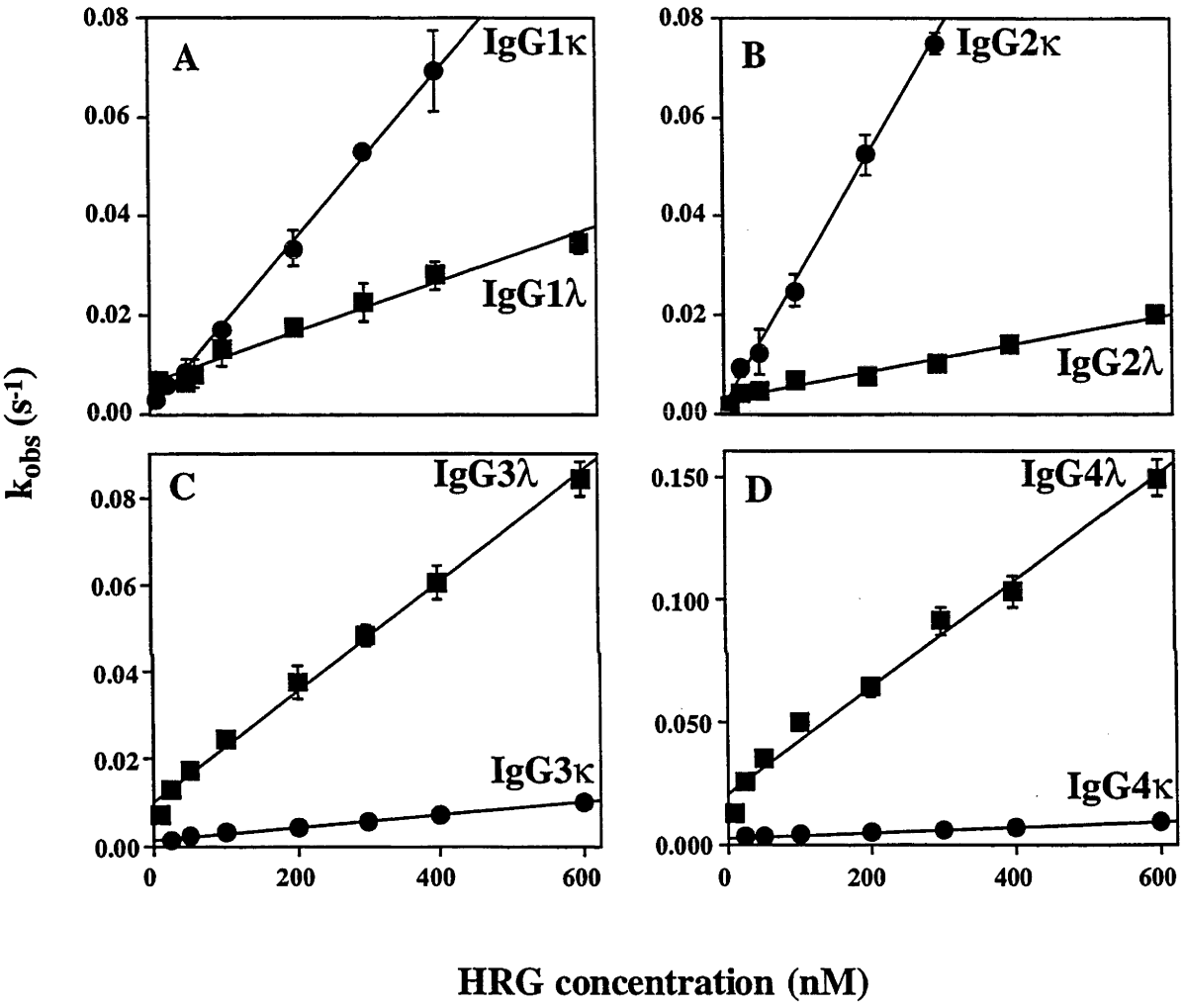
A
IgG1κ
IgG1λ
B
IgG2κ
IgG2λ
C
IgG3λ
IgG3κ
D
IgG4λ
IgG4κ
k_{obs} (s^{-1})
HRG concentration (nM)
0.08
0.06
0.04
0.02
0.00
0.150
0.100
0.050
0.000
0
200
400
600

Therefore, to study the binding of HRG to different λ-containing IgG subclasses, each subclass IgG1λ, IgG2λ, IgG3λ and IgG4λ was immobilized onto a separate biosensor cuvette, and the binding of soluble HRG to each subclass was analysed using the biosensor. The binding of HRG to each different IgG subclass was carried out separately at a range of different concentrations of HRG (10 - 600 nM) in PBS-T-BSA. The binding of HRG to each IgGλ subclass was found to be saturable and dependent on HRG concentration (data not shown). The biosensor read out for each concentration of HRG was fitted to a single exponential to obtain the average k_{obs} for the interaction, and the average k_{obs} was then plotted against the HRG concentration.

To facilitate comparison of the results from IgG subclasses containing either κ or λ light chains, the data for each λ-containing subclass was plotted on the same graph as the corresponding κ-containing subclass; the results for IgG1 and IgG2 are shown in Figure 4.2 (A,B), and those for IgG3 and IgG4 are shown in Figure 4.2 (C,D). From the line of best fit it was calculated (Table 4.1) that the on-rate for the interaction of HRG with IgG1λ and IgG2λ was $0.44 \pm 0.024 \times 10^5$ $M^{-1}s^{-1}$ and $0.27 \pm 0.011 \times 10^5$ $M^{-1}s^{-1}$, respectively; these values are 5-10-fold slower than for the binding of HRG to IgG1κ and IgG2κ (Figure 4.2A and B). The off-rates and K_d were found to be $8.07 \pm 1.36 \times 10^{-3}$ s^{-1} and 188.73 ± 43.26 nM for HRG-IgG1λ, and $3.07 \pm 0.20 \times 10^{-3}$ s^{-1} and 111.93 ± 2.68 nM for HRG-IgG2λ interactions, respectively. Interestingly, the dissociation constants were 20-60 fold higher than those observed for IgG1κ and IgG2κ (see Figure 4.2 and Table 4.1).

As shown in Figure 4.2 and Table 4.1, similar studies indicated that the binding of HRG to immobilized IgG3λ and IgG4λ is faster than the binding of HRG to IgG1λ and IgG2λ. The on-rate, off-rate and K_d for the HRG-IgG3λ interaction were $1.16 \pm 0.090 \times 10^5$ $M^{-1}s^{-1}$, $12.20 \pm 2.10 \times 10^{-3}$ s^{-1} and 109.31 ± 28.95 nM, respectively (Figure 4.2C). The corresponding values for the HRG-IgG4λ interaction were $2.16 \pm 0.030 \times 10^5$ $M^{-1}s^{-1}$, $20.8 \pm 0.77 \times 10^{-3}$ s^{-1} and 96.10 ± 4.78 nM, respectively (Figure 4.2D).

The data indicate that although the on-rate of these interactions are similar to those observed for the interaction of HRG with IgG1κ and IgG2κ, the off-rates are much higher, resulting in a higher K_d (approximately 20-fold higher) than for the interaction of HRG with IgG1κ and IgG2κ (see Table 4.1). The on-rates for the binding of HRG to IgG subclasses containing the λ light chain followed

the relationship IgG4λ > IgG3λ >>> IgG1λ > IgG2λ (see Figure 4.2 and Table 4.1).

4.2.3 Effect of Zn^{2+} on the binding of HRG to IgG subclasses

As described in Chapter 3, the presence of Zn^{2+} potentiates the binding of HRG to human IgG (from pooled human serum), but inhibits the binding of HRG to the complement component C1q (Gorgani et al., 1997 and Chapter 3). To determine the effect of Zn^{2+} on the binding of HRG to IgG subclasses, biosensor experiments were performed using separate cuvettes containing each immobilized IgG subclass (as described above). The binding of HRG to each different IgG subclass was carried out in PBS-BSA-T containing 20 μM added Zn^{2+} (PBS-BSA-T-Zn). As shown in Figure 4.3 and Table 4.2, in the presence of Zn^{2+} the on-rate of the HRG-IgG1κ interaction was increased from 1.73 ± 0.04 x 10^5 to 6.21 ± 0.13 x 10^5 $M^{-1}s^{-1}$, whereas the off-rate was decreased from 0.53 ± 0.02 x 10^{-3} to 0.37 ± 0.17 x 10^{-3} s^{-1}. The dissociation constant was decreased ~ 5 fold changing from 3.04 ± 0.13 to 0.6 ± 0.01 nM (see Table 4.2).

Experiments also were performed to examine the effect of Zn^{2+} on the binding of HRG to immobilized IgG1λ. In contrast to the HRG-IgG1κ interaction, the presence of Zn^{2+} slightly decreased the on-rate of the HRG-IgG1λ interaction from 0.44 ± 0.024 x 10^5 to 0.34 ± 0.025 x 10^5 $M^{-1}s^{-1}$, (without affecting the off-rate of this interaction). Thus the K_d was increased from 188.73 ± 43.26 to 266.33 ± 34.60 nM (see Figure 4.3A and Table 4.3). Similarly, the effect of Zn^{2+} on the binding of HRG to other IgG subclasses was studied as described above. The results show that although the presence of Zn^{2+} generally increases the affinity of the binding of HRG to all IgG subclasses possessing κ light chains, it tends to decrease the affinity of the binding of HRG to IgG subclasses possessing λ light chains (see Table 4.2 and 4.3). However, except for IgG1κ, the effects of Zn^{2+} on the HRG-IgG interaction were small and, in most cases, not statistically significant.

4.2.4 Binding of HRG to Bence Jones proteins

The above studies indicated that the type of constituent light chain may be a major factor determining the kinetics and behavior of the interaction between HRG and IgG subclasses containing different light chains. To further characterise the interaction of HRG with IgG, studies also were carried out using κ and λ light chains of BJ proteins. For these studies, lyophilized BJ

FIGURE 4.3 **Effect of Zn^{2+} on the binding of HRG to IgG1κ, IgG1λ and κ and λ Bence Jones proteins (BJκ and BJλ).**

The binding of human HRG to immobilized IgG1κ, IgG1λ, BJκ and BJλ was examined in the presence and absence of Zn^{2+}. All experiments were performed as described in the legend to Figure 4.1 with exception that for some experiments HRG was added in PBS-BSA-T buffer containing 20 μM Zn^{2+} instead of PBS-BSA-T. For each concentration of HRG, the k_{obs} value for the binding of HRG was determined by fitting to a curve (as detailed in the text) and each k_{obs} value was plotted against HRG concentration for the HRG-IgG1κ interaction in PBS-BSA-T buffer (●, control), and for the same interaction in PBS-BSA-T buffer containing 20 μM Zn^{2+} (○) as shown in (A). Similarly, (A) shows the k_{obs} values plotted against the HRG concentration for the HRG-IgG1λ interaction in PBS-BSA-T (■, control) and in PBS-BSA-T containing 20 μM Zn^{2+} (□). The data for the effect of Zn^{2+} on the HRG-BJκ and HRG-BJλ interactions are presented in (B) which shows plot k_{obs} against HRG concentration for the HRG-BJκ interaction in PBS-BSA-T (●, control), and for the same interaction in PBS-BSA-T buffer containing 20 μM Zn^{2+} (○). Also shown is the plot of k_{obs} against HRG concentration for the HRG-BJλ interaction in PBS-BSA-T (■, control), and for the same interaction in PBS-BSA-T containing 20 μM Zn^{2+} (□). Error bars represent ± SEM obtained from three separate experiments for each concentration of HRG.

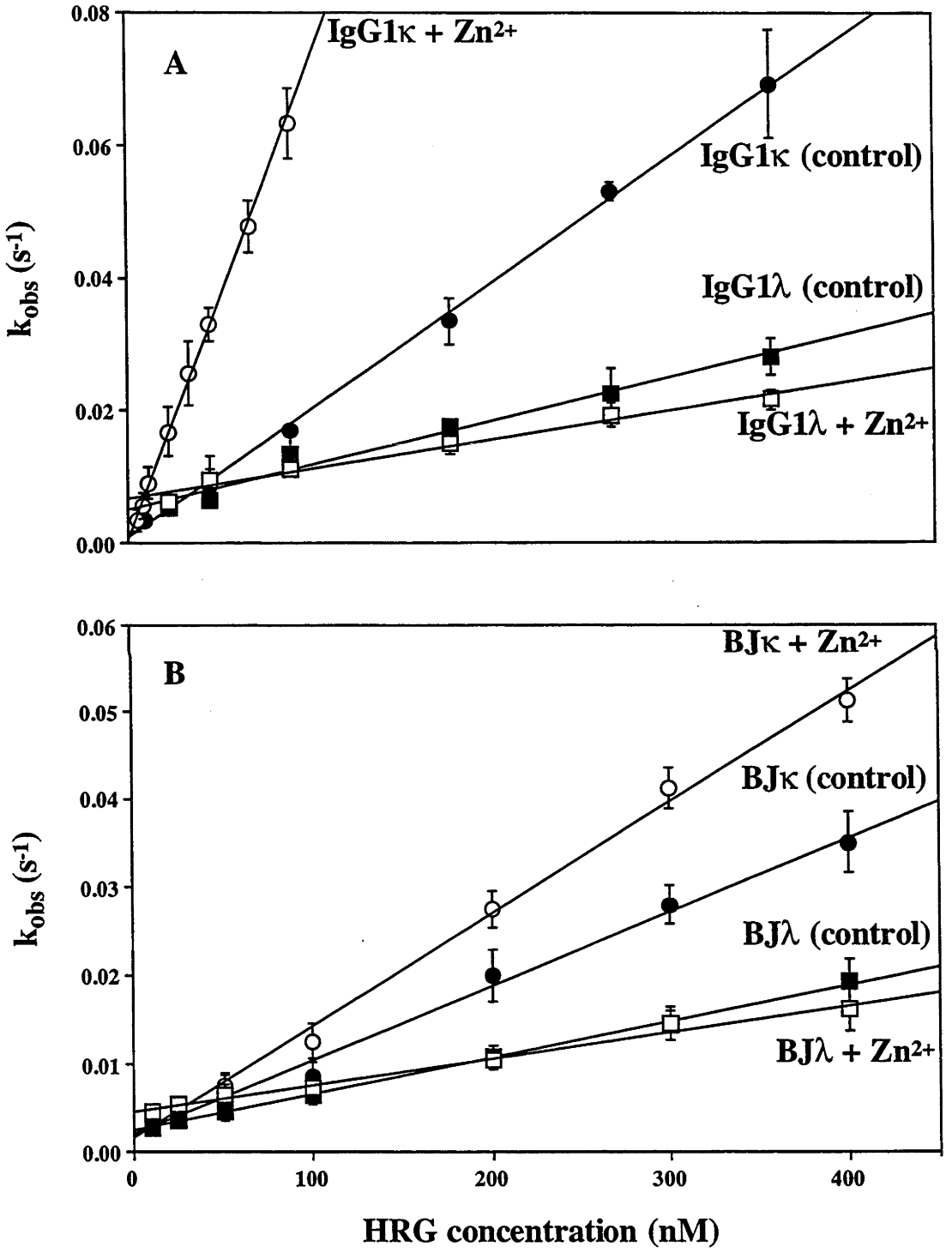
A
IgG1κ + Zn2+
IgG1κ (control)
IgG1λ (control)
IgG1λ + Zn2+
kobs (s-1)
0.08
0.06
0.04
0.02
0.00
B
BJκ + Zn2+
BJκ (control)
BJλ (control)
BJλ + Zn2+
kobs (s-1)
0.06
0.05
0.04
0.03
0.02
0.01
0.00
0
100
200
300
400
HRG concentration (nM)

TABLE 4.2 **Rate and dissociation constants for the interaction of HRG with various κ light chain containing ligands in the presence and absence of Zn^{2+}.**

Kinetic constants for the interactions indicated were determined by applying the "Fast Fit" program to the binding data obtained using the IAsys biosensor. All experiments were performed by the addition of HRG to a dextran cuvette containing the immobilized protein in PBS-T-BSA buffer (pH 7.4) in the absence (control) or presence of 20 μM Zn^{2+}. Each constant represents the mean ± SEMs of three independent experiments. Asterisks indicate that the presence of Zn^{2+} significantly affected the HRG-ligand binding constant.

* $p < 0.05 > 0.01$; ** $p < 0.01 > 0.001$; *** $p < 0.001$

Interactions	k_{on} ($M^{-1}s^{-1}$) x 10^{-5}	k_{off} (s^{-1}) x 10^{3}	K_d (nM)
HRG to immob. IgG1κ			
Control	1.73 ± 0.04	0.53 ± 0.02	3.04 ± 0.13
+ 20 μM Zn^{2+}	6.21 ± 0.13***	0.37 ± 0.17	0.60 ± 0.01**
HRG to immob. IgG2κ			
Control	2.76 ± 0.27	1.36 ± 0.22	5.04 ± 1.29
+ 20 μM Zn^{2+}	3.40 ± 0.37	1.12 ± 0.17	3.28 ± 0.14
HRG to immob. IgG3κ			
Control	0.13 ± 0.004	1.92 ± 0.11	147.57 ± 13.01
+ 20 μM Zn^{2+}	0.20 ± 0.01*	1.83 ± 0.08	91.93 ± 8.60
HRG to immob. IgG4κ			
Control	0.11 ± 0.005	2.86 ± 0.16	268.01 ± 26.98
+ 20 μM Zn^{2+}	0.15 ± 0.02	2.53 ± 0.14	167.03 ± 26.44
HRG to immob. BJκ			
Control	0.77 ± 0.04	2.56 ± 0.29	35.21 ± 4.89
+ 20 μM Zn^{2+}	1.30 ± 0.04**	1.35 ± 0.69	10.38 ± 1.21*

TABLE 4.3 **Rate and dissociation constants for the interaction of HRG with various λ light chain containing ligands in the presence and absence of Zn^{2+}.**

Kinetic constants for the interactions indicated were determined by applying the "Fast Fit" program to the binding data obtained using the IAsys biosensor. All experiments were performed by the addition of HRG to a dextran cuvette containing the immobilized protein in PBS-T-BSA buffer (pH 7.4) in the absence (control) or presence of 20 μM Zn^{2+}. Each constant represents the mean ± SEMs of three independent experiments. Asterisks indicate that the presence of Zn^{2+} significantly affected the HRG-ligand binding constant.

* $p < 0.05 > 0.01$; ** $p < 0.01 > 0.001$; *** $p < 0.001$

Interactions	k_{on} ($M^{-1}s^{-1}$) x 10^{-5}	k_{off} (s^{-1}) x 10^{3}	K_d (nM)
HRG to immob. IgG1λ			
Control	0.44 ± 0.02	8.07 ± 2.36	188.73 ± 43.26
+ 20 μM Zn^{2+}	0.34 ± 0.02	9.08 ± 3.07	266.33 ± 34.60
HRG to immob. IgG2λ			
Control	0.27 ± 0.01	3.07 ± 0.20	111.93 ± 2.68
+ 20 μM Zn^{2+}	0.21 ± 0.05	3.14 ± 0.35	149.60 ± 52.29
HRG to immob. IgG3λ			
Control	1.16 ± 0.09	12.20 ± 2.10	109.31 ± 28.95
+ 20 μM Zn^{2+}	1.11 ± 0.18	13.20 ± 1.58	113.45 ± 22.82
HRG to immob. IgG4λ			
Control	2.16 ± 0.03	20.8 ± 0.77	96.10 ± 4.78
+ 20 μM Zn^{2+}	1.91 ± 0.04*	19.80 ± 1.89	103.50 ± 7.84
HRG to immob. BJλ			
Control	0.38 ± 0.02	2.87 ± 0.042	76.35 ± 5.60
+ 20 μM Zn^{2+}	0.32 ± 0.05	4.48 ± 0.113**	139.75 ± 4.60*
HRG to immob. IgM			
Control	0.036 ± 0.005	7.11 ± 0.10	1989.50 ± 50.50
+ 20 μM Zn^{2+}	0.016 ± 0.003*	11.84 ± 1.60***	7754.0 ± 1707.0

proteins were dissolved in PBS and purified by gel filtration on FPLC using a Superose 12 column. Two protein peaks were obtained with the BJκ preparation and a single higher molecular weight peak, with BJλ. Subsequently, SDS-PAGE analysis of the protein peaks showed that BJκ consisted of a lower molecular weight monomeric and a higher molecular weight dimeric form, whereas only a single peak of the dimeric form of BJλ could be detected (see Figure 4.4). The dimeric forms of both BJκ and BJλ were biotinylated as described in the Materials and Methods (Chapter 2), and then used in ELISA assays to assess their ability to bind immobilized HRG. Preliminary experiments indicated that both biotinylated κ and λ BJ proteins bound to immobilized HRG in an ELISA assay, that the binding was concentration dependent, and that HRG bound more strongly to the κ than to the λ light chains (data not shown).

The interaction of HRG with BJ proteins also was studied using the biosensor. For these studies each BJ protein was immobilized onto a separate biosensor cuvette to permit an analysis of the binding of HRG in solution. The biosensor data indicated that the binding of HRG to both BJκ and BJλ proteins was saturable and dependent on the HRG concentration. Three sets of experiments were performed for the interaction of HRG with either κ or λ BJ proteins. Before each repeat experiment, bound HRG was removed from the cuvette by acid wash or using Pierce gentle Ag/Ab elution buffer. Similar to the analysis of other biosensor data described above, for each concentration of HRG, the observed rate constant (k_{obs}) was obtained by fitting the binding curve to a single exponential using the "FAST FIT program". As shown in Figure 4.3B (control experiments, in PBS-T-BSA buffer) the change of the k_{obs} for the interaction of HRG with both BJκ and the BJλ was dependent on the HRG concentration. The results (Table 4.1) indicate that the on-rate, off-rate and the K_d for the binding of HRG to immobilized BJκ are $0.77 \pm 0.042 \times 10^5$ $M^{-1}s^{-1}$, $2.56 \pm 0.29 \times 10^{-3}$ s^{-1} and 35.21 ± 4.89 nM, respectively; and that the corresponding values for the binding of HRG to immobilized BJλ are $0.38 \pm 0.022 \times 10^5$ $M^{-1}s^{-1}$, $2.87 \pm 0.042 \times 10^{-3}$ s^{-1} and 76.35 ± 5.60 nM, respectively. The results indicate, therefore, that the affinity for the binding of HRG to BJκ is significantly higher than for the binding of HRG to BJλ.

To determine whether Zn^{2+} affects the ability of HRG to interact with the light chains (κ and λ), biosensor experiments to study the binding of HRG to immobilized BJκ and BJλ also were carried out as described above, with the exception that the HRG was added to the cuvette in PBS-BSA-T-Zn. As shown

FIGURE 4.4 **SDS-PAGE analysis of the kappa and lambda Bence Jones proteins.**

The κ and λ BJ proteins (BJκ and BJλ) obtained from Dr Bob Raison, University of Technology, Sydney, were each dissolved in PBS and then subjected to gel filtration by FPLC (using a Superose 12 column). The FPLC indicated that the BJκ preparation contained two protein peaks (a lower molecular weight and a higher molecular weight peak), whereas, BJλ preparations contained only a higher molecular weight protein peak. Aliquots of the protein peaks resolved by FPLC were analysed by SDS-PAGE (10% gel) under non-reducing conditions, and the proteins then stained with Coomassie Brilliant Blue. The analysis indicate that BJκ consists of monomeric and dimeric forms, whereas, the BJλ was only in dimeric form. Lane M (molecular weight markers) was analysed under reducing conditions; whereas lane A (dimeric BJλ), lane B (monomeric BJλ) and lane C (dimeric BJκ) were all analysed under non-reducing conditions.

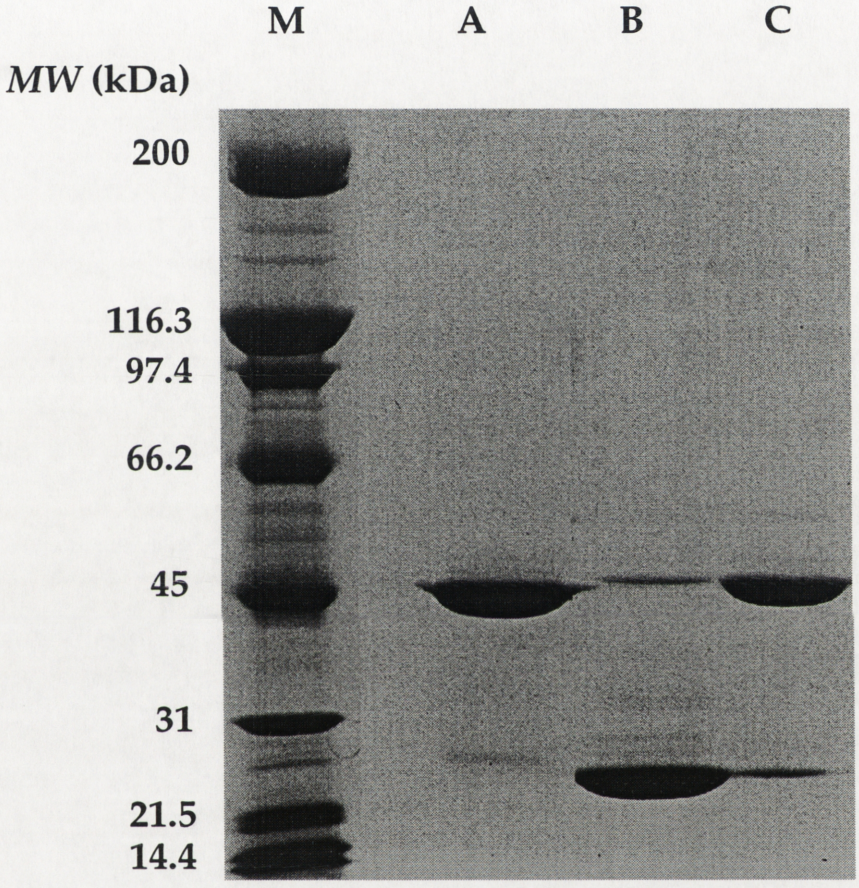
M
A
B
C
MW (kDa)
200
116.3
97.4
66.2
45
31
21.5
14.4

in Figure 4.3B and Table 4.2, in the presence of Zn^{2+} the on-rate of the HRG-BJκ interaction was increased from 0.77 ± 0.042 x 10^5 to 1.30 ± 0.038 x 10^5 $M^{-1}s^{-1}$ and the off-rate was decreased from 2.56 ± 0.29 x 10^{-3} to 1.35 ± 0.69 x 10^{-3} s^{-1}. The K_d was significantly reduced from 35.21 ± 4.89 to 10.38 ± 1.21 nM.

Similarly, an investigation of the effect of Zn^{2+} on the HRG-BJλ interaction (Figure 4.3B and Table 4.3) indicated that the presence of Zn^{2+} decreases the on-rate of the interaction from 0.38 ± 0.022 x 10^5 to 0.32 ± 0.048 x 10^5 $M^{-1}s^{-1}$, and increases the off-rate of the interaction from 2.87 ± 0.042 x 10^{-3} to 4.48 ± 0.11 x 10^{-3} s^{-1}. The K_d was thus significantly increased from 76.35 ± 5.60 to 139.75 ± 4.60 nM. These results show that Zn^{2+} potentiates the binding of HRG to BJκ, but inhibits the binding of HRG to BJλ (Figure 4.3B and Tables 4.2 and 4.3).

4.2.5 Binding of HRG to IgM

The ability of HRG to interact with IgG subclasses (particularly IgG1κ) with high affinity in a Zn^{2+}-dependent manner prompted an examination of whether HRG also binds to other Igs such as IgM. For these studies, experiments were conducted to determine whether human b-IgM binds to immobilized HRG in an ELISA assay. A concentration dependent increase in the binding of b-IgM to the immobilized HRG was detected. In subsequent studies the IAsys biosensor was used to determine the kinetic constants for the interaction of HRG with immobilized IgM. The b-IgM (20 ng/cuvette) was immobilized onto the sensing surface of a biosensor cuvette by coupling it to immobilized STP, and the association and dissociation of HRG in PBS-BSA-T buffer was monitored using the biosensor. As shown in Figure 4.5A, the binding of HRG to immobilized IgM was saturable and was dependent on the concentration of added HRG in the range of 0.5 - 5 μM. For each concentration of HRG the observed rate constant (k_{obs}), was determined from the biosensor data and the results are presented in Figure 4.5B. It was calculated (Table 4.3) that the on-rate and off-rate for the binding of HRG to IgM was 0.036 ± 0.005 x 10^5 $M^{-1}s^{-1}$ and 7.11 ± 0.102 x 10^{-3} s^{-1}, respectively, and that the K_d for this interaction was 1989.50 ± 50.50 nM.

Experiments also were carried out to assess the binding of HRG (1 μM) to immobilized IgM in the presence of different concentrations of Zn^{2+} (5-20 μM). The results showed a decrease in the binding of HRG to IgM with increasing concentrations of Zn^{2+} (data not shown). Studies of the binding of HRG at different concentrations (0.5-5 μM) to immobilized IgM in the presence of 20 μM

FIGURE 4.5 **Determination of the binding constant for the interaction of HRG with immobilized IgM.**

The IAsys biosensor was used to study the binding of HRG to biotinylated IgM immobilized onto the biosensor cuvette by coupling to immobilized STP. After equilibrating the system in PBS-BSA-T to obtain a base line, HRG was added at the indicated concentration (in the same buffer) and the binding of HRG was monitored for 5 minutes. The cuvette was then washed three times with PBS-BSA-T and dissociation of the bound HRG was monitored for 5 minutes. Overlay plots representing the binding of HRG at concentrations of 0.5 - 5 μM to the immobilized IgM are shown in (A). Overlay plots for similar experiments carried out in buffer containing 20 μM Zn^{2+} (PBS-BSA-T-Zn) instead of PBS-BSA-T also were obtained (not shown). The value of k_{obs} for the binding curve at each concentration of HRG in the presence or absence of added Zn^{2+} was determined using the linearization method (FAST FIT program). The results in (B) show plots of k_{obs} against HRG concentration for the HRG-IgM interaction in PBS-BSA-T buffer (■, control) and for the same interaction in PBS-BSA-T containing 20 μM Zn^{2+} (□). The slope of the line of best fit for each set of data represents the k_{on} and the y-intercept represents the k_{off} for the interaction. Error bars represent ± SEM obtained from three separate experiments for each concentration of HRG.

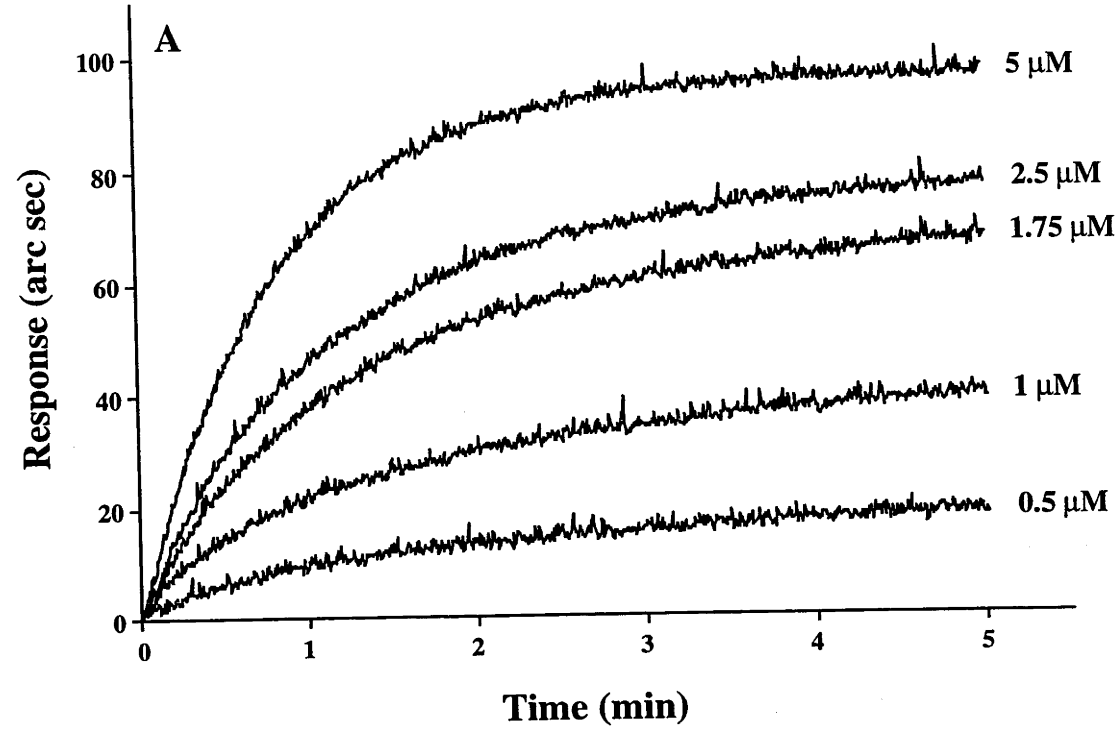
A
Response (arc sec)
Time (min)
5 μM
2.5 μM
1.75 μM
1 μM
0.5 μM
0
20
40
60
80
100
0
1
2
3
4
5

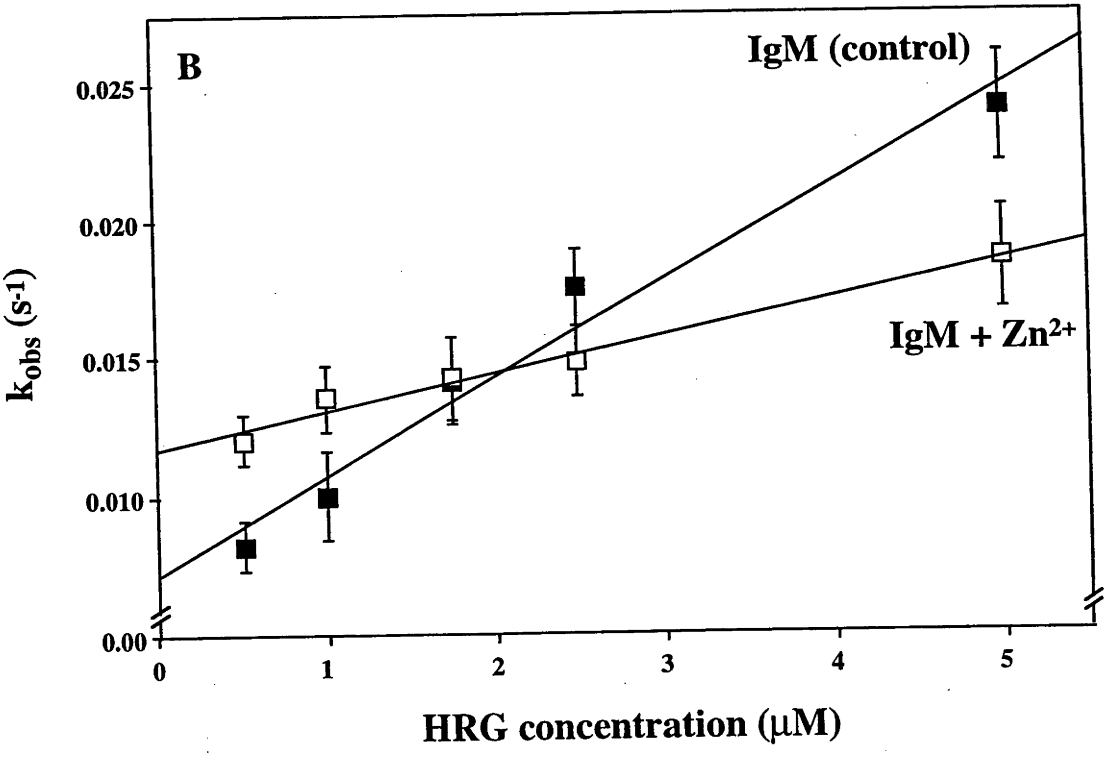
B
IgM (control)
IgM + Zn2+
kobs (s-1)
HRG concentration (μM)
0.00
0.010
0.015
0.020
0.025
0
1
2
3
4
5

Zn^{2+} were carried out to determine the effect of Zn^{2+} on the on- and off-rates of the HRG-IgM interaction (see Figure 4.5B and Table 4.3). These experiments indicated that in the presence of Zn^{2+} the on-rate of the interaction is decreased from $0.036 \pm 0.005 \times 10^5$ to $0.016 \pm 0.003 \times 10^5$ $M^{-1}s^{-1}$ (~ 2.3 fold decrease), whereas the off-rate is increased from $7.11 \pm 0.102 \times 10^{-3}$ to $11.84 \pm 1.60 \times 10^{-3}$ s^{-1} (~ 1.7 fold increase). The presence of Zn^{2+} therefore results in a 3.9 fold increase in the K_d for the HRG-IgM interaction, increasing it from 1989.50 ± 50.50 to 7754.0 ± 1707.0 nM (see Figure 4.5B and Table 4.3).

4.2.6 Effect of HRG on the formation of insoluble ICs between ovalbumin and κ containing anti-ovalbumin IgG (IgGκ)

The ability of HRG to interact with IgG1κ and IgG2κ with high affinity raised the question of whether HRG can inhibit the formation of insoluble ICs containing IgGκ. To explore this possibility experiments were aimed at examining the effect of HRG on the formation of insoluble ICs between ovalbumin and rat anti-ovalbumin IgGκ *in vitro*. These experiments required the production and use of polyclonal anti-ovalbumin IgG which was obtained by immunizing rats with ovalbumin. The anti-ovalbumin IgG was purified from the sera of rats immunized with ovalbumin using Avid-Al beads (see Materials and Methods). The proportion of κ and λ light chain in this IgG preparation was assessed using two commercially available mAbs specific for rat κ or λ light chains in ELISA assays. These assays showed that the rat anti-ovalbumin IgG used contained only the κ light chain, since no λ light chain could be detected using anti-λ mAb (data not shown). Only the preparations of IgGκ for which the purity was > 95% (as assessed by SDS-PAGE analysis, see Figure 4.6) were used in studies of insoluble IC formation.

The formation and increase in the size of insoluble ICs can be monitored by measuring the absorbance of the suspension at 350 nm as a function of time, since the increase in absorbance can be correlated with the size of the particles in suspension (Gorgani et al., 1996). The effect of HRG on the formation of insoluble ICs was examined by the addition of ovalbumin to a solution of IgGκ (that was either untreated or pre-treated with indicated concentrations of HRG) in PBS at 37°C. As shown in Figure 4.7A, the formation of insoluble ICs in a control experiment in which ovalbumin was added to a cuvette containing anti-ovalbumin IgGκ (200 μg/ml) in PBS buffer indicated that the maximum absorbance was increased from 0.00 initially to 0.07 after 30 minutes. In some experiments the anti-ovalbumin IgGκ (200 μg/ml) was pre-incubated with

FIGURE 4.6 **SDS-PAGE analysis of purified κ containing rat IgG (IgGκ).**

IgGκ was purified from ovalbumin immunized rat serum as described in Materials and Methods (Chapter 2) and then analysed by SDS-PAGE (10 % gel) under reducing and non-reducing conditions. After electrophoresis, the gel was stained with Coomassie Brilliant Blue. Lane M_1, high molecular weight markers; lane B, IgGκ (non-reduced); lane C, IgGκ (reduced); lane M_2, low molecular weight markers (reduced).

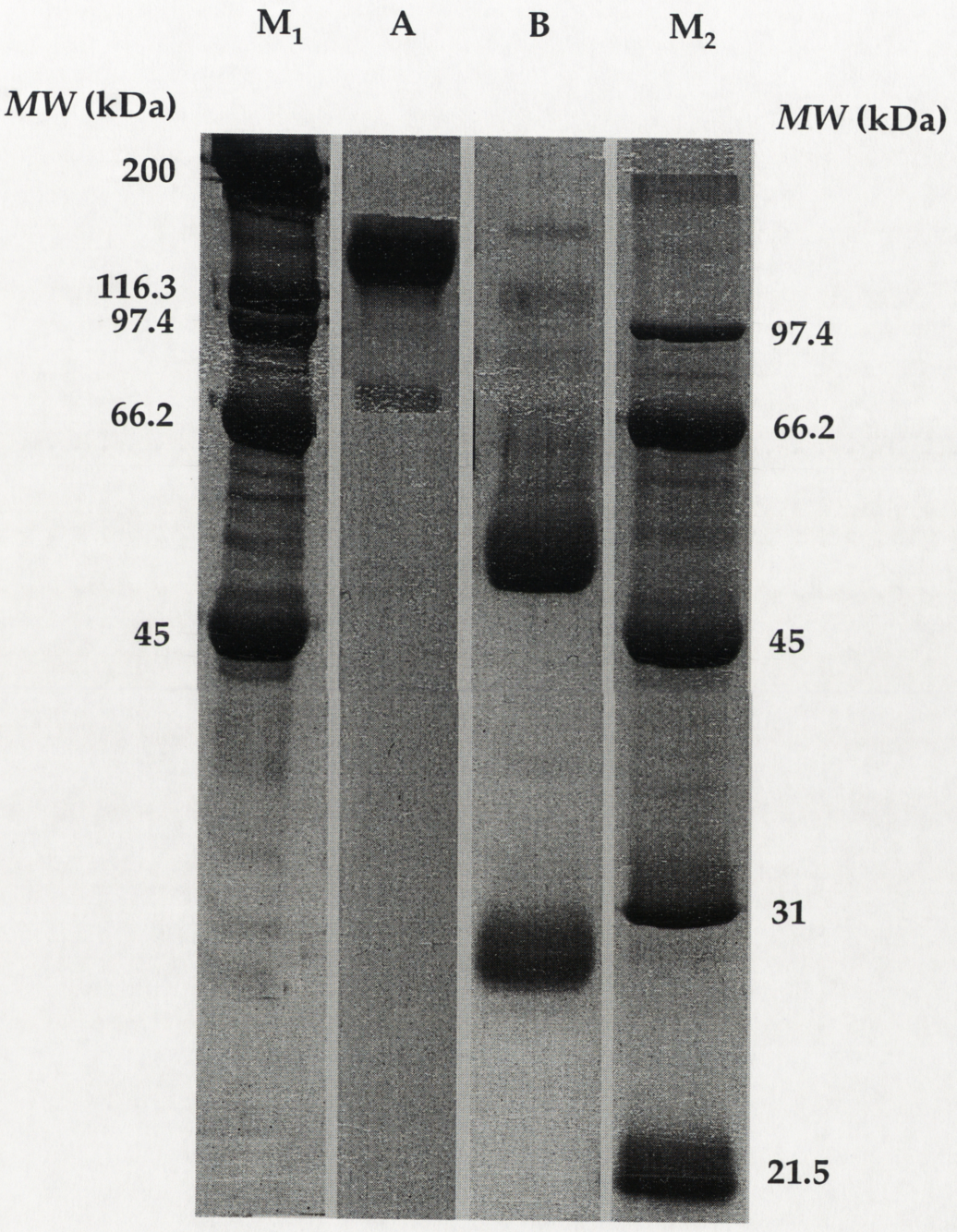
M1
A
B
M2
MW (kDa)
200
116.3
97.4
66.2
45
MW (kDa)
97.4
66.2
45
31
21.5

FIGURE 4.7 **The effect of HRG on the formation of insoluble ICs containing IgG with the κ light chain (IgGκ).**

Ovalbumin was mixed with a solution of anti-ovalbumin IgGκ in PBS (with or without native HRG) at 37°C and the formation of insoluble ICs was monitored by measuring the absorbance of the suspension at 350 nm using the light scattering technique. The formation of insoluble ICs was initiated either by addition of ovalbumin (6 μg/ml) to a solution of IgGκ (200 μg/ml) in PBS (○, control), or by the addition of ovalbumin to a solution of IgGκ which was pre-incubated for 5 minutes with 75 μg/ml (▲), 150 μg/ml (■) or 300 μg/ml (●) of native human HRG. The results for the absorbance of the suspension as a function of time is shown in (A). For each inhibition assay the time to reach 50% maximum absorbance was plotted versus HRG concentration (●) and is shown in (B). The data shown is representative of four experiments performed in duplicate.

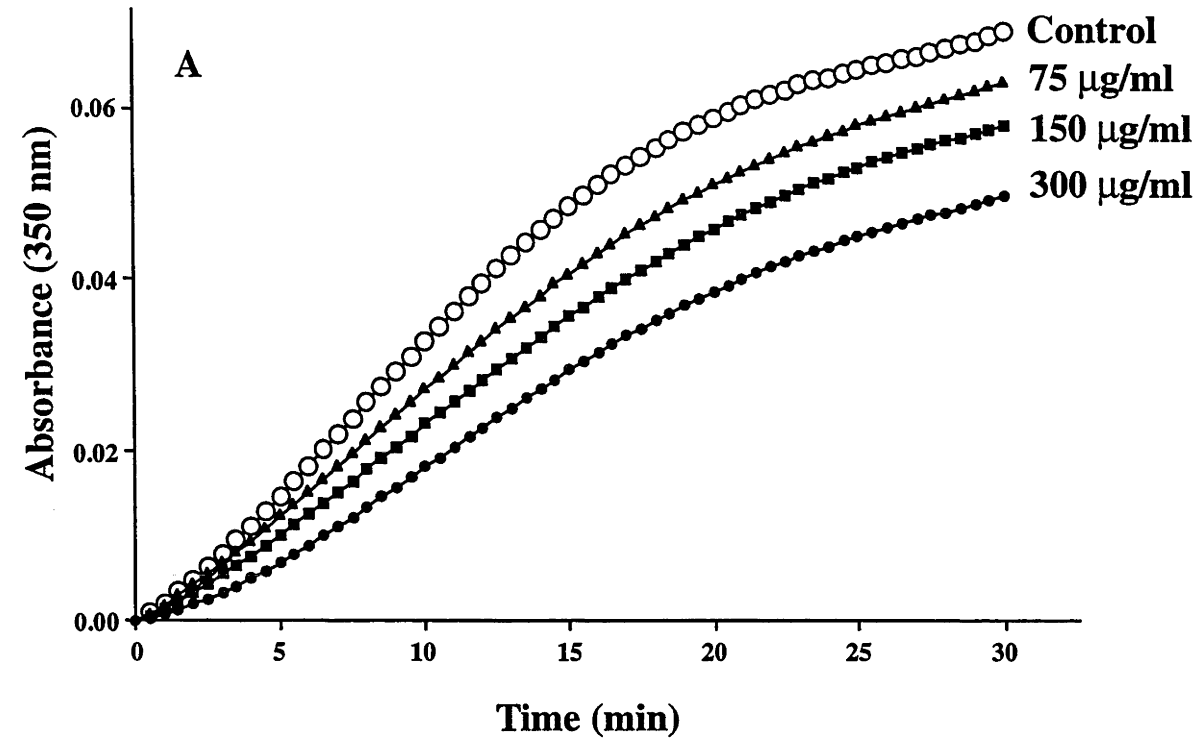
A
Control
75 μg/ml
150 μg/ml
300 μg/ml
Absorbance (350 nm)
0.00
0.02
0.04
0.06
0
5
10
15
20
25
30
Time (min)

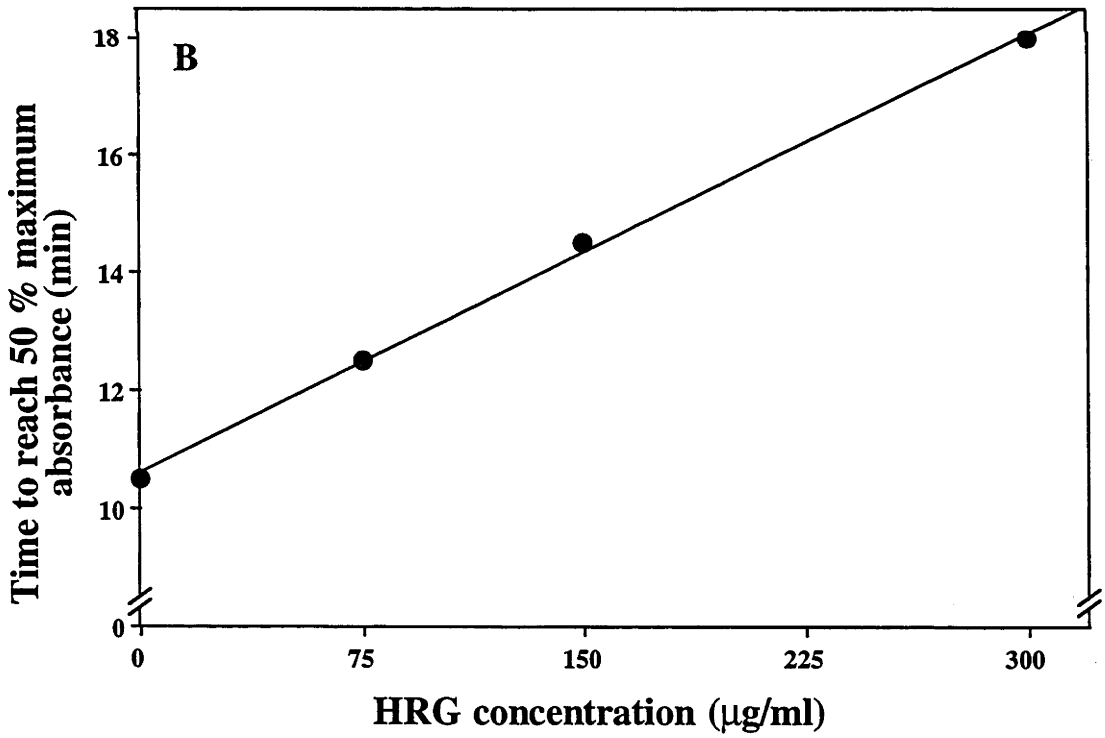
B
Time to reach 50 % maximum absorbance (min)
0
10
12
14
16
18
0
75
150
225
300
HRG concentration (μg/ml)

HRG before the addition of ovalbumin to initiate the formation of insoluble ICs. Interestingly, the presence of HRG at a concentration between 75 and 300 μg/ml decreased the initial rate of formation of rat IgGκ containing insoluble ICs (see Figure 4.7A). A plot of the time to reach 50% maximum absorbance against the HRG concentration is shown in Figure 4.7B, where it can be seen that at the higher HRG concentrations there is a longer lag time to reach 50% maximum absorbance, consistent with an ability of HRG to inhibit insoluble IC formation.

4.3 Discussion

The present study shows that HRG binds to different IgG subclasses and that the affinity of the interaction depends on the subclass. Thus, HRG interacts with IgG1κ and IgG2κ with much faster on-rate (and higher affinities) than with IgG3κ and IgG4κ. In contrast, although the affinities of the binding of HRG to IgG subclasses possessing λ light chains were similar, HRG interacts much faster with IgG4λ and IgG3λ than with IgG2λ and IgG1λ.

Interestingly, the results show that the affinity for the binding of HRG to IgG1κ is ~ 60-fold greater than the affinity for the binding of HRG to IgG1λ (see Figure 4.2A and Table 4.1). Similarly the affinity of the binding of HRG to IgG2κ is ~ 20-fold greater than that for binding to IgG2λ (Figure 4.2B and Table 4.1). In contrast, the binding of HRG to IgG3 and IgG4 (when each contained the λ light chain instead of κ) showed a different pattern. HRG bound to IgG3λ with ~ 1.3-fold higher affinity than it bound to IgG3κ. Similarly, HRG bound to IgG4λ with ~ 2.8-fold greater affinity than it bound to IgG4κ (see Figure 4.2 C,D and Table 4.1). These findings, therefore, suggest that human HRG interacts with all human IgG subclasses and the kinetics of binding are dependent not only on the particular subclass (or constituent heavy chain) of the IgG molecules, but also on the type of its constituent light chains. Thus, this study provides the first direct evidence for a functional role for the κ and λ light chains of Igs.

Structure studies have shown that most of the amino acid sequence differences between the different IgG subclasses are located in the hinge region, which may give rise to differences in the length and flexibility of this region of the IgG molecule. This also may reflect possible differences in the function of the different IgG subclasses (see Figure 4.8). Although the amino acid sequence of the constant region of the κ light chain is different to that of the constant region of the λ light chain, evidence suggests that the the constant region of the κ and λ light chains are homologous and structurally related. The structural homology between the variable regions of the κ and λ light chains, however, is less pronounced (Abbas et al., 1991).

The finding that HRG binds with different affinities to different IgG subclasses depending upon whether κ or λ light chains are present raised the intriguing possibility that HRG binds directly to the κ or λ light chains of IgG. An analysis of the binding of HRG to BJ proteins with κ or λ light chains using the IAsys biosensor revealed that HRG binds to both BJκ and BJλ, but that the on-rate for

FIGURE 4.8 **Three dimensional structure of IgG subclasses.**

The illustrations, reproduced from (Abbas et al., 1991), represent computer-generated space filling models of the different IgG subclasses. The models indicate that the structure of each subclass of IgG is distinct, and that the major differences in structure occurs in the IgG hinge region. This conclusion was also confirmed by comparing the amino acid sequence of each IgG subclass (Abbas et al., 1991).

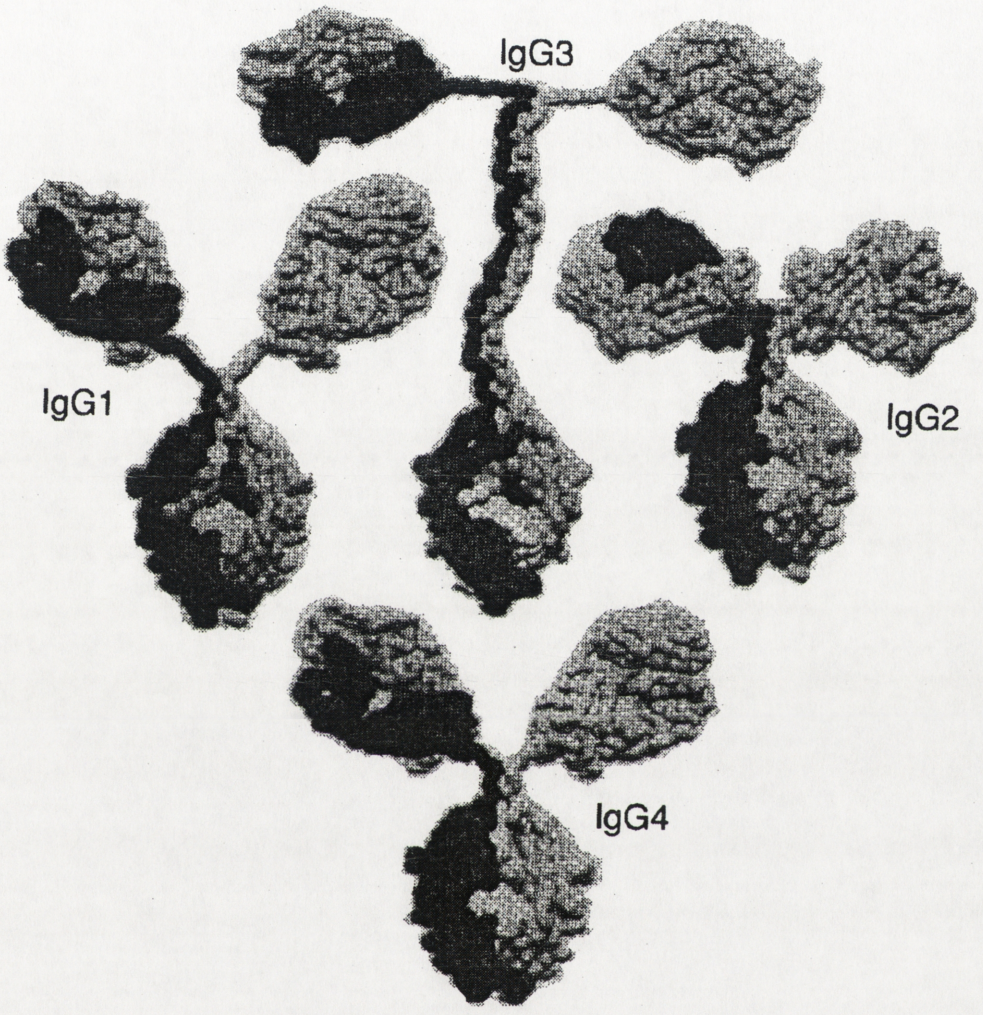
IgG3
IgG1
IgG2
IgG4

the HRG-BJκ interaction is 2-fold faster than for the HRG-BJλ interaction. This difference resulted in the affinity of the binding of HRG to immobilized BJκ being ~2 fold higher than for the binding of HRG to immobilized BJλ (see Figure 4.3B and Table 4.1). The higher affinity of the binding of HRG to BJκ suggests that the κ light chain in the IgG1κ and IgG2κ molecules is a factor in the high affinity interaction between HRG and these IgG subclasses. This conclusion may have implications for the function of HRG and IgG subclasses (see below).

Consistent with our recent finding that Zn^{2+} potentiates the binding of HRG to IgG (from pooled serum) (Gorgani et al., 1997), the present study shows that Zn^{2+} also potentiates binding of HRG to specific IgG subclasses. Physiological concentrations of Zn^{2+} had little if any effect on the binding of HRG to IgG1λ, but substantially potentiated the binding of HRG to IgG1κ. Figure 4.3A shows that the presence of Zn^{2+} led to an approximately 5-fold increase in the affinity of the binding of HRG to IgG1κ and led to a slight decrease in the affinity of the binding of HRG to IgG1λ (~ 1.4 fold). Therefore, in the presence of Zn^{2+}, HRG binds to IgG1κ with ~ 440-fold higher affinity than to IgG1λ, suggesting that Zn^{2+} strongly potentiates interaction of HRG with IgG1 containing the κ light chain, but only slightly effects the interaction of HRG with IgG1 containing the λ light chain.

Additional studies on the binding of HRG to IgG subclasses showed that 20 μM Zn^{2+} slightly increased the overall affinity of the binding of HRG to other IgG subclasses possessing κ light chains, and generally slightly reduced the affinity of binding of HRG to IgG subclasses possessing λ light chain, although in most cases these effects were not statistically significant. These results are consistent with each molecule of HRG interacting with both a heavy chain (presumably hinge region or CH1 domain) and a light chain (constant region) of the IgG molecule. Compared to the interaction of HRG with other IgG subclasses, the HRG-IgG1κ interaction was substantially affected by Zn^{2+} (5-fold increase), indicating that Zn^{2+} also potentiates the binding of HRG to the heavy chain of IgG (subclass difference). Similar results were obtained when different myeloma sources of the same IgG subclass and light chain isotype were used, indicating that the constant regions of heavy and light chains, rather than the variable regions, determine HRG binding.

Another interesting finding from the present work relates to the effect of Zn^{2+} on the binding of HRG to BJ proteins. As shown in Figure 4.3B and Table 4.2, the presence of Zn^{2+} led to a ~ 3.4-fold increase in the affinity of the binding of HRG

to BJκ and a ~ 1.8-fold decrease in the affinity of the binding of HRG to BJλ. Therefore, in the presence of Zn^{2+} the affinity of binding of HRG to BJκ is ~ 14-fold higher than the affinity of binding to BJλ. These findings are consistent with an effect of Zn^{2+} on the HRG-κ light chain interaction, and further support the notion that HRG binds more strongly to the κ light chain.

BJ proteins are of pathological importance in renal and systemic diseases associated with elevated levels of light chains in the blood circulation. The deposition of BJ proteins as tubular casts can cause diseases such as light chain deposition disease (LCDD). These light chain deposits, which may involve deposition of κ light chain in ~ 80 % of LCDD patients (Preud'homme et al., 1994), may result in the loss of renal function and account for morbidity and mortality in these patients (Solomon et al., 1991). Evidence suggests that the insolubilisation and aggregation of the unfolded protein may occur via intermolecular hydrophobic interactions (Bellotti et al., 1996). However, no protective mechanisms against insolubilisation and the deposition of these light chains in the kidney or blood vessel wall has yet been described. Clearly, in view of the present findings, it will be important, therefore, to establish whether HRG plays a role in inhibiting the insolubilisation and aggregation of BJ proteins, and hence whether HRG may play a role in protecting against their pathological effects.

Although it has been proposed that the IgG form of RF is the more pathogenic in relation to RA and SLE, the IgM form of RF is the most predominant form detected in the sera of these patients. It was important, therefore, to determine whether HRG also interacts with IgM. Kinetic studies of the binding of soluble HRG to immobilized IgM showed that HRG binds to IgM with a very low affinity. The affinity of the binding of HRG to IgM was ~ 650 fold lower than for the binding of HRG to IgG1κ (see Figure 4.5 and Table 4.2 and 4.3). In addition, the presence of 20 μM Zn^{2+} reduced the affinity of the HRG-IgM interaction by ~ 3.9 fold. Since the physiological concentration of HRG in plasma is ~ 2 μM, these observation suggest that the interaction of HRG with IgM may not be physiologically relevent. Importantly, the interaction of HRG with IgM and other immobilized ligands tested in the present work was inhibitable by pre-incubation of the HRG with a 4-fold molar excess of the ligand in solution (not shown), indicating that the binding of HRG was specific for each immobilized ligand.

It has been shown that of the total IgG in normal human plasma approximately 65 % and 25 % is in the IgG1 and IgG2 form, respectively (Abbas et al., 1991). HRG may be expected, therefore, to be more efficient at inhibiting the formation of insoluble ICs containing IgG1κ or IgG2κ than the formation of insoluble ICs containing other IgG subclasses. These observations suggest that the observed stronger interaction of HRG with IgG subclasses possessing κ light chains may be important in regulating the formation and clearance of ICs under normal conditions. Thus, the ability of HRG to interact with IgG1κ with a higher affinity than with IgG1λ, also may inhibit the insolubilisation of IgG1κ containing ICs more efficiently than those containing IgG1λ. On the other hand, the faster binding of HRG to IgG4λ may indicate a role for HRG in other pathological conditions where the IgG4λ concentration is high compared to IgG4κ. The differential binding of HRG to IgG subclasses may also allow ICs containing different IgG subclasses to insolubilise at different rates. The insolubilisation rate of ICs may prevail the persistence of Ags in insoluble ICs. This finding may also imply that HRG can direct ICs to different Ag presenting cells (see Chapter 5). Thus, HRG may lead to the clearance of insoluble ICs by the RES, whereas, soluble ICs may be used as an Ag depot.

Functional studies using light scattering techniques revealed that HRG efficiently inhibits the formation of insoluble ICs between ovalbumin and the purified polyclonal rat anti-ovalbumin IgG containing > 98 % IgGκ (see Figure 4.7A). The inhibition was similar to that seen for the formation of insoluble ICs containing rabbit IgG (see Chapter 3) and was dependent on the HRG concentration. As shown in Figure 4.7B, the time to reach 50% maximum absorbance was positively correlated with the HRG concentration, indicating that human HRG can inhibit the formation of insoluble ICs containing IgGκ. This finding is consistent with our previous observation on the effect of HRG on the formation of insoluble ICs containing ovalbumin and rabbit anti-ovalbumin IgG (Gorgani et al., 1997). The finding that human HRG inhibits the formation of insoluble ICs containing IgG from different species (eg. rabbits and rats) also further strengthens the notion that this function of HRG is physiologically relevant. These findings provided the basis for the studies in Chapter 6, the results of which also support the notion that HRG regulates the formation of insoluble ICs in humans, *in vivo*.

CHAPTER 5

HISTIDINE-RICH GLYCOPROTEIN REGULATES THE BINDING OF MONOMERIC IgG AND IMMUNE COMPLEXES TO MONOCYTES

Abstract

HRG is a relatively abundant plasma protein which I have shown previously inhibits the formation of insoluble ICs. In this study the ability of HRG to regulate the binding of monomeric IgG and ICs to monocytes was examined. Initial studies demonstrated that HRG interacts with FcγRI on the monocytic cell line THP1 and blocks the binding of monomeric IgG to these cells. However, despite totally blocking the binding of monomeric IgG to FcγRI, preincubation of THP1 cells with HRG had no effect on the binding of ICs to these cells. In contrast, depending on the HRG : IgG molar ratio, preincubation of monomeric IgG with HRG resulted in either enhanced or reduced IgG binding to FcγRI. Similarly, under certain highly defined conditions, incorporation of HRG in IgG containing ICs potentiated the binding of ICs to THP1 cells. The key conditions involved incorporating approximately equimolar concentrations of HRG and IgG in the ICs, the ICs being formed at a near equivalence Ag : Ab ratio and usually physiological concentration (20 μM) of Zn^{2+} being present. Based on these observations, a model is proposed where the IgG binding domain of HRG can interact with FcγRI on monocytes and block monomeric IgG binding. In contrast, if HRG interacts with monomeric IgG or IgG containing ICs the FcγRI binding site on HRG is masked and HRG enhances IC binding to monocytes, probably via its heparan sulfate binding domain.

5.1 Introduction

The recognition of a cognate Ag by polyclonal Ab molecules in the blood circulation may result in the formation of soluble and insoluble ICs. The mechanisms by which such ICs are cleared from the circulation and from tissues are not well understood, but the binding of ICs to FcRs (Anderson, 1989; Abrass, 1984) and, following complement fixation, to CRs (Schifferli et al., 1988; Walport and Davies, 1996) on mononuclear phagocytic cells is known to be important. Three different types of FcRs specific for IgG, namely FcγRI, FcγRII and FcγRIII (each similar in biological function but capable of binding distinct IgG subclasses) are known to exist in humans (Van de Winkel and Anderson, 1991; Van de Winkel and Capel, 1993). Evidence suggests that the binding of IgG to FcRs on mononuclear cells can trigger a number of responses; including the phagocytosis, uptake and clearance of ICs. Thus, under normal physiological conditions ICs may be recognized by the RES including the peripheral blood mononuclear phagocytic cells (Anderson and Abraham, 1980; Anderson, 1982; Anderson, 1989) and the resident mononuclear phagocytic cells in liver and/or spleen, and cleared from the circulation (Schifferli et al., 1988; Emlen et al., 1992; Davies et al., 1992). Similarly, in many tissues ICs may be cleared by tissue macrophages and monocytes which are recruited from the circulation as part of the inflammatory response (Walport and Davies, 1996).

A role for components of complement in the uptake and clearance of ICs by phagocytic cells was first suggested by the demonstration that receptors for complement C3 exist on monocytes (Huber et al., 1968), and that large ICs in blood can activate complement, and both generate and incorporate C3 fragments such as C3b and C3d (Schifferli, 1987). Subsequent studies showed that blood borne C3b-opsonized ICs are usually recognized by C3b binding receptors (CR1) on erythrocytes (Veerhuis et al., 1986; Schifferli et al., 1988 and Davies et al., 1992). Erythrocytes, upon entering the liver and/or spleen (Cornacoff et al., 1983, 1984) may release bound ICs (Yokoyama and Waxman, 1994) which are then free to interact with resident tissue mononuclear cells such as macrophages and monocytes via receptors for Fc, C3b and C3d (Ehlenberger and Nussenzweig, 1977; Emlen et al., 1992; Taylor et al., 1997).

Studies described in Chapter 3 showed that HRG binds to IgG-containing soluble ICs, and inhibits the formation of insoluble ICs *in vitro* by promoting the maintenance of ICs in a soluble form (Gorgani et al., 1997). HRG also is reported to bind to macrophages and to regulate FcR expression and phagocytosis

(Chang et al., 1992b, 1994). Since HRG incorporates in ICs and binds to macrophages, it was important to examine whether HRG plays any role in the uptake of ICs by mononuclear cells. The present work uses flow cytometry to study the effect of HRG on the binding of IgG and ICs to the human mononuclear phagocytic cell line THP1. The results show that HRG inhibits the binding of monomeric human or rabbit IgG to FcγRI on THP1 cells, but promotes the binding of ICs containing either human or rabbit IgG to these cells in a Zn^{2+}-dependent manner. The results indicate that HRG regulates the binding of both monomeric IgG and ICs to mononuclear cells, and provides strong evidence for the existence of a complement-independent mechanism for enhancing the clearance of ICs from the circulation.

5.2 Results

5.2.1 Binding of human IgG and HRG to THP1 cells

It is well established that monomeric IgG binds to monocytes and macrophages through $Fc_{\gamma}RI$ on the surface of these cells (Anderson and Abraham, 1980; Anderson, 1982; Woof et al., 1986; Ravetch and Kinet, 1991; Sylvestre and Ravetch, 1994; Abrass, 1991). Initial experiments were aimed at determining the level of binding of human IgG to the monocytic cell lines THP1 and U937 by flow cytometry. For these studies the cells were incubated with different concentrations of human b-IgG in PBS-BSA, washed and then stained with FITC-STP. The data in Figure 5.1A show histograms representing the FITC-fluorescence of THP1 cells incubated either with 20 nM b-BSA (control), or with 1.25, 5, and 20 nM b-IgG. A plot of the Median FIU of the cells against different b-IgG concentrations indicates that the level of b-IgG binding to the cells increases with increasing concentrations in the range of 40 pM - 40 nM (Figure 5.1B). These results indicate that binding of the IgG to THP1 cells is saturable with near-maximal binding occurring at an IgG concentration of ~ 20 nM. A similar value for near-maximal binding also was obtained when U937 cells were used instead of THP1 cells (not shown).

Previous studies have shown that HRG binds to peritoneal macrophages and regulates phagocytosis of Ab opsonized erythrocytes (Chang et al., 1992b, 1994). To determine whether binding of HRG to THP1 and U937 cells also can be detected by flow cytometry, experiments were performed in which the cells were incubated in PBS-BSA in the presence of human b-HRG, and the binding of the b-HRG to the cells assessed by fluorescence activated cell sorter (FACS) analysis after staining with FITC-STP. The fluorescence profiles for the binding of 5 μM b-BSA (control) and different concentrations of HRG (0.28, 1.12 and 4.5 μM) to THP1 cells are shown in Figure 5.1C. Similar experiments were carried out at a number of different HRG concentrations in the range 9nM to 9 μM, at each concentration the Median FIU of the cells being plotted against the concentration of HRG (see Figure 5.1D). These data show that HRG binds to THP1 cells, and that the binding is concentration-dependent and saturable, with near-maximal binding occurring at ~ 4.5 μM HRG. A similar value for near-maximal binding also was obtained using U937 cells instead of THP1 cells (not shown).

FIGURE 5.1 **The binding of human IgG or HRG to THP1 cells**

THP1 cells were incubated with biotinylated human IgG (b-IgG) in the concentration range of 40 pM - 40 nM or biotinylated human HRG (b-HRG) in the concentration range of 9 nM - 9 μM in PBS-BSA for 1 hr on ice. After washing off unbound b-IgG or b-HRG, the cells were stained with FITC-STP, and the FITC-fluorescence profile of the cells was determined by FACS. The histograms in (A) show the fluorescence profiles representing the binding of 1.25 nM (Blue line), 5 nM (red line) and 20 nM (green line) of b-IgG to THP1 cells. The black line represents the fluorescence profile of control cells incubated with 20 nM b-BSA instead of b-IgG. For clarity the profiles for only three concentrations of b-IgG are shown. The histograms in (C) represent the FITC-fluorescence profiles due to the binding of HRG at 0.28 μM (blue line), 1.12 μM (red line) and 4.5 μM (green line) to the THP1 cells. The black line represents the fluorescence profile of cells incubated with 5 μM b-BSA instead of b-HRG (control experiment). The Median FIU of the cells incubated at each different concentration of b-IgG or b-HRG was determined using the computer program "Cell Quest". The plot of the relative Median FIU against the concentrations of b-IgG (●) and b-HRG (■) are shown in (B) and (D), respectively. Each histogram in (A) and (C) and each of the data points in (B) and (D) are representative results obtained from 3 separate experiments carried out at the indicated concentration of IgG or HRG.

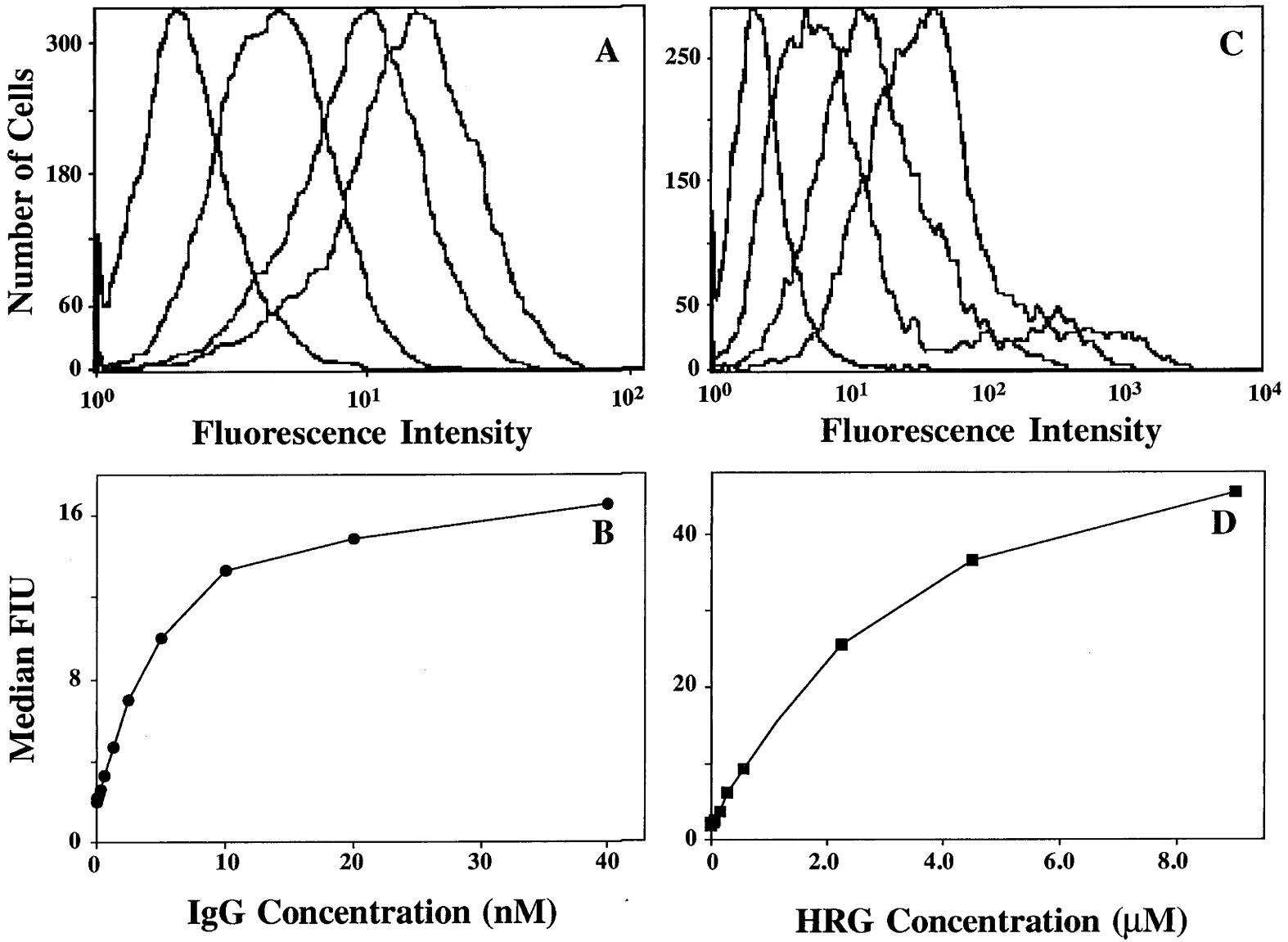
A
Number of Cells
300
180
60
0
10^0
10^1
10^2
Fluorescence Intensity
C
250
150
50
0
10^0
10^1
10^2
10^3
10^4
Fluorescence Intensity
B
Median FIU
16
8
0
0
10
20
30
40
IgG Concentration (nM)
D
40
20
0
0
2.0
4.0
6.0
8.0
HRG Concentration (μM)

Additional experiments indicated that preincubation of b-HRG (2 μM) with heparin (50 μg/ml) inhibited the binding of b-HRG to THP1 cells by ~ 60 %, whereas, preincubation with 2 μM IgG inhibited binding by ~ 35 %. Furthermore, these inhibitory effects were additive: preincubation of HRG (2 μM) with both heparin (50 μg/ml) and IgG (4 μM) inhibiting the binding of HRG to THP1 cells by 80 - 90 %. In addition, preincubation of THP1 cells with a saturating amount of a mouse mAb (MRII) specific for human FcγRI partially inhibited (35%) the subsequent binding of HRG to the cells, at a wide range of concentrations (9 nM - 9 μM), supporting the notion that HRG interacts with FcγRI (not shown). As previously shown for other cell types, the presence of physiological concentrations (20 μM) of Zn^{2+} potentiated the binding of HRG to THP1 cells by ~ 45% (data not shown), an effect which has been shown to be due to an enhancement of heparin-inhibitable binding (Olsen et al., 1996; Borza and Morgan 1998). These results are consistent with HRG interacting with at least two different binding sites on THP1 cells: sites inhibitable by heparin (presumably cell surface heparan sulfates), and sites inhibitable by IgG (the cell surface FcγRI).

5.2.2 Effect of pre-treating THP1 cells with HRG on IgG binding

The observation that HRG binds to FcγRI on THP1 cells raised the question of whether cell-bound HRG affects the ability of the cells to bind monomeric IgG. To explore this, THP1 cells were either preincubated in PBS-BSA or preincubated in PBS-BSA containing 2, 4 and 8 μM HRG, before washing and incubating the cells with different concentrations (40 pM - 40 nM) of b-IgG. After washing away unbound b-IgG the cells were then stained with FITC-STP and subjected to FACS analysis. The data in Figure 5.2A show the Median FIU of cells following incubation with different IgG concentrations and indicate that preincubation of THP1 cells with 2, 4 and 8 μM HRG strongly inhibited subsequent binding of IgG. In fact, at the higher concentrations of HRG (4 and 8 μM) an almost total inhibition of IgG binding was observed. Similar experiments also were carried out in which the effect of preincubating THP1 cells with different concentrations of HRG (9nM - 9 μM), on the subsequent binding of a constant concentration of IgG (20 nM) was examined (Figure 5.2B). The results indicate that the pre-treatment of THP1 cells with HRG inhibits the subsequent binding of IgG, and that this inhibition is dependent on the HRG concentration with HRG concentrations ≥ 2 μM inhibiting monomeric IgG binding by 90% or more (Figure 5.2B).

FIGURE 5.2 **Effect of HRG on the binding of IgG to THP1 cells**

THP1 cells were either left untreated (control) or preincubated for 1 hr on ice with different concentrations of HRG in PBS-BSA or in PBS-BSA-Zn. All cells were then washed to remove any unbound HRG, and incubated with the indicated concentration of biotinylated IgG (b-IgG). In some experiments, the b-IgG also was pre-incubated with the HRG (either in PBS-BSA or in PBS-BSA-Zn) before incubation with the THP1 cells. After the incubation(s) the cells were then washed, stained with FITC-STP, and subjected to FACS analysis. Each data point in (A) shows the median fluorescence due to the binding of a different concentration of b-IgG to control THP1 cells (●), and to THP1 cells pre-treated with 2 μM (○), 4 μM (△) and 8 μM (□) HRG. The binding of b-IgG (20 nM) to THP1 cells pre-treated with different concentrations of HRG (9 nM -9 μM) in either PBS-BSA (■) or in PBS-BSA-Zn (□) is shown in (B). In some experiments, the b-IgG (20 nM) was pre-incubated with different concentration of HRG (9 nM -9 μM) and this mixture was then incubated with THP1 cells in either PBS-BSA (▲) or in PBS-BSA-Zn (△) and the effect on b-IgG binding determined (B). Each point is a representative result obtained from 3 separate experiments carried out at each concentration of IgG (A) and HRG (B).

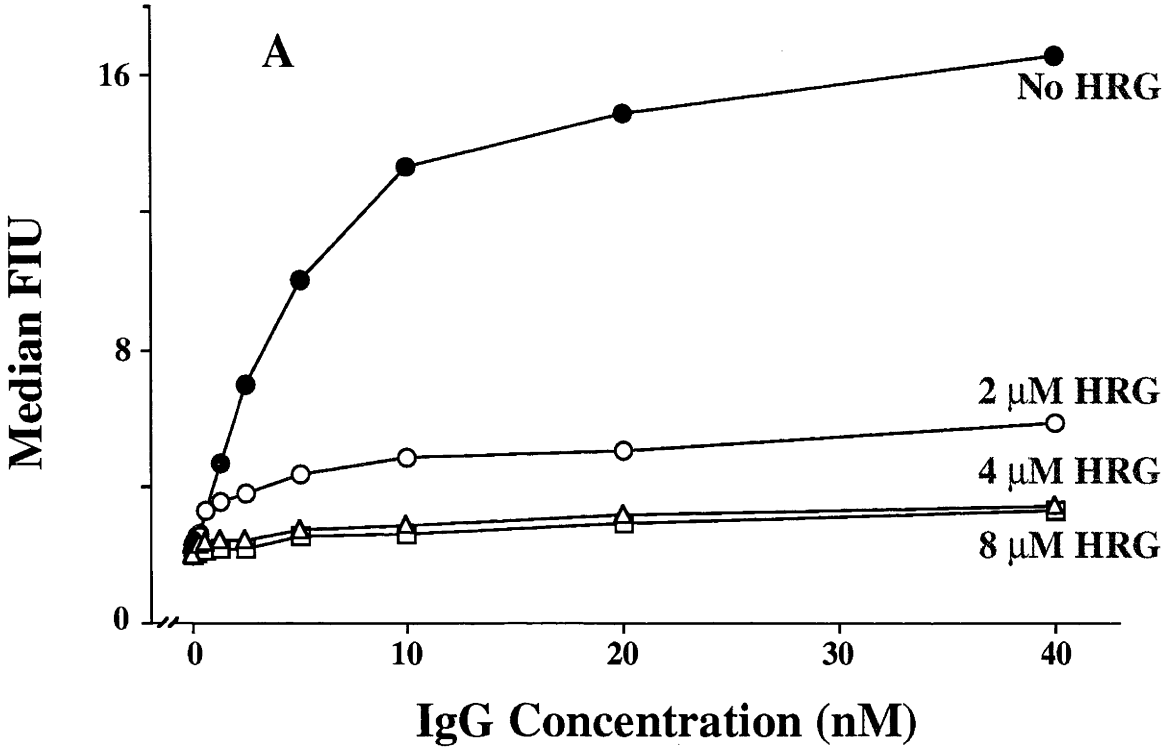
A
16
8
0
Median FIU
No HRG
2 μM HRG
4 μM HRG
8 μM HRG
0
10
20
30
40
IgG Concentration (nM)

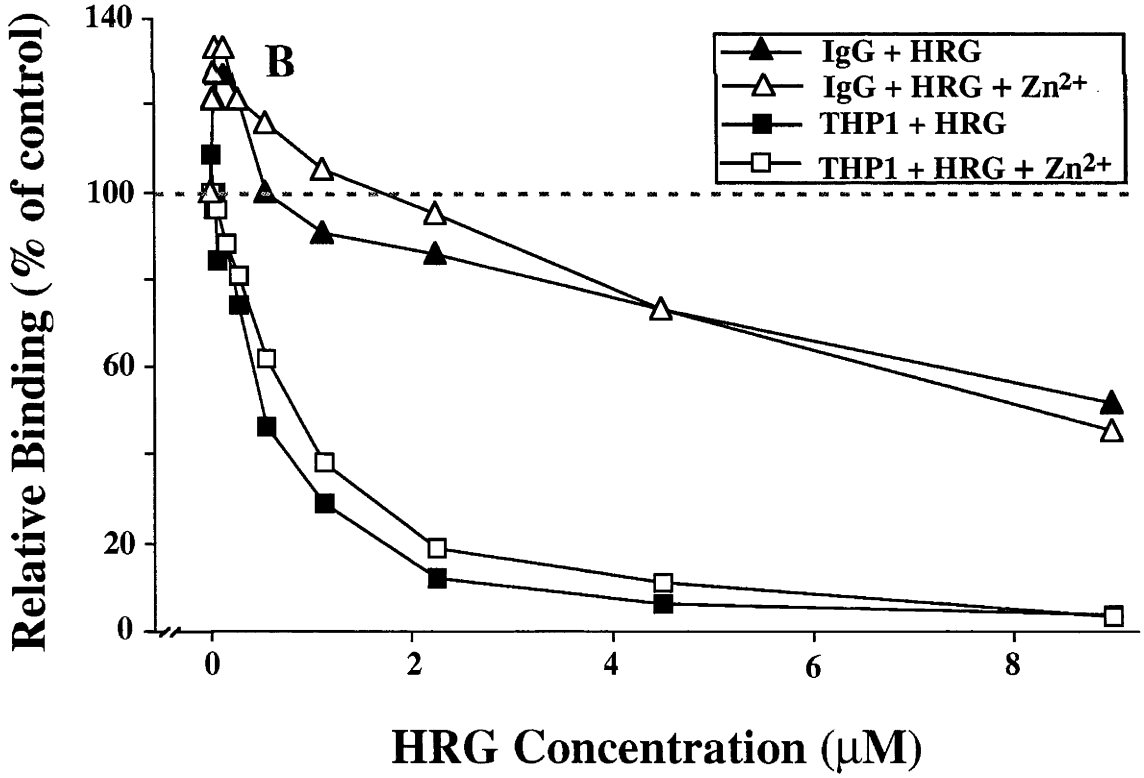
B
140
100
60
20
0
Relative Binding (% of control)
IgG + HRG
IgG + HRG + Zn2+
THP1 + HRG
THP1 + HRG + Zn2+
0
2
4
6
8
HRG Concentration (μM)

Recently we showed that the presence of Zn^{2+} modulates the binding of HRG to several different T cell lines (Olsen et al., 1996) and to IgG (Gorgani et al., 1997). To determine whether Zn^{2+} also can modulate the effect of HRG on the binding of IgG to THP1 cells, the experiments described above also were performed with 20 μM Zn^{2+} being included in the binding buffer (PBS-BSA-Zn). The results of these studies indicate that the presence of 20 μM Zn^{2+} had no significant effect on the binding of IgG to THP1 cells (not shown), and had little or no modulatory action on the inhibitory effect of HRG on IgG binding (Figure 5.2B, open squares).

5.2.3 Effect of preincubating IgG with HRG on IgG binding to THP1 cells

The ability of HRG to bind IgG (see Chapter 3), suggested that the pre-incubation of IgG with HRG also might influence the binding of IgG to FcγRI on THP1 cells. To explore this possibility b-IgG was first pre-incubated with different concentrations of HRG in PBS-BSA, and the mixture was then incubated with THP1 cells. Binding of the IgG to the cells again was assessed by FACS analysis after staining the cells with FITC-STP. As shown by the plot of relative binding against HRG concentration (Figure 5.2B), the pre-incubation of b-IgG (20 nM) with relatively low concentrations (~ 20 - 280 nM) of HRG enhanced binding of the IgG to THP1 cells, whereas pre-incubation of the IgG with higher concentrations (1.12 - 9 μM) of HRG partially inhibited binding of the IgG to these cells (Figure 5.2B filled triangles). Parallel experiments also were carried out in which 20 nM b-IgG was pre-incubated with different concentrations of HRG in PBS-BSA-Zn before incubating the mixture with THP1 cells. Overall Zn^{2+} had little or no effect on the ability of HRG to modulate the binding of IgG to THP1 cells, although there was a suggestion that at low concentrations of HRG (approximately 20 nM - 1 μM) Zn^{2+} further potentiated the effect of HRG on IgG binding (see Figure 5.2B, open triangles). Control experiments indicated that Zn^{2+} alone had no effect on the binding of IgG to THP1 cells (not shown).

5.2.4 The binding of monomeric rabbit IgG and rabbit IgG containing ICs to THP1 cells

To facilitate studies on the binding of ICs to THP1 cells, the binding of FITC labeled monomeric rabbit anti-ovalbumin IgG (FITC-IgG) to THP1 cells was first examined by FACS analysis. As reflected by the increase in FITC-fluorescence

of the cells, the binding of the FITC-IgG to THP1 cells was dependent on the FITC-IgG concentration and was saturable, with near-maximal binding occurring at ~ 10 nM FITC-IgG (see Figure 5.3A). This result is similar to that observed for the binding of biotinylated human IgG to THP1 cells (see Figure 5.1B). Also, an analysis of the precipitin curve (see Materials and Methods) for ICs containing ovalbumin and FITC-anti-ovalbumin IgG indicated that maximum precipitation (~ 38% of the total added FITC-IgG) occurs when the ratio of ovalbumin : FITC-IgG is between 0.02 and 0.04 (Figure 5.3C, open squares). This ratio is similar to that obtained from an analysis of ovalbumin and non-FITC labelled anti-ovalbumin IgG containing ICs (not shown). These results suggest that the labelling of the anti-ovalbumin IgG with FITC does not significantly affect the ability of the monomeric IgG to bind to THP1 cells or to form ICs with ovalbumin.

To study the binding of ICs to THP1 cells, different concentrations of ovalbumin were pre-incubated with FITC-IgG (0.5 μM) for 30 minutes in PBS-BSA buffer to allow the formation of ICs and then each mixture was incubated separately with THP1 cells. Ovalbumin/FITC-IgG ratios were used to yield ICs in Ab excess, Ag excess and at equivalence. After incubation with ICs, the cells for each IC preparation were washed to remove unbound fluorescent ICs and subjected to FACS analysis. The data in Figure 5.3B shows that relative to cells incubated with 0.5 μM of free FITC-IgG (control, blue line), THP1 cells incubated with ICs formed in Ag excess (Ag: Ab ratio = 0.06) showed a homogenous increase in FITC-fluorescence (Figure 5.3B, green line) as a consequence of the binding of FITC-containing ICs to the cells. When THP1 cells were exposed to ICs formed at an equivalence Ag : Ab ratio, the binding of fluorescent ICs became more heterogeneous and broadly distributed, with some cells showing a very high level of fluorescence while others showed a level of IC binding similar to that seen with ICs formed in Ag excess (Figure 5.3B, red line). This broad distribution in fluorescent IC binding to the cells most likely reflects great heterogeneity in the size of ICs formed at equivalence. Figure 5.3C clearly shows that ICs formed at equivalence or in slight Ab excess bind best to THP1 cells whereas IC binding is less evident when the complexes are formed in Ag excess (Figures 5.3B and C). Interestingly, the inclusion of 20 μM Zn^{2+} in the reaction buffer (PBS-BSA-Zn) resulted in a decrease in the binding of ICs formed at near equivalence Ag : Ab ratios to THP1 cells (Figure 5.3C, triangles).

FIGURE 5.3 **The binding of ICs containing FITC-labelled rabbit IgG to THP1 cells**

THP1 cells were incubated with different concentrations (0 - 36 nM) of FITC labelled rabbit anti-ovalbumin IgG (FITC-IgG) in PBS-BSA for 1 hr on ice. The cells were washed to remove unbound FITC-IgG and the FITC-fluorescence profile of the cells was determined by FACS analysis. The Median FIU obtained for the cells incubated at each different concentration of FITC-IgG was plotted against the concentration of FITC-IgG (▲) as shown in (A). To examine the binding of ICs to THP1 cells, ICs were formed by incubating FITC-IgG (0.5 μM) with ovalbumin at different Ag : Ab ratios in the range of 0.005-0.06 in PBS-BSA buffer for 30 minutes on ice and the IC mixture was then incubated with THP1 cells. The cells were washed to remove unbound ICs, and the fluorescence profile of the cells was determined by FACS analysis. The histograms in (B) represent the FITC-fluorescence profiles due to the binding to THP1 cells of ICs formed either at Ag excess (0.06 Ag : Ab ratio) (green line) or at equivalence (0.03 Ag : Ab ratio) (red line) . The blue line represents the fluorescence profile of cells incubated with 0.5 μM of free FITC-IgG (no ovalbumin added control). The binding to THP1 cells of fluorescent ICs formed at different Ag : Ab ratios is shown in (C), IC binding being assessed either in PBS-BSA (●) or in PBS-BSA containing 20 μM Zn^{2+} (▲). The precipitin curve analysis (□) for the formation of insoluble ICs containing FITC-IgG and ovalbumin also is shown in (C), with the percent precipitation of FITC-IgG at each Ag : Ab ratio being depicted. The data are representative results obtained from 3 separate experiments carried out at each concentration of FITC-IgG in (A) and at each Ag : Ab ratio (B and C).

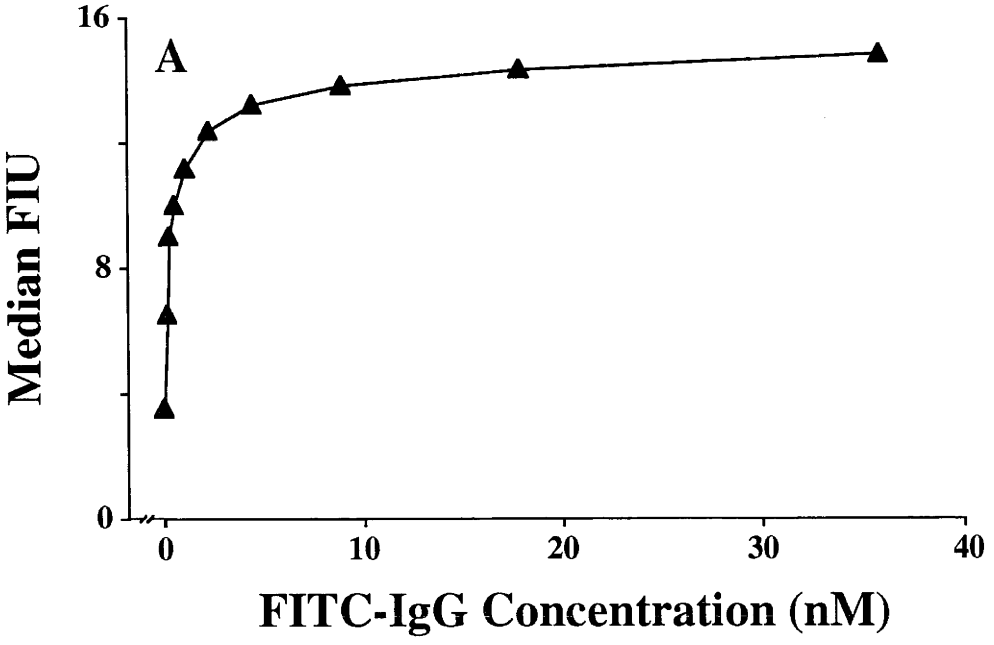
A
16
8
0
Median FIU
0
10
20
30
40
FITC-IgG Concentration (nM)

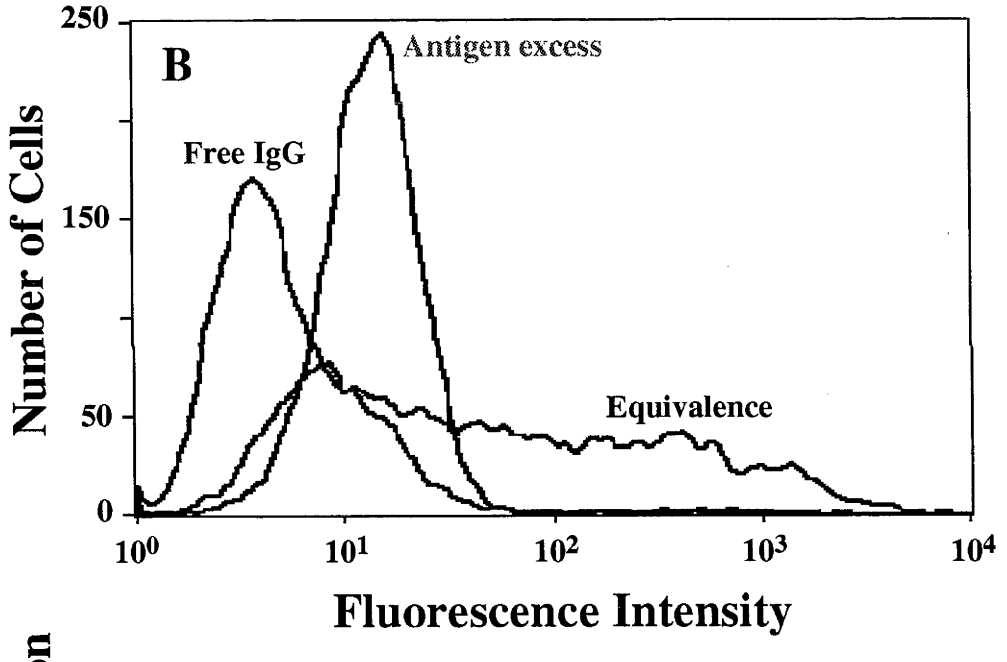
B
250
150
50
0
Number of Cells
Antigen excess
Free IgG
Equivalence
10^0
10^1
10^2
10^3
10^4
Fluorescence Intensity

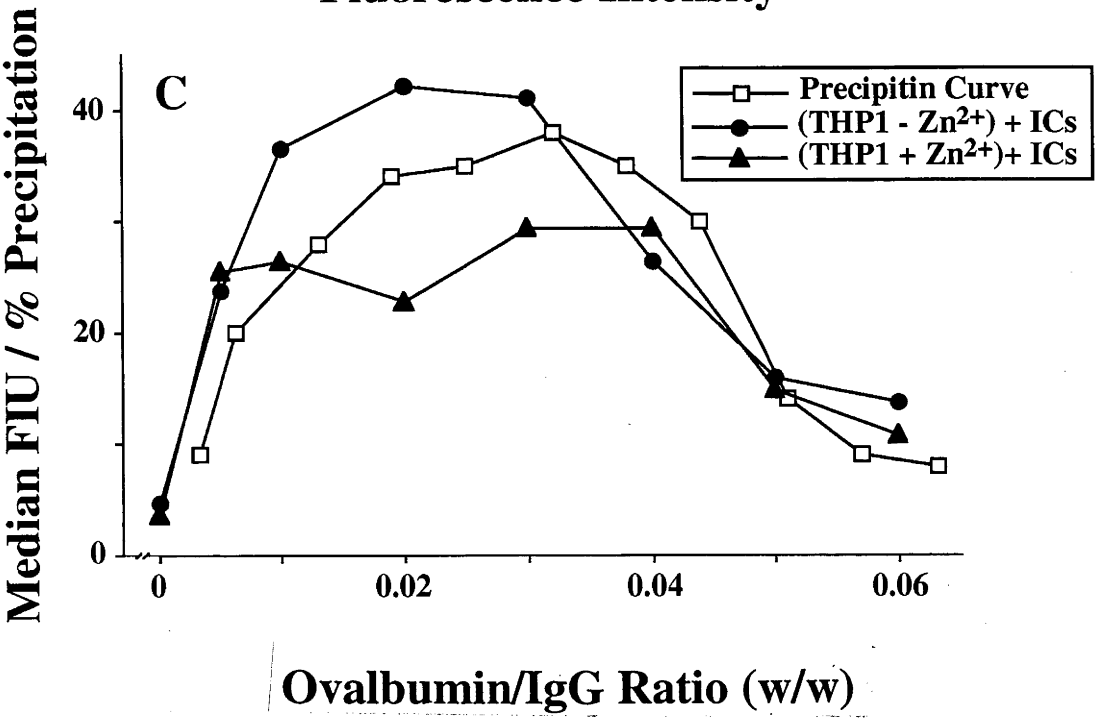
C
40
20
0
Median FIU / % Precipitation
Precipitin Curve
(THP1 - Zn^{2+}) + ICs
(THP1 + Zn^{2+})+ ICs
0
0.02
0.04
0.06
Ovalbumin/IgG Ratio (w/w)

5.2.5 Effect of pretreating THP1 cells with HRG on IC binding

The binding of ICs containing ovalbumin and anti-ovalbumin FITC-IgG to THP1 cells pre-incubated with HRG also was investigated. For these experiments THP1 cells were either left untreated (control), or were pre-incubated with 2 μM HRG in PBS-BSA buffer, and then washed to remove unbound HRG. Subsequently, the cells were incubated with preformed fluorescent ICs, the cells washed to remove unbound ICs and analysed for bound IC by fluorescence flow cytometry. From the fluorescence profiles of the cells, it can be seen that pre-treatment of the THP1 cells with HRG inhibited the binding of free FITC-IgG (Figure 5.4A), but had little if any affect on the binding of ICs formed at equivalence (Ag : Ab ratios of 0.03) or in Ag excess (Ag : Ab ratios of 0.06) (see Figures 5.4B and C).

To determine whether the presence of Zn^{2+} alters the effect of HRG in this system, parallel experiments also were carried out in which 20 μM Zn^{2+} was included in the incubations. It was found that HRG, when preincubated with cells, also had no effect on the binding of ICs to THP1 cells when Zn^{2+} was present.

5.2.6 Effect of pretreating ICs with HRG on the binding of ICs to THP1 cells

The results presented in section 5.2.3 indicate that the binding of human IgG to THP1 cells is enhanced when monomeric human IgG is preincubated with HRG (HRG : IgG molar ratio ~ 1 - 10 : 1) before incubating the HRG-IgG mixture with the cells. To determine whether HRG also enhances the binding of ICs to THP1 cells, HRG was incorporated in ICs by preincubating anti-ovalbumin FITC-IgG with HRG prior to the addition of ovalbumin, and then incubating the resultant ICs with THP1 cells. The pre-incubation of FITC-IgG (0.5 μM) with HRG (0.25 μM) had no effect on the binding of free FITC-IgG to the THP1 cells (Figure 5.5A), but slightly potentiated the binding of ICs formed at Ag : Ab equivalence to THP1 cells (Figure 5.5B) an effect not seen with ICs formed in Ag excess (Figure 5.5C). Interestingly, the binding of ICs formed at Ag : Ab equivalence to THP1 cells was slightly potentiated by increasing concentrations of HRG up to an HRG : IgG molar ratio of ~ 0.5, but further increases in the concentration of HRG resulted in a less efficient enhancement of the binding of ICs (not shown).

FIGURE 5.4 **Effect of preincubating THP1 cells with HRG on IC binding**

THP1 cells were preincubated with 2 μM HRG in either PBS-BSA or PBS-BSA-Zn on ice for 1 hr. After the preincubation the cells were washed to remove any unbound HRG, and then incubated with IC-mixture formed by preincubating anti-ovalbumin FITC-IgG (0.5 μM) for 30 minutes with no ovalbumin (A, D) or with ovalbumin at Ag : Ab ratios of 0.03 (equivalence; B, E) and 0.06 (Ag excess; C, F). The fluorescence profiles for the binding of IgG and ICs to untreated THP1 cells (thin line) or THP1 cells pre-treated with 2 μM HRG (thick line) in PBS-BSA are shown in A-C and in PBS-BSA-Zn are shown in D-F. Each histogram is a representative result obtained from three separate experiments.

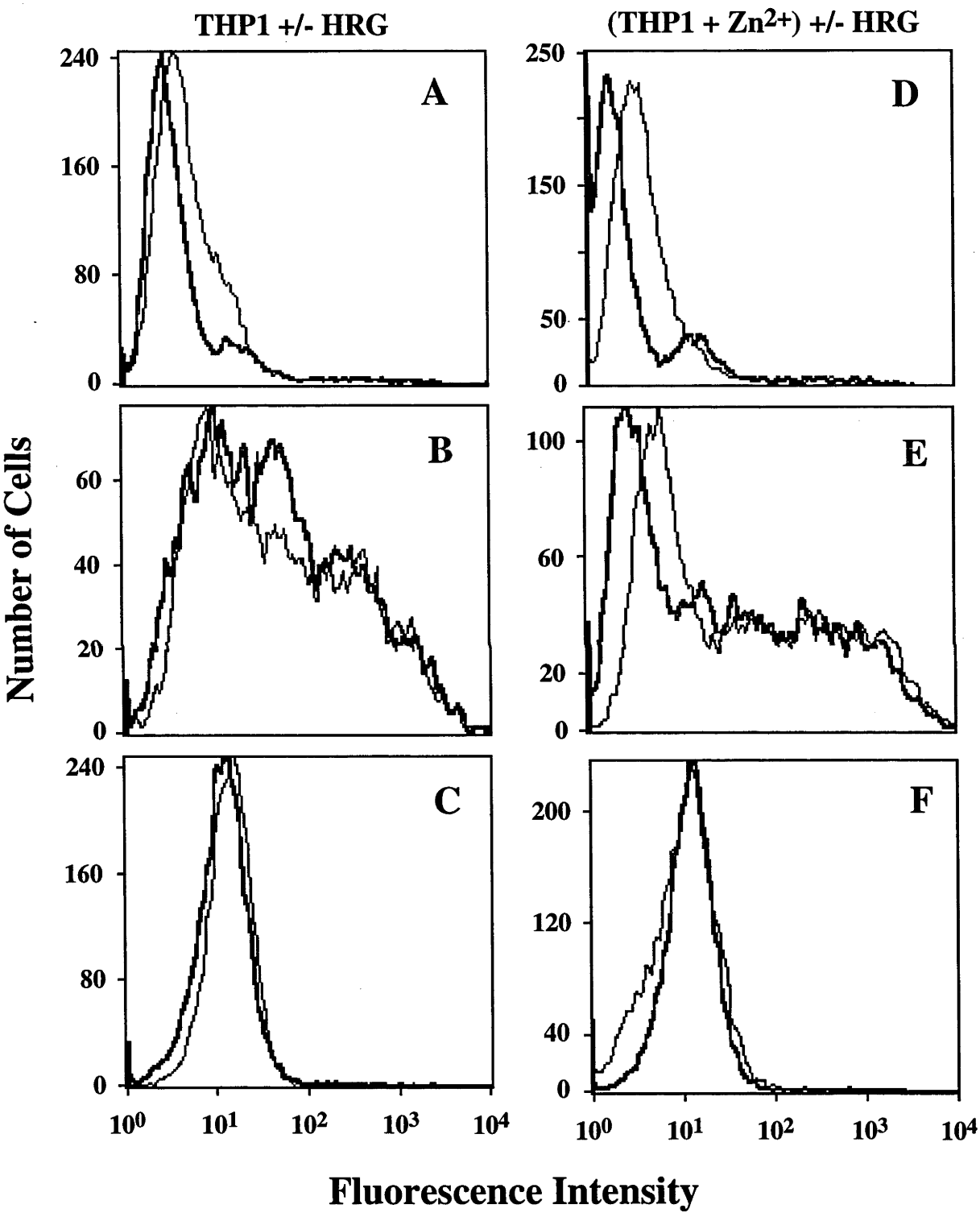
THP1 +/- HRG
(THP1 + Zn2+) +/- HRG
A
B
C
D
E
F
Number of Cells
Fluorescence Intensity
240
160
80
0
60
40
20
250
150
50
100
200
120
40
10^0
10^1
10^2
10^3
10^4

FIGURE 5.5 **Effect of preincubating ICs with HRG on IC binding to THP1 cells**

ICs were formed by preincubating anti-ovalbumin FITC-IgG (0.5 μM) with or without 0.25 μM HRG and with no ovalbumin (A, D) or with ovalbumin at Ag : Ab ratios of 0.03 (equivalence; B, E) and 0.06 (Ag excess; C, F). The FITC-fluorescence profiles of the THP1 cells which were incubated with IgG and ICs untreated with HRG (thin line), or pretreated with 0.25 μM HRG (thick line) in PBS-BSA are shown in (A-C) and in PBS-BSA-Zn are shown in (D-F). Each histogram is a representative result obtained from three separate experiments.

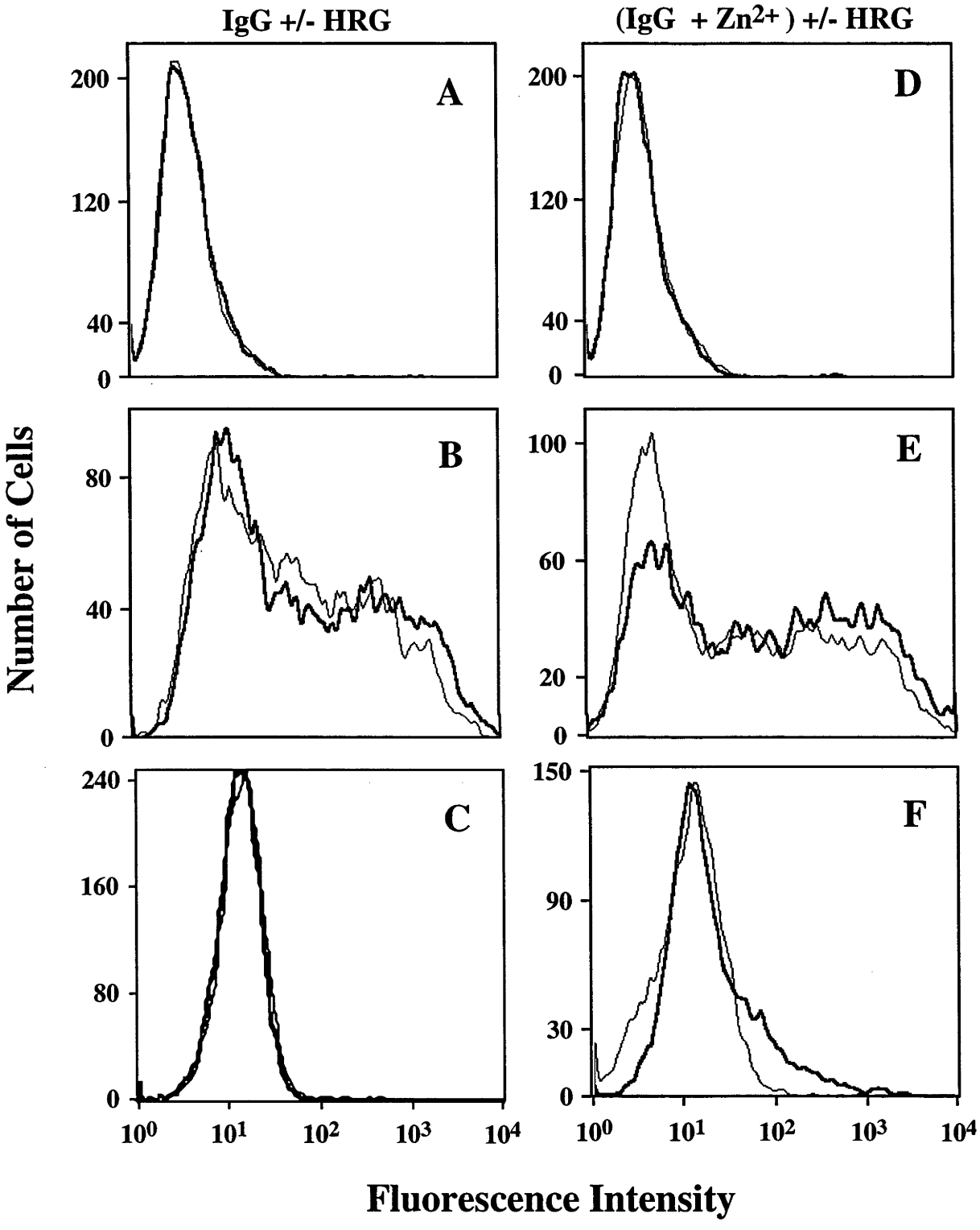
IgG +/- HRG
(IgG + Zn2+) +/- HRG
A
B
C
D
E
F
Number of Cells
Fluorescence Intensity
200
120
40
0
80
40
0
240
160
80
0
100
60
20
0
150
90
30
0
10^0
10^1
10^2
10^3
10^4

Subsequent experiments also revealed that in the presence of 20 μM Zn^{2+}, HRG (0.25 μM) still had no effect on the binding of free FITC-IgG (0.5 μM) to THP1 cells. However, Zn^{2+} did result in HRG substantially enhancing the binding of ICs formed at Ag : Ab equivalence to THP1 cells (compare Figures 5.3B and 5.3E). In the presence of HRG a higher proportion of THP1 cells bound ICs and more cells bound high levels of ICs (Figure 5.3E). Furthermore, HRG also slightly enhanced the binding of ICs formed in Ag excess, an effect not seen in the absence of Zn^{2+} (compare Figures 5.5C and 5.5F). This potentiating effect of HRG, in the presence of Zn^{2+}, on the binding of ICs to THP1 cells was seen when the HRG : IgG molar ratio approached 0.5 - 1 (Figure 5.6A). However, at higher HRG : IgG molar ratios little potentiation occured and, in fact, HRG at a 4-fold molar excess to IgG began to inhibit IC binding (Figure 5.6A). A similar effect of the HRG : IgG molar ratio on IC binding to THP1 cells was observed when ICs were formed over a wide range of Ag : Ab ratios (Figure 5.6B).

FIGURE 5.6 **Effect of the HRG : IgG molar ratio on the binding of ICs to THP1 cells**

ICs were formed between ovalbumin and anti-ovalbumin FITC-IgG (0.5 μM) at different Ag : Ab ratios and in the presence of different HRG : FITC-IgG molar ratios. Binding of fluorescent ICs to THP1 cells was then determined by flow cytometry and the data in (A) presented as relative binding (RB) for each HRG : FITC-IgG molar ratio where RB = (fluorescence of THP1 cells incubated with HRG treated ICs - background THP1 cell fluorescence) / (fluorescence of THP1 cells incubated with HRG untreated ICs - background THP1 cell fluorescence) x 100. In (A) the effect of the HRG : IgG molar ratio on the binding of ICs to THP1 cells formed at Ag : Ab ratios of 0.01 (○) , 0.02 (□) and 0.03 (△) is depicted. (B) shows overlay plots of the binding to THP1 cells of ICs containing 0.5 μM anti-ovalbumin FITC-IgG formed at different Ag : Ab ratios when ICs were either untreated (●) or were pretreated with 0.25 (△), 0.5 (□), 1 (▲) and 2 (■) μM HRG in PBS-BSA-Zn. Experiments in (B) were performed at six different concentrations of HRG in the range of 62.5 nM - 2 μM however, for clarity, only the data for four concentrations of HRG are plotted against the different Ag : Ab ratios. The data are representative results obtained from three separate experiments.

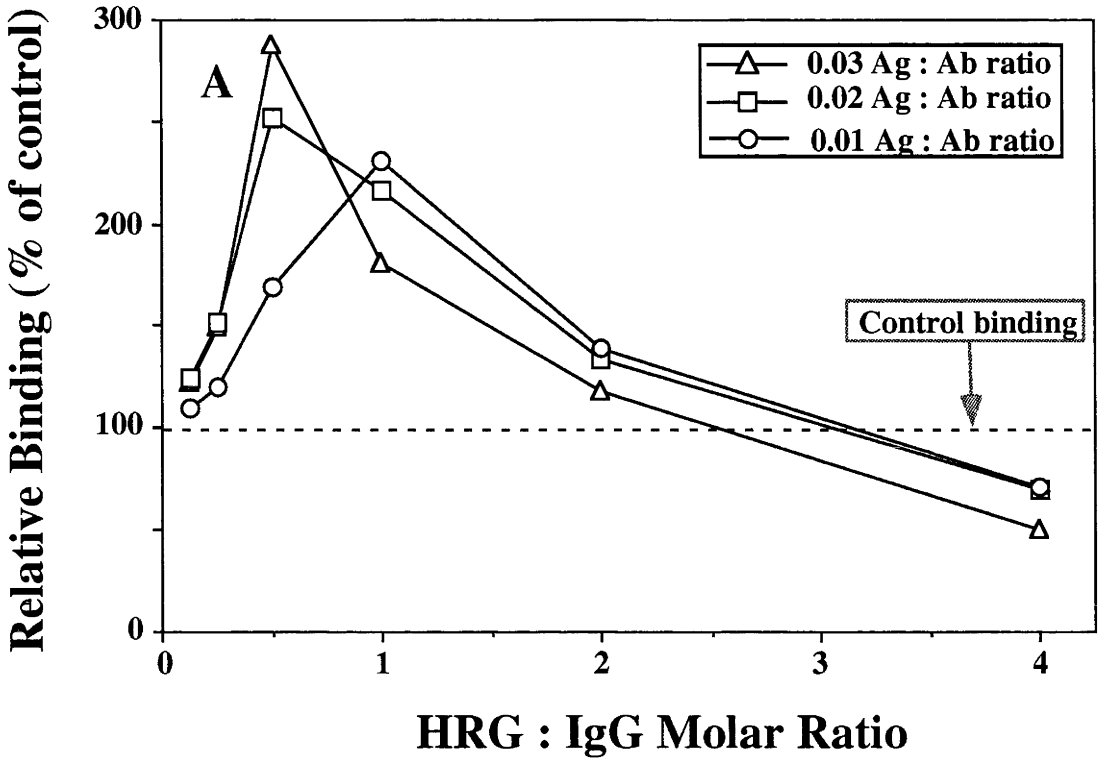
A
0.03 Ag : Ab ratio
0.02 Ag : Ab ratio
0.01 Ag : Ab ratio
Control binding
Relative Binding (% of control)
300
200
100
0
0
1
2
3
4
HRG : IgG Molar Ratio

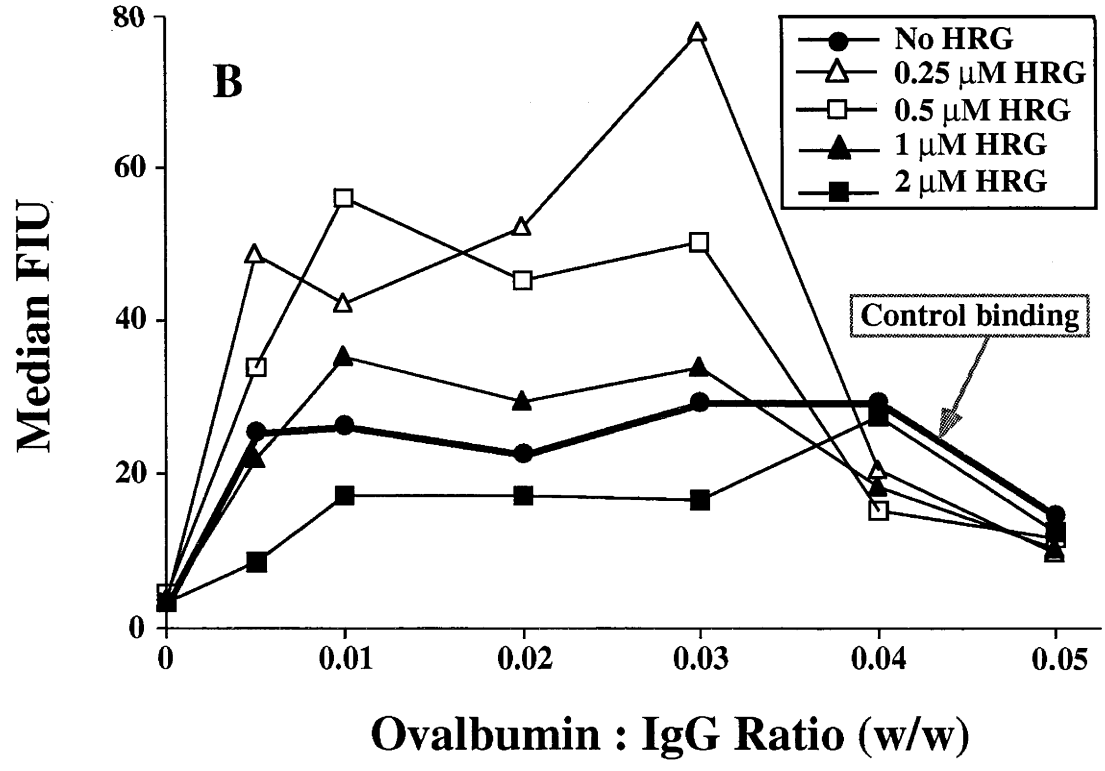
B
No HRG
0.25 μM HRG
0.5 μM HRG
1 μM HRG
2 μM HRG
Control binding
Median FIU
80
60
40
20
0
0
0.01
0.02
0.03
0.04
0.05
Ovalbumin : IgG Ratio (w/w)

5.3 Discussion

This study shows that the presence of human HRG markedly affects the binding of free human IgG and IgG-containing ICs to the human monocytic cell lines THP1 and U937. Consistent with the known ability of monomeric IgG to bind to FcγRI on mononuclear cells (Anderson, 1982; Anderson and Abraham, 1980; Woof et al, 1984; Woof et al., 1986; Ravetch and Kinet, 1991), and the reported interaction of HRG with mouse peritoneal macrophages (Chang et al., 1992b, 1994), our flow cytometric analyses indicate that biotinylated human IgG and biotinylated human HRG each binds to THP1 cells in a concentration-dependent manner with near-maximal binding of the IgG to THP1 cells occurring at a concentration of 20 nM IgG, a result similar to that reported in previous studies (Anderson and Abraham, 1980; Allen and Seed, 1989; Anderson, 1982; Fries et al., 1982; Kurlander and Batker, 1982; Cohen et al., 1983; Perussia et al., 1983). Near-maximal binding of b-HRG to THP1 cells occurred at ~ 4.5 μM HRG (Figure 5.1D). Of particular interest, however, was the finding that HRG binds to FcγRI on THP1 cells. Three lines of evidence support this conclusion. Firstly, the binding of HRG to THP1 cells is inhibited by monomeric human or rabbit IgG which are known to interact only with FcγRI. Secondly, the mAb MRII against FcγRI (anti-CD64) partially inhibited (35%) the binding of HRG to THP1 cells. Thirdly, IgG does not interfere with the binding of HRG to the T cell lines Jurkat and MT4 which lack FcγRI (not shown).

A major finding of the present study is that the pretreatment of THP1 cells with HRG significantly inhibits the binding of monomeric human IgG to THP1 cells, with the binding being inhibited about 90% by 2 μM HRG. It should be noted that this observation is physiologically relevant as the plasma concentration of human HRG is approximately 2 μM. Interestingly, the preincubation of THP1 cells with HRG also inhibited the binding of both monomeric human IgG1 and IgG3 to these cells (not shown), but the presence of Zn^{2+} did not alter the effect of HRG on the interaction of IgG with THP1 cells (Figure 5.2B). Since monomeric IgG binds to FcγRI on THP1 cells, these findings suggest that the pre-treatment of the THP1 cells with HRG can mask the IgG binding site on the FcγRI. Interestingly, the presence of ICs in the reaction vessel did not change the ability of HRG to inhibit the subsequent binding of monomeric IgG to THP1 cells. However, the fact that pretreatment of the cells with HRG did not affect the binding of ICs to these cells (Figure 5.4) may be explained by the ability of the ICs to bind to low affinity FcRs (FcγRII, etc.) on THP1 cells which may not be blocked by HRG. Another possibility is the established ability of ICs to bind to

cells multivalently and hence with higher avidity, a process which may displace HRG from FcγRI on the cell surface.

Despite the fact that preincubation of THP1 cells with HRG inhibited subsequent binding of monomeric IgG, the binding of IgG to THP1 cells was potentiated when IgG was preincubated with HRG (Figure 5.2B, triangles). Similarly, the preincubation of HRG with monomeric human IgG1 and IgG3 also resulted in an enhanced binding of these IgG subclasses to THP1 cells (not shown). The potentiating effect of HRG under these conditions is likely to be due to the binding of the IgG-HRG complexes to heparan sulfates on the cell surface via heparan sulfate binding sites on HRG (Brown and Parish, 1994; Olsen et al, 1996). The ability of Zn^{2+} to potentiate the augmenting effect of HRG on the binding of IgG to THP1 cells (Figure 5.2B, open triangles), presumably occurs through the ability of Zn^{2+} to increase both the binding of HRG to heparan sulfates on the cell surface (Olsen et al., 1996), and the binding of HRG to IgG molecules (Gorgani et al., 1997). The data presented also show that the molar ratio of HRG : IgG is an important factor in determining whether HRG potentiates (HRG : IgG molar ratio ~ 1 - 10 : 1) or inhibits (HRG : IgG molar ratio ≥ 50 : 1) the binding of monomeric IgG to FcγRI. Thus, when the concentration of HRG exceeds that of IgG (~ 50-fold in this system), free HRG blocks the binding of IgG to FcγRI receptors even after pre-incubation of the HRG with IgG (Figure 5.2B, filled triangles). It would be expected that under physiological conditions plasma HRG (2 μM) would not enhance the binding of monomeric plasma IgG (~ 60 μM) to monocytes since the molar ratio of HRG : IgG is ~ 1 : 30. This notion is also supported by the data shown in Figures 5.5A and D in which preincubation of HRG with FITC-IgG did not affect the binding of FITC-IgG to THP1 cells when the HRG : IgG molar ratio was ~ 1 : 2.

Another major finding from the present work is that HRG potentiates the binding of IgG-containing ICs to THP1 cells. ICs containing FITC-IgG and ovalbumin were used to study the effect of HRG on the interaction of ICs with THP1 cells. Turbidity assays and precipitin curve analysis of insoluble IC formed using FITC-IgG and ovalbumin indicated that insoluble IC formation in this system was indistinguishable from that which occurred when using unlabelled IgG and ovalbumin (not shown). Also, the binding of ICs to THP1 cells showed a similar pattern to the precipitin curve analysis of FITC-IgG-ovalbumin IC (see Figure 5.3C, compare circles with squares). These findings indicate that the binding of ICs to FcγR is dependent on the Ag : Ab ratio of the IC-mixture, and that maximum binding of ICs occurs at or near the equivalence

Ag : Ab ratio. This result is consistent with the observation that ICs formed at an equivalence Ag : Ab ratio are more effective in stimulating mouse peritoneal macrophages (Tripathi et al., 1993). Interestingly, at the equivalence Ag : Ab ratio the presence of Zn^{2+} slightly decreased the binding of ICs to THP1 cells (see Figure 5.3C, triangles), despite Zn^{2+} having no effect on the binding of free IgG to THP1 cells. Consistent with previous findings (Bauer et al., 1997), our studies show that Zn^{2+} increases IC insolubilisation and promotes the formation of larger insoluble ICs (not shown), but Zn^{2+} may also interfere with the ability of insoluble ICs to bind to FcγRs.

ICs containing FITC-IgG, ovalbumin and HRG were found to bind to THP1 cells at much higher levels than ICs containing only FITC-IgG and ovalbumin (Figure 5.5B) particularly when 20 μM Zn^{2+} was present. Although, the presence of 20 μM Zn^{2+} slightly inhibited the binding of ICs to THP1 cells (Figure 5.3C, triangles), in the presence of Zn^{2+} the binding of ICs to THP1 cells was markedly increased by HRG (Figure 5.5E). The results show, therefore, that HRG promotes the binding of ICs to THP1 cells in a Zn^{2+}-dependent fashion. There are two possible explanations for this phenomenon. First, my previous studies showed that Zn^{2+} substantially enhances the binding of HRG to IgG (Gorgani et al., 1997). Second, Zn^{2+} enhances the binding of HRG to heparan sulfate structures on cell surfaces (Olsen et al., 1996). HRG appears to maximally potentiate the binding of ICs to monocytes when the ICs are formed with a HRG : IgG molar ratio of ~ 1. However, at higher HRG : IgG molar ratios little or no enhancement of the binding of ICs occurs and, in fact, when the HRG : IgG molar ratio was ≥ 4 inhibition of IC binding was observed, presumably due to excess HRG masking FcRs on monocytes.

The findings presented herein, in conjunction with my previous findings that HRG binds to IgG and IgG-containing ICs and inhibits the formation of insoluble ICs *in vitro* (Gorgani et al., 1997), allows me to propose a model for the regulation of the binding and uptake of monomeric IgG and ICs by monocytes. As illustrated in Figure 5.7A HRG can inhibit the binding of monomeric IgG molecules to FcγRI on monocytes by interacting with FcγRI and masking their Fc binding site. The interaction of HRG, via its heparan sulfate binding domain, with heparan sulfate moieties on the monocyte surface would be expected to further stabilize the binding of HRG to FcγRI. In contrast, if HRG is incorporated into ICs it enhances IC binding to FcγRI, probably via its heparan sulfate-binding domain (Figures 5.7 B and C). This model implies that the region of HRG which binds IgG also binds to FcγRI, a distinct possibility since

the extracellular portion of FcγRI contains three truncated Ig-like domains (Allen and Seed, 1989). The ability of monomeric IgG to inhibit the capacity of HRG to mask FcγRI on monocytes supports this view. Interestingly, the interaction of HRG with IgG in ICs does not interfere with the binding of IgG to FcγR. This is probably due to the fact that HRG binds to the $F(ab')_2$ region of IgG (Chapter 3) and not the Fc region, as is the case with FcγR.

To date the uptake of ICs by the RES has been proposed to involve two mechanisms; namely, the binding of ICs to FcRs, and the binding of ICs complexed with complement C3b to CRs. The production of C3b or C3d requires activation of the complement cascade which results in the release of other factors (eg. anaphylatoxins, MAC) not yet shown to be involved in the clearance of ICs (Schifferli et al., 1988; Davies et al., 1992). The present study provides evidence for the existence of a third mechanism for enhancing the uptake of ICs by monocytes namely by incorporation of HRG in ICs. These results indicate that HRG can promote the binding of ICs to FcRs probably via binding to the GAG, heparan sulfate, and possibly to other HRG receptors on the cell surface. The binding or incorporation of HRG into ICs also may increase the avidity of these ICs for the cell surface due to the formation of multivalent interactions between ICs and heparan sulfate receptors for HRG (Figure 5.7C).

The finding that HRG inhibits the binding of monomeric IgG to monocytes has major implications for the role of HRG in regulating immune function. Importantly, the absence of HRG in plasma may lead to the complete saturation of FcγRI on mononuclear cells by monomeric IgG and hence to a serious disruption of the clearance of ICs by RES. Moreover, the fact that HRG does not usually affect the binding of ICs to these cells may ensure that FcRs are still available to bind ICs that may be present in the circulation. Whether HRG can interact with FcRs other than FcγRI and regulate their function needed to be investigated.

It has been shown that the deposition of CICs in various organs (eg. kidney, joint and the blood vessel wall) may lead to the development of pathological conditions such as GN, arthritis and vasculitis (Abrass, 1997; Haynes, 1992). It also has been shown that tissue IC deposits are in equilibrium with CICs (Abrass, 1997; Abrass, 1984) and that a reduction of ICs in the circulation is necessary for therapy in the majority of ICDs (Balint, 1996). Attenuation of the activation of complement also was proposed to be a clinical strategy to treat

these pathological conditions (Savige et al., 1989; Waxman et al., 1984; Causer et al., 1995; Shumak and Rock, 1984). Since HRG is a plasma protein, it is possible that in the treatment of ICDs HRG may be used as a therapeutic agent for the prevention of the pathogenic effects of ICs in terms of keeping ICs in a soluble form and potentiating their uptake by the RES.

CHAPTER 6

HISTIDINE-RICH GLYCOPROTEIN BLOCKS THE BINDING OF RHEUMATOID FACTOR TO HUMAN IgG AND SOLUBILISES ALREADY FORMED INSOLUBLE IMMUNE COMPLEXES

Abstract

In Chapters 3 and 4 it was demonstrated that HRG inhibits the formation of insoluble ICs. Results in this chapter demonstrate that HRG, when incorporated in ICs, blocks the binding of RF to ICs and inhibits the subsequent insolubilisation of ICs by RF. Biosensor studies also support this view and show that preincubation of HRG with immobilized IgG blocks the subsequent binding of RF to IgG. Based on these data it is proposed that HRG plays important roles in regulating IC size in humans and that HRG may control the production of RF and the pathogenic effects arising from excessive production of RF *in vivo*. This Chapter also provides evidence that HRG can solubilise already formed insoluble ICs, a phenomenon which may be important in preventing the pathogenic effects of insoluble ICs deposited in tissues.

6.1 Introduction

RFs are aAbs produced against antigenic determinants on the Fc portion of IgG molecules and have been detected as IgM, IgA and IgG forms in plasma and tissues (Panush et al., 1971). Two general types of RFs have been described; namely, pathologic RFs associated with RA (Stewart et al., 1997), and natural RFs which exist in healthy individuals (Nasu et al., 1980). Both types of RF are known to bind to the Fc portion of IgG, but RFs within each type possess several characteristic differences such as use of different variable region sequences and different Ig isotypes (Stewart et al., 1997). It has also been proposed that pathologic RF can be tolerized at the B cell level by competition with natural RF (Stewart et al., 1997). Although pathologic RF may be present at low levels in normal human plasma, the concentration of this RF is often elevated in the plasma of patients suffering from infections such as infectious mononucleosis and hepatitis C virus infection (Johnson and Page Faulk, 1976; Capra et al., 1969; Carson et al., 1981). On the other hand, sustained levels of pathologic RF are observed in ICD such as RA, SLE and vasculitis (Johnson and Page Faulk, 1976; Carson et al., 1981; Schifferli, 1996; Walport and Davies, 1996).

It is reported that the plasma level of pathologic RF is correlated with the severity of RA (Nasu et al., 1980; Johnson and Page Faulk, 1976), and that patients with high RF titers have a higher frequency of rheumatoid nodules (Naranjo et al., 1997). The high level of pathologic RF production in these patients may be associated with the presence of high concentrations of pathogenic ICs. Although IgM-RF is increased in the plasma of patients with RA, IgG-RF is the predominant RF present in pathogenic ICs (both soluble and insoluble) found in the synovial fluid, with IgG4 containing κ light chains being the major IgG-RF found in the synovium of RA patients (Zach et al., 1995; Corper et al., 1997), despite IgG4 representing only 4% of normal serum IgG. This predominance of IgG4 in synovial IC in RA patients may be due to IgG4 interacting with the Fc region of most IgG subclasses via its constant rather than its variable region (Zach et al., 1995). Evidence also indicates that the widespread vascular complications associated with RA are mediated, at least in part, by CICs containing IgG and RF (Weisman and Zvaifler, 1975).

Although evidence suggests that natural RF may be involved in the clearance of ICs (Mellow and Clarkson, 1982; Heyman, 1990), the precise function of RFs and the mechanism(s) regulating their production *in vivo* is unclear. Kinetic studies have shown that IgM-RF or IgG-RF each interact with aggregated IgG or ICs

with much greater affinity (~ 100 fold) than with monomeric IgG, indicating that RF binds specifically to ICs containing IgG (Johnson and Page Faulk, 1976; Normansell, 1971). Other studies have shown that human peripheral blood mononuclear leukocytes secrete RF when cultured in the presence of ICs, but not when cultured in the presence of monomeric IgG, suggesting that only ICs can appropriately display antigenic determinants which activate B cells to secrete RF (Pisko et al., 1982). In addition, only prolonged immunization of mice or rabbits with bacterial Ags has been shown to induce RF production (Coulie and Van Snick, 1983; Nemazee and Sato, 1983) indicating that the production of pathologic RF, particularly of the IgG4 subclass, may be a secondary phenomena that occurs during chronic infections. These studies collectively suggest that the production of RF may be a physiological phenomena which potentiates the clearance of primary ICs.

As reviewed in part I of Chapter 1 HRG has been shown to bind several plasma proteins. As outlined in Chapter 3, I identified two previously undescribed ligands for HRG, namely IgG and C1q. My additional studies indicated that HRG inhibits the formation of insoluble ICs by maintaining ICs in a soluble form, thus implicating HRG as a key endogenous regulator of the formation of ICs (Gorgani et al., 1997), In fact, recent studies indicate that when HRG is incorporated in ICs the ICs more effectively interact with macrophages (Chapter 5).

In the present work, experiments were designed to mimic the interaction of RFs with ICs in order to examine the effect of HRG on the binding of RF to ICs. Additional experiments using an IAsys biosensor studied the binding of RF to immobilized human IgG1κ and the effect of the plasma protein HRG on this interaction. The results show that physiological concentrations of HRG can block the formation of insoluble ICs between aggregated human IgG and RF *in vitro*. Furthermore, the biosensor studies show that the binding of RF to IgG1κ is blocked by HRG, indicating that HRG masks the epitope on IgG recognized by RFs. The findings suggest a novel mechanism by which the binding of RF to autologous IgG containing ICs can be regulated. HRG also was found to solubilise already formed insoluble ICs.

6.2 RESULTS

6.2.1 Formation of insoluble ICs containing human IgG and anti-human IgG antibodies

Previous studies have shown that the formation of insoluble ICs between ovalbumin and anti-ovalbumin IgG can be studied *in vitro* by monitoring changes in insoluble IC particle size by absorbance measurements at 350 nm (Gorgani et al., 1997). In the present work insoluble ICs containing human IgG and anti-human IgG Abs were formed by: (1) the incubation of polyclonal rabbit anti-human IgG (specific for the Fc region of human IgG) with monomeric human IgG, (2) the incubation of human RF with heat-aggregated human IgG, and (3) the incubation of human RF with monomeric human IgG.

To study the formation of insoluble ICs between rabbit anti-human IgG and monomeric human IgG, rabbit anti-human IgG (69 μg/ml) was incubated in PBS-BSA buffer and the formation of insoluble ICs was initiated by the addition of human IgG at different concentrations in the range 3.9 - 15.5 μg/ml (Ag : Ab ratio between ~ 0.056 - 0.22). The increase in the average size of the insoluble ICs formed in the suspension was monitored by measuring the absorbance of the turbid suspension at 350 nm (as described in Materials and Methods) for 20 minutes (see Figure 6.1A). These data show that incubation of rabbit anti-human IgG with monomeric human IgG (from pooled human serum) resulted in the formation of insoluble ICs, with maximum formation occuring at an Ag : Ab ratio of 0.1. To determine whether the nature of the light chain of human IgG (κ or λ), as Ag, affects the formation of insoluble ICs, insoluble IC formation also was carried out by mixing human IgG1κ or IgG1λ with rabbit anti-human IgG. These experiments indicated that the light chain of human IgG (as Ag) has no effect on the formation and precipitation of insoluble ICs (not shown).

The formation of insoluble ICs between human RF and aggregated human IgG was carried out by the addition of RF (8 IU/ml) to different concentrations of aggregated human IgG (20 - 120 μg/ml) in PBS-BSA buffer. SDS-PAGE analysis showed that the majority of RF used in these studies is the IgG form (not shown). As can be seen from the data in Figure 6.1B the formation of insoluble ICs under these conditions was dependent on the concentration of aggregated IgG used in the incubations. Interestingly, these experiments also indicate that little if any insolubilisation and formation of insoluble ICs between RF and monomeric human IgG occurs in this system (see Figure 6.1C).

FIGURE 6.1 **Formation of insoluble ICs between human IgG and either rabbit anti-human IgG antibodies or RF as measured by light scattering at 350 nm.**

The results in (A) show the increase in absorbance as a function of time due to formation of insoluble ICs containing rabbit anti-human IgG (69 μg/ml) and human IgG at the Ag : Ab ratios of 0.056 (■), 0.1 (□). 0.17 (●) and 0.22 (○). The results in (B) show the increase in absorbance as a function of time due to formation of insoluble ICs containing human RF (8 IU/ml) and aggregated human IgG at concentrations of 20 (■), 40 (□), 60 (●), 80 (○) and 120 (△) μg/ml. The results in (C) show the increase in absorbance as a function of time due to formation of insoluble ICs containing human RF (8 IU/ml) and monomeric human IgG at concentrations of 60 (■), 120 (□) and 240 (●) μg/ml. Data are a representative of three separate experiments.

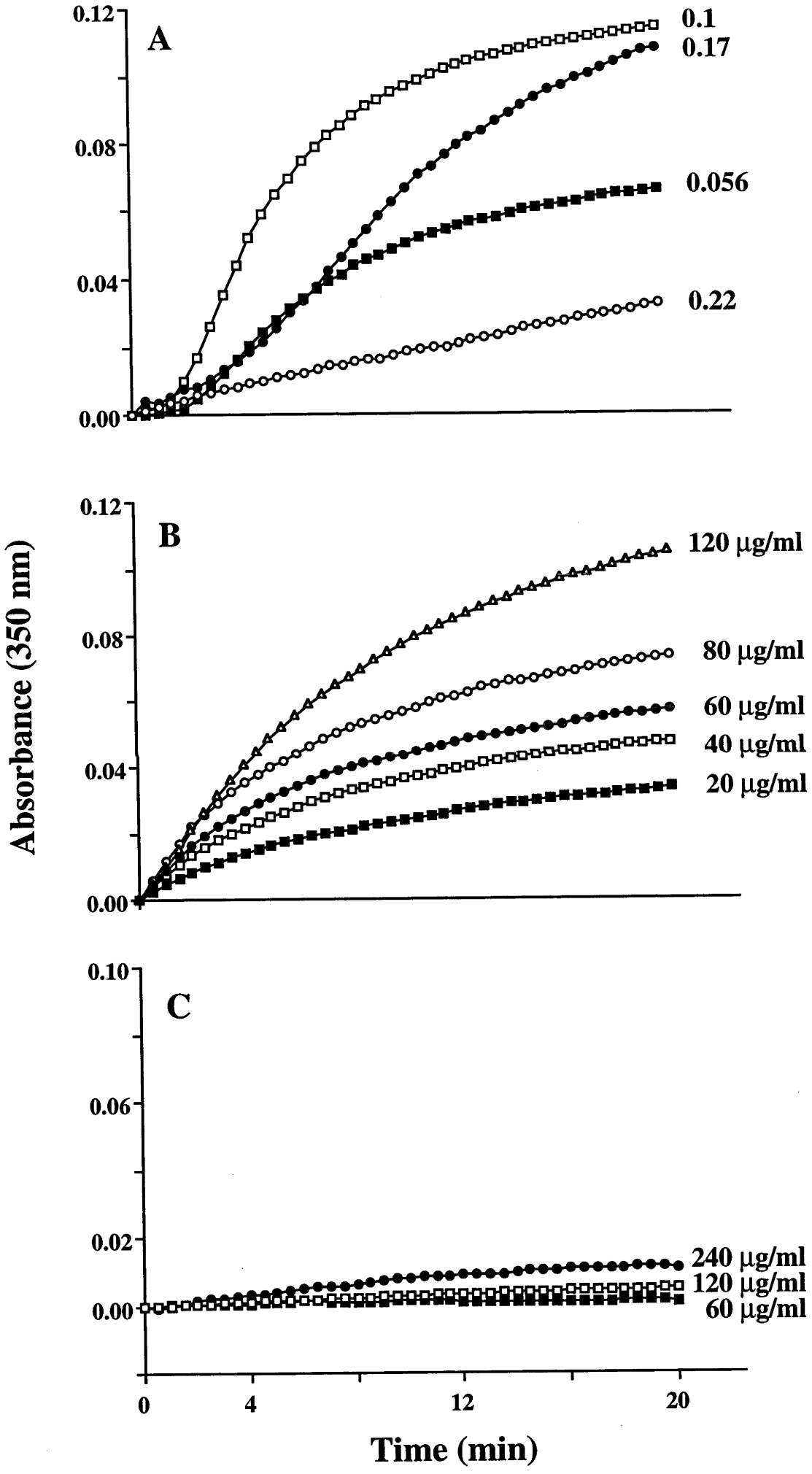
A
0.12
0.08
0.04
0.00
0.1
0.17
0.056
0.22
B
0.12
0.08
0.04
0.00
120 µg/ml
80 µg/ml
60 µg/ml
40 µg/ml
20 µg/ml
C
0.10
0.06
0.02
0.00
240 µg/ml
120 µg/ml
60 µg/ml
0
4
12
20
Absorbance (350 nm)
Time (min)

6.2.2 HRG blocks the formation of insoluble ICs between human IgG and anti-human IgG antibodies

The effect of HRG on the formation of insoluble ICs between rabbit anti-human IgG (69 μg/ml) and monomeric human IgG (6.9 μg/ml) was examined. As shown in Figure 6.2A pre-incubation of rabbit anti-human IgG and human IgG with HRG at 22.5, 45 and 60 μg/ml inhibited the formation of insoluble ICs in a dose-dependent manner. Whereas little effect was seen at 22.5 μg/ml HRG, higher concentrations (75 and 150 μg/ml) of HRG resulted in an almost complete blockage of the formation of insoluble ICs in this system.

Interestingly, the pre-incubation of RF (8 IU/ml) with different concentrations of HRG in the range 37.5 - 300 μg/ml resulted in a HRG concentration-dependent inhibition of the formation of insoluble ICs between RF and aggregated human IgG (~ 120 μg/ml) (see Figure 6.2B). However, HRG was much less effective at inhibiting insoluble IC formation in this system (compare Figures 6.2A and 6.2 B)

6.2.3 HRG blocks the formation of insoluble ICs between RF and STP aggregated biotinylated human IgG

Since HRG was relatively ineffective at blocking the formation of insoluble ICs between human RF and heat aggregated human IgG, another form of aggregated human IgG was investigated as Ag. In particular, there was the concern that heat treatment may destroy HRG binding sites on human IgG. Thus it was considered essential to establish whether HRG could block the formation of insoluble ICs between RF and biotinylated human IgG aggregated with STP.

Experiments were conducted to determine the optimum ratio of STP : b-IgG to produce aggregated b-IgG which subsequently formed insoluble ICs upon addition of RF (8 IU/ml). The b-IgG (30 μg/ml) was incubated with different concentrations of STP (6 - 60 μg/ml) in PBS-BSA-Zn in a quartz reaction cuvette for 20 minutes at 37 °C. It should be noted that crosslinking b-IgG with STP resulted in no significant detectable light scattering (Figure 6.3A). However, addition of RF to some solutions of STP-b-IgG resulted in an increase in absorbance due to light scattering by insoluble ICs. These experiments indicated that the formation of insoluble ICs with RF (8 IU/ml) and STP-b-IgG

FIGURE 6.2 **Effect of HRG on the formation of insoluble ICs between human IgG and either rabbit anti-human IgG antibodies or human RF as measured by light scattering at 350 nm.**

The results in (A) show the increase in absorbance as a function of time due to formation of insoluble ICs containing human IgG and rabbit anti-human IgG (69 μg/ml) at equivalence Ag : Ab ratio for a control experiment (■, no additions), and for experiments carried out in the presence of 22.5 (□), 45 (●), 60 (○), 75 (▲) and 150 (△) μg/ml of human HRG. The results in (B) show the increase in absorbance as a function of time due to formation of insoluble ICs containing RF (8 IU/ml) and aggregated human IgG (120 μg/ml) for a control experiment (■, no additions), and for experiments carried out in the presence of 37.5 (□), 75 (●), 150 (○) and 300 (△) μg/ml of human HRG. Data are a representative of three separate experiments.

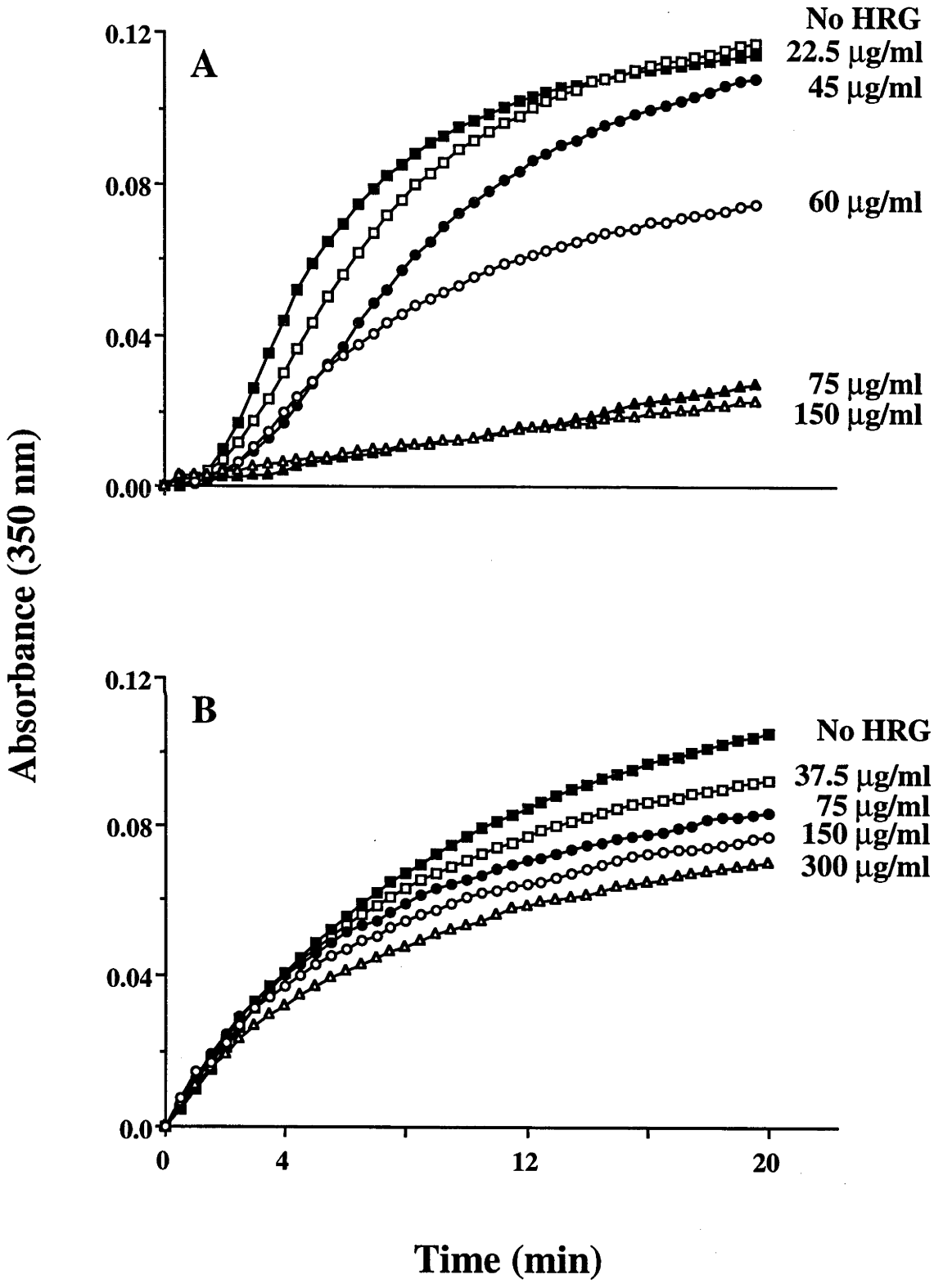
A
B
No HRG
22.5 µg/ml
45 µg/ml
60 µg/ml
75 µg/ml
150 µg/ml
No HRG
37.5 µg/ml
75 µg/ml
150 µg/ml
300 µg/ml
0.12
0.08
0.04
0.00
0.0
0
4
12
20
Absorbance (350 nm)
Time (min)

FIGURE 6.3 **Effect of HRG on the formation of insoluble ICs between RF and streptavidin-aggregated biotinylated human IgG (b-IgG).**

In (A) b-IgG (30 μg/ml) was incubated with STP at 6 (■), 12 (□), 18 (●), 24 (○) and 60 (▲) μg/ml for 20 minutes, then RF (8 IU/ml) was added to the STP-b-IgG complexes and insoluble IC formation was monitored by light scattering. In (B) b-IgG was pre-incubated without (■) or with human HRG at 15 (□), 30 (●), 75 (○), and 150 (▲) μg/ml for 20 minutes before aggregation by STP (18 μg/ml) for 20 minutes and the addition of RF (8 IU) to form insoluble ICs. Data are a representative of three separate experiments.

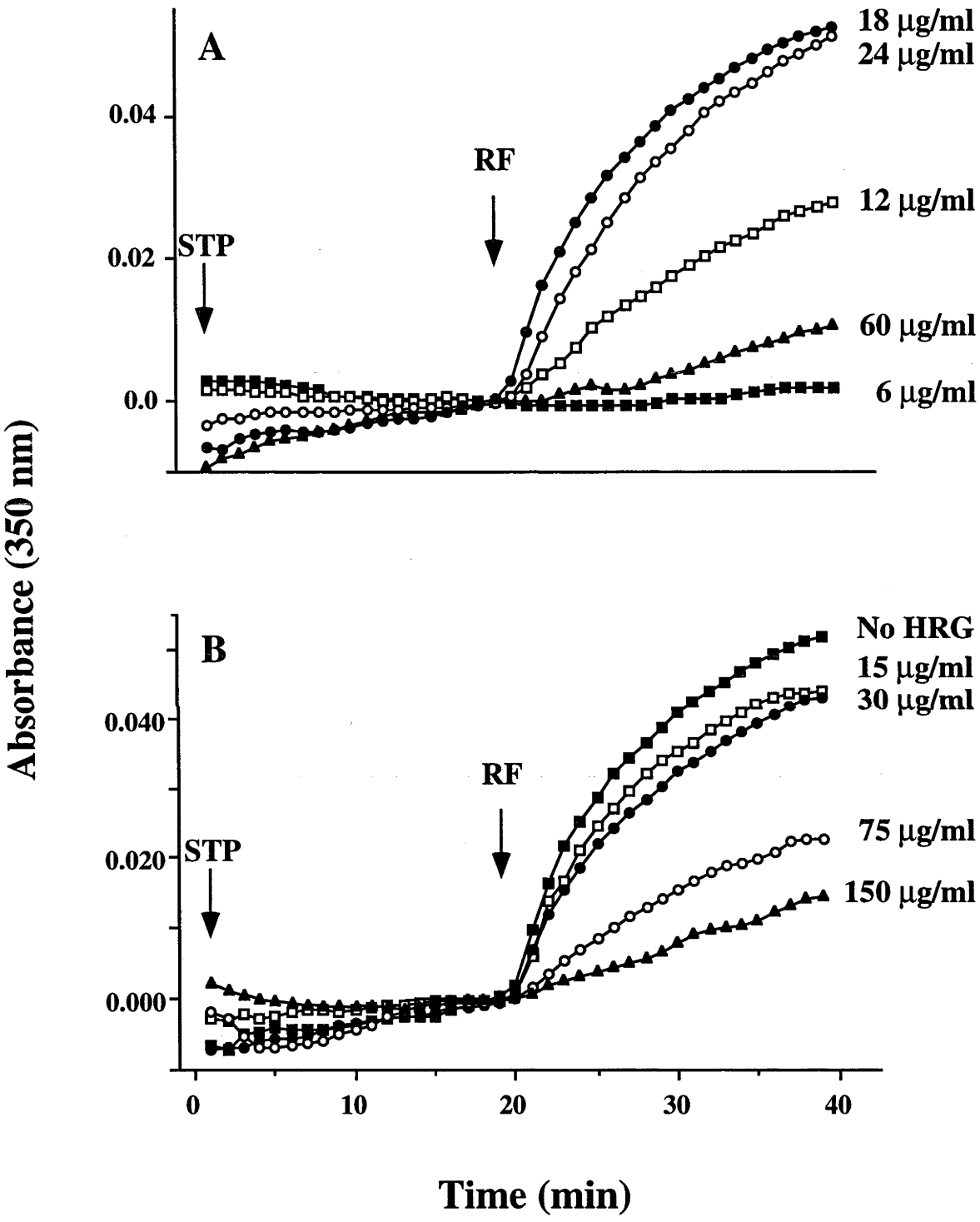
A
0.04
0.02
0.0
STP
RF
18 µg/ml
24 µg/ml
12 µg/ml
60 µg/ml
6 µg/ml
B
0.040
0.020
0.000
STP
RF
No HRG
15 µg/ml
30 µg/ml
75 µg/ml
150 µg/ml
0
10
20
30
40
Absorbance (350 nm)
Time (min)

is optimal when 18 μg/ml of STP is used for b-IgG crosslinking (see Figure 6.3A).

The effect of HRG on the formation of insoluble ICs between RF and STP-b-IgG was examined by preincubating b-IgG (30 μg/ml) with different concentrations of HRG (15 - 150 μg/ml) for 20 min before the addition of STP (18 μg/ml). After incubating this mixture for 20 min RF was added to initiate the formation of insoluble ICs. Gel filtration studies showed that the presence of HRG had no effect on the cross-linking of b-IgG by STP (data not shown). The data show that preincubation of IgG with HRG inhibits formation of insoluble ICs; inhibition was significant at 15 and 30 μg/ml HRG, with over 60% to 80% blockage of insoluble IC formation occurring at 75 and 150 μg/ml HRG, respectively (see Figure 6.3B). This is similar to the inhibitory effect of HRG on the formation of insoluble IC between human IgG and rabbit anti-human IgG (compare Figure 6.2 A and Figure 6.3B).

6.2.4 Use of optical biosensor to examine the effect of HRG on RF-IgG interaction

Since HRG is an IgG binding protein, it may mask epitopes on IgG recognized by RF. Thus an IAsys optical biosensor was used to study the binding of human RF to IgG and the effect of human HRG on this interaction. Human IgG1κ was biotinylated and bound to STP immobilized onto the sensing surface of an IAsys dextran cuvette. The binding of RF to immobilized IgG1κ, which may resemble immobilized ICs, was carried out by the addition of RF to the cuvette at different concentrations in the range 2-16 IU/ml in PBS-T-BSA. In this study, the concentration of RF is expressed as IU/ml (instead of molarity) since most published work and clinical evaluations of RF levels in patients use this unit. As shown in Figure 6.4A the binding of RF to IgG1κ over a 10 minute period exhibited saturation kinetics with near maximal binding occurring at ~ 16 IU/ml RF. The biosensor signal obtained was specific for the binding of RF to the immobilized IgG1κ since pre-incubation of the RF (8 IU/ml) with 120 μg/ml of soluble IgG1κ inhibited the binding of RF to immobilized IgG1κ (not shown). Analysis of the data using the "Fast Fit" program showed that the association curves could be fitted to a single exponential. For each binding curve the observed rate constant (k_{obs}) was determined and plotted against the titer of RF. As shown in Figure 6.4B the plot of k_{obs} against the RF concentration (IU/ml) approximated a straight line with the slope or on-rate being $14.92 \pm 2.43 \times 10^{-5}$

FIGURE 6.4 **Interaction of RF with immobilized human IgG1κ**

(A) Human IgG1κ immobilized onto the sensing surface of a biosensor cuvette was reacted with different concentrations (2-16 IU/ml) of RF, the overlay plots representing the binding of different RF concentrations to the immobilized IgG1κ. (B) The value of k_{obs} for the binding curve for each RF titer was determined using the linearization method (FAST FIT program) and each value plotted against the concentration of RF. The plot of k_{obs} against RF concentration (IU/ml) approximates a straight line (●); the slope represents k_{on} and the y-intercept represents k_{off} for this interaction. (C) In some experiments before monitoring the binding of RF (8 IU/ml) to IgG1κ the cuvette was either untreated (no HRG) or pre-treated (+HRG) with HRG (15 μg/ml) for 5 minutes. Each data point in (B) represents the mean ± SEM obtained from three separate experiments. The data in (A) and (C) are a representative of three separate experiments.

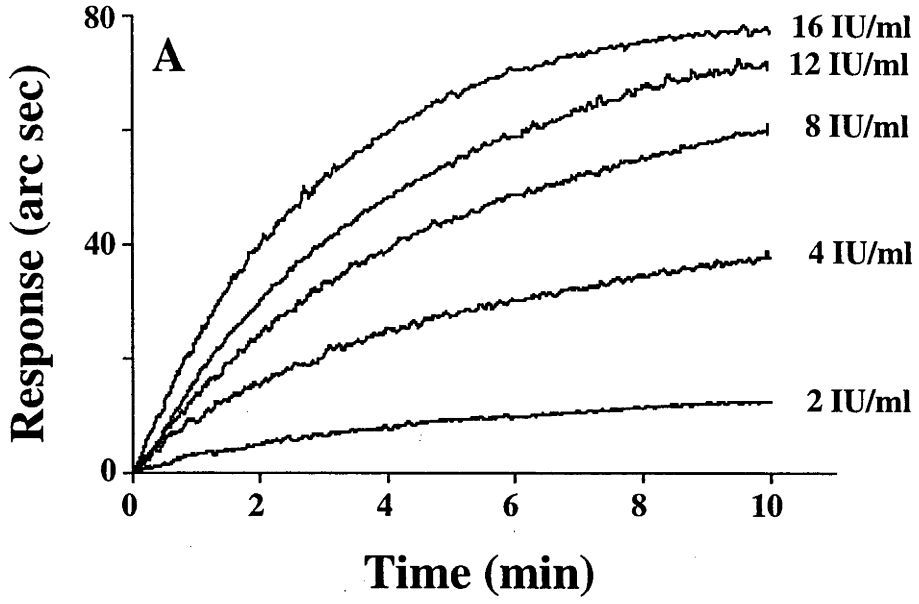
A
Response (arc sec)
80
40
0
0
2
4
6
8
10
Time (min)
16 IU/ml
12 IU/ml
8 IU/ml
4 IU/ml
2 IU/ml

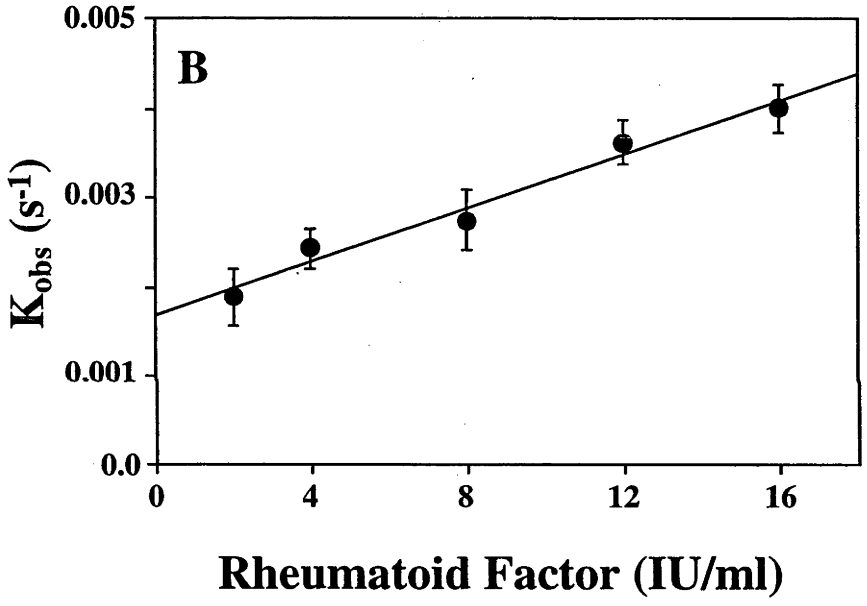
B
K_{obs} (s^{-1})
0.005
0.003
0.001
0.0
0
4
8
12
16
Rheumatoid Factor (IU/ml)

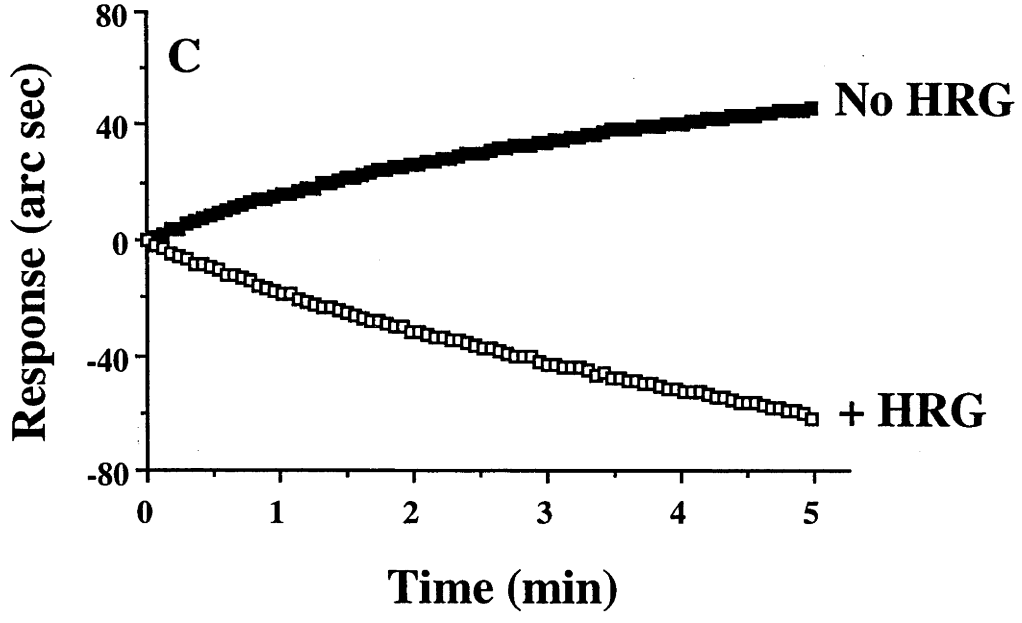
C
Response (arc sec)
80
40
0
-40
-80
0
1
2
3
4
5
Time (min)
No HRG
+ HRG

IU/ml^{-1} s^{-1} and the y-intercept (off-rate) for the interaction being 1.69 ± 0.41x10^{-3} s^{-1}.

The ability of HRG to bind with high affinity to immobilized IgG (Gorgani et al., 1997) raised the question of whether HRG can mask epitopes on IgG1κ recognized by RF. Consistent with the data shown in Figure 6.4A, the addition of 8 IU/ml RF in PBS-T-BSA to the cuvette increased the binding signal (association pattern, no HRG) (see Figure 6.4C). However, the addition of RF (8 IU/ml) to a cuvette containing immobilized IgG1κ that had been pretreated with 15 μg/ml HRG did not result in an increased binding signal, suggesting that HRG blocks the binding of RF to immobilized IgG1κ. Interestingly, under these conditions the addition of RF to the HRG pretreated-cuvette actually showed a dissociation response, rather than the expected association (see Figure 6.4C, + HRG). This result may be due to RF displacing some of the HRG bound to the immobilized IgG1κ. Collectively, since the immobilization of b-IgG on the sensing surface may have created cross-linked IgG molecules resembling ICs, the biosensor data further supports the view that HRG has the ability to block the binding of RF to IgG containing ICs.

6.2.5 HRG promotes solubilisation of already formed insoluble ICs

Activation of the classical and alternative complement pathways has been shown to inhibit the formation of insoluble ICs and to promote solubilisation of already formed insoluble ICs (Schifferli et al., 1986). Therefore, it was important to examine whether HRG, apart from inhibiting the formation of insoluble ICs and regulating the binding of RF to IgG containing ICs, could promote the solubilisation of already formed insoluble ICs. Different concentrations of ovalbumin were added to rabbit anti-ovalbumin IgG (900 μg/ml) to form insoluble ICs and the insoluble ICs either left untreated, or treated with HRG (150 μg/ml), and then incubated overnight at 37°C. After incubation, the insoluble ICs that remained in each sample were collected by centrifugation, dissolved in NaOH, and the absorbance of each solution was measured to determine the percent IgG precipitation as described in the Materials and Methods. A comparison of the precipitin curves shown in Figure 6.5A indicates that there was slightly less precipitate in the incubations in which HRG was included with the preformed insoluble ICs at almost all Ag : Ab ratios.

To explore whether the effect of HRG on the solubilisation of already formed insoluble ICs is dependent on the concentration of HRG, insoluble ICs were

FIGURE 6.5 **Effect of HRG on solubilization of already formed insoluble ICs.**

In (A) insoluble ICs were formed between ovalbumin and anti-ovalbumin IgG (900 μg/ml) at different Ag : Ab ratios (0.005 - 0.05) and then HRG (150 μg/ml) examined for its ability to solubilize the insoluble ICs overnight at 37°C (■), insoluble IC incubated in the absence of HRG indicated as (●). Data expressed as percent precipitation of anti-ovalbumin IgG (for details see Materials and Methods). (B) shows the ability of different concentrations of HRG, following incubation overnight at 37°C, to solubilize ovalbumin anti-ovalbumin IgG (900 μg/ml) insoluble IC formed at an equivalence (0.03) Ag : Ab ratio. Each data point in (B) represents mean ± SEM of three experiments. Asterisks indicate the ability of different concentrations of HRG to significantly solubilize the preformed insoluble ICs when compared to insoluble IC formation in the absence of HRG, i.e. * $P = 0.02$, ** $P = 0.006$.

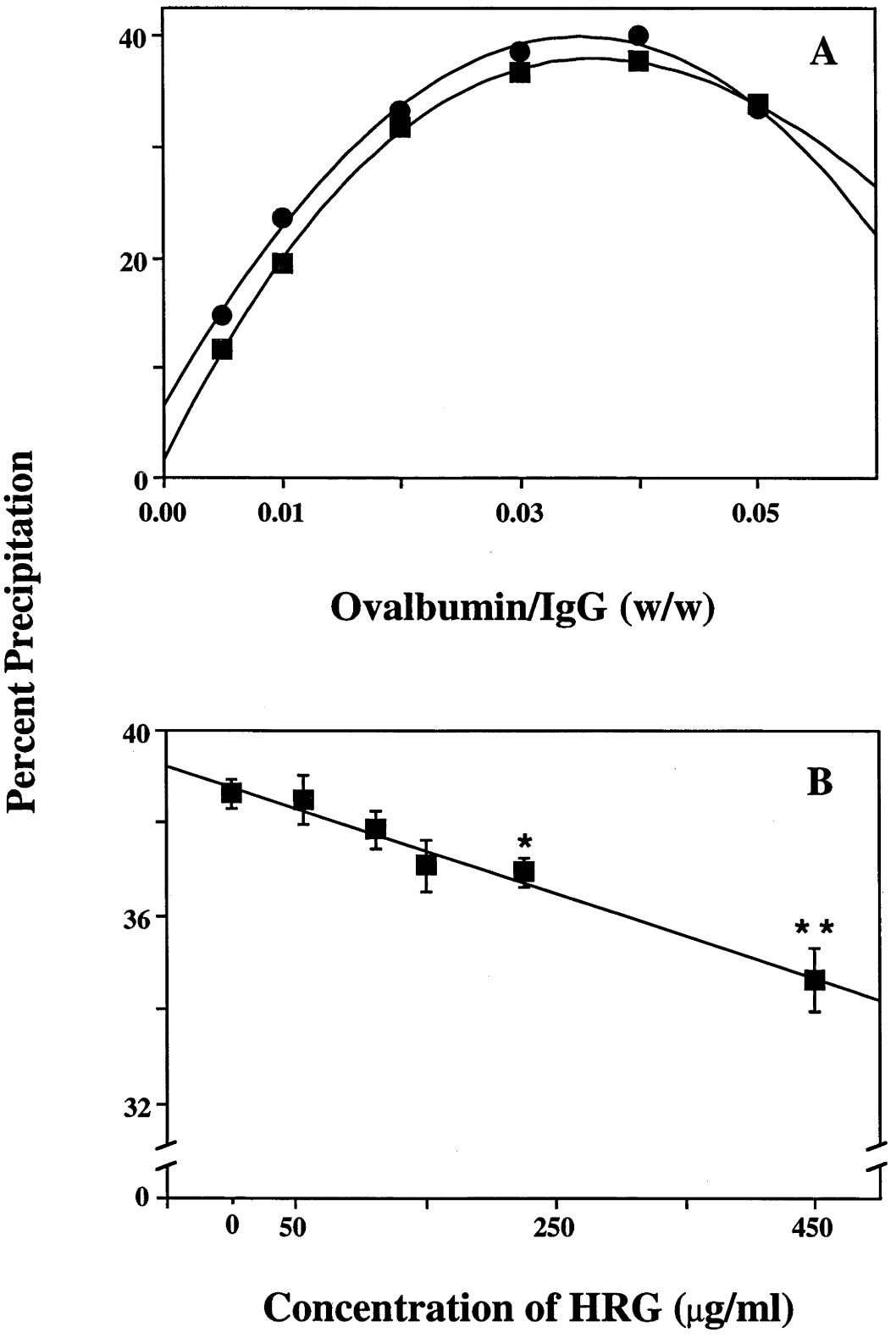
A
40
20
0
0.00
0.01
0.03
0.05
Ovalbumin/IgG (w/w)
Percent Precipitation
B
40
36
32
0
0
50
250
450
*
* *
Concentration of HRG (μg/ml)

formed at the equivalence Ag : Ab ratio (ie. 0.03), and then incubated with different concentrations (56 - 450 μg/ml) of HRG. The results indicate that HRG promotes solubilisation of already formed insoluble ICs, and that the solubilisation is dependent on the concentration of HRG (Figure 6.5B), with very significant solubilisation ($P < 0.006$) occurring when the molar ratio of HRG : IgG is ~ 1, i.e., 450 μg/ml HRG. There was also significant solubilisation of insoluble ICs at 225 μg/ml ($P=0.02$) of HRG, with 150 μg/ml of HRG producing almost significant solubilisation ($P=0.07$).

6.3 Discussion

Earlier studies described in Chapter 3 demonstrated that HRG can inhibit the formation of insoluble ICs. Thus it was important to examine whether HRG could also inhibit formation of insoluble ICs resulting from the interaction of RFs with human IgG. In order to answer this question three RF models were used. The first involved a xenogeneic system, namely the interaction of rabbit IgG specific for human IgG (Fc region-specific) with monomeric human IgG. The other two systems entailed the formation of insoluble ICs between human RF and human IgG aggregated either by heat or by crosslinking with STP following biotinylation. It was found that, in order for RF to form insoluble ICs, the human IgG needed to be aggregated (Figure 6.1C), indicating that RF may bind weakly to monomeric IgG, and that multimeric interactions may be required for the formation of insoluble ICs. These results are consistent with the reported binding affinity of RF for ICs being 100-fold higher than for monomeric IgG (Johnson and Page Faulk, 1976; Normansell, 1971).

A major finding from the present work is that in all three models of the RF-human IgG interaction, HRG blocks the formation of insoluble ICs. It is interesting to note that with the rabbit anti-human IgG-human IgG interaction and the RF-STP aggregated b-IgG interaction, HRG could completely inhibit insoluble IC formation (see Figures 6.2A and 6.3B). This effect was not observed in the rabbit anti-ovalbumin/ovalbumin interaction, where HRG only partially inhibited insoluble IC formation (Gorgani et al., 1997). This difference is probably due to HRG both directly blocking the epitopes on human IgG recognized by RF and inhibiting insolubilisation of RF-human IgG containing ICs. In the case of the ovalbumin/anti-ovalbumin system HRG would only inhibit IC insolubilisation. The failure of high concentrations (300 μg/ml) of HRG to completely block the formation of insoluble ICs between human RF and heat aggregated human IgG (see Figure 6.2B) may be an indication of inefficient binding of the HRG to aggregated human IgG and/or possible alterations in the HRG binding site upon exposure to heat.

To clarify whether HRG inhibits insoluble IC formation by masking epitopes on IgG recognized by RF, additional studies were performed using the optical biosensor. These studies indicated that human RF binds to immobilized human IgG1κ (presumably mimicing immobilized ICs) in a concentration-dependent and saturable manner (Figure 6.4A). In contrast, preincubation of IgG1κ immobilized on the biosensor surface with HRG resulted in a total inhibition of

RF binding and, in fact, significant dissociation of bound HRG was observed. Dissociation of HRG presumably occurs through the competitive binding of the HRG to RF in solution. These biosensor data are consistent with HRG masking the site on IgG1κ recognized by the RF used in this study.

Another major finding from the present work is that the presence of HRG can promote solubilisation of already formed insoluble ICs. HRG was much more effective at inhibiting the formation of insoluble ICs (50 % inhibition when the HRG : IgG molar ratio was ~ 1) (Gorgani et al., 1997), than at promoting solubilisation (15 % solubilisation occurred when the HRG was incubated with insoluble ICs at a HRG : IgG molar ratio of ~ 1) (see Figure 6.5B), although such a result is not that surprising when one considers the poor accessibility of HRG to insoluble ICs. Nevertheless, the ability of HRG to promote solubilisation of already formed insoluble ICs *in vitro*, suggests that HRG may play an important role in the solubilisation and subsequent clearance of insoluble ICs *in vivo*. Furthermore, I have recently shown that the incorporation of HRG into ICs leads to enhanced uptake of the ICs by monocytes (Chapter 5).

The present work represents the first report that a plasma protein (i.e. HRG) is able to block the binding of RF to ICs. The results also suggest that when it is incorporated in ICs, HRG may prevent ICs from being recognized by the surface Igs on RF-producing B cells. This proposal, therefore, suggests that HRG may directly interfere with the production of RFs *in vivo*. These findings have major implications for the role of HRG in regulating the production of RF and hence the regulation of the humoral immune response. Similarly, HRG-mediated solubilisation of already formed insoluble ICs has major implications for the prevention of the deposition of pathogenic insoluble ICs in tissues (eg. synovia, kidney, blood vessel wall) in some ICD. The presence of HRG, by promoting the solubilisation and enhanced clearance of the insoluble ICs trapped in tissues, may reduce the pathogenic effects and immunological consequences associated with the deposition of insoluble ICs.

CHAPTER 7

GENERAL DISCUSSION

7 General Discussion

As reviewed in part II of Chapter 1, the formation and clearance of ICs from the circulation has been shown to be largely regulated by plasma complement proteins, erythrocyte CR1 and FcRs on cells associated with the RES. This thesis describes an additional abundant plasma protein, HRG, which plays an important role in regulating the formation and clearance of ICs in a number of unique ways. Initially the results outlined in Chapter 3 indicated that HRG is the dominant endogenous inhibitor in normal plasma of insoluble IC formation and may represent a natural mechanism for controlling IC size. My additional studies have shown that HRG *(i)* binds differentially to Igs which carry κ and λ light chains, thus providing a possible functional role for the κ and λ light chains of Igs (Chapter 4), *(ii)* can solubilise already formed insoluble ICs (Chapter 6), and *(iii)* regulates the interaction of monomeric IgG and ICs with monocytes by inhibiting the binding of monomeric IgG to FcγRI and enhancing the binding of ICs to FcγR on monocytes (Chapter 5). These latter data imply that when HRG is bound to IgG in ICs it does not interfere with the Fc : FcR interaction but can augment macrophage binding of ICs, presumably via other domains of the HRG molecule which bind to cells. Furthermore, studies described in Chapter 6 showed that when HRG is incorporated in ICs it blocks the binding of RF to ICs. This finding suggests that the major IgG epitope recognised by RF could be masked *in vivo* by HRG. Additional studies in Chapter 3 showed, for the first time, that C1q is a high affinity HRG ligand. By binding to C1q, HRG may regulate activation of the classical complement cascade by either inhibiting or enhancing C1 binding to ICs and subsequent activation of the classical complement pathway.

My findings, together with the published report showing that the level of HRG is dramatically decreased in the plasma of patients with SLE (Castel et al., 1983), has led me to hypothesise that HRG represents a key molecule for controlling IC-mediated tissue injury observed in syndromes such as vasculitis, arthritis and GN by (a) regulating the size of ICs and keeping ICs in a soluble form, (b) enhancing the clearance of ICs from the circulation by the RES, (c) solubilizing already formed insoluble ICs, (d) preventing the action of RF and (e) inhibiting the inflammatory effects of complement. Thus, as discussed below in more detail, HRG appears to play an important role in preventing IC-mediated tissue injury.

7.1 Regulation of the size of ICs by HRG

A key feature of IC formation is that, following the initial Ag-dependent cross-linking of Ag and Ab, there is an Ag-independent phase of IC insolubilisation (Gorgani et al., 1996). The Ag-independent insolubilisation of ICs (which leads to the formation of very large hydrophobic particles millimetres in size) appears to be an important phenomenon for efficient clearance of Ags from the circulation, as ICs need to be kept within a critical size range for optimal ingestion by macrophages.

Hitherto, the size of ICs has been shown to be regulated largely by complement proteins (as outlined in Chapter 1). Chapter 3 of this thesis presents evidence that the plasma protein HRG also regulates the size of ICs. This function of HRG may provide two important protective mechanisms. First, as a plasma protein which is always present in the circulation, unlike the complement components which require activation, HRG is immediately available to regulate the size of ICs. Second, by binding C1q HRG may inhibit activation of the classical complement pathway by ICs, thus decreasing the inflammatory effects of complement activation, although further work is required to validate this point.

7.2 Differential binding of HRG to IgG

An unexpected finding described in Chapter 4 of this thesis is that changing the light chain type of IgG from κ to λ has a profound effect on the kinetics of interaction of HRG with all IgG subclasses. Thus the ability of IgG molecules to interact with HRG and, consequently, form soluble versus insoluble ICs is dependent on the light chain isotype they express. In addition, HRG also interacts with the IgG1κ and IgG2κ subclasses faster and stronger, compared to other IgG subclasses, suggesting that HRG also would be more efficient in inhibiting the formation of insoluble ICs containing IgG1κ and IgG2κ, these two subclasses constituting the majority of IgG in human plasma. Since HRG is found to enhance the uptake of ICs by macrophages (Chapter 5), the differential binding of HRG to IgG subclasses may indicate that the light chain and the IgG isotype are important factors in determining whether ICs are eliminated by the RES or are deposited in tissues, possibly providing an Ag depot. Interestingly, HRG binds to human IgG4κ with the lowest affinity. Thus, the finding that the majority of pathogenic ICs in some ICD (eg. ICs in the synovium of RA patients

or anti-ANCA Abs in patients with vasculitis) contain Abs of the IgG4 subclass is particularly relevant.

7.3 Regulation by HRG of the uptake of ICs by monocytes

The uptake of ICs by the RES is the major process for elimination of foreign Ags and has been proposed to involve two mechanisms, namely the binding of ICs to FcRs, and the binding of ICs complexed with complement C3b to CRs. The study presented in Chapter 5 provides evidence for the existence of a third mechanism for enhancing the uptake of ICs by monocytes, namely by the incorporation of HRG in ICs. Furthermore, the finding that HRG inhibits the binding of monomeric IgG to monocytes has major implications for the role of HRG in regulating immune function. Depletion of HRG in plasma may lead to the complete saturation of FcγRI on mononuclear cells by monomeric IgG and hence to a serious disruption of the clearance of ICs by the RES. The deposition of CICs in various organs (eg. kidney, joint and the blood vessel wall) has been shown to lead to the development of pathological conditions such as GN, arthritis and vasculitis (Abrass, 1997; Haynes, 1992). The finding that tissue IC deposits are in equilibrium with CICs (Abrass, 1997; Abrass, 1984) and that a reduction of ICs in the circulation is necessary to limit IC-mediated tissue injury (Balint, 1996; Charlesworth et al., 1982) has led me to the hypothesise that, *in vivo*, HRG may play an important role in reducing the pathogenic effects of ICs by keeping ICs at an optimal size for ingestion and enhancing FcγR-mediated uptake of ICs by the RES.

7.4 Regulation of binding of RF to ICs by HRG

Chapter 6 of this thesis represents the first report that a plasma protein (i.e. HRG) is able to block the binding of RF to ICs. Based on these results it is tempting to hypothesise that when it is incorporated in ICs, HRG may prevent ICs from being recognized by the surface Igs on RF-producing B cells. This proposal, therefore, suggests that HRG may directly interfere with the production of RFs *in vivo*. These findings have major implications for the role of HRG in regulating the production of RF, an Ab type which may play an important immunoregulatory as well as a pathological role.

7.5 Ability of HRG to solubilise already formed insoluble ICs

The ability of HRG to promote solubilisation of already formed insoluble ICs *in vitro*, suggests that HRG may play an important role in the solubilisation and subsequent clearance of insoluble ICs *in vivo*. Thus HRG, by promoting the solubilisation and clearance of insoluble ICs trapped in tissues, may reduce the pathogenic effects and immunological consequences associated with the deposition of insoluble ICs.

7.6 Summary

In summary, HRG appears to play a crucial role in IC clearance at several levels in both health and disease, its major function being to prevent IC-mediated tissue injury. First, HRG is the dominant plasma protein which prevents Ag-independent insolubilisation of ICs, thereby maintaining the complexes in a soluble form and optimal size that can be more readily cleared by the RES. Second, when associated with ICs, HRG enhances uptake of the complexes by macrophages. Third, when bound to IgG, HRG masks the IgG epitope recognised by RF, thereby limiting potential pathogenic effects of RF. Fourth, HRG binds C1q and may well inhibit complement activation by ICs and reduce the inflammatory action of complement, a point yet to be established. Fifth, HRG can promote the solubilisation of insoluble ICs, and this may reduce the pathogenic effects associated with insoluble ICs trapped in tissues.

8 FUTURE DIRECTIONS

With a multifunctional protein such as HRG there are many questions that need to be answered. An obvious one is the location of various ligand binding sites on the molecule. At the functional level, the role of HRG in coagulation and fibrinolysis clearly needs to be clarified. However, in this final discussion I will concentrate on the IC-associated functions of HRG, basing my discussion on a general hypothesis which is outlined below.

8.1 Hypothesis

Studies presented in this thesis have demonstrated that HRG, a relatively abundant plasma protein, may represent a key endogenous protein for controlling IC-mediated tissue injury by directing ICs for clearance by the RES. Thus, it is hypothesized that *(i)* since HRG binds ICs, plasma HRG (~ 2 μM)

may be depleted in severe or chronic infections, *(ii)* a primary genetic defect in patients with syndromes such as vasculitis, arthritis and GN may be the presence of HRG molecules which have lost their ability to bind IgG and/or C1q, and *(iii)* a secondary defect in RA may be the presence of IgG glycoforms and/or the IgG4 subclass that are unable to interact efficiently with HRG. Under such circumstances defective clearance of ICs would be anticipated. Depending on their structure, ICs may accumulate in blood vessel walls, renal glomeruli or synovia.

Future studies can be designed to explore whether the ability of HRG to potentiate the clearance of ICs is physiologically relevant and whether there is a functional defect in the IgG and C1q binding capacity of HRG in patients with ICD. This can be done by *(a)* examining the effect of HRG on the clearance of ICs *in vivo* in mice, *(b)* examining the IC handling ability of plasma from SLE or RA patients, *(c)* clarifying whether HRG from humans with SLE or RA are defective in IgG and/or C1q binding, and *(d)* examining the ability of normal HRG to bind pathogenic IgG associated with RA. Future experiments are discussed below.

8.2 Assessment of the role of HRG in IC clearance *in vivo*.

The effect of HRG on the clearance of ICs *in vivo* can be examined in an IC model (eg. using C57BL/6J mice) (Gauthier et al., 1996; Haakenstad and Mannik, 1974). ICs can be injected into animals and plasma at different times after injection can be examined for HRG depletion using an ELISA assay. If HRG is depleted by IC administration this would be consistent with HRG interacting with ICs *in vivo*. Subsequent experiments, if HRG is depleted by IC injection, can assess in HRG depleted animals the clearance and tissue localization of radiolabelled ICs which have or have not been preincubated with HRG. If HRG is found to prevent the tissue localization and to potentiate the clearance of ICs, genetically engineered fragments of HRG can be examined for their activity in this system. These experiments will provide insights into the importance of HRG in regulating the handling of ICs *in vivo*. This information also will be useful in the future design of synthetic HRG molecules that may well have therapeutic potential.

8.3 Effect of HRG on activation of the classical complement pathway by ICs

As detailed in Chapter 3, optical biosensor experiments clearly demonstrated that human HRG binds C1q with high affinity, with a K_d of ~ 10 nM. These findings suggest that HRG, by binding to C1, the first complement component, may regulate activation of the classical complement pathway by ICs, a point which needs to be clarified, although there is one study which suggests that HRG can modulate the activation of complement by opsonised erythrocytes.

In an attempt to define whether HRG is a pro-inflammatory or anti-inflammatory protein, experiments can be designed to test the effects of HRG on complement activation via the classical pathway. Briefly, ovalbumin can be immobilised on plastic, reacted with polyclonal rabbit anti-ovalbumin IgG and exposed at 37°C to HRG-depleted human plasma. The fixation of human C1q, C3 and C5 by the immobilised IgG could be monitored by ELISA using mAbs against these complement components. The effect of HRG on complement activation, when preincubated with the IgG or added back to the human plasma, can then be assessed. By examining C1q, C3 and C5 fixation the effect of HRG on early and late events in complement activation can be ascertained.

8.4 Effect of HRG on the uptake of ICs by other Fc receptors

Potentially one of the most important functions of HRG may be to direct CICs for clearance by the RES. As described in Chapter 5, HRG enhances uptake of ICs by monocytes. Although three lines of evidences indicate that HRG binds to FcγRI and inhibits monomeric IgG binding, it is important to examine the interaction of HRG with transfected cell lines expressing FcγRI (eg. Cos-7 cells expressing FcγRI). In addition, examination of the binding of HRG to FcγRII, FcγRIII and FcαRI transfected cells would establish whether HRG can interact with other FcR family members. If binding to other FcR is detected it would be important to examine the effect of HRG, when incorporated in ICs, on the ingestion of ICs by cells expressing these FcRs.

8.5 Assessment of IC handling ability of HRG in SLE/RA-plasma.

As outlined in Part II of Chapter 1, two major mechanisms have been shown to inhibit IC-mediated tissue injury, namely removal of ICs from the circulation and attenuation of complement activation. Since a series of findings outlined in

this thesis indicate that HRG may play an important role in the clearance of ICs in healthy states, this raises the intriguing possibility that a genetic defect in HRG's function or the dramatic depletion of HRG in severe infections may lead, at least in part, to deranged clearance of ICs and initiation of diseases such as GN, vasculitis and arthritis.

At the genetic level, mutations in the HRG molecule which destroy its IgG or C1q binding site could represent a risk factor for the development of some ICD. A major aim of future work would be to test this hypothesis by examining the IgG and C1q binding activity of HRG from SLE and RA patients. Initially the effect of different HRG preparations on the formation of insoluble ICs can be examined using turbidity assays (Gorgani et al., 1997) and on the potentiation of uptake of fluoresceinated ICs by macrophages (Chapter 5). The interaction between IgG and different HRG preparations also can be assessed using both ELISA and biosensor techniques (Gorgani et al., 1997). Biosensor or ELISA binding studies can examine whether HRG from SLE/RA patients can bind C1q. The assays can be identical to those performed with IgG except that C1q, rather than IgG, can be immobilised on the biosensor surface/ELISA plates.

Although the HRG molecule itself may be defective in certain ICD, another possibility is that HRG is functionally active but the IgG molecules are defective in their binding to HRG. A degalactosyl form of IgG has been noted in RA patients which may be unable to interact with HRG. The circulating IgG molecules in patients with RA are glycosylated differently, the oligosaccharide sidechain on the Fc portion of IgG lacking terminal galactose (Parekh et al., 1985). Recently it was demonstrated that this degalactosyl-IgG can directly activate the lectin complement cascade via interaction with the MBP in plasma (Malhotra et al., 1995). Based on this finding it has been proposed that IgG containing ICs in RA are highly pathogenic due to their dramatically increased ability to activate complement (Malhotra et al., 1995). Recent studies have also shown that the degalactosyl glycans expressed on IgG in RA, rather than being immobilised in a pocket on the surface of the Fc region of IgG, are highly mobile and extend away from the surface of the Fc region (Wormald et al., 1997). Thus the degalactosyl glycan is much more likely to sterically interfere with the interaction of proteins, such as HRG, with IgG. If this was the case, HRG would be unable to prevent the formation of insoluble ICs and to potentiate the clearance of ICs containing agalactosyl IgG in RA patients, with a resultant accumulation of potentially pathogenic ICs in tissues. In order to investigate this possibility, normal IgG can be enzymatically degalactosylated

with *Streptococcus* β-galactosidase as previously described (Wormald et al., 1997) and the binding of normal HRG to this degalactosyl-IgG assessed on the biosensor or by ELISA assays. Since only approximately 30-50% of circulating IgG from rheumatoid patients bears the abnormal glycoform, the binding of HRG to purified preparations of this abnormal IgG can be examined.

On the other hand, based on my recent findings that HRG binds to IgG4κ with the lowest affinity (Chapter 4) and since IgG4κ is the predominant Ig in pathogenic ICs in ICD (eg. RF in the synovium of patients with RA), this may indicate that HRG does not regulate the formation and clearance of ICs containing IgG4κ. Interestingly, recent studies also have shown that Fc : Fc interactions can occur between purified IgG4κ and other IgG subclasses in the absence of Ag, suggesting that this Ag-independent Fc : Fc interaction can result in the formation of pathogenic ICs in RA (Zach et al., 1995). Thus, HRG also can be examined for its ability to block the Ag-independent interaction of IgG4κ with other subclasses of Igs.

9 FUTURE CLINICAL SIGNIFICANCE

In this final section I would like to speculate about the future clinical significance of HRG in ICDs. ICs are an important pathogenic feature of both SLE and RA. In RA the ICs appear in the joints whereas in SLE they are predominant in the circulation. Both RA and SLE have a strong genetic component but the genes which are associated with disease susceptibility have only been partially characterized. However, it would be anticipated that the genes which regulate the pathogenic effects of ICs would be important.

It is important to note, however, that HRG is likely to be more relevant in SLE than RA patients since ICs are believed to be fundamental in the pathogenesis of SLE, whereas their role in the joint manifestations associated with RA is much less clear. Thus, serum complement levels are invariably high in RA and low in active SLE. Similarly, ICGN is common in SLE, but does not occur in RA suggesting that the pathogenesis of SLE is different from that of RA. However, since my *in vitro* studies suggest that HRG blocks the binding of RF to ICs and may inhibit the pathogenic effects of RFs *in vivo* it also would be important to test the function of HRG in RA patients.

If it is established that HRG is able to potentiate the clearance of ICs in an *in vivo* model, this will provide the first physiologically relevant evidence that a

plasma protein is able to control, by a complement-independent mechanism, the pathogenic effects of ICs and may have therapeutic potential in IC-mediated tissue injury. In addition, if it is found that HRG from autoimmune patients is defective in IgG or C1q binding, this has profound implications for both the diagnosis and treatment of these diseases. First, it implies that "mutated" HRG may be a risk factor for diseases such as SLE and thus patients at risk from the development of ICD could be readily identified. Second, since HRG is a plasma protein, replacement of the defective protein by administration of normal HRG may be a viable treatment strategy, analogous to Factor VIII replacement therapy in haemophiliacs or administration of insulin in patients with diabetes mellitus. At a more theoretical level, if HRG function is found to be seriously compromised in SLE or RA patients, it will strongly suggest that deranged clearance of ICs is an initiating factor in these autoimmune diseases. If the HRG is not defective but is depleted in patients with ICDs, administration of HRG will be a viable treatment strategy to direct pathogenic ICs for clearance by the RES and therefore limit IC-mediated tissue injury. If HRG is normal but the IgG associated with RA is defective in HRG binding, genetically engineered forms of HRG-like molecules with higher affinity for IgG isoform associated with RA may be a viable strategy to potentiate the clearance of ICs from the synovium.

References

Abbas, A.K., Lichtman, A.H. and Pober, J.S. (1991) In Cellular and molecular immunology. *W. B. Saunders publications, Philadelphia,* pp. 45-50.

Abrass, C.K. (1984) Autologous immune complex nephritis in rats. Influence of modification of mononuclear phagocytic system function. *Lab. Invest.* **51**, 162-171.

Abrass, C.K. (1991) Fc receptor-mediated phagocytosis: abnormalities associated with diabetes mellitus. *Clin. Immunol. Immunopathol.* **58**, 1-17.

Abrass, C.K. (1997) Mechanisms of immune complex formation and deposition in renal structure. In Immunological renal diseases, Edited by Neilson, E.G. and Couser, W.G. *Lippincott-Raven publishers, Philadelphia.* pp. 291-307.

Agodoa, L.Y.C., Gauthier, V.J. and Mannik, M. (1983) Precipitating antigen-antibody systems are required for the formation of subepithelial electron dense immune deposits in rat glomeruli. *J. Exp. Med.* **158**, 1259-1271.

Allen, J.M. and Seed, B. (1989) Isolation and expression of functional high affinity Fc receptor cDNA. *Science* **243**, 378-380.

Anderson, C.L. (1982) Isolation of the receptor for IgG from a human monocyte cell line (U937) and from human peripheral blood monocytes. *J. Exp. Med.* **156**, 1794-1806.

Anderson, C.L. (1989) Human IgG Fc receptors. *Clin. Immunol. Immunopathol.* **53**, S63-S71.

Anderson, C.L. and Abraham, G.N. (1980) Characterization of the Fc receptor for IgG on a human macrophage cell line U937. *J. Immunol.* **125**, 2735-2741.

Andrassy, K., Darai, G. and Koderisch, et al., (1983) Anti-Ro antibodies in Wegener's Granulomatosis. *Klin. Wochenschr* **61**, 873-875.

Angles-Cano, E., Gris, J.C., Loyau, S. and Schved, J.F. (1993) Familial association of high levels of histidine-rich glycoprotein and plasminogen activator inhibitor-1 with venous thromboembolism *J. Lab. Clin. Med.* **121**, 646-653.

Anton, L.C., Ruiz, S., Barrio, E., Marques, G., Sanchez, A. and Vivanco, F. (1994) C3 binds with similar efficiency to Fab and Fc regions of IgG immune aggregates. *Eur. J. Immunol.* **24**, 599-604.

Appay, M-D., Kazatchkine, M.D., Levi-Strauss, M., Hinglais, N. and Bariety, J. (1990) Expression of CR1 (CD35) mRNA in podocytes from adult and fetal human kidney. *Kidney Int.* **38**, 289-293.

Balint, J.P. (1996) Immune modulation associated with extracorporeal immunoadsorption treatments utilizing protein A/silica column. *Artif. Organs* **20**, 906-913.

Bariety, J., Hinglais, N., Bhakdi, S., Mandet, C., Rouchon, M. and Kazatchkine, M.D. (1989) Immunohistochemical study of complement S protein (vitronectin) in normal and diseased human kidney: relationship to neoantigens of the C5b-9 terminal complex. *Clin. Exp. Immunol.* **75**, 76-81.

Bauer, R., Muller, A., Richter, M., Schneider, K., Frey, J. and Engelhardt, W. (1997) Influence of heavy metal ions on antibodies and immune complexes investigated by dynamic light scattering and enzyme linked immunosorbent assay. *Biochim. Biophys. Acta* **1334**, 98-108.

Bellotti, V., Stoppini, M., Mangione, P.P., Fornasieri, A., Min, L., Merlini, G. and Ferri, G. (1996). Structural and functional characterization of three human immunoglobulin kappa light chains with different pathological implications. *Biochim. et Biophys. Acta* **1317**, 161-167.

Beynon, H.L., Davies, K.A., Haskard, D.O. and Walport, M.J. (1994) Erythrocyte complement receptor type 1 and interactions between immune complexes, neutrophils, and endothelium. *J. Immunol.* **153**, 3160-3167.

Birmingham, D.J., Hebert, L.A., Cosio, F.G. and Van Aman, M.E. (1990) Immune complex erythrocyte complement receptor interactions *in vivo* during induction of glomerulonephritis in nonhuman primates. *J. Lab. Clin. Med.* **116**, 242-252.

Blobel, G., Walter, P., Chang, C.N., Goldman, B.M., Erickson, A.H. and Lingappa, R. (1979) Translocation of proteins across membranes: the signal hypothesis and beyond. *Symp. Soc. Exp. Biol.* **33**, 9-36.

Borza, D-B., Tatum, F.M. and Morgan, W.T. (1996) Domain structure and conformation of histidine-proline-rich glycoprotein. *Biochemistry* **35**, 1925-1934.

Borza, D-B. and Morgan, W.T. (1997) Acceleration of plasminogen activation by tissue plasminogen activator on surface-bound histidine-proline-rich glycoprotein. *J. Biol. Chem.* **272**, 5718-5726.

Borza, D-B. and Morgan, W.T. (1998) Histidine-proline-rich glycoprotein as plasma pH sensor. *J. Biol. Chem.* **273**, 5493-5499.

Bowness, P., Davies, K.A., Norsworthy, P.J. et al. (1994) Hereditary C1q deficiency and systemic lupus erythematosus. *Quart. J. Med.* **87**, 455-464.

Brasile, L., Kremer, J.L., Clarke, J.L. and Cerelli, J. (1989) Identification of an autoantibody to vascular endothelial cell-specific antigen in patients with systemic vasculitis. *Am. J. Med.* **87**, 74-80.

Brown, B.P., Nardella, F.A. and Mannik, M. (1982) Human complement activation by self associated IgG rheumatoid factors. *Arthritis & Rheum* **25**, 1101-1107.

Brown, K.J. and Parish, C.R. (1994) Histidine-rich glycoprotein and platelet factor 4 mask heparan sulfate proteoglycans recognized by acidic and basic fibroblast growth factor. *Biochemistry* **33**, 13918-13927.

Buckle, P.E., Davies, R.J., Kinning, T., Yeung, D., Edwards, P.R., Pollard-Knight, D. and Lowe, C.R. (1993) The resonant mirror: a novel optical biosensor for direct sensing of biomolecular interactions. Part II: Applications. *Biosensor Bioelectron.* **8**, 355-363.

Burch, M.K., Blackburn, M.N. and Morgan, W.T. (1987) Further characterization of histidine-rich glycoprotein with heparin: Evidence for the binding of two molecules of histidine-rich glycoprotein by high molecular weight heparin and for the involvement of histidine residues in heparin binding. *Biochemistry* **26**, 7477-7482.

Burton, D.B., Boyd, J.B., Brampton, A.D., et al. (1980) The C1q receptor site on immunoglobulin G. *Nature* **288**, 338-344.

Capra, J.D., Winchester, R.J. and Kunkel, H.G. (1969) Cold-reactive rheumatoid factors in infectious mononucleosis and other diseases. *Arthritis and Rheum.* **12**, 67-73.

Carayannopoulos, L. and Capra, J.D. (1993) Immunoglobulins. Structure and Function. In Fundamental Immunology, Third Edition, Edited by William E. Paul, *Raven Press, New York.* pp. 283-314.

Carson, D.A., Pasquali, J.-L., Tsoukas, C.D., Fong, S., Slovin, S.F., Lawrance, S.K., Slaughter, L. and Vaughan, J.H. (1981) Physiology and pathology of rheumatoid factors. *Springer Semin. Immunopathol.* **4**, 161-179.

Castaman, G., Ruggeri, M., Burei, F. and Rodeghiero, F. (1993) High levels of histidine-rich glycoprotein and thrombotic diathesis. *Thromb. Res.* **69**, 297-305.

Castel, M., Horellou, M.H., Conard, J. and Samama, M. (1983) Immunochemical determination of histidine-rich glycoprotein in healthy subjects and in a clinical population. In: Davidson, J.F., Bachmann, F., Bouvier, C.A., Kruithof, E.K.O., eds. Progress in fibrinolysis. *Edinburgh: Churchill Livingstone,* pp. 370-373.

Causer, W.G., Johnson, R.J., Young, B.A., Yeh, C.G., Toth, C.A. and Rudolph, A.R. (1995) The effect of soluble recombinant complement receptor 1 on complement-mediated experimental glomerulonephritis. *J. Am. Soc. Nephrol.* **5**, 1888-1894.

Chang, N.-S., Leu, R.W., Rummage, J.A., Anderson, J.K. and Mole J.E. (1992a) Regulation of complement functional efficiency by histidine rich glycoprotein. *Blood* **79**, 2973-2980.

Chang, N.-S., Leu, R.W., Rummage, J.A., Anderson, J.K. and Mole J.E. (1992b) Regulation of macrophage Fc receptor expression and phagocytosis by histidine-rich glycoprotein. *Immunology* **77**, 532-538.

Chang, N.-S., Leu, R.W., Anderson, J.K. and Mole J.E. (1994) Role of N-terminal domain of histidine-rich glycoprotein in modulation of macrophage Fcγ receptor-mediated phagocytosis. *Immunology* **81**, 296-302.

Charlesworth, J.A., Endre, Z.H., Pussell, B.A., Yasmeen, D. and Peake, P.W. (1982) Complement behavior in infectious mononucleosis: possible mechanisms for the prevention of immune complex injury. *J. Infect. Dis.* **145**, 505-513.

Cines, D., Lyss, A., Reeber, M., Bina, M. and DeHoratius R. (1984) Presence of complement fixing anti-endothelial cell antibodies in systemic lupus erythematosus. *J. Clin. Immunol.* **73**, 611-625.

Cohen, L., Sharp, S. and Kulczycki, A. Jr. (1983) Human monocytes, B lymphocytes and non-B lymphocytes each have structurally unique Fc receptors. *J. Immunol.* **131**, 378-383.

Cole, J.L., Housley, G.A., Dykman, T.R., et al. (1985) Identification of an additional class of C3 binding membrane proteins of human peripheral blood leukocytes and cell lines. *Proc. Natl. Acad. Sci. (USA)* **82**, 859-863.

Corper, A.L., Sohi, M.K., Bonagura, V.R., Steinitz, M., Jefferis, R., Feinstein, A., Beale, D., Taussing, M.J. and Sutton, B.J. (1997) Structure of human IgM rheumatoid factor Fab bound to its autoantigen IgG Fc reveals a novel topology of antibody-antigen interaction. *Nature structural biology* **4**, 374-381.

Cornacoff, J.B., Hebert, L.A., Smead, W.L., Van Aman, M.E., Birmingham, D.J. and Waxman, F.J. (1983) Primate erythrocyte-immune complex-clearing mechanism. *J. Clin. Invest.* **71**, 236-247.

Cornacoff, J.B., Hebert, L.A., Birmingham, D.J. and Waxman, F.J. (1984) Factors influencing the binding of large immune complexes to primate erythrocyte CR1 receptor. *Clin. Immunol. Immunopathol.* **30**, 255-264.

Corrigan, J.J., Jr., Jeter, M.A., Bruck, D. and Feinberg, W.M. (1990) Histidine-rich glycoprotein levels in children: The effect of age. *Thromb. Res.* **59**, 681-686.

Cosio, F.G., Birmingham, D.J., Sexton, D.J. and Herbet, L.A. (1987) Interaction between precipitating and non-precipitating antibodies in the formation of immune complexes. *J. Immunol.* **138**, 2587-2592.

Cosio, F.G., Shen, X.P., Birmingham, D.J., Van Aman, M.E., and Herbet, L.A. (1990) Evaluation of the mechanisms resposible for the reduction in erythrocyte complement receptors when immune complexes form in vivo in primates. *J. Immunol.* **145**, 4198-4206.

Coulie, P. and Van Snick, J. (1983) Rheumatoid factors and secondary immune responses in the mouse. II. Incidence, kinetics and induction mechanism. *Eur. J. Immunol.* **13**, 895-899.

Cousins, R.J. (1989) Systemic transport of zinc. In: Zinc in human biology. Mills, C.F., ed. *Springer-Verlag, London* pp. 80-81.

Cupps, T. and Fauci, A.S. (1981) The vasculitides. In: Major problems in internal medicine, XXI. Philadelphia: *WB Saunders.* pp.

Cupps, T. and Fauci, A.S. (1982) The vasculitis syndrome. *Adv. Intern. Med.* **27**, 315-344.

Cush, R., Cronin, J.M., Stewart, W.J., Maule, C.H., Molloy, J. and Goddard, N.J. (1993) The resonant mirror: a novel optical biosensor for direct sensing of biomolecular interactions. Part I: Principles of operation and associated instrumentation. *Biosensors Bioelectron.* **8**, 347-354.

Danielsson, C., Pascual, M., French, L., Steiger, G. and Schifferli, J.A. (1994) Soluble complement receptor type 1 (CD35) is released from leukocytes by surface cleavage. *Eur. J. Immunol.* **24**, 2725-2731.

Davies, A., Simmons, D.L., Hale, G., et al. (1989) CD59, and LY-6-like protein expressed in human lymphoid cells, regulates the action of the complement membrane attack complex on homologous cells. *J. Exp. Med.* **170**, 637-654.

Davies, K.A., Hird, V., Stewart, S. et al. (1990a) A study of *in vivo* immune complex formation and clearance in man. *J. Immunol.* **144**, 4613-4620.

Davies, K.A., Mathieson, P., Winearls, C.G., Rees, A.J. and Walport, M.J. (1990b) Serum sickness and acute renal failure after streptokinase therapy for myocardial infarction. *Clin. Exp. Immunol.* **80**, 83-88.

Davies, K.A., Peters, A.M., Beynon, H.L. and Walport, M.J. (1992) Immune complex processing in patients with systemic lupus erythematosus. *In vivo* imaging and clearance studies. *J. Clin. Invest.* **90**, 2075-2083.

Davies, K.A., Erlendsson, K., Beynon, H.L. et al. (1993) Splenic uptake of immune complexes in man is complement-dependent. *J. Immunol.* **151**, 3866-3873.

Davies, K.A., Chapman, P.T., Norsworthy, P.J. et al. (1995) Clearance pathway of soluble immune complexes in the pig: insights into the adaptive nature of antigen clearance in human. *J. Immunol.* **155**, 5760-5768.

Dienstag, J.L. (1981) Hepatitis B as an immune complex disease. *Semin. Liver Dis.* **1**, 45-57.

Dorff, B. and Lind, K. (1976) Two fatal cases of meningoencephalitis associated with mycoplasma pnenumoniae infection. Scand. *J. Infect. Dis.* **8**, 49-51.

Drasin, T. and Sahud, M. (1996) Blood-type and age affect human plasma levels of histidine-rich glycoprotein in a large population. *Thromb. Res.* **84**, 179-188.

Easterbrook-Smith, S. B. (1993) A light scattering method for measuring the sizes of insoluble immune complexes. *Molec. Immunol.* **30**, 637-640.

Easterbrook-Smith, S.B., Vandenberg, R.J. and Alden, J.A. (1988) The role of Fc : Fc interactions in insoluble immune complex formation. *Molec. Immunol.* **25**, 1331-1337.

Edwards, J.C. and Cambridge, G. (1998) Rheumatoid arthritis: the predictable effect of small immune complexes in which antibody is also antigen. *Br. J. Rheumatol.* **37**, 126-130.

Ehlenberger, A.G. and Nussenzweig, V. (1977) The role of membrane receptors for C3b and C3d in phagocytosis. *J. Exp. Med.* **145**, 357-371.

Eisenberg, S.P., Dripps, D.J., Evans, R.J., Childs, J.D. and Thompson, R.C. (1991) Structural and biological studies on IL1 receptor antagonist. *J. Cell Biochem. [Suppl]* 15E : 151A

Eisenberg, S.P., Evans, R.J., Arenel, W.P., Verderber, E., Brewer, M.T., Hannumi, C.H. and Thompson, R.C. (1990) Primary structure and functional expression from complementary DNA of a human IL1 receptor antagonist. *Nature* **343**, 341-346.

Emlen, W., Carl, V. and Burdick, G. (1992) Mechanism of transfer of immune complexes from red blood cell CR1 to monocytes. *Clin. Exp. Immunol.* **89**, 8-17.

Failla, M.L., Van De Veerdonk, M. and Morgan, W.T. (1982) Characterization of zinc-binding proteins of plasma in familial hyperzincemia. *J. Lab. Clin. Med.* **100**, 943-952.

Fauci, A.S. (1983) Vasculitis. *J. Allergy Clin. Immunol.* **72**, 211-223.

Fauci, A.S., Haynes, B.F. and Katz, P. (1978) The spectrum of vasculitis: Clinical, pathological, immunologic, and therapeutic considerations. *Ann. Intern. Med.* **89**, 660-676.

Fearon, D.T. (1983) The human C3b receptor. *Springer Semin. Immunopathol.* **6**, 159-172.

Fearon, D.T. and Austen, K.F. (1975) Properdin: binding to C3b and the stabilization of the C3b-dependent C3 convertase. *J. Exp. Med.* **142**, 856-863.

Fernald, G.W. (1982) Immunologic interactions between host cells and mycoplasmas *Rev. Infect. Dis.* **4**, S201-S204.

Fleit, H.B. and Kuhnle, M. (1988) Biochemical characterization of an Fc gamma receptor purified from human neutrophils *J. Immunol.* **140**, 3120-3125.

Freeman, C. and Parish C.R. (1998) Human platelet heparanase: purification, characterization and catalytic activity. *Biochem J.* **330**, 1341-1350.

Fries, L.F., Hall, R.P., Lawley, T.J., Crabtree, G.R. and Frank, M.M. (1982) Monocyte receptors for the Fc portion of IgG studied with monomeric human IgG1: Normal *in vitro* expression of Fcγ receptors in HLA-B8/Drw 3 subjects with defective Fc-mediated *in vivo* clearance. *J. Immunol.* **129**, 1041-1049.

Furness, P.N. (1993) Degradation of insoluble immune complexes by glomerular mesangial cells. *Exp. Nephrol.* **1**, 372-375.

Gauthier, V.J. and Abrass, C.K. (1992) Circulating immune complexes in renal injury. *Semin. Nephrol.* **12**, 379-394.

Gauthier, V.J., Tyler, L.N. and Mannik, M. (1996) Blood clearance kinetics and liver uptake of mononucleosomes in mice *J. Immunol.* **156**, 1151-1156.

Gavin, A.L., Wines, B.D., Powell, M.S. and Hogarth, P.M. (1995) Recombinant soluble FcγRII inhibits immune complex precipitation. *Clin. Exp. Immunol.* **102**, 620-625.

George, A.J.T., French, R.R. and Glennie, M.J. (1995) Measurement of kinetic binding constants of a panel of anti-saporin antibodies using a resonant mirror biosensor. *J. Immunol. Methods* **183**, 51-63.

Geronski, P., Bodenbender, L., Kanzy E-J., Loos, M. and Seiler, F.R. (1985) The modulation of immune complex aggregation by classical pathway-mediated reactions. *Immunobiol.* **169**, 346-361.

Giacomelli, F. and Weiner, J. (1974) Regional variation in the permeability of rat thoracic aorta. *Am. J. Pathol.* **75**, 513-528.

Gocke, D., Hsu, K., Morgan, C., Bombarieri, S., et al. (1970) Association between polyarteritis and australia antigen. Lancet **2**, 1149-1153.

Golan, M.D., Hitschold, T. and Loos, M. (1981) The reconstitution of human C1, the first complement component: binding of C1r and C1s to C1q influences the C1q conformation. *FEBS Lett.* **128**, 281-285.

Goodnough, L.T., Saito, H., Bell, W.R. and Heimburger, N. (1985) Histidine-rich glycoprotein and changes in the components of the fibrinolytic system after streptokinase therapy in patients with pulmonary thromboembolism. *Am J. Hematol.* **19**, 245-253.

Gorgani, N.N., Easterbrook-Smith, S.B. and Altin, J.G. (1996) The formation of insoluble immune complexes between ovalbumin and anti-ovalbumin IgG occurs in at least two distinct phases dependent on reactant concentration and ionic strength. *Biochim. Biophy. Acta* **1317**, 45-54.

Gorgani, N.N., Parish, C.R., Easterbrook-Smith, S.B., and Altin, J.G. (1997) Histidine-rich glycoprotein binds to human IgG and C1q and inhibits the formation of insoluble immune complexes. *Biochemistry* **36**, 6653-6662.

Guthans, S.L. and Morgan, W.T. (1982) The interaction of zinc, nickel and cadmium with serum albumin and histidine-rich glycoprotein assessed by equilibrium dialysis and immunoadsorbent chromatography. *Arch. Biochem. Biophys.* **218**, 320-328.

Haakenstad, A.O. and Mannik, M. (1974) Saturation of the reticuloendothelial system with soluble immune complexes *J. Immunol.* **112**, 1939-1943.

Haakenstad, A.O., Striker, G.E. and Mannik, M. (1976) The glomerular deposition of soluble immune complexes prepared with reduced and alkylated antibodies and with intact antibodies in mice. *Lab. Invest.* **35**, 293-301.

Hajjar, D.P., Boyd, D.B., Harpel, P.C. and Nachman, R.L. (1987) Histidine-rich glycoprotein inhibits the anti-proliferative effect of heparin on smooth muscle cells. *J. Exp. Med.* **165**, 908-913.

Hakansson, L., Hallgren, R. and Venge, P. (1982) Kinetic studies of phagocytosis: III. The complement-dependent opsonic and anti-opsonic effects of normal and SLE sera. *Immunology* **47**, 91-99.

Halbmayer, W.M., Hopmeier, P., Mannhalter, C., Heuss, F., Leodolter, S., Rubi, K. and Fischer, M. (1991) C1-Esterase inhibitor in uncomplicated pregnancy and mild and moderate preeclampsia. *Thromb. Haemost.* **65**, 134-138.

Halbmayer, W.M., Hopmeier, P., Feichtinger C., Rubi, K. and Fischer, M. (1992) Histidine-rich glycoprotein (HRG) in uncomplicated pregnancy and mild and moderate preeclampsia. *Thromb. Haemost.* **67**, 585-586.

Halkier, T., Andersen, H., Vestergaard, A. and Magnusson, S. (1994) Bovine histidine-rich glycoprotein is a substrate for bovine plasma factor XIIIa. *Biochem. Biophys. Res. Commun.* **200**, 78-82.

Hansch, G.M., Hammer, C.H., Vanguri, P. et al. (1981) Homologous species restriction in lysis of erythrocytes by terminal complement proteins. *Proc. Natl. Acad. Sci. USA.* **78**, 5118-5121.

Haukkamaa, M., Morgan, W.T., and Koskelo, P. (1983) Serum histidine-rich glycoprotein during pregnancy and hormone treatment. *Scand. J. Clin. Lab. Invest.* **43**, 591-595.

Haupt, H. and Heimburger, N. (1972) Human serum proteins with high affinity for carboxymethyl cellulose. I. Isolation of lysozyme, C1q and 2 hitherto unknown globulins. *I. Hoppe-seyler's Z.physiol. Chem. Bd.* **353**, S. 1125-1132.

Haynes B.F. (1992) Vasculitis. Pathogenic mechanisms of vessel damage. In: Inflammation: Basic Principles and Clinical Correlates, Edited by Gallin, J.I., Goldstein, I.M. and Snyderman, R. *Raven press Ltd., NY* pp. 921-941.

Haynes B.F., Allen, N.B. and Fauci A.S. (1986) Diagnostic and therapeutic approach to the patient with vasculitis. *Med. Clin. North Am.* **70**, 355-368.

Hebert, L.A. (1987) The erythrocyte-immune complex- glomerulonephritis connection in man. *Kidney Int.* **31**, 877-885.

Hebert, L.A. (1991) Clearance of immune complexes from the circulation of man and other primates. *Am. J. Kidney Dis.* **17**, 352-361.

Hebert, L.A., Cosio, F.G., Birmingham, D.J., Mahan, J.D., Sharma, H.M., Smead, W.L. and Goel, R. (1991a) Experimental immune complex mediated glomerulonephritis in the nonhuman primate. *Kidney Int.* **39**, 44-56.

Hebert, L.A., Cosio, F.G., Birmingham, D.J. and Mahan, J.D. (1991b) Biological significance of the erythrocyte complement receptor: a primate prerequisite. *J. Lab. Clin. Med.* **118**, 301-308.

Hebert, L.A., Cosio, F.G. and Neff, J.C. (1991c) Diagnostic significance of hypocomplementemia. *Kidney Int.* **39**, 811-821.

Hebert, L.A., Cosio, F.G. and Birmingham, D.J. (1997) Complement and complement regulatory proteins in renal disease. In Immunological renal diseases, *Lippincott-Raven publishers, Philadelphia.* pp. 377-395.

Heidelberger, M. (1941) Quantitative chemical studies on complement or alexin.- I. A method. *J. Exp. Med.* **73**, 691-694.

Heimburger, N., Haupt, H., Kranz, T. and Baudner, S. (1972) Humanserumproteine mit hoher affinitat zu carboxymethylcellulose, II. *Hoppe-Seyler's Z. Physiol. Chem.* **353**, 1133-1140.

Heimer, R., Wolf, L.D. and Abruzzo, J.L. (1982) IgM and IgG anti-F(ab')2 antibodies in rheumatoid arthritis and systemic lupus erythematosus. *Arthritis Rheum.* **25**, 1298-1306.

Hennis, B.C., De Maat, M.P.M., Quax, P.H.A., Le Clercq E.J., Kuiper, J. and Kluft, C. (1991) Evaluation of sites of synthesis of histidine-rich glycoprotein. *Thromb. Haemost.* **65**, pp. 884 (abstract 660).

Hennis, B.C., Frants, R.R., Bakker, E., Vossen, R.H.A.M., van der Poort, E.W., Blonden, L.A., Cox, S., Meera Khan, P., Spurr, N.K. and Kluft, C. (1994) Evidence for the absence of intron H of the histidine-rich glycoprotein (HRG) gene: genetic mapping and in situ localization of HRG to chromosome 3q28-q29. *Genomics* **19**, 195-197.

Hennis, B.C., van Boheemen, P.A., Wakabayashi, S., Koide, T., Hoffmann, J.J.M.L., Kievit, P., Dooijewaard, G., Jansen, J.G. and Kluft, C. (1995) Identification and genetic analysis of a common molecular variant of histidine-rich glycoprotein with a difference of 2KD in apparent molecular weight. *Thromb. Haemost.* **74**, 1491-1496.

Heyman, B. (1990) Fc-dependent IgG-mediated suppression of the antibody response: fact or artefact. *Scand. J. Immunol.* **31**, 601-607.

Holers, V.M., Cole, J.L., Lublin, D.M., Seya, T. and Atkinson, J.P. (1989) Human C3b and C4b regulatory proteins: a new multi-gene family. *Immunol. Today* **6**, 188-192.

Holguin, M.H., Fredrick, L.R., Bernshow, N.J., Wilcox, L.A. and Parker, C.J. (1989) Isolation and characterization of a membrane protein from normal human erythrocytes that inhibit reactive lysis of the erythrocyte of paroxysmal nocturnal hemoglobinuria. *J. Clin. Invest.* **84**, 7-17.

Holmskov, U., Malhotra, R., Sim, R.B. and Jensenius, J.C. (1994) Collectins: collagenous C-type lectins of the innate immune defense system. *Immnol. Today* **15**, 67-74.

Huber, H., Polley, M.J., Linscott, W.D., Fudenberg, H.H. and Muller-Eberhard, H.J. (1968) Human monocytes: distinct receptor sites for the third component of complement and immunoglobulin G. *Science* **162**, 1281-1283.

Hulett, M.D. and Hogarth, P.M. (1994) Molecular basis of Fc receptor function. *Advances in Immunol.* **57**, 1-128.

Huttner, I., More, R. and Rona, G. (1970) Fine structural evidence of specific mechanism for increased endothelial permeability in experimental hypertension. *Am. J. Pathol.* **61**, 395-404.

Iida, K., Mornaghi, R. and Nussenzweig, V. (1982) Complement receptor (CR1) deficiency in erythrocytes from patients with systemic lupus erythematosus. *J. Exp. Med.* **155**, 1427-1438.

Isenman, D. and Kells, D.I.C. (1982) Conformational and functional changes in the fourth component of human complement produced by nucleophilic modification and by proteolysis with C1s. *Biochemistry* **21**, 1109-1117.

Isenman, D.E., Kells, D.I., Cooper, N.R., Muller-Eberhard, H.J. and Pangburn, M.K. (1981) Nucleophilic modification of human complement protein C3: correlation of conformational changes with acquisition of C3b-like functional properties. *Biochemistry* **20**, 4458-4467.

Iskandar, S.S. and Jennette J.C. (1983) Influence of antibody avidity on glomerular immune complex localization. *Am. J. Pathol.* **112**, 155-159.

Jackson, R.L., Busch, S.J. and Cardin, A.D. (1991) Glycosaminoglycans: Molecular properties, protein interactions, and role in physiological processes. *Physiol. Rev.* **71**, 481-539.

Jaffe, E.A., Leung, L.L.K., Nachman, R.L., Levin, R.I. and Mosher, D.F. (1982) Thrombospondin is the endogenous lectin of human platelets. *Nature* **295**, 246-248.

Jefferis, R. and Pound, J.D. (1992) Immunoglobulins. In: Inflammation: Basic Principles and Clinical Correlates. Sec. Ed. Gallin, J.I., Goldstein, I.M. and Snyderman, R. Eds. *Raven Press Ltd. NY* pp. 11-31.

Johnson, P.M. and Page Faulk, W. (1976) Rheumatoid factor: its nature, specificity, and production in rheumatoid arthritis. *Clin. Immunol. Immunopathol.* **6**, 414-430.

Kallenberg, C.G.M., Cohen Tervaert, J.W., van der Woude, F.J., Goldschmeding, R., von dem Borne, A.E.G. and Weeming, J.J. (1991) Autoimmunity to lysosomal enzymes: new clues to vasculitis and glomerulonephritis? *Immunol. Today* **12**, 61-64.

Kamoun, M., Martin, P.J., Hansen, J.A., Brown, M.A., Siadak, A.W. and Nowinski, R.C. (1981) Identification of a human T lymphocyte surface protein associated with the E-rosette receptor. *J. Exp. Med.* **153**, 207-212.

Kavanaugh, A.F. (1998) Anti-tumor necrosis factor-alpha monoclonal antibody therapy for rheumatoid arthritis. *Rheum. Dis. Clin. North Am.* **24**, 593 ff.

Kawakami, M., Ilhara, I., Ilhara, S., Suzuki, S. and Fukui, K. (1984) A group of bactericidal factors conserved by vertebrates for more than 300 million years. *J. Immunol.* **132**, 2578-2581.

Kazama, Y. and Koide, T. (1992) Modulation of protein C inhibitor activity by histidine-rich glycoprotein and platelet factor 4: Role of zinc and calcium ions in the heparin-neutralizing ability of histidine-rich glycoprotein. *Thromb. Haemos.* **67**, 50-55.

Kijlstra, A., Allegonda, V.D.L., Knutson, D.W., Fleuren, G.J. and Van Es, L.A. (1978) The influence of phagocyte function on glomerular localization of aggregated IgM in rats. *Clin. Exp. Immunol.* **32**, 207-217.

Klein, J. and Horejsi, V. (1997) B cell receptors, immunoglobulins and Fc receptors, In: Immunology. Sec. Ed., *Oxford: Blackwell Science Ltd.* pp. 204-270.

Klopstock, A., Schwartz, J., Bleiberg, Y., Adam, A. and Szeinberg, A. (1965) Hereditary nature of the behaviour of erythrocytes in the immune adherence haemagglutination phenomenon. *Vox Sang* **10**, 177-187.

Koide, T. (1988) Human histidine-rich glycoprotein gene: evidence for evolutionary relatedness to cystatin supergene family. *Thromb. Res.* **Suppl VIII**, 91-97.

Koide, T., Foster, D., Yoshitaki, S. and Davie, E.W. (1986) Amino acid sequence of human histidine-rich glycoprotein derived from the nucleotide sequence of its cDNA. *Biochemistry* **25**, 2220-2225.

Koide, T., Odani, S. and Ono, T. (1982) The N-terminal sequence of human plasma histidine-rich glycoprotein homologous to antithrombin with high affinity for heparin. *FEBS Lett.* **141**, 222-224.

Koide, T., Odani, S. and Ono, T. (1985) Human histidine-rich glycoprotein: Simultaneous purification with antithrombin III and characterization of its gross structure. *J. Biochem.* **98**, 1191-1200.

Kozarsky, K.F., Tsai, C., Bott, C.M., Allada, G., Li, L.L. and Fox, D.A. (1993) An anti-CD2 monoclonal antibody that both inhibits and stimulates T cell activation recognizes a subregion of CD2 distinct from known ligand-binding sites. *Cell Immunol.* **150**, 235-246.

Kurlander, R.J. and Batker, J. (1982) The binding of human immunoglobulin G1 monomer and small covalently cross-linked polymers of immunoglobulin G1 to human peripheral blood monocytes and polymorphonuclear leukocytes. *J. Clin. Invest.* **69**, 1-8.

Kyte, J. and Doolittle, R.F. (1982) A simple method for displaying the hydropathic character of a protein. *J. Mol. Biol.* **157**, 105-132.

Lachmann, P.J. and Hughes-Jones, N.C. (1984) Initiation of complement activation. *Springer Semin. Immunopathol.* **7**, 143-162.

Lachmann, P.J. and Walport, M.J. (1987) Deficiency of the effector mechanisms of the immune response and autoimmunity. in Autoimmunity and Autoimmune diseases Whelan, J. Eds *Wiley, Chichester.* pp. 149 - 171.

Laemmli, U.K. (1970) Cleavage of structural proteins during the assembly of the head of the bacteriophage T4. *Nature* **227**, 680-685.

Lamb-Wharton, R.J. and Morgan, W.T. (1993) Induction of T lymphocyte adhesion by histidine-proline-rich glycoprotein and concanavalin A. *Cellular Immunol.* **152**, 544-555.

Lane, D.A., Peijler, G., Flynn, A.M., Thompson, E.A. and Lindahl, U. (1986) Neutralization of heparin-related saccharides by histidine-rich glycoprotein and platelet factor 4. *J. Biol. Chem.* **261**, 3980-3986.

Leber, P. and McCluskey, R. (1974) Immune complex disease. In: The inflammatory process. Zweifach, B. and McCluskey R. eds., vol 3, sec. ed., *NY Acamedic Press* pp. 401-438.

Leebeek, F.W.G., Kluft, C., Knot, E.A.R. and De Maat, M.P.M. (1989) Histidine-rich glycoprotein is elevated in mild liver cirrhosis and decreased in moderate and severe liver cirrhosis. *J. Lab. Clin. Med.* **113**, 493-497.

Lehman, D.H., Wison, C.B. and Dixon, F.J. (1975) Extraglomerular immunoglobulin deposits in human nephritis. *Am. J. Med.* **58**, 765-786.

Lerch, P.G., Nydegger, U.E., Kuyas, C. and Haeberli, A. (1988) Histidine-rich glycoprotein binding to activated human platelets. *Br. J. Haematol.* **70**, 219-224.

Leung, L.L.K. (1986) Interaction of histidine-rich glycoprotein with fibrinogen and fibrin. *J. Clin. Invest.* **77**, 1305-1311.

Leung, L.L.K. and Nachman, R.L. (1982) Complex formation of thrombospondin with fibrinogen. *J. Clin. Invest.* **70**, 542-549.

Leung, L.L.K., Harpel, P.C., Nachman, R.L. and Rabellino, E.M. (1983) Histidine-rich glycoprotein is present in human platelets and is released following thrombin stimulation. *Blood* **62**, 1016-1021.

Leung, L.L.K., Nachman, R.L. and Harpel, P.C. (1984) Complex formation of platelet thrombospondin with histidine-rich glycoprotein. *J. Clin. Invest.* **73**, 5-12.

Leung, L.L.K., Saigo, K. and Grant, D. (1989) Heparin binds to human monocytes and modulates their procoagulant activities and secretory phenotypes. Effect of histidine-rich glycoprotein. *Blood* **73**, 177-184.

Lewis, S.M. (1994) The mechanism of V(D)J joining: lessons from molecular, immunological, and comparative analyses. *Adv. Immunol.* **56**, 27-151.

Lijnen, H.R. and Collen, D. (1983) Turn over of histidine-rich glycoprotein during heparin administration in man. *Thromb. Res.* **30**, 671-676.

Lijnen, H.R., Jacobs, G. and Collen, D. (1981a) Histidine-rich glycoprotein in a normal and a clinical population. *Thromb. Res.* **22**, 519-523.

Lijnen, H.R., De Cock, F. and Collen, D. (1981b) Turn over of histidine-rich glycoprotein in healthy subjects and during thrombolytic therapy. *Thromb. Res.* **23**, 121-131.

Lijnen, H.R., Hoylaerts, M. and Collen D. (1980) Isolation and characterization of a human plasma protein with affinity for the lysine binding site in plasminogen. *J. Biol. Chem.* **255**, 10214-10222.

Lijnen, H.R., Rylatt, D.B. and Collen, D. (1983a) Physicochemical, immunochemical and functional comparison of human histidine-rich glycoprotein and autorosette inhibition factor. *Biochem. Biophys. Acta* **742**, 109-115.

Lijnen, H.R., Hoylaerts, M. and Collen, D. (1983b) Heparin binding properties of human histidine-rich glycoprotein. Mechanism and role in the neutralization of heparin in plasma. *J. Biol. Chem.* **258**, 3803-3808.

Lijnen, H.R., Van Hoef, B. and Collen, D. (1984) Histidine-rich glycoprotein modulates the anticoagulant activity of heparin in human plasma. *Thromb. Haemos.* **51**, 266-268.

Liszewski, M.K., Post, T.W. and Atkinson, J.P. (1991) Membrane cofactor protein (MCP or CD46): newest member of the regulators of complement activation gene cluster. *Ann. Rev. Immunol.* **9**, 431-455.

Liu, Y.C., Tomashefski, J.F., Tomford, J.W. and Green, H. (1989) Necrotizing Pneumocystis carinii vasculitis associated with lung necrosis and cavitation in a patient with acquired immunodeficiency syndrome. *Arch. Pathol. Lab. Med.* **113**, 494-497.

Lorenz, H.M. and Kalden, J.R. (1998) Biological agents in Rheumatoid Arthritis - Which ones could be used in combination. *Biodrugs* **9**, 303-324.

Lu, J., Thiel, S., Wiedemann, H., Timpl, R. and Reid, K.B.M. (1990) Binding of the pentamer/hexamer forms of mannan-binding protein to zymosan activates the proenzyme $C1r_2C1s_2$ complex, of the classical pathway of complement, without involvement of C1q. *J. Immunol.* **144**, 2287-2294.

Lublin, D.M. and Atkinson, J.P. (1989) Decay-accelerating factor: biochemistry, molecular biology and function. *Annu. Rev. Immunol.* **7**, 35-38.

Malhotra, R., Wormald, M.R., Rudd, P.M., Fischer, P.B., Dwek, R.A. and Sim, R.B. (1995) Glycosylation changes of IgG associated with rheumatoid arthritis can activate complement via the mannose-binding protein. *Nature Med.* **1**, 237-243.

Mannik, M., Agodoa, L.Y.C. and David, K.A. (1983) Rearrangement of immune complexes in glomeruli leads to persistence and development of electron dense deposits. *J. Exp. Med.* **157**, 1516-1528.

Mannik, M. and Person, R.E. (1994) Deep penetration of antibodies into the articular cartilage of patients with rheumatoid arthritis. *Rheumatol. Int.* **14**, 95-102.

Mancilla-Jimenez, R., Appay, M.D., Bellon, B., Kuhn, J., Bariety, J. and Druet, P. (1984) IgG Fc membrane receptor on normal human glomerular visceral epithelial cells. *Virchows Arch.* **404**, 139-158.

Mathieson, P.W., Cobbold, S.P., Hale, G. et al. (1990) Monoclonal antibody therapy in systemic vasculitis. *N. Engl. J. Med.* **323**, 250-254.

Matsushita, M. and Fujita, T. (1992) Activation of the classical complement pathway by mannose binding protein in association with a novel C1s-like serine proteases. *J. Exp. Med.* **176**, 1497-1502.

Matsushita, M., Takahashi, A., Hatsuse, H., Kawakami, M. and Fujita, T. (1992) Human mannose-binding protein is identical to a component of Ra-reactive factor. *Biochem. Biophys. Res. Commun.* **183**, 645-651.

Matsumoto, A.K., Kopicky-Burd, J., Carter, R.H., Tuveson, D.A., Tedder, T.F. and Fearon, D.T. (1991) Intersection of the complement and immune system: a signal transduction complex of the B lymphocyte-containing complement receptor type 2 and CD19. *J. Exp. Med.* **173**, 55-64.

Mauer, S.M., Fish, A.J., Blau, E.B. and Michael, A.F. (1972) The glomerular mesangium: I. Kinetic studies of macromolecular uptake in normal and nephrotic rats. *J. Clin. Invest.* **51**, 1091-1101.

Max, E.E. (1993) Immunoglobulins. Molecular genetics. In Fundamental Immunology, Third Ed., Paul, W.E. ed. *Raven Press, NY* pp. 315-382.

Mellow, G.H. and Clarkson, A.B. jr. (1982) Trypanosoma lewisi: enhanced resistance in naive lactating rats and their suckling pups. *Exp. Parasitol.* **53**, 217-228.

McCluskey, R. and Bhan, A. (1983) Cell-mediated mechanisms in renal diseases. *Hum. Pathol.* **14**, 305-315.

Miller, G.W. and Nussenzweig, V. (1975) A new complement function: solubilisation of antigen-antibody aggregates. *Proc. Natl. Acad. Sci. USA*, **72**, 418-422.

Milstein, C. (1986) From antibody structure to immunological diversification of the immune response. *Science* **231**, 1261-1268.

Miyakawa, Y., Yamada, A., Kosaka, K., Tsuda, F., Kosugi, E. and Mayumi, M. (1981) Defective immune-adherence (C3b) receptor on erythrocytes from patients with systemic lupus erythematosus. *Lancet* **2**, 493-497.

Møller, N.P.H. (1979) Fc-mediated immune precipitation - I. A new role for the Fc-portion of IgG. *Immunology* **38**, 631-640.

Møller, N.P.H. and Bak, J.F. (1984) A general theory for the precipitin reaction based on Fc-mediated immune precipitation. *Acta Path. Microbiol. Scand. Sect.* C **92**, 237-246.

Møller, N.P.H. and Steensgard, J. (1979) Fc-mediated immune precipitation - II. Analysis of precipitating immune complexes by rate-zonal centrifugation *Immunology* **38**, 641-648.

Monahan, J.B. and Sodetz, J.M. (1981) Role of the b-subunit in the interaction of the 8th component of human complement with the membrane-bound cytolytic complex. *J. Biol. Chem.* **256**, 3258-3262.

Moreland, L.W. (1998) Soluble tumor necrosis factor receptor (p75) fusion protein (enbrel) as a therapy for rheumatoid arthritis. *Rheum. Dis. Clin. North Am.* **24**, 579 ff.

Morgan, W.T. (1978) Human serum histidine-rich glycoprotein. I. Interactions with heme, metal ions and organic ligands. *Biochim. Biophys. Acta.* **533**, 319-333.

Morgan, W.T. (1981) Interaction of the histidine-rich glycoprotein of serum with metals. *Biochemistry* **20**, 1054-1061.

Morgan, W.T. (1985) The histidine-rich glycoprotein of serum has a domain rich in histidine, proline, and glycine that binds heme and metals. *Biochemistry* **24**, 1496-1501.

Morgan, W.T. (1986) Serum histidine-rich glycoprotein levels are decreased in acquired immune deficiency syndrome and by steroid therapy. *Biochem. Med. Metabolic Biol.* **36**, 210-213.

Morgan, W.T., Koskelo, P., Koenig, H. and Conway, T.P. (1978) Human histidine-rich glycoprotein. II. Serum levels in adults, pregnant woman and neonates. *Proc. Soc. Exp. Biol. Med.* **158**, 647-651.

Mountz, J.D., Wu, J., Cheng, J. and Zhou, T. (1994) Autoimmune disease - A problem of defective apoptosis. *Arthritis and Rheum.* **37**, 1415-1420.

Muller-Eberhard, H.J. (1992) Complement. Chemistry and pathway. In: Inflammation: Basic Principles and Clinical Correlates. Second Edition. Edited by Gallin, J.I., Goldstein, I.M. and Snyderman, R. *Raven Press Ltd., NY* pp. 33-62.

Muller-Eberhard, H.J. and Gotze, O. (1972) C3 proactivator convertase and its mode of action. *J. Exp. Med.* **135**, 1003-1008.

Murphy, R.M., Slayter, H., Schurtenberger, P., Chamberlin, R.A., Colton, C.K. and Yramush, M.L. (1988) Size and structure of antigen-antibody complexes. Electron microscopy and light scattering studies. *Biophys. J.* **54**, 45-56.

Myones, B.L., Dalzell, J.G., Hogg, N. et al., (1988) Neutrophil and monocyte cell surface p150,95 has iC3b-receptor (CR4) activity resembling CR3. *J. Clin. Invest.* **82,** 640-651.

Nagasawa, S. and Stroud, R.M. (1977) Cleavage of C2 by C1s into the antigenically distinct fragments C2a and C2b: demonstration of binding of C2b to C4b. *Proc. Natl. Acad. Sci. USA* **74,** 2998-3001.

Naranjo, H.A., Rodriguez, G.T., Rodriguez, L.C., Ojeda, B.S., Francisco, H.F., Sanchez , G.F. and Bilbao, C.A. (1997) High titers of rheumatoid factor : clinical significance. *Rev. Clin. Esp.* **197,** 232-236.

Nasu, H., Chia, D.S., Knutson, D.W. and Barnett, E.V. (1980) Naturally occuring human antibodies to the $F(ab')_2$ portion of IgG. *Clin. Exp. Immunol.* **42,** 378-386.

Nemazee, D.A. and Sato, V.L. (1983) Induction of rheumatoid antibodies in the mouse: regulated production of autoantibody in the secondary humoral response. *J. Exp. Med.* **158,** 529-545.

Neuwirth, R., Singhal, P., Diamond, B., et al. (1988) Evidence for immunoglobulin Fc receptor-mediated prostaglandin2 and platelet-activating factor formation by cultured rat mesangial cells *J. Clin. Invest.* **82,** 936-944.

Nickells, M.W., Subramanian, V.B., Clemenza, L. and Atkinson, J.P. (1995) Identification of complement receptor type 1-related proteins on primate erythrocytes. *J. Immunol.* **154,** 2829-2837.

Normansell, D.E. (1971) Anti-globulins in rheumatoid arthritis sera. II. the reactivity of anti-globulin rheumatoid factors with altered G-globulin. *Immunochemistry* **8:** 593-602.

O'Brien, R.O., Roeth, P.J., Thomson, S.A., Bartell,G. and Easterbrook-Smith, S.B. (1994) The effects of histidine residue modification on the immune precipitating ability of rabbit IgG. *Arch. Biochem. Biophys.* **310,** 25-31.

Ohta, M., Okada, M., Yamashina, I. and Kawasaki, T. (1990) The mechanism of carbohydrate-mediated complement activation by the serum mannan-binding protein. *J. Biol. Chem.* **265,** 1980-1984.

Olsen, H.M., Parish, C.R. and Altin, J.G. (1996) Histidine-rich glycoprotein binding to T-cell lines and its effect on T-cell substratum adhesion is strongly potentiated by zinc. *Immunology* **88,** 198-206.

Pangburn, M.K., Schreiber, R.D. and Muller-Eberhard, H.J. (1981) Formation of the initial C3 convertase of the alternative complement pathway: acquisition of C3b-like activities by spontaneous hydrolysis of the putative thioester in native C3. *J. Exp. Med.* **154,** 856-867.

Panush, R.S., Bianco, N.E. and Schur, D.H. (1971) Serum and synovial fluid IgG, IgA, and IgM anti-immunoglobulins in rheumatoid arthritis. *Arthritis Rheum.* **14**, 737-747.

Parekh, R.B., Dwek, R.A., Sutton, B.J., et al., (1985) Association of rheumatoid arthritis and primary osteoarthritis with changes in the glycosylation pattern of total serum IgG. *Nature* 316: 452-457.

Parish, C.R., Rylatt, D.B. and Snowden, J.M. (1984) Demonstration of lymphocyte surface lectins that recognize sulfated polysaccharides. *J. Cell Science* **67**, 145-158.

Perussia, B., Starr, S., Abraham, S., Fanning, V. and Trinchieri, G. (1983) Human natural killer cells analysed by B73.1, a monoclonal antibody blocking Fc receptor function. *J. Immunol.* **130**, 2133-2141.

Pisko, E.J., Turner, R.A. and Foster, S.L. (1982) Induction of human rheumatoid factor producing cells by aggregated IgG. *Arthritis Rheum.* **25**, 1108-1116.

Podack, E.R. (1984) Molecular composition of the tubular structure of the membrane attack complex of complement. *J. Biol. Chem.* **259**, 8641-8647.

Porter, R. and Reid, K. (1979) Activation of the complement system by antibody-antigen complexes: the classical pathway. *Adv. Protein Chem.* **33**, 1-71.

Preud'homme, J. -L., Aucouturier, P., Touchard, G., Striker, L., Khamlichi, A. A., Rocca, A., Denoroy, L. and Cogne, M. (1994) Monoclonal immunoglobulin deposition disease. Relationship with structural abnormalities of immunoglobulin chains. *Kidney Int.* **46**, 965-972.

Purkerson, J. and Isakson, P. (1992) A two-signal model for regulation of immunoglobulin isotype switching. *FASEB J.* **6**, 3245-3252.

Qi, M. and Schifferli J.A. (1995) Inhibition of complement activation by intravenous immunoglobulins. *Arthritis Rheum.* **38**, 146.

Ramm, L.E, Whitlow, M.B. and Mayer, M.M. (1984) Complement lysis of nucleated cells: effect of temperature and puromycin on the number of channels required for cytolysis. *Mol. Immunol.* **21**, 1015-1021.

Randen, I., Thompson, K.M., Thorpe, S.J., Forre, O. and Natvig, J.B. (1993) Human monoclonal IgG rheumatoid factors from the synovial tissue of patients with rheumatoid arthritis. *Scand. J. Immunol.* **37**, 638-642.

Ranieri-Raggi, M., Montali, U., Ronca, F., Sabbatini, A., Brown, P.E., Moir, A.J.G. and Raggi, A. (1997) Association of purified skeletal-muscle AMP deaminase with a histidine-proline-rich glycoprotein-like molecule. *Biochem. J.* **326**, 641-648.

Ravetch, J.V. and Kinet, J.P. (1991) Fc receptors. *Annu. Rev. Immunol.* **9**, 457-492

Reid, K.B. (1974) A collagen-like amino acid sequence in a polypeptide chain of human C1q (a subcomponent of the first component of complement). *Biochem. J.* **141**, 189-203.

Riesen, W., Keller, H., Skvaril, F., Morrell, A. and Barandun, S. (1976) Restriction of immunoglobulin heterogeneity, autoimmunity and serum protein levels in aged people. *Clin. exp. immnol.* **26**, 280-285.

Robinson, J.J., Watson, F., Bucknall, R.C. and Edwards, S.W. (1994) Stimulation of reactive oxidant production in neutrophils by soluble and insoluble immune complexes occurs via different receptors/signal transduction system. *FEMS Immunol. Med. Microbiol.* **8**, 249-258.

Rodwell, J.D., Tang, L-H. and Schumaker, V.N. (1980) Antigen valence and Fc-localized secondary forces in antibody precipitation. *Molec. Immunol.* **17**, 1591-1597.

Rosen, H. and Gorden, S. (1989) Current status review: Adhesion molecules and myelomonocytic cells-endothelial interactions. *Br. J. Exp. Pathol.* **70**, 385-394.

Ruiz de Souza, V., Kaveri, S.V. and Kazatchkine, M.D. (1993) Intravenous immunoglobulin (IVIgs) in the treatment of autoimmune and inflammatory disease. *Clin. Exp. Rheumatol.* **11**, S33-36.

Rylatt, D.B., Sia, D.Y., Mundy, J.P. and Parish, C.R. (1981) Autorosette inhibition factor: Isolation and properties of the human plasma protein. *Eur. J. Biochem.* **119**, 641-646.

Saez, C.T., Jansen, G.J., Smith, A. and Morgan, W.T. (1995) Interaction of histidine-proline-rich glycoprotein with plasminogen: Effect of ligands, pH, ionic strength and chemical modification. *Biochemistry* **34**, 2496-2503.

Saigo, K., Shatsky, M., Levitt, L.J. and Leung, L.L.K. (1989) Interaction of histidine-rich glycoprotein with human T lymphocytes. *J. Biol. Chem.* **264**, 8249-8253.

Saigo, K., Yoshida, A., Sugano, W., Ryo, R. and Yamaguchi, N. (1990a) Histidine-rich glycoprotein in blood during inflammation, surgical operation or hemodialysis. *Jpn. J. Clin. Hematol.* **31**, 1914-1919.

Saigo, K., Yoshida, A., Ryo, R., Yamaguchi, N. and Leung, L.L.K. (1990b) Histidine-rich glycoprotein as a negative acute phase reactant. *Am. J. Hematol.* **34**, 149-150.

Saito, H., Goodnough, L.T., Boyle, J.M. and Heimburger, N. (1982) Reduced histidine-rich glycoprotein levels in plasma of patients with advanced liver cirrhosis. Possible implications for enhanced fibrinolysis. *Am. J. Med.* **73**, 179-182.

Sakuragawa, N., Niwa, M. and Yamagishi, R. (1985) Studies on the purification and characteristics of histidine-rich glycoprotein. *Sem. Thromb. Hemost.* **11**, 384-386.

Savige, J.A., Dash, A.C. and Rees, A.J. (1989) Exaggerated glomerular albuminuria after cobra venom factor in anti-glomerular basement membrane disease. *Nephron* **52**, 29-35.

Savin, V.J. (1993) Mechanism of proteinuria in noninflammatory glomerular disease. *Am. J. Kidney Dis.* **21**, 347-362.

Schifferli, J.A. (1987) The classical pathway of complement prevents the formation of insoluble antigen-antibody complexes: biological implications. *Immunol. Lett.* **14**, 225-228.

Schifferli, J.A. (1996) Complement and immune complexes. *Res. Immunol.* **147**, 109-110

Schifferli, J.A., Ng, Y.C., Estreicher, J. and Walport, M.J. (1988) The clearance of tetanus toxoid/anti-tetanus toxoid immune complexes from the circulation of humans. Complement- and erythrocyte complement receptor 1-dependent mechanisms. *J. Immunol.* **140**, 899-904.

Schifferli, J.A., Pascual, M., Steiger, G., Schapira, M., Ryser, J.E., Estreicher, J. and Dash, A. (1987) Fast liver catabolism of C1q in patients with paraproteinemia and depletion of the classical pathway of complement. *Clin. Exp. Immunol.* **69**, 188-197.

Schifferli, J.A., Steiger, G. and Paccaud, J.P. (1986) Complement mediated inhibition of immune precipitation and solubilisation generate different concentrations of complement anaphylatoxins. *Clin. Exp. Immunol.* **64**, 407-414.

Schifferli, J.A., Steiger, G. and Schapira, M. (1985) The role of C1, C1 inhibitor and C4 in modulating immune precipitation. *Clin. Exp. Immunol.* **60**, 605-612.

Schifferli, J.A., Woo, P. and Peters, D.K. (1982) Complement-mediated inhibition of immune precipitation. Role of the classical and alternative pathways. *Clin. Exp. Immunol.* **47**, 555-562.

Schinke, T., Koide, T. and Jahnen-Dechent, W. (1997) Human histidine-rich glycoprotein expressed in SF9 insect cells inhibits apatite formation. *FEBS lett.* **412**, 559-562.

Sem, A., Sumbhara, S., Chadwick, B.S. and Miller, R.G. (1991) Dependence of mouse thymocyte-erythrocyte rosette formation on complete identity at Class I MHC. *J. Cell Physiol.* **148**, 485-492.

Shatsky, M., Saigo, K., Burdach, S., Leung, L.L.K. and Levitt, L.J. (1989) Histidine-rich glycoprotein blocks T cell rosette formation and modulates both T cell activation and immunoregulation. *J. Biol. Chem.* **264**, 8254-8259.

Shigekiyo, T., Kanazuka, M., Azuma, H., Ohshima, T., Kusaka K. and Saito, S. (1995) Congenital deficiency of histidine-rich glycoprotein : Failure to identify abnormalities in routine laboratory assays of hemostatic function, immunological function, and trace elements. *J. Lab. Clin. Med.* **125**, 719-723.

Shigekiyo, T., Yoshida, H., Matsumoto, K., Azuma, H., Wakabayashi, S., Saito, S., Fujikawa, K. and Koide, T. (1998) HRG-Tokushima : molecular and cellular characterization of histidine-rich glycoprotein (HRG) deficiency. *Blood* **91**, 128-133.

Shimada, K., Kawamoto, A., Matsubayashi, K. and Ozawa, T. (1989) Histidine-rich glycoprotein does not interfere with interactions between antithrombin III and heparin-like compounds on vascular endothelial cells. *Blood* **73**, 191-193.

Shumak, K.H. and Rock, G.A. (1984) Therapeutic plasma exchange. *N. Engl. J. Med.* **310**, 762-771.

Sia, D.Y., Rylatt D.B. and Parish, C.R. (1982) Anti-self receptors. V. Properties of a mouse serum factor that blocks autorosetting receptors on lymphocytes. *Immunology* **45**, 207-216.

Silverstein, R.L., Leung, L.L.K., Harpel, P.C. and Nachman, R.L. (1985a) Platelet thrombospondin forms a trimolecular complex with plasminogen and histidine-rich glycoprotein. *J. Clin. Invest.* **75**, 2065-2073.

Silverstein, R.L., Nachman, R.L., Leung, L.L.K. and Harpel, P.C. (1985b) Activation of immobilised plasminogen by tissue activator. Multicellular complex formation. *J. Biol. Chem.* **260**, 10346-10352.

Sittampalam, G. and Wilson, G.S. (1984a) Experimental observations of transient light scattering complexes formed during immunoprecipitin reactions. *Analyt. Chem.* **56**, 2170-2175.

Sittampalam, G. and Wilson, G.S. (1984b) Theory of light scattering measurement as applied to immunoprecipitin reactions. *Analyt. Chem.* **56**, 2176-2180.

Smiley, J.D. and Moore, S.E. (1989) Immune complex vasculitis: role of complement and IgG-Fc receptor function. *Am. J. Med. Sci.* **298**, 267-277.

Smith, A., Nuiry, I. and Morgan, W.T. (1985) Proteolysis of histidine-rich glycoprotein in plasma and in patients undergoing thrombolytic therapy *Thromb. Res.* **40**, 653-661.

Smoller, B.R., McNutt, N.S. and Contreras, F. (1990) The natural history of vasculitis. What the histology tells us. *Arch. Dermatol.* **126**, 84-89.

Solomon, A., Weiss, D.T. and Kattine, A.A. (1991) Nephrotoxic potential of Bence Jones proteins. *N. Engl. J. Med.* **324**, 1845-1851.

Sorensen, C.B., Krogh-Pedersen, H. and Petersen, T.E. (1993) Determination of disulphide bridge arrangement of bovine histidine-rich glycoprotein. *FEBS* **328**, 285-290.

Souto, J.C., Gari, M., Falkon, L. and Fontcuberta, J. (1996) A new case of hereditary histidine-rich glycoprotein deficiency with familial thrombophilia. *Thromb. Haemos.* **75**, 372-377.

Stacey, K. A. (1956) In: Light Scattering in Physical Chemistry. *Butterworths Scientific Publications.* London, U. K. pp. 53-56.

Steward, M.W. (1979) Chronic immune complex disease in mice: the role of antibody affinity. *Clin. Exp. Immunol.* **38**, 414-423.

Stewart, J.J., Agosto, H., Litwin, S., Welsh, J.D., Shlomchik, M., Weigert, M. and Seiden, P.E.A. (1997) Solution to the rheumatoid paradox - pathologic rheumatoid factors can be tolerized by competition with natural rheumatoid factors. *J. Immunol.* **159**, 1728-1738.

Sylvestre, D.L. and Ravetch, J.V. (1994) Fc receptors initiate the arthus reaction: redefining the inflammatory cascade. *Science* **265**, 1095-1098

Takata, Y., Tamura, N. and Fujira, T. (1984) Interaction of C3 with antigen-antibody complexes in the process of solubilisation of immune precipitates. *J. Immunol.* **132**, 2531-2537.

Tartour, E., Delasalle, H., Delasalle, C., Teillaud, C., Camoin, L., Galinha, A., Latour, S., Hanau, D., Fridman, W.H. and Sautes, C. (1993) Identification, in mouse macrophages and in serum, of a soluble receptor for the Fc portion of IgG (Fc-gamma-R) encoded by an alternatively spliced transcript of the Fc-gamma-RII gene. *Int. Immunol.* **5**, 859-868.

Taylor, R.P., Ferguson, P.J., Martin, E.N., Cooke, J., Greene, K.L., Grinspun, K., Guttman, M. and Kuhn, S. (1997) Immune complexes bound to the primate erythrocyte complement receptor (CR1) via anti-CR1 mAb are cleared simultaneously with loss of CR1 in a concerted reaction in a rhesus monkey model. *Clin. Immunol. Immunopathol.* **82**, 49-59.

Tenner, A.J., Lesavre, P.H. and Cooper, N.R. (1981) Purification of radiolabelling of human C1q. *J. Immunol.* **127**, 648-653.

Theofilopoulos, A.N. (1980) Evaluation and clinical significance of circulating immune complexes. *Prog. Clin. Immunol.* **4**, 63-106.

Theofilopoulos, A.N. and Dixon, F.J. (1980) Immune complexes in human disease. *Am. J. Pathol.* **100**, 529-594.

Tosca, N. and Stratigos, J.D. (1988) Possible pathogenetic mechanisms in allergic cutaneous vasculitis. *Intern. J. Dermatol.* **27**, 291-296.

Tosi, M.F. and Berger, M.F. (1988) Functional differences between 40 kDa and 50-70 kDa IgG Fc receptors on human neutrophils revealed by elastase treatment and anti-receptor antibodies. *J. Immunol.* **141**, 2097-2106.

Tripathi, A.K., Chakrabarty, A.K. and Gupta, P.S. (1993) Biochemical studies on stimulation of mouse peritoneal macrophages by interaction with preformed immune complexes. *Indian J. Exp. Biol.* **31**, 5-11.

Tripp, C.S., Beckerman, K.P. and Unanue, E.R. (1995) Immune complexes inhibit antimicrobial responses through interleukin-10 production. Effects in severe combined immunodeficiency mice during listeria infection. *J. Clin. Invest.* **95**, 1628-1634.

Tschopp, J., Chonn, A., Hertig, S. and French, L.E. (1993) Clusterin, the human apolipoprotein and complement inhibitor, binds to complement C7, C8B and the b domain of C9. *J. Immunol.* **151**, 2159-2165.

Unkeless, J.C., Boros, P. and Fein, M. (1992) Structure, signalling and function of FcγR. In: Inflammation: Basic Principles and Clinical Correlates. Sec. Ed. Gallin, J.I., Goldstein, I.M. and Snyderman, R. *Raven Press Ltd., NY* pp. 497-510.

Van Den Berg, E.A., Le Clercq, E., Koide, T., Van Der Zee, A., Oldenburg, M., Wijnen, J. and Khan, P.M. (1990) Assignment of the human gene for histidine-rich glycoprotein to chromosome 3. *Genomics* **7**, 276-279.

Van Der Woude, F., Rasmussen, N., Lobatto, S., Wiik,, A., Permin, H., Van Es, L., Van Der Giessen, M., Van Der Hem, G. (1985) Autoantibodies to neutrophils and monocytes: a new tool for diagnosis and a marker of disease activity in wegener's granulomatosis. *Lancet* **1**, 425-429.

Van De Winkel, J.G.J. and Anderson, C.L. (1991) Biology of human immunoglobulin G Fc receptors. *J. Leuk. Biol.* **49**, 511-524.

Van De Winkel, J.G.J. and Capel, P.J.A. (1993) Human IgG Fc receptor heterogeneity: molecular aspects and clinical implications. *Immunol. Today* **14**, 215-221.

Van Es, L., Daha, M., Valentijn, R. and Kauffman, R. (1984) The pathogenetic significance of circulating immune complexes. *Neth. J. Med.* **27**, 350-358.

Veerhuis, R., Krol, M.C., Es L.A. and Van Daha, M.R. (1986) Differences in clearance kinetics of particulate immune complexes and soluble aggregates of IgG *in vivo*. *Clin. Immunol. Immunopathol.* **41**, 379-391.

Vellenga, E., Kluft, C., Mulder, N.H., Wijngaards, G. and Nieweg, H.O. (1984) The influence of L-asparaginase therapy on the fibrinolythic system. *Br. J. Haem.* **57**, 247-254.

Walport, M.J. and Davies, K.A. (1996) Complement and immune complexes. *Res. Immunol.* **147**, 103-109.

Walport, M.J., Ng, Y.C. and Lachmann, P.J. (1987) Erythrocytes transfused into patients with SLE and haemolytic anaemia lose complement receptor type 1 from their cell surface. *Clin. Exp. Immunol.* **69**, 501-507.

Walport, M.J. and Lachmann, P.J. (1988) Erythrocytes complement receptor type 1, immune complexes and the rheumatic diseases. *Arthritis Rheum.* **31** 153-158.

Waxman, F.J., Herbert, L.A., Cornacoff, J.B. et al. (1984) Complement depletion accelerates the clearance of immune complexes from the circulation of primates. *J. Clin. Invest.* **74**, 1329-1340.

Waxman, F.J., Herbert, L.A., Cosio, F.G., Smead, W.L., Van Aman, M.E., Taguiam, J.M. and Birmingham, D.J. (1986) Differential binding of immunoglobulin A and immunoglobulin G1 immune complexes to primate erythrocytes *in vivo*.: immunoglobulin A immune complexes binds less well to erythrocytes and are preferentially deposited in glomeruli. *J. Clin. Invest.* **77**, 82-89.

Weis, W.I., Drickamer, K. and Hendrickson, W.A. (1992) Structure of a C-type mannose-binding protein complexed with an oligosaccharide. *Nature* **360**,127-134.

Weisman, M. and Zvaifler, N. (1975) Cryoglobulinemia in rheumatoid arthritis. Significance in serum of patients with rheumatoid vasculitis. *J. Clin. Invest.* **56**, 725-739

Wener, M.H. and Mannik, M. (1986) Mechanism of immune deposit formation in renal glomeruli. *Springer Semin. Immunopathol.* **9**, 219-235.

Wilson, J.G., Wong, W.W., Schur, P.H. and Fearon, D.T. (1982) Mode of inheritance of decreased C3b receptors on erythrocytes of patients with systemic lupus erythematosus. *N. Engl. J. Med.* **307**, 981-986.

Winchester, R. J. (1975). Characterization of IgG complexes in patients with rheumatoid arthritis. *Ann. NY Acad. Sci.* **256**, 73-81.

Woof, J.M., Nik Jaafar, M.I., Jefferis, R. and Burton, D.R. (1984) The monocyte binding domain(s) on human immunoglobulin G. *Mol. Immunol.* **21**, 523-527.

Woof, J.M., Partridge L.J., Jefferies, R. and Burton, D.R. (1986) Localization of the monocyte-binding region on human immunoglobulin G. *Mol. Immunol.* **23**, 319-330.

Wormald, M.R., Rudd, P.M., Harvey, D.J., Chang, S-C., Scragg, I.G. and Dwek, R.A. (1997) Variation in oligosaccharide-protein interactions in immunoglobulin G determine the site specific glycosylation profiles and modulate the dynamic motion of the Fc oligosaccharides. *Biochemistry* 36: 1370-1380.

Yamashina, M., Ueda, E., Kinoshita, T., et al. (1990) Inherited complete deficiency of 20-kilodalton homologous restriction factor (CD59) as a cause of paroxysmal nocturnal. *N. Engl. J. Med.* **323**, 1184-1188.

Yarmush, D.M., Murphy, R.M., Colton, C.K., Fisch, M. and Yarmush, M.L. (1988) Quasi-elastic light scattering of antigen-antibody complexes. *Molec. Immunol.* **25**, 17-32.

Yokoyama, I. and Waxman, F. (1994) Differential susceptibility of immune complexes to release from the erythrocytes CR1 receptor by factor I. *Mol. Immunol.* **29**, 935-947.

Zach, D.J., Stempniak, M., Wong, A.L. and Weisbart, R.H. (1995) Localization of an Fc binding reactivity to the constant region of human IgG4. Implications for the pathogenesis of rheumatoid arthritis. *J. Immunol.* **155**, 5057-5063.

Zanetti, M. and Wilson, C.B. (1986) A role for anti-idiotypic antibodies in immunologically mediated nephritis. *Am. J. Kidney Dis.* **7**, 445-451.

Zhang, S.O., Schultz, D.R. and Ryan, U.S. (1986) Receptor-mediated binding of C1q on pulmonary endothelial cells. *Tissue-Cell* **18**, 13-18.

Ziccardi, R.J. (1981) Activation of the early component of the classical complement pathway under physiologic conditions. *J. Immunol.* **126**, 1769-1773.